Molecular Pharmacology of DNA topoisomerase II drugs

Ka Cheong Lee

Thesis submitted for the degree of
Doctor of Philosophy

Institute for Cell and Molecular Biosciences
Faculty of Medical Sciences
Newcastle University

July 2016

Abstract

Topoisomerase II (TOP2) is an important anti-cancer drug target. This study demonstrates that proteasomal inhibition by MG132 or PS341 potentiates the effect of TOP2 poisons on cell growth inhibition. Mitoxantrone was potentiated the most. The presence of the proteasome inhibitor MG132 prolonged the half-life of drug-induced DNA-TOP2 complexes stabilised by mitoxantrone or etoposide.

Genotoxicity was measured in K562 cells using *in vitro* micronucleus assays for combinations of a proteasome inhibitor (MG132 or PS341) and mitoxantrone and for each agent alone. Combinations that potentiated the cytotoxicity reduced the genotoxicity. This suggests that combining a proteasome inhibitor with a TOP2 drug has the potential to reduce late toxicities such as therapy related leukaemia.

The genotoxicity of six TOP2 poisons was determined by high throughput *in vitro* micronucleus assays in three Nalm-6 cell lines with differing TOP2 levels. Lower genotoxicity was observed in TOP2B knock-out and TOP2A knock-down cells, suggesting both TOP2A and TOP2B have a role in genotoxicity triggered by TOP2 poisons.

Acknowledgements

The completion of my thesis would not have been possible without these people. Firstly, I would like to express my deepest appreciation to both my supervisors Professor Caroline Austin and Dr Ian Cowell for their guidance, encouragement, and patience throughout these years. Thank you for their advice and critical reading of my thesis. Thank you to Bloodwise for their support and for funding this study.

I would also like to thank Rebecca Bramley, and Dr. Laura Neilson for their help in proof reading this thesis. I would also like to thank Mandeep Atwal and Mushtaq Khazeem who have provided help and support to me in different ways.

Finally many thanks to my family. I could not have got to this point of my life without their help, especially my son and wife, Lucas and Lindy, they have been very understanding, patient and full of love.

Table of Contents

Table of figures:

Table of Tables:

Abbreviations

ANOVA	Analysis of variance
AP	Apurine/ Apyrimidine
APE1/APEX1	Human apurinic/apyrimidinic (AP) endonuclease 1
ATM	Ataxia-Telangiectasia Mutated
ATP	Adenosine triphosphate
Av. MNi	Average percentage of Micronculei
BER	Base excision repair
Bp	Base pairs
BSA	Bovine serum albumin
CML	Chronic myelogenous (or myeloid) leukaemia
CO_2	Carbon dioxide
CtIP	CtBP-interacting protein
Da	Daltons
DAPI	4', 6-diamidino-2-phenylindole
Dau	Daunorubicin
DDR	DNA damage response
DMEM	Dulbecco's Modified Eagle's Medium
DMSO	Dimethyl sulfoxide
DNA	Deoxyribonucleic acid
DNA-PK	DNA-dependent protein kinase
DNA-PK_{cs}	DNA-PK catalytic subunit
Dox	Doxorubicin

DSBs	double strand breaks
DTT	Dithiothreitol
ECL	Electrochemiluminescence
EDTA	Ethylenediaminetetraacetice acid
EMA	Ethidium Monoazide Bromide
Epi	Epirubicin
FACS	Fluorescence activated cell sorting
FBS/FCS	Heat-inactivated Foetal Bovine Serum/ Foetal calf Serum
FDA	Food and Drug Administration
FITC	fluorescein isothiocyanate
HEPES	4-(2-hydroxyethyl)-1-piperazineethanesulfonic acid
HR	Homologous recombination
Ida	Idarubicin
IF	Integrated fluorescence
IgA	Immunoglobulin A
IgD	Immunoglobulin D
IgE	Immunoglobulin E
IgG	Immunoglobulin G
IP	Immunoprecipitation
IR	Irradiation
KCl	Potassium Chloride
Ku70/80	human Ku70/80 protein complex
$MgCl_2$	Magnesium chloride

min(s)	minute(s)
miRNA	microRNA
MLL	Mixed-lineage leukaemia
MMS	Methyl methanesulfonate
MN/MNi	Micronucleus/ Micronuclei
MRE11	Meiotic recombination 11
MRN complex	Mre11/NBS1/Rad50 complex of proteins
MTX	Mitoxantrone
NaCl	Sodium chloride
NaOH	Sodium hydroxide
$NaPO_4$	Sodium phosphate
NBS1	Nijmegen Breakage Syndrome 1
NER	Nucleotide excision repair
NHEJ	Non-homologous end joining
OECD	Organisation for Economic Co-operation and Development
Oligo	Oligonucleotide
PARP1	Poly (ADP-ribose) polymerase
PBS	Phosphate-buffered saline
PIs	Protease inhibitors
PMSF	Phenylmethanesulphonylfluoride
RCF	Relative centrifugal force
RICC	Relative Increase of Cell Count

RNA	Ribonucleic acid
RNAi	RNA interference
RPM	Revolutions per minute
SEM	Standard Error of the Mean
SDS	Sodium dodecyl sulphate
SDS- PAGE	SDS polyacrylamide gel electrophoresis
siRNA	small interfering RNA
SSBs	Single stand breaks
TARDIS	Trapped in Agarose DNA immunostaining assay
TDP1	tyrosyl DNA phosphodiesterase-1
TDP2	tyrosyl DNA phosphodiesterase-2
TOP	DNA topoisomerase
TOP2	DNA topoisomerase II
TOP2A	DNA topoisomerase II α
TOP2B	DNA topoisomerase II β
TTRAP/TDP2	TRAF and TNF receptor-associated protein/ tyrosyl DNA phosphodiesterase-2
UK	United Kingdom
UPS	Ubiquitin-Proteasome System
USA	United States of America
VM26	Teniposide
VP16	Etoposide
v/v	volume/ volume

w/v	weight/ volume
XTT	tetrazolium salt; sodium 3’-[1-(phenoaminacarbonyl)-3,4,-tetrazolium] bis(4-methoxy-6-nitro)benzene sulfonic acid hydrate
+ve	positive
-ve	negative

Chapter 1. Introduction

1.1 DNA topoisomerases

DNA topoisomerases are enzymes that catalyse changes in DNA topology. They transiently break and re-join DNA as part of their reaction mechanism. This involves a covalent intermediate in which the DNA is cleaved and covalently linked to the active site tyrosine within the topoisomerase (Figure 1.1). There are two main classes of topoisomerases, type I and type II. Type I enzymes cleave a single strand, and type II cleave both strands. The reactions they catalyse include relaxation of DNA supercoils and decatenation of interlinked DNA molecules (Figure 1.2). Biochemical studies have revealed key mechanistic details for type II topoisomerases (Figure 1.3). The introduction of protein-bound DNA double strand breaks allows the passage of a second DNA helix through the enzyme. Eukaryotic TOP2 is a dimer. The monomers have three functional domains; an N-terminal ATPase domain, a middle "core" domain that houses the catalytic tyrosine residue, and a C-terminal domain that has many sites for post-translational modifications such as phosphorylation. The core domains for yeast TOP2, human TOP2A and human TOP2B have been crystallised and the structures solved (Berger *et al.*, 1996; Wu *et al.*, 2011; Wendorff *et al.*, 2012). The work in this thesis focuses on human type II DNA topoisomerases. Vertebrate cells possess two isoforms of topoisomerase II, termed alpha (TOP2A) and beta (TOP2B). TOP2A is essential for cells, required for segregation of chromosomes during cell division (Akimitsu *et al.*, 2003). Cells can survive without TOP2B but whole organisms cannot (Dereuddre *et al.*, 1997; Yang *et al.*, 2000). Both isoforms are involved in gene regulation (Tiwari *et al.*, 2012; Thakurela *et al.*, 2013; Madabhushi *et al.*, 2015).

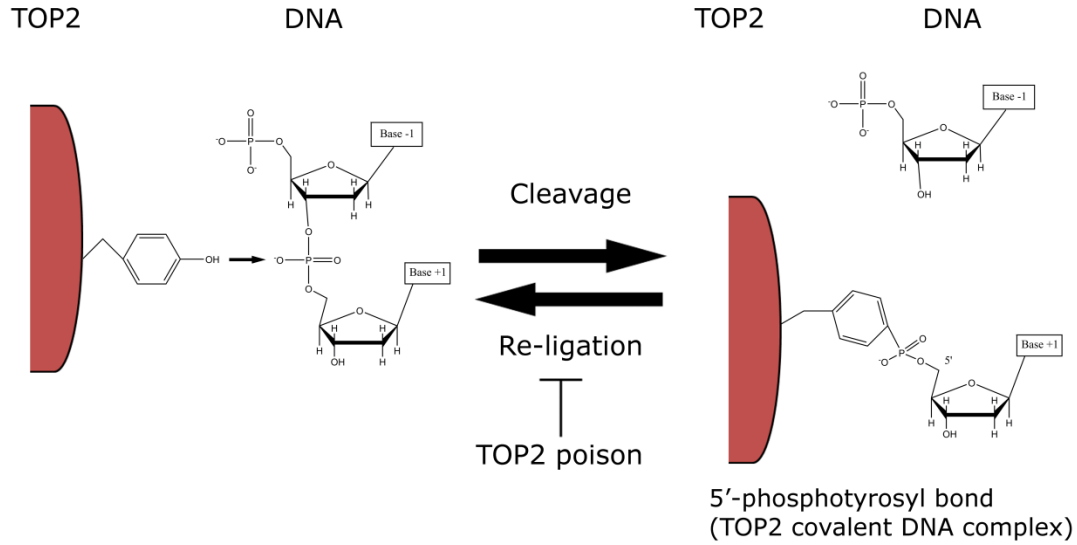

Figure 1.1 DNA cleavage reaction of TOP2.

TOP2 active site with tyrosine cleaves DNA at the 5' position, resulting in a DNA double strand break with 5'-phosphotyrosyl linkage.

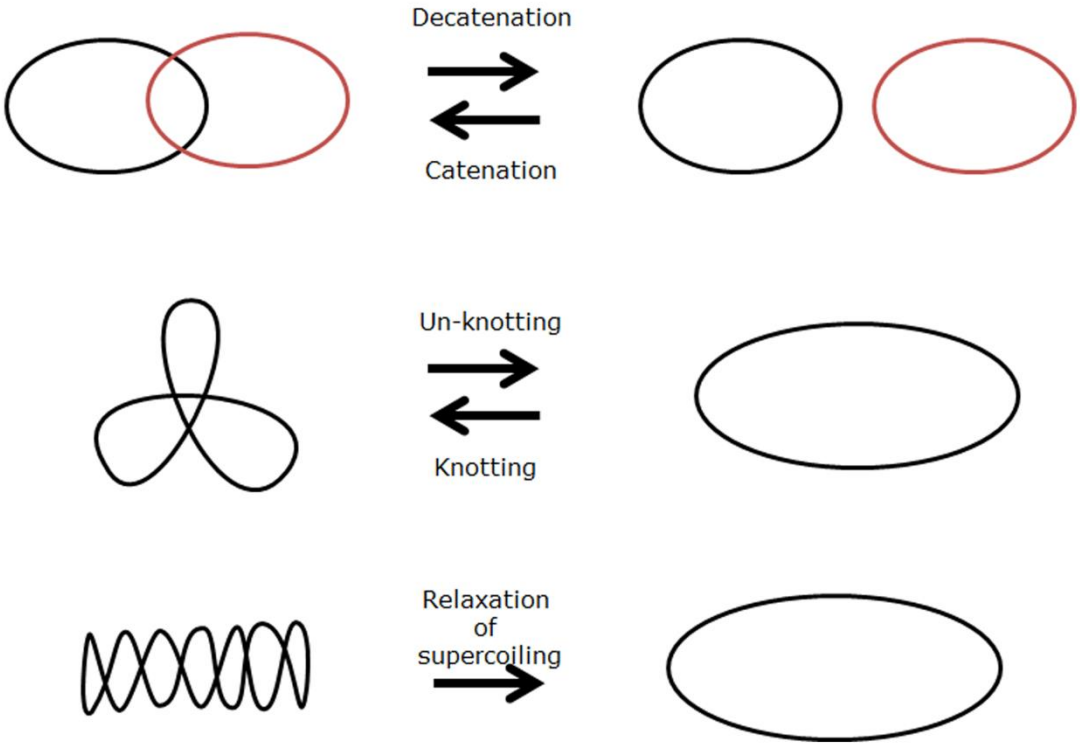

Figure 1.2 Schematic of reactions catalysed by TOP2 including decatenation, un-knotting DNA and relaxation of supercoiled DNA.

Adapted with permission from Pommier *et al.,* 2010.

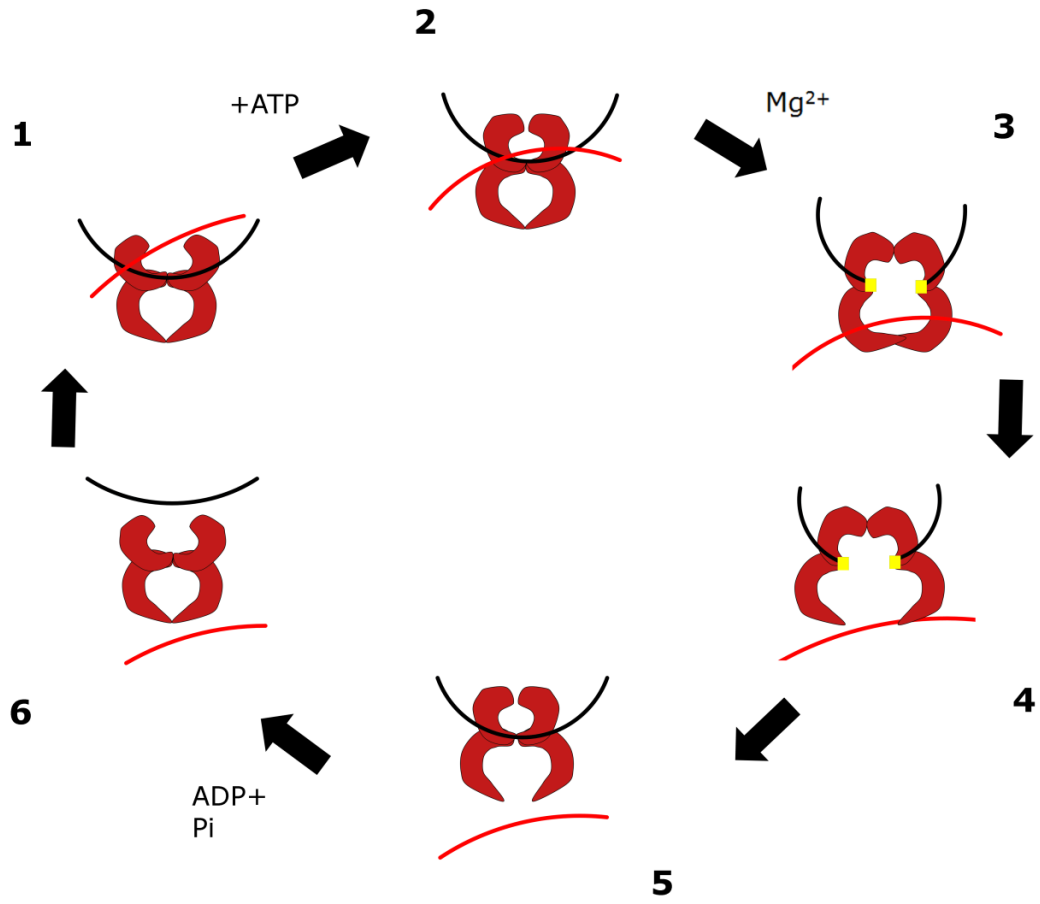

Figure 1.3 Catalytic cycle of TOP2.
The catalytic cycle of TOP2 starts from the binding of the first duplex of DNA to TOP2 (1) and then with the binding of ATP and the second duplex of DNA. TOP2 changes to a closed clamp position (2). In the presence of Mg^{2+}, TOP2 breaks the first duplex of DNA and allows the second DNA duplex to pass through (3). Once the second DNA duplex is released, TOP2 re-ligates the first DNA duplex (4 and 5). TOP2 releases the first DNA duplex and returns to the open clamp position by ATP-hydrolysis (6). Adapted with permission from Pommier *et al.,* 2010.

1.2 Drugs targeting human TOP2

DNA topoisomerase II is an important anti-cancer drug target. Several classes of drug target TOP2, including epipodophyllotoxins (etoposide and teniposide), anthracyclines (doxorubicin and epirubicin), anthracenediones (mitoxantrone) and acridines (mAMSA) (Figure 1.6). These drugs can target both TOP2A and TOP2B. TOP2 drugs can act in two ways; TOP2 poisoning or catalytic inhibition. Catalytic inhibition is defined as inhibiting the TOP2 catalytic cycle but not via the cleaved intermediate (Larsen *et al.*, 2003; Nitiss, 2009; Pommier *et al.*, 2010). TOP2 poisoning means stabilising the normally transient covalent TOP2-DNA complex whilst the DNA is cleaved (Wang, 2002; Pommier *et al.*, 2010). This results in a trapped TOP2 cleavage complex where the DNA has protein-linked strand

breaks. Both types of targeting can kill cells (Wang, 2002). TOP2 targeting drugs have been implicated in the initiation of chromosome translocations that lead to treatment-related leukaemia (Rowley, 1998; Smith *et al.*, 1999; Felix, 2001; Felix *et al.*, 2006; Cowell *et al.*, 2012) (Figure 1.4).

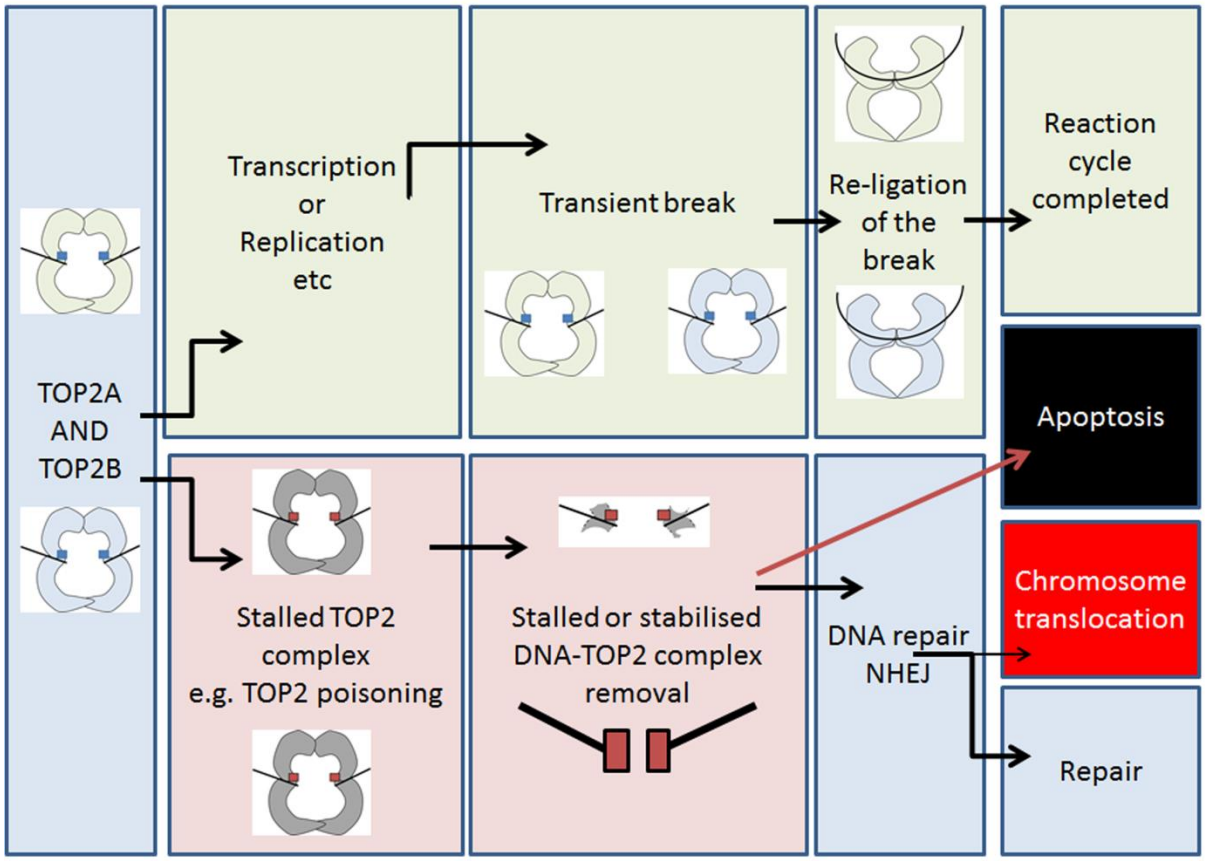

Figure 1.4 Schematic of TOP2 reaction cycle and endpoints.

To study the isoform specificity of drug targeting, an isoform-specific assay was previously developed here in Newcastle called the trapped in agarose DNA immunostaining (TARDIS) assay (Figure 1.7). This is a microscopy-based assay in which TOP2 specific primary antibodies and a FITC-labelled secondary antibody are used to detect covalent TOP2-DNA complexes formed in cells in response to drugs *(Willmore et al., 1998; Cowell et al., 2011)*. The TARDIS assay can be used to study the rate of disappearance of drug-induced DNA-TOP2 complexes from cells (Willmore *et al.*, 2004; Sunter *et al.*, 2010) to determine the half-life of the complexes under different conditions. Complexes decrease after removal

of the drug. They can reverse via the normal re-ligation step of the TOP2 reaction mechanism or they can be repaired by the cellular DNA repair machinery. This latter process is essential for "stalled complexes". In human cells, the main pathway to repair DNA double-strand breaks is Non-Homologous End joining (NHEJ). This requires DNA-dependent protein kinase (DNA-PK). However, activation of DNA-PK requires DNA breaks without bound protein (Martensson *et al.*, 2003). Therefore, TOP2 must be removed before the double-strand break can be repaired by NHEJ. Protein removal is thought to occur by proteases in the proteasome (Lee *et al.*, 2016). This will leave a short peptide attached to the DNA, which can be removed by 5'-tyrosyl DNA phosphodiesterase, TDP2 (Cortes Ledesma *et al.*, 2009; Zeng *et al.*, 2011; Schellenberg *et al.*, 2012; Gao *et al.*, 2014a; Pommier *et al.*, 2014). Alternatively, the DNA end bearing the TOP2 may be cleaved by a nuclease such as MRE11, or an AP lyase activity such as KU or APE1 (Ayene *et al.*, 2005; Roberts *et al.*, 2010; Lee *et al.*, 2012) (Figure 1.5).

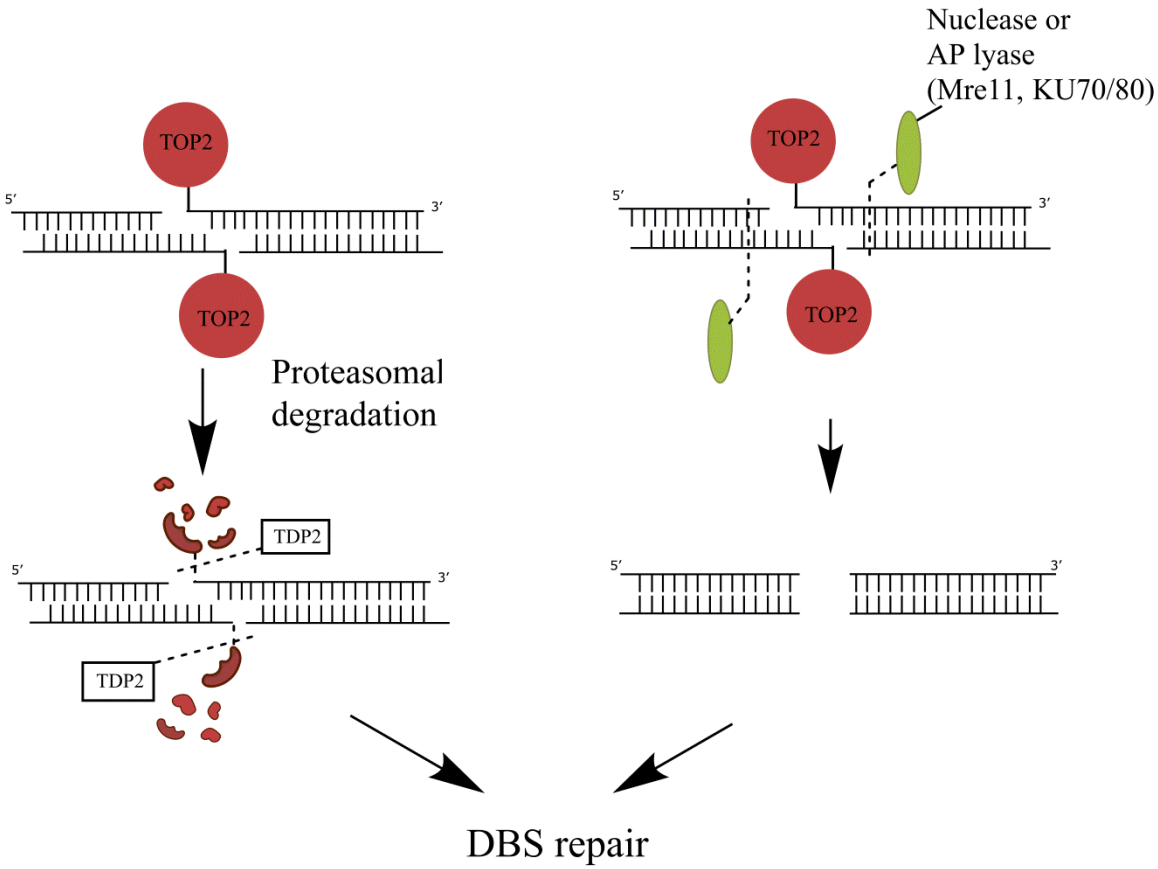

Figure 1.5 Schematic diagram representing possible mechanism(s) of TOP2 protein removal.

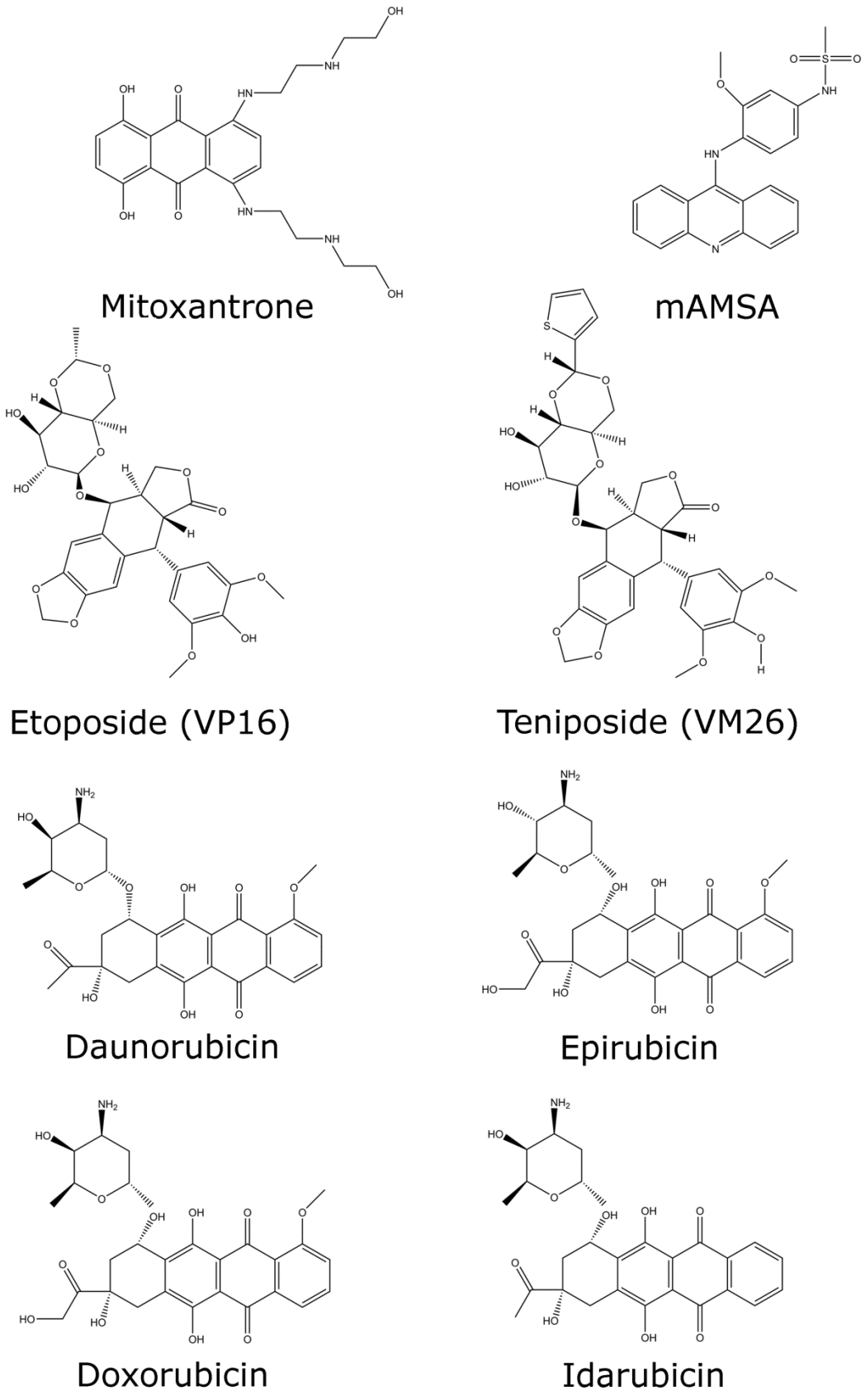

Figure 1.6 Chemical structure of TOP2 poisons.

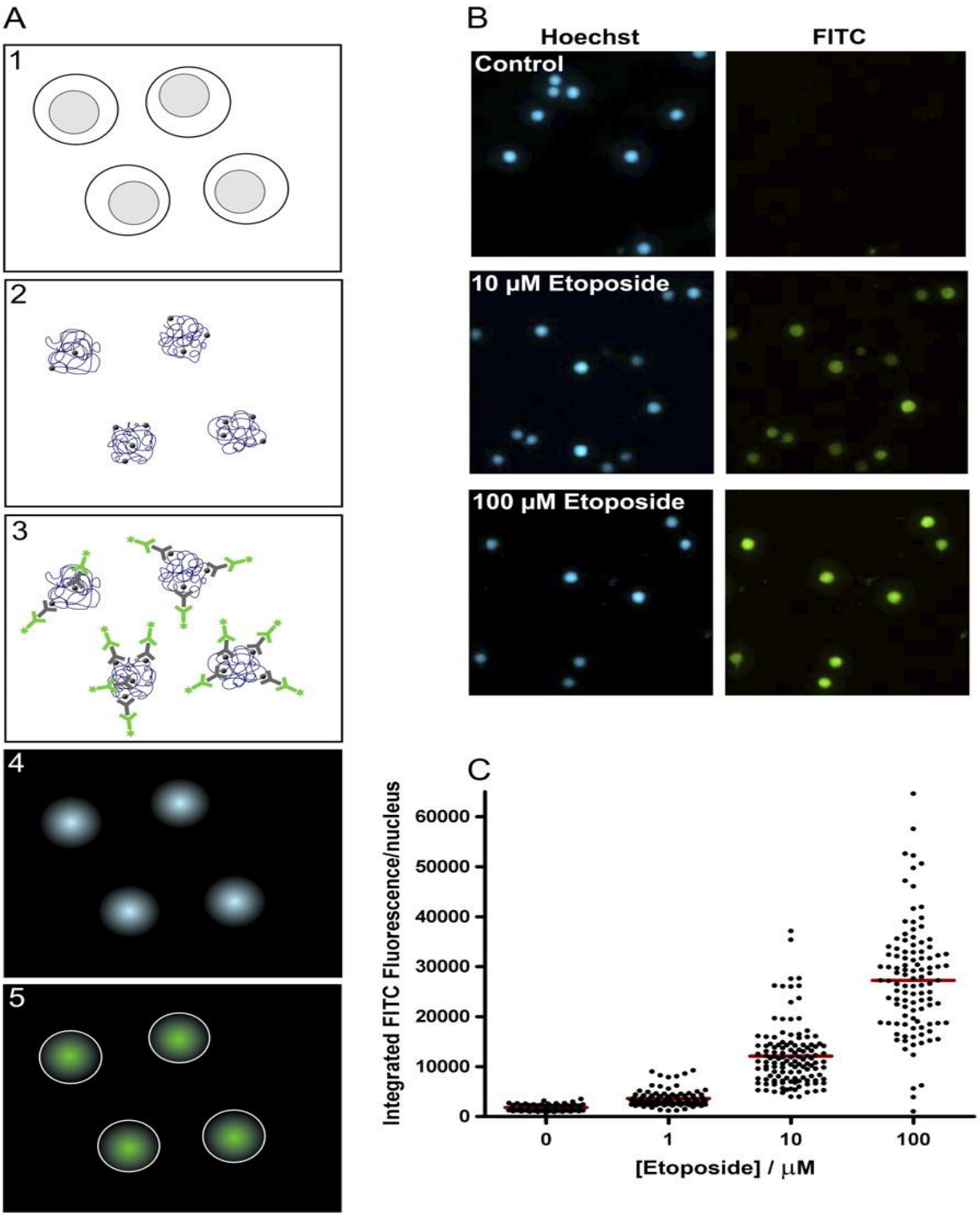

Figure 1.7 Basis of TARDIS analysis.

A) Schematic diagram of the steps involved in processing cells for TARDIS analysis: (1) cells are embedded in agarose on a glass slide; (2) after extraction with SDS and salt, most cellular components are removed but genomic DNA and covalent adducts remain; (3) adducts are detected by immunofluorescent staining using specific primary antibodies and FITC-labelled secondary antibody; (4) areas occupied by genomic DNA are identified by Hoechst fluorescence; (5) FITC fluorescence is quantified within the areas defined as containing DNA. (B) Representative images recorded for etoposide-treated K562 cells. Immunofluorescence was carried out with anti-TOP2A and FITC-conjugated second antibody. (C) Scattergram representation of the TOP2A signal derived from etoposide-treated K562 cells. Each filled circle represents the integrated fluorescence value of a single nucleus. The horizontal lines represent the median values. This figure was adapted from Cowell *et al.,* 2011 with permission.

1.3 Proteasome pathway and TOP2

Proteasomes are important for protein degradation. Proteins are unfolded prior to translocation into the multi-protein barrel shaped proteasome. Proteins can be targeted to the proteasome either in a ubiquitin-dependent or a ubiquitin-independent manner. The ubiquitin-dependent pathway starts with an E1 enzyme to activate ubiquitin and transfer the activated ubiquitin to an E2 ubiquitin conjugation enzyme. The E2 and target protein are bound to an E3 ubiquitin ligase and the activated ubiquitin is transferred to the target. This step can be repeated forming poly-ubiquitin chain. Once a ubiquitin chain is formed on the target protein it can be targeted to the proteasome. The proteasome will be triggered to degrade the target protein (Ciechanover, 2005; Nalepa *et al.*, 2006; Goldberg, 2007) (Figure 1.8).

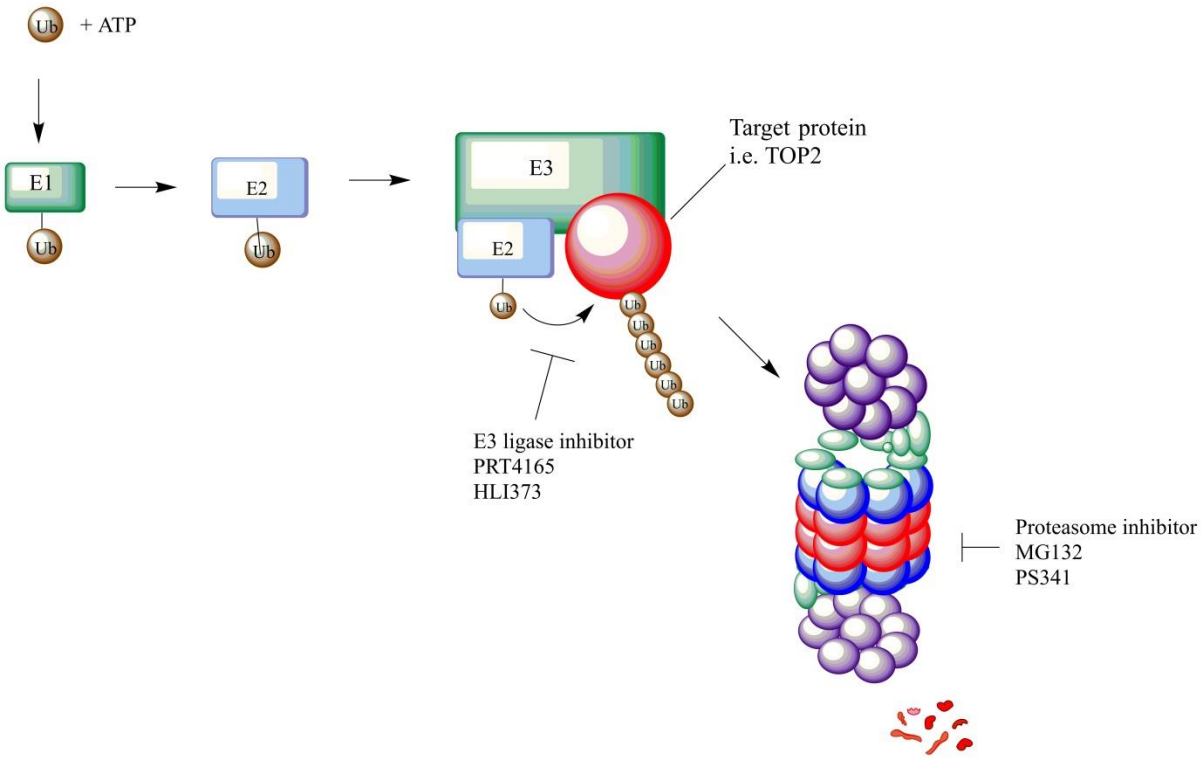

Figure 1.8 Ubiquitin-proteasome degradation pathway

Ubiquitin activated by E1-ubiqutin activation enzyme. Activated ubiquitin transfers to E2 conjugation enzyme. E3 ligase binds to target protein and E2 then E2 labels target protein with activated ubiquitin. This step will be repeated until a poly ubiquitin chain has formed and then the proteasome may degrade the target protein. Adapted with permission from Ciechanover, 2005.

Proteasomal degradation is involved in regulating cellular TOP2 levels (Salmena *et al.*, 2001). Also E3 ubiquitin ligases such as BRCA1, FBW7, MDM2, BMI1/RING1A and ECV, have been reported to be associated with TOP2A (Nayak *et al.*, 2007; Shinagawa *et al.*, 2008; Alchanati *et al.*, 2009; Yun *et al.*, 2009; Chen *et al.*, 2011).

TOP2 poisons appear to alter TOP2 protein levels in a proteasome-dependent manner (Mao *et al.*, 2001; Xiao and Goodrich, 2005; Zhang *et al.*, 2006; Nayak *et al.*, 2007; Alchanati *et al.*, 2009). To determine if proteasomal inhibition can potentiate the effect of TOP2 poisons, cells were treated with TOP2 poison alone or in combination with a proteasome inhibitor (Figure 1.8 and Figure 1.9). The effect of proteasome inhibition on growth inhibition was determined using an XTT growth inhibition assay and by RICC determination.

Two E3 ligases, Bmi1/Ring1A and HDM2, have been implicated in TOP2A degradation after exposure to TOP2 poison (Nayak *et al.*, 2007; Kitagaki *et al.*, 2008; Alchanati *et al.*, 2009; Conradt *et al.*, 2013). To determine whether E3 ubiquitin ligase inhibition can potentiate the effect of TOP2 poisons in cells, two E3 ligase inhibitors of these E3 ligases, PRT4165 and HLI373 respectively, were used in combination with TOP2 poisons to study potentiation using an XTT growth inhibition assay (Figure 1.8 and Figure 1.9).

Proteasomal inhibition and E3 ligases inhibition potentiated the growth inhibition of TOP2 poisons. The biggest effect was seen with mitoxantrone.

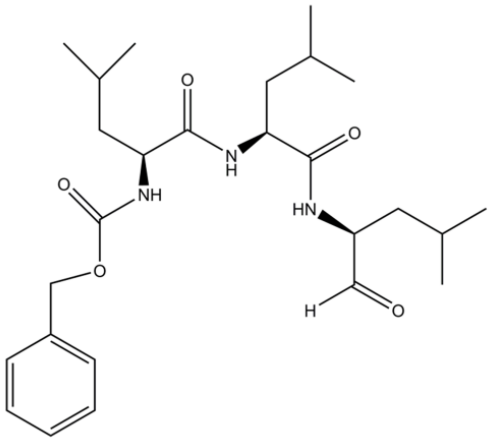

MG132

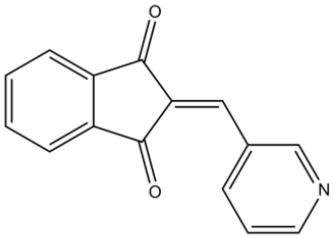

PRT4165
Bmi1/Ring1A
inhibitor

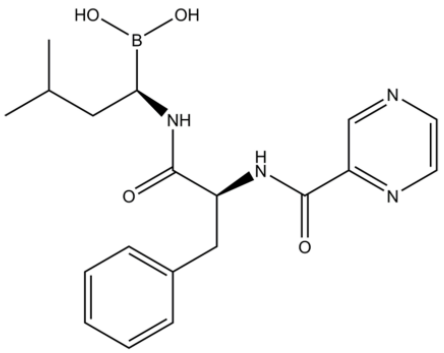

PS341

Proteasome inhibitors

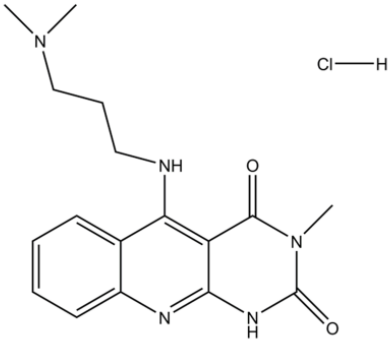

HLI373
HDM2 inhibitor

E3 ligase inhibitors

Figure 1.9 Chemical structure of proteasome inhibitors and E3 ligase inhibitors.

1.4 Genotoxicity of TOP2 poisons

TOP2 poisons are useful anti-cancer drugs. Their adverse effects include the development of secondary malignancies, such as therapy-related acute myeloid leukaemia (t-AML) (Felix, 1998; Felix, 2001). t-AML is thought to be caused by chromosome translocations, including those with the mixed lineage leukaemia (MLL) gene (Rowley and Olney, 2002). TOP2B is implicated in the generation of therapy-related malignancies, for example, etoposide (VP16) induced fewer melanomas in a skin-specific TOP2B knock-out mice than in the wild type mice (Azarova *et al.*, 2007). The absence of TOP2B reduces the levels of VP16-mediated chromosome breaks in the MLL gene (Cowell *et al.*, 2012). In this study, three Nalm-6 cells line with different levels of TOP2 (wild type, TOP2B knock-out and TOP2A knock-down) have been used to determine the role of TOP2 isoforms in growth inhibition, cytotoxicity and genotoxicity after treatment with different TOP2 poisons. Genotoxicity was determined using the *in vitro* micronucleus assay (Fenech, 2000; Fenech *et al.*, 2011). The effect of proteasome inhibitors on TOP2 poison induced genotoxicity was also determined in K562 cells using *in vitro* micronucleus assays.

1.5 Aims

TOP2 poisons are widely used in the treatment of cancers. These drugs are cytotoxic agents that act by stabilising TOP2-DNA complexes. The number of complexes and the longevity of these complexes vary depending on which drug is used. The number of stabilised complexes depends upon the rate of formation and the rate of removal of the stabilised complexes. The removal of the stabilised complexes is mediated by a range of processes, including reversal when drug is removed or repair via one of several pathways. Repair can be mediated by nucleases such as MRE11 (Lee, 2012; Lee *et al.*, 2012) or proteasomal degradation removing the drug-induced stabilised TOP2-DNA complexes. The role of the proteasome in processing of stabilised TOP2-DNA complexes is investigated and reported in this thesis. TOP2 poison induced DNA damage can lead to genotoxicity such as the formation of

micronuclei. There are two human TOP2 isoforms, TOP2A and TOP2B and it is possible they contribute differently to the formation of genotoxicity.

- To investigate the effect of proteasome inhibition on TOP2 poison-induced growth inhibition (Chapter 3).
- To study the genotoxic effects between mitoxantrone (MTX) alone and in combination with a proteasome inhibitor (Chapter 4).
- To determine the effect of E3 ligase inhibition on TOP2 poison-induced growth inhibition (Chapter 5).
- To study the role of TOP2 isoforms in TOP2 poison-induced genotoxicity (Chapter 6).

Chapter 2. Materials and Methods

2.1 Chemicals and Reagents

In this study, chemicals were obtained from Sigma-Aldrich (Gillingham, Dorset, UK) unless otherwise stated. Cell culture reagents were obtained from Invitrogen (Paisley, UK) unless otherwise stated.

2.2 Sterilisation

Glass and plastic-ware were autoclaved for 15 minutes at 134 °C for sterilisation. Solutions were autoclaved for two hours at 121 °C. Solutions were prepared using de-ionised water unless otherwise stated.

2.3 Cell lines

Four suspension human cell lines were used in this study; these were K562, Nalm-6 WT, Nalm-$6^{TOP2B-/-}$ and Nalm-$6^{TOP2A+/-}$.

The K562 cell line was derived from a patient with chronic myelogenous leukaemia (CML) in terminal blast phase and its metabolism is therefore similar to that of acute myeloid leukaemia (AML) blasts. K562 is an undifferentiated blast cell with a diameter of about 20 μm (Koeffler and Golde, 1980). The cell has a basophilic cytoplasm containing no granules and two or more prominent nucleoli. The K562 cells have an average doubling time of 24 hours.

Nalm-6 is a human pre-B cell line, and Nalm-$6^{TOP2A+/-}$ and Nalm-$6^{TOP2B-/-}$ are derivatives of Nalm-6 (Toyoda *et al.*, 2008). The Nalm-6 cell lines have an average doubling time of 24 hours.

These cell lines were maintained in Roswell Park Memorial Institute (RPMI) 1640 medium containing 10% (v/v) heat-inactivated foetal bovine serum (FBS), 50 U/ml of penicillin and 50 U/ml of streptomycin at 37 °C. Cells were sub-cultured approximately every 2 days and disposed of after 20 passages.

Liquid nitrogen stocks and defrosting cells

Exponentially growing cells were harvested and centrifuged for 3 minutes at 500 RCF. The supernatant was removed and the cell pellet was re-suspended with complete media with 10% DMSO. Re-suspended cells were in aliquots kept at -80 °C for 24 to 48 hours. Finally, the cell stocks were stored in liquid nitrogen. Cells stocks stored in liquid nitrogen remain viable for several years.

To defrost cells, cell stocks were warmed in a water bath at 37 °C and mixed with 5 ml of media. Cells were centrifuged for 3 minutes at 500 RCF. After centrifugation, the medium was removed and the cell pellet was re-suspended in 10 ml of fresh medium. Centrifugation and re-suspension was then repeated. The re-suspended cells were pipetted into a 25 cm^2 tissue culture flask (Greiner BioOne, Stonehouse, UK) and returned to the incubator. Defrosted cells were sub-cultured on the following day.

Sub-culturing Cells

Cells were sub-cultured when 70-90% confluent and transferred to 75 cm^2 or 175 cm^2 tissue culture flasks (Greiner BioOne, Stonehouse, UK). The cell number was determined and the culture diluted to 5 $x10^4$ cells/ml. Cells were incubated in a humid air atmosphere containing 5% CO_2. During sub-culture, cells were maintained between 5 x 10^4 to 1 x 10^6 cells/ml.

Determination of cell density

Cell densities were determined using a TC20 automated cell counter (Bio-Rad, USA). Ten microlitres of cell culture were transferred to a cell counting slide (Bio-Rad, USA) and inserted into the cell counter.

2.4 XTT growth inhibition assay

Exponentially growing cells were seeded into 96-well plates for 24 hours, and then drug(s) were added and incubated for 120 hours. The growth inhibition effects were quantified by using a sodium 3'-[1-(phenoaminacarbonyl)-3,4,-tetrazolium] bis(4-methoxy-6-nitro)benzene sulfonic acid hydrate (XTT) cell proliferation kit (Roche, Lewes, United Kingdom). Fifty microlitres of XTT reagent (50:1 XTT reagent to electron coupling reagent, XTT Cell Proliferation kit, Roche, UK) were added per well and cells were incubated for a further 4 hours at 37 °C.

Plates were read on a Bio-Rad iMARK plate reader (Hercules, CA) at wavelength 450 nm, and the OD_{450nm} data was analysed using GraphPad Prism software version 4.03 (GraphPad Software, USA).

The OD_{450nm} values of TOP2 poison alone were normalised to 0 nM TOP2 poison as 100%. The OD_{450nm} values of TOP2 poison in combination with proteasome inhibitor or E3 ligase inhibitor were normalised to 0 nM TOP2 poison control in the presence of proteasome inhibitor or E3 ligase inhibitor as 100%. The values of media alone were set as 0%. The normalisation method used in this study is the same as Willmore et al., 2004 (Willmore *et al.*, 2004).

The 50% inhibitory concentrations (IC_{50}) of TOP2 poison alone and the combination were determined using GraphPad Prism. The effect of the combination on TOP2 poison was determined by potentiation factor (Pf_{50}), calculated using the below equation.

$$\frac{IC_{50} of\ TOP2\ poison\ alone}{IC_{50} of\ the\ combination}$$

A Pf_{50} value greater than one means that the combination has potentiated the TOP2 poison. For example, if the Pf_{50} is two, this means that the combination requires half of the concentration of TOP2 poison to inhibit cell growth by 50%. The mean of Pf_{50} values in the results chapters represents the mean of at least three individual Pf_{50} values.

2.5 TARDIS assay—reversal of drug-stabilised TOP2-DNA complexes

Seeding and treating cells

Exponentially growing K562 cells were seeded at approximately 1 x 10^5 cells/ml in 6-well plates for 24 hours, followed by two hours of drug treatment. Cells were centrifuged at 500 RCF for three minutes. Cell pellets were washed with ice-cold phosphate-buffer saline (PBS) and centrifuged at 500 RCF for three minutes. The supernatant was removed and replaced with fresh drug-free media, then placed back in the incubator. Samples were collected at different time points after fresh drug-free medium was added.

The collected samples were centrifuged and washed with PBS, then re-suspended in 50 µl of PBS. Fifty microlitres of a 2% agarose solution was added to the 50 µl PBS cell mixture.

Embedding slides and cell lysis stage

Microscopy slides were coated with 0.5% melted agarose (Lonza, USA) and allowed to air dry. The cell cultures mentioned above were mixed with 50 µl of a 2% agarose solution and evenly spread on the 0.5% agarose. The slides with cells embedded in agarose were placed on an ice-cold surface to set. Slides were incubated in lysis buffer containing 80mM potassium phosphate pH 6.5, 1% SDS, 10mM ethylenediaminetetraacetic acid (EDTA) and protease inhibitors (1 mM benzamidine, 1 mM phenylmethanesulphonylfluoride, 2 ng/ml leupeptin and 2 ng/ml pepstatin) for 30 minutes. After lysis the slides were incubated with 1 M sodium chloride (NaCl) with PIs for 30 minutes then washed 3 times (30 seconds, 2 x 5 minutes) with PBS containing PIs.

Immunofluorescent visualisation

The slides were incubated with an appropriate primary antibody at a suitable dilution in 1% BSA-PBS-T [1% (w/v) bovine serum albumin (BSA),

PBS and 0.1% (v/v) Tween] for 1.5 hours. The slides were then washed 3 times (30 seconds, 2 x 5 minutes) with PBS including PIs and 0.1% v/v Tween. An appropriate secondary antibody, Alexa Fluor® 488 (Life technologies, USA) at a suitable dilution in 1% BSA-PBS-T, was incubated with the slides in the dark for 90 minutes, then washed twice (30 seconds and 5 minutes) with PBS including PIs and 0.1% v/v Tween, and for a further 30 minutes with PBS. From this point, slides were light sensitive, so were stored in the dark and exposure to visible light was minimised.

Slides were stained with 2 µg/ml Hoechst 33258 (Life technologies, USA) in PBS (1:5000) for 5 minutes. After draining off any surplus Hoechst solution, slides were mounted with mounting media Vectashield (without DAPI) (Vector laboratories, CA).

Slides were stored at 4 °C until visualised by microscopy. Microscopy was done within 2 days.

Microscopy and analysis

An Olympus IX81 microscope system was used with a Hamamatsu Orca-AG camera. Captured microscope images were analysed using Volocity 6.4 software (Perkin Elmer, Massachusetts, USA). Statistical analysis was carried out using GraphPad Prism software (GraphPad Software, USA). The mean integrated fluorescence signal for cells incubated with 100 µM VP16 was used as a positive control in each experiment. Immunofluorescence levels varied between experiments, so data was normalised to enable comparison between experiments.

The mean integrated fluorescence of the positive control was set as 100% and the integrated fluorescence signal from individual cells was normalised to it. The mean of normalised means with standard error from at least three individual experiments was plotted unless otherwise stated.

2.6 *In vitro* micronucleus assay—microscopy

Cells were treated for a designated length of time and the cell density for each culture was determined by using a TC20 automated cell counter (Bio-Rad, USA). Relative increase of cell count (RICC) was calculated using the equation below:

$$RICC = \frac{(Increase\ in\ number\ of\ cells\ in\ treated\ cultures(finish - starting))}{(Increase\ in\ number\ of\ cells\ in\ untreated\ control\ (finish - starting))} \times 100$$

After cell counting, a volume containing 5 x 10^5 cells was transferred to a fresh 15 ml centrifuge tube. Cells were centrifuged at 300 x *g* for 5 minutes and supernatants were aspirated. Three hundred microlitres of PBS containing 2 µg/ml ethidium monoazide bromide (EMA) was added and the pellet was re-suspended. Samples were exposed to a cool white fluorescent light source for 30 minutes on ice to allow photoactivation of EMA. As the samples were light sensitive, exposure to visible light was kept to a minimum. The samples were centrifuged at 300 x *g* for 5 minutes and the supernatant was removed. 2.5 ml media containing 10% pluronic solution (Sigma) was added to the samples. Samples were (100 µl) spread across a Polysine™ slide (VWR, UK). Slides were left to air dry in the dark.

Slides were fixed with 100% methanol for 10 minutes then stained with 2 µg/ml Hoechst 33258 (Life Technologies, USA) in PBS (1:5000) for 5 minutes. After draining off any surplus Hoechst dye, slides were mounted with Vectashield mounting media (without DAPI) (Vector Laboratories, CA). Mounted slides were examined and images were taken using an Olympus IX81 microscope system (10x objective) with a Hamamatsu Orca-AG camera within 3 days of mounting. Volocity 6.4 software (Perkin Elmer, USA) was used to analyse the microscopy images.

Microscopy slide scoring

At least 2000 cells were counted per slide. Nuclei stained with EMA (red) and Hoechst dye (blue) were excluded. The number of nuclei and micronucleated cells were recorded.

Criteria for defining micronucleated cells:

1. The size of a micronucleus should be between 1/16th and 1/3rd of diameter of the main nucleus (Figure 2.1A).
2. The micronucleus must not be connected to the main nucleus.
3. The micronucleus/micronuclei may touch but not overlap with the main nucleus. The boundaries should be distinguishable (Figure 2.1B).
4. Micronuclei are non-refractile to distinguish them from staining artefacts.
5. The intensity of micronuclei should be the same as the main nucleus but occasionally may be more intense. (Fenech, 2000)

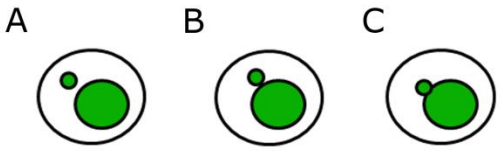

Figure 2.1 Micronucleus scoring.

(A) A micronucleated cell meeting all the criteria mentioned above. (B) Cell with micronucleus touching but not overlapping with the main nucleus. (C) Micronucleus overlapped with the main nucleus (this is not classed as a micronucleus).

Average percentage of micronuclei and the fold-increase of micronuclei were calculated using the equations shown below:

Average percentage of micronuclei

$$\frac{Number\ cells\ with\ micronuclei}{Total\ number\ of\ cells\ counted} \times 100$$

Fold increase of micronuclei:

$$\frac{Drug\ treated\ (Average\ micronuclei\ \%)}{Untreated\ control\ (Average\ micronuclei\ \%)}$$

2.7 *In vitro* micronucleus assay—Flow cytometry

Exponentially growing cells were seeded at 5 x 10^4 cells/ml (K562) or 1 x 10^5 cells/ml (Nalm-6) for 24 hours prior to drug treatment. After treatment, Relative Increase of Cell Count (RICC) was calculated using an automatic cell counter (Bio-Rad, USA). The flow cytometry method was carried out following the "basic" or "high content protocol 1" for suspension cells from the instruction manual of the *in vitro* MicroFlow kit (Litron laboratories, USA).

A consistent volume of cells from each sample was transferred to 15 ml centrifuge tubes separately. The volume used was equivalent to 1 x 10^6 cells of the negative control cultures. The samples were centrifuged at 300 x *g* for 5 minutes. The supernatant was removed carefully by aspiration without disturbing the pellet and samples were placed on ice for 20 minutes. Three hundred microlitres of nucleic acid dye A working solution, containing 1% ethidium monoazide bromide (EMA) and 2% FBS, was added to each sample tube. The samples were exposed to a cool white fluorescent light source for 30 minutes on ice, to allow photoactivation of EMA. As the samples were light sensitive, exposure to visible light was kept to a minimum. For the high content protocol, green fluorescent beads (Life Technologies, USA) were added to ice-cold 1x buffer solution (approximately 1 drop of bead suspension per 10ml). Three millilitres of the above solution was added to the samples followed by centrifugation at 300 x *g* for 5 minutes and removal of the supernatant.

Five hundred microlitres of Complete Lysis Solution 1, containing 0.4% nucleic acid dye B (SYTOX green) and 0.5% RNase solution, was added to the samples and vortexed on low speed for 5 seconds. The samples were incubated in the dark for an hour at room temperature. Five hundred microlitres of Complete Lysis Solution 2, including 0.4% SYTOX green, was added to the samples and then vortexed immediately and incubated at room temperature for 30 minutes in dark. At this stage, the samples were stored at 4 °C ready for flow cytometric analysis within 72 hours.

Before analysis, the samples were retrieved from the refrigerator to allow them to equilibrate to room temperature.

Data acquisition was carried out using a BD fluorescence-activated cell sorting (FACS) Canto™ II cytometer (BD Biosciences, New Jersey, USA) and analysed with BD FACSDiva v8.0 software (BD Biosciences, New Jersey, USA). The samples were excited with a 488 nm laser. EMA and SYTOX Green fluorescence was collected using 585/42 and 530/30 filters of the flow cytometer, respectively.

The positive methyl methanesulfonate (MMS) and negative (DMSO and H_2O) control samples were used to set up and confirm the parameter settings and gating of the system. The stopping gate was set as 30,000 nuclei counted. For each sample, 30,000 nuclei events were counted and the number of micronuclei, counting beads and EMA positive events were recorded. The ratio of Nuclei-to-Counting Beads was calculated to determine relative survival.

Data was analysed and presented as relative survival, average percentage of micronuclei, fold increase of micronuclei and fold increase of EMA events. The following equations were used.

Relative survival:

$$\frac{Ratio\ of\ drug\ treated\ sample}{Ratio\ of\ untreated\ control} \times 100$$

Average percentage of micronuclei:

$$\frac{Number\ of\ micronculei\ counted}{Number\ of\ healthy\ nuclei\ counted} \times 100$$

Fold increase of micronuclei:

$$\frac{Drug\ treated\ (Average\ micronuclei\ \%)}{Untreated\ control\ (Average\ micronuclei\ \%)}$$

Fold increase of EMA events:

$$\frac{Drug\ treated\ (\frac{Number\ of\ EMA\ events}{Number\ of\ nuclei})}{Untreated\ control\ (\frac{Number\ of\ EMA\ events}{Number\ of\ nuclei})}$$

DNA content of nuclei provides cell cycle distribution information. The data was plotted as frequency against DNA content histograms and analysed by FlowJo v8.1 software (FlowJo, Oregon, USA).

If the dose or treatment of a sample caused a relative survival lower than 40%, it was classed as a cytotoxic dose.

If a sample had more than a two-fold increase in the frequency of the micronuclei above the negative control, and the difference was statistically significant, it was classed as a genotoxic response.

MMS was included as a positive control in every experiment. This positive control should induce micronuclei more than two-fold compared to the micronuclei of negative control. If not, the results should be excluded.

The instruction manual from Litron Laboratories was utilised to determine the flow cytometry gating parameters in addition to the micronuclei scoring criteria. An example of the gating and identification of micronuclei is shown on figure 2.2 and figure 2.3.

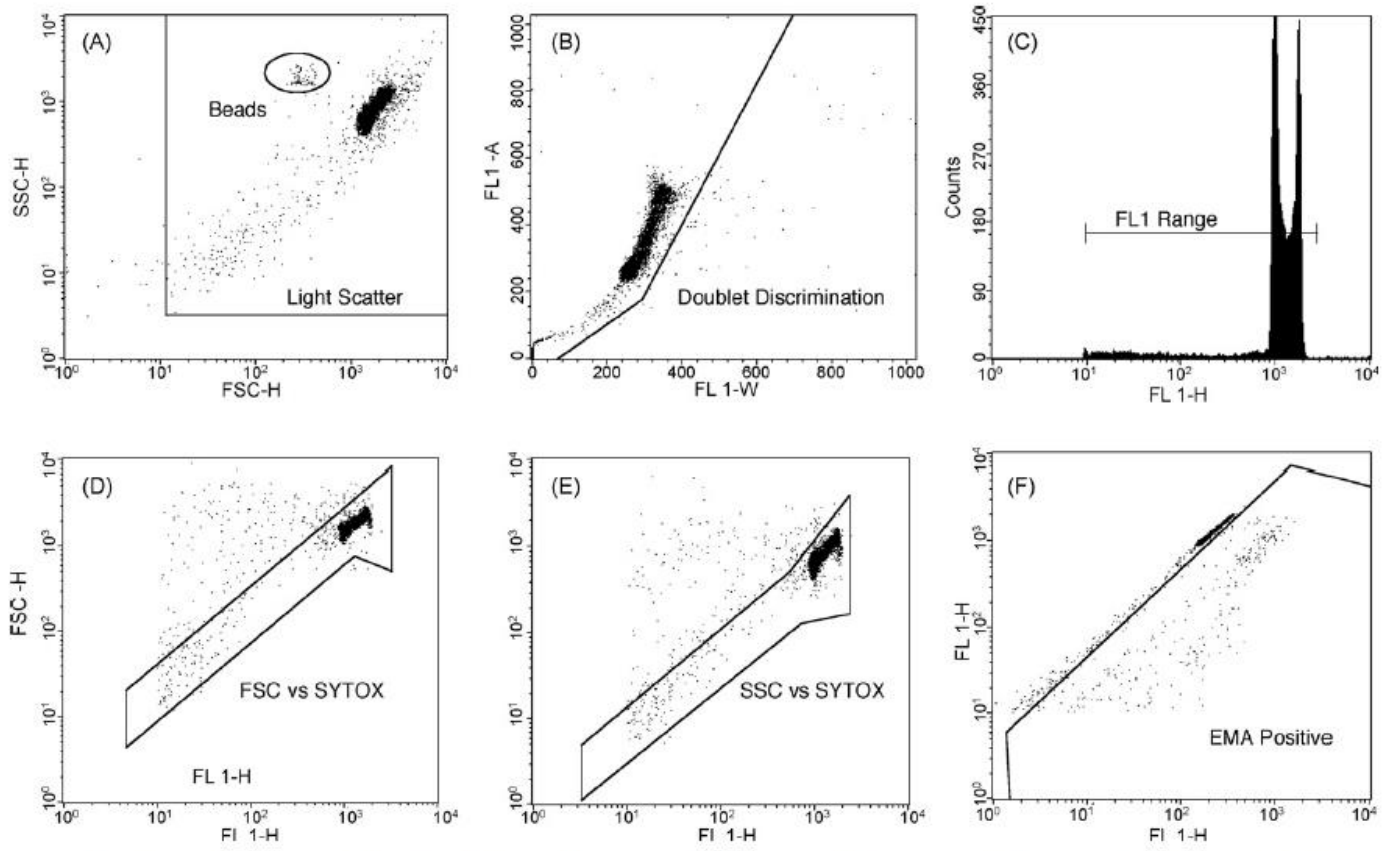

Figure 2.2 Identifying micronuclei by flow cytometry (1).

Histogram and bivariate plots of TK6 nuclei and other subcellular particles as analysed by flow cytometry. These panels illustrate the gating strategy used to discriminate nuclei and micronuclei from apoptotic chromatin as well as other spurious events. In order for events to be scored as nuclei or micronuclei, they needed to meet each of the following six criteria: within a side scatter vs. forward scatter region, panel A; within a region that excludes doublets, plot B; at least 1/100 the SYTOX-associated fluorescence as G1 nuclei, panel C; within a forward scatter vs. SYTOX fluorescence region, plot D; within a side scatter vs. SYTOX fluorescence region, plot E; ethidium monoazide-negative, panel F. Note that once the dimensions and locations of these regions were set, they were not varied within or between experiments. Adapted with permission from Bryce et al., 2007 (Bryce *et al.*, 2007).

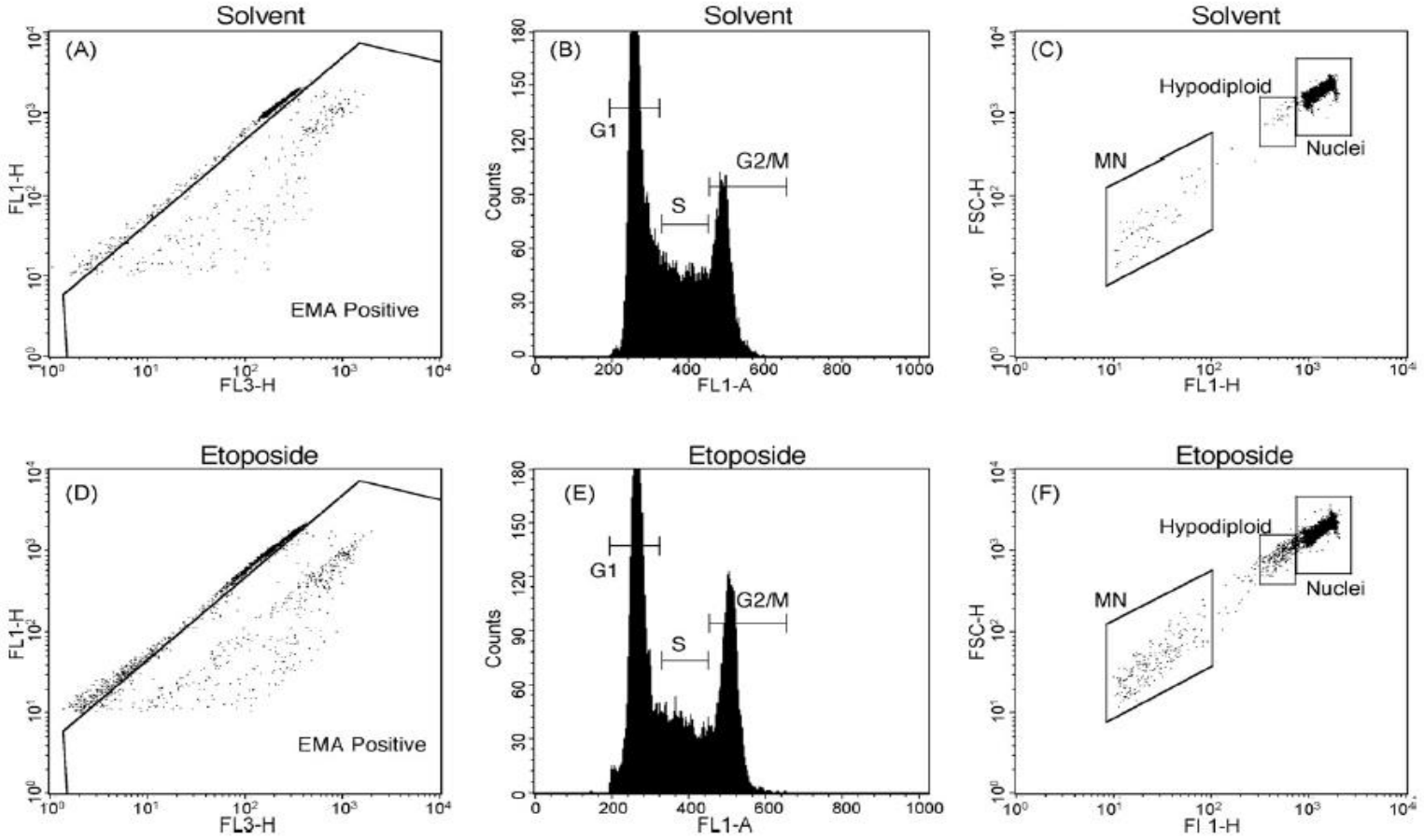

Figure 2.3 Identifying micronuclei by flow cytometry (2).

(Panels A and D) These bivariate plots were used to quantify the percentage of EMA-positive events. Only events that fell within the side scatter vs. forward scatter region (Figure 2.2A) and a region that excludes doublets (Figure 2.2B) were plotted and used in the %EMA-positive calculation. (Panels B and E) These SYTOX fluorescence histograms were used to quantitatively evaluate cell cycle distribution. These gated events had to exhibit light scatter and fluorescence characteristics of healthy nuclei as illustrated by Figure 2.2. (Panel C and F) These bivariate plots were used to quantify the incidence of nuclei, hypodiploid nuclei, and micronuclei (MN). These gated events had to exhibit light scatter and fluorescence characteristics of healthy cells as illustrated by Figure 2.2. Adapted with permission from Bryce et al., 2007 (Bryce *et al.*, 2007).

Chapter 3. Proteasomal inhibition potentiates growth inhibition by TOP2 targeting drugs

3.1 Introduction

Topoisomerase II (TOP2) is an important cellular enzyme during replication, transcription, chromosome condensation and segregation. The catalytic cycle of TOP2 involves cleaving and re-ligating double stranded DNA. A group of chemotherapy agents called "TOP2 poisons" target this cycle to stabilise TOP2 while it is covalently bound to the DNA double strand break (DSB). This stabilised cleavable complex is the primary damage within the cell. Repair of this damage may lead to genotoxicity, resulting in secondary cancer (Cowell *et al.*, 2012).

The stabilised TOP2 needs to be removed before DNA double-strand break (DSB) repair can occur by NHEJ. DSBs with stabilised TOP2 do not activate DNA-PK *in vitro* (Martensson *et al.*, 2003) and a number of lines of evidence suggest cellular processing is required to remove stabilised TOP2 prior to triggering a DNA damage response.

A number of potential mechanisms exist to remove stabilised TOP2 complexes. One mechanism involves a multi-step process that starts with proteasome degradation to break down the poisoned TOP2, leaving a peptide fragment on the 5' end of the DNA double strand break. Then TDP2 removes the 5'- adduct to allow the DSB to be repaired (Cortes Ledesma *et al.*, 2009; Zeng *et al.*, 2011; Gao *et al.*, 2012; Schellenberg *et al.*, 2012; Shi *et al.*, 2012; Gao *et al.*, 2014a; Gao *et al.*, 2014b; Pommier *et al.*, 2014).

To address the question of whether proteasomal inhibition increase (potentiates) the growth inhibition of TOP2 poisons, the XTT assay was used. The XTT assay is a growth inhibition assay widely used in drug testing. Sodium 3'-[1-(phenoaminacarbonyl)-3,4,-tetrazolium] bis(4-methoxy-6-nitro)benzene sulfonic acid hydrate (XTT) is a yellow tetrazolium salt. This is cleaved by metabolically active cells to form an

orange formazan dye. Importantly, the formazan dye formed is soluble in aqueous solutions. The intensity of this dye can be measured by a microplate reader and the optical density indirectly represents the number of viable cells.

In order to determine whether proteasomal inhibition alters the kinetics of formation and removal of covalent TOP2-DNA complexes, the Trapped in Agarose DNA immunostaining (TARDIS) assay was used to measure the removal rate of drug-induced DNA-TOP2 complexes in K562 cells with or without MG132 proteasome inhibitor.

3.2 Growth curve of K562 cells (XTT assay to determine optimal cell density for potentiation experiments)

The K562 cell line was used to study the effect of proteasome inhibitors on the growth inhibitory effects of TOP2 poisons. Cell growth and growth inhibition of K562 cells were determined by XTT assay.

To determine an optimal cell density for the potentiation study, K562 cells were seeded at a range of cell densities in 96-well plates and incubated for up to 144 hours (6 days). 96-well plates were stained and read every 24 hours after seeding. After seeding, K562 cells grew exponentially from one to five days. As shown in figure 3.1, cells seeded at approximately 2 x 10^3 cells per well demonstrated exponential growth over days 1-5 with the absorbance remaining fairly constant at day 6 (144 hours). A cell density of 2 x 10^3 cells per well was used in all XTT potentiation studies including 120 hours incubation for the K562 cell line.

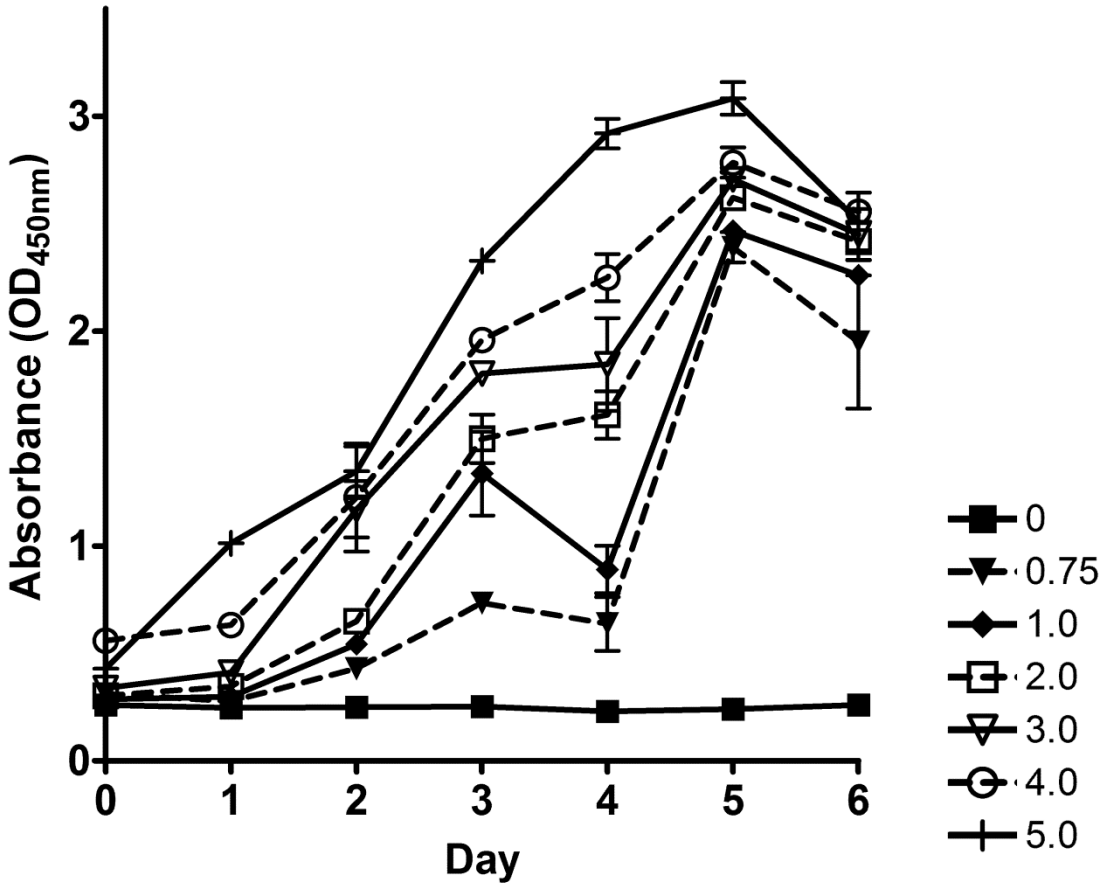

Figure 3.1 Growth curve of K562 cell line.

K562 cells were seeded at approximately 0, 0.75, 1, 2, 3, 4 and 5 x10^3 cells/well in 96-well plates. Plates were stained with XTT and the OD_{450nm} was determined every 24 hours after seeding up to 6 days (144 hours).

3.3 Proteasome inhibition and the effect of MTX on K562 cell line

Proteasome inhibitor MG132 effects on growth inhibition

MG132 is a low molecular weight proteasome inhibitor. It can enter cells and selectively inhibit protein degradation (Lee and Goldberg, 1998).

MG132 dose-response for growth inhibition in K562 cells was determined by XTT assay. K562 cells were seeded for 24 hours followed by 120 hour exposure to a range of concentrations of MG132 (0 -200 nM). Absorbance of non-treated cells was set as 100% and all the readings were normalised to it.

Willmore *et al.* demonstrated that a low level of DNA-PK inhibitor potentiates the cytotoxicity of TOP2 poisons (20% growth inhibition)

(Willmore *et al.*, 2004). Based on the above experimental setup, the results showed that 95 nM MG132 inhibited cell growth by 20% (figure 3.2). This concentration was used in combination with TOP2 poisons to study potentiation.

Proteasomal inhibition potentiates MTX

Mitoxantrone (MTX) is an anthracenedione TOP2 poison which is commonly used to treat breast cancer, prostate cancer, lymphoma and leukaemia. K562 cells were seeded at 2 x 10^3 cells per well in 96-well plates for 24 hours, then treated with a range of concentrations of MTX alone or in the presence of a fixed concentration of 95 nM MG132 for 120 hours. After drug treatment, growth inhibition was detected by XTT assay. The OD_{450nm} values of MTX alone were normalised to 0 nM MTX as 100%, and OD_{450nm} values of MTX in combination with MG132 were normalised to 0 nM MTX control in the presence of 95 nM MG132 as 100%.

IC_{50} refers to the dose which exhibited 50% growth inhibition. The difference between the IC_{50} of MTX alone and the IC_{50} in the presence of MG132 was determined by unpaired *t*-test. The potentiation of MTX by MG132 was presented as potentiation factors (Pf_{50}). It was calculated using the IC_{50} value of MTX alone over the IC_{50} value of MTX in combination with MG132.

Figure 3.3 shows K562 cell growth inhibition by MTX. When combined with MG132 cell growth inhibition was increased. The potentiation factor (Pf_{50}) of MTX and MG132 was 4.58 (Table 3.1). The IC_{50} of MTX alone and in the presence of MG132 was statistically significant ($p \leq 0.0001$). This suggests inhibition of the proteasome potentiates the growth inhibition effects of MTX.

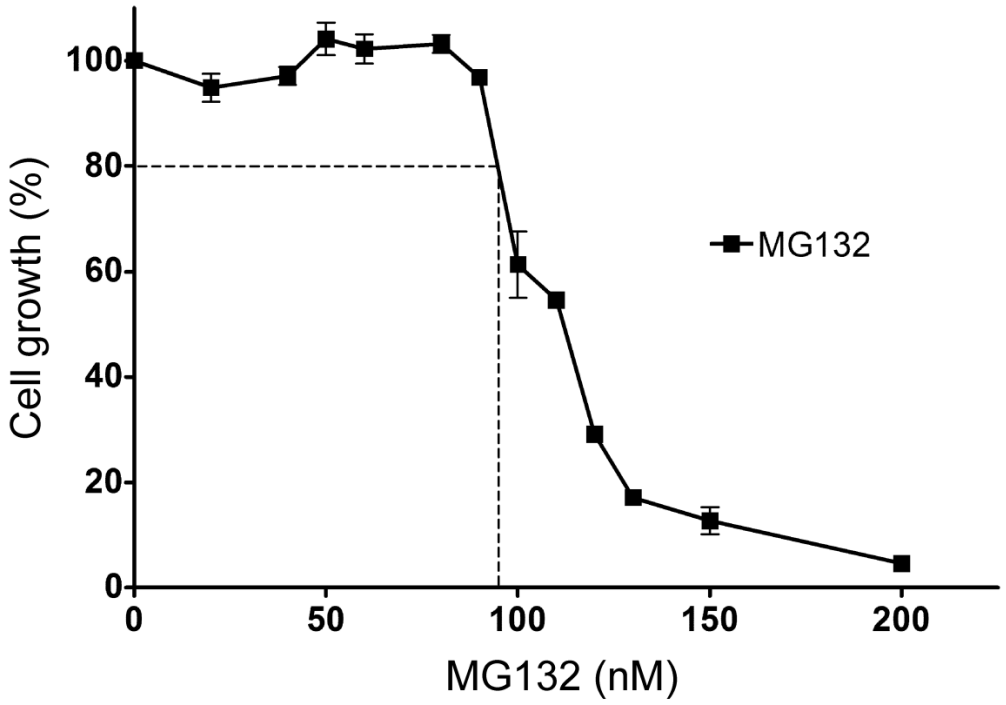

Figure 3.2 Growth inhibition curve of proteasome inhibitor MG132 in K562 cells.

K562 cells were seeded at approximately $2x10^3$ cells/well in 96-well plates for 24 hours prior to MG132 drug treatment. After 120 hours of drug exposure, cells were stained with XTT and OD_{450nm} was quantified. Results are means of four experiments ± standard error of the mean.

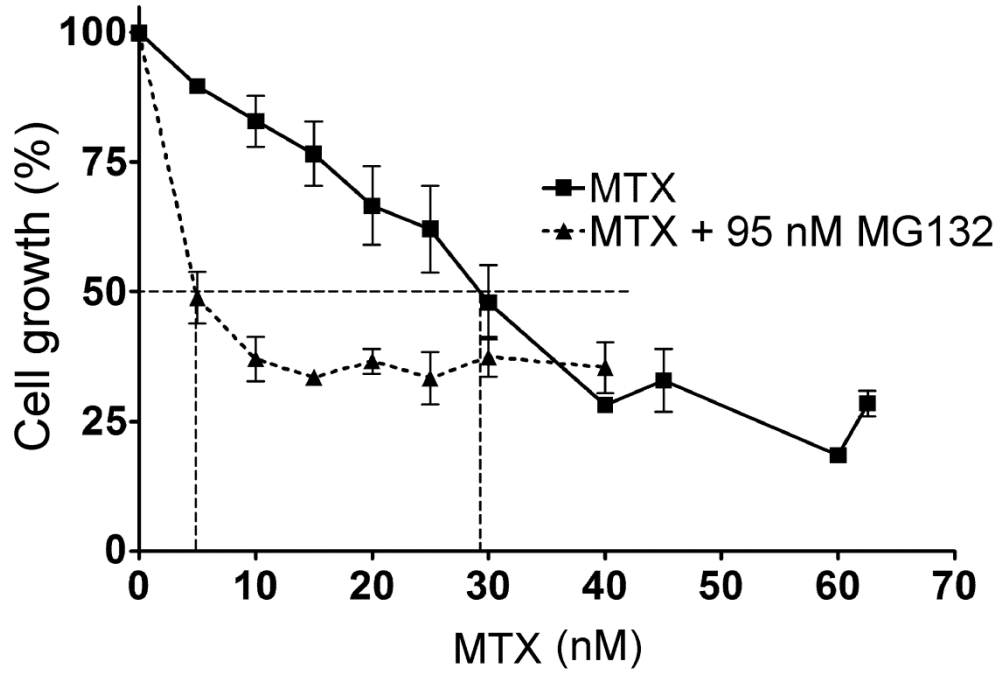

Figure 3.3 Potentiation of MTX by MG132 in K562 cells.

Cells were treated with increasing concentrations of MTX alone or in combination with 95 nM MG132 for 5 days followed by XTT staining. Dose–response curves were used to estimate the IC_{50} of MTX alone or in combination with MG132. Error bars represent the mean ± SEM of at least 3 separate experiments for both + and - MG132 conditions. Values were normalised to the 0 nM MTX value (100%).

Proteasome inhibitor PS341 (bortezomib, Velcade) effects on growth inhibition

PS341 (bortezomib, Velcade) is a proteasome inhibitor used successfully in the treatment for multiple myeloma. The dose response curve of PS341 in K562 cells was determined by XTT assay. K562 cells were seeded at 2 x 10^3 cells per well for 24 hours prior to the exposure to a range of concentrations of PS341. The absorbance of untreated cells was set as 100% and all the readings were normalised to it.

The dose demonstrating 20% growth inhibition was 5.2 nM and this dose was used in the potentiation assay (Figure 3.4).

PS341 potentiates the growth inhibitory effects of MTX

K562 cells were treated with MTX alone or in the presence of 5.2 nM PS341. After 120 hours of incubation, XTT assays were used to determine growth inhibition. The OD_{450nm} values were normalised as described for the combination with MG132. Potentiation was presented as Pf_{50} and statistical significance determined by unpaired *t*-test. The presence of 5.2 nM PS341 significantly potentiated MTX (Pf_{50}=2.95) (Figure 3.5 and Table 3.1). The results show the proteasome inhibitor currently used in treatment can potentiate the growth inhibitory effect of MTX.

Mitoxantrone +	Mean of Pf_{50}	SEM	*p*-value
MG132	4.58	0.54	<0.0001
PS341	2.95	0.11	0.002

Table 3.1 Potentiation factor (Pf_{50}) summary of mitoxantrone (MTX) in combination with proteasome inhibitors.

Statistical significance between IC_{50} values of MTX alone and in combination with proteasome inhibitors by unpaired *t*-test (*p*-value).

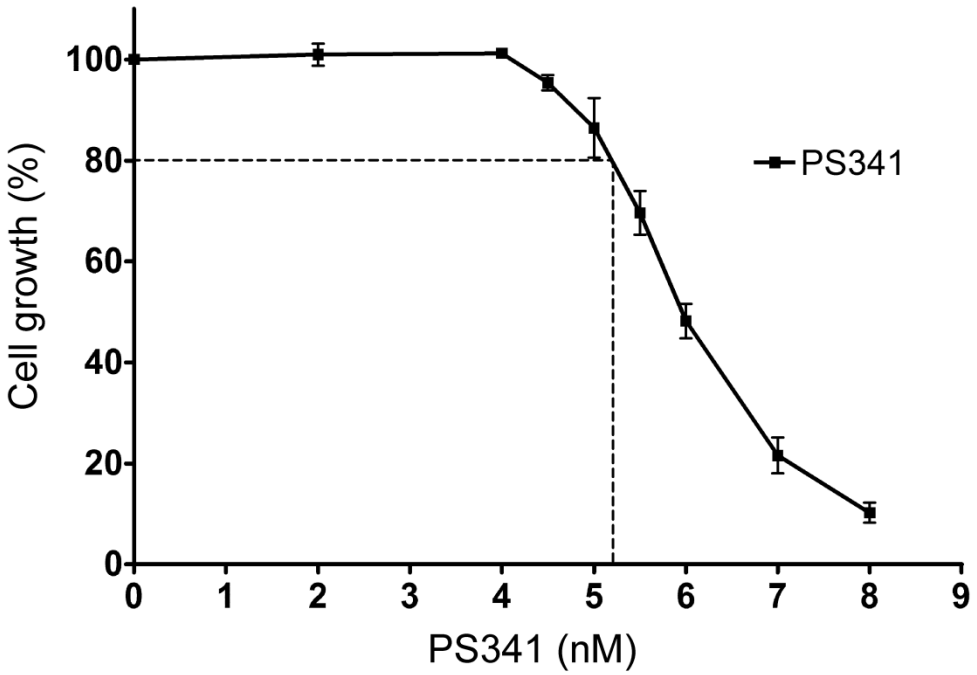

Figure 3.4 Growth inhibition curve of proteasome inhibitor PS341 in K562 cells.

K562 cells were seeded at approximately $2x10^3$ cells/well in 96-well plate for 24 hours prior to PS341 drug treatment. After 120 hours of drug exposure, cells were stained with XTT and OD_{450nm} was quantified. Results are means of four experiments ± standard error of the mean.

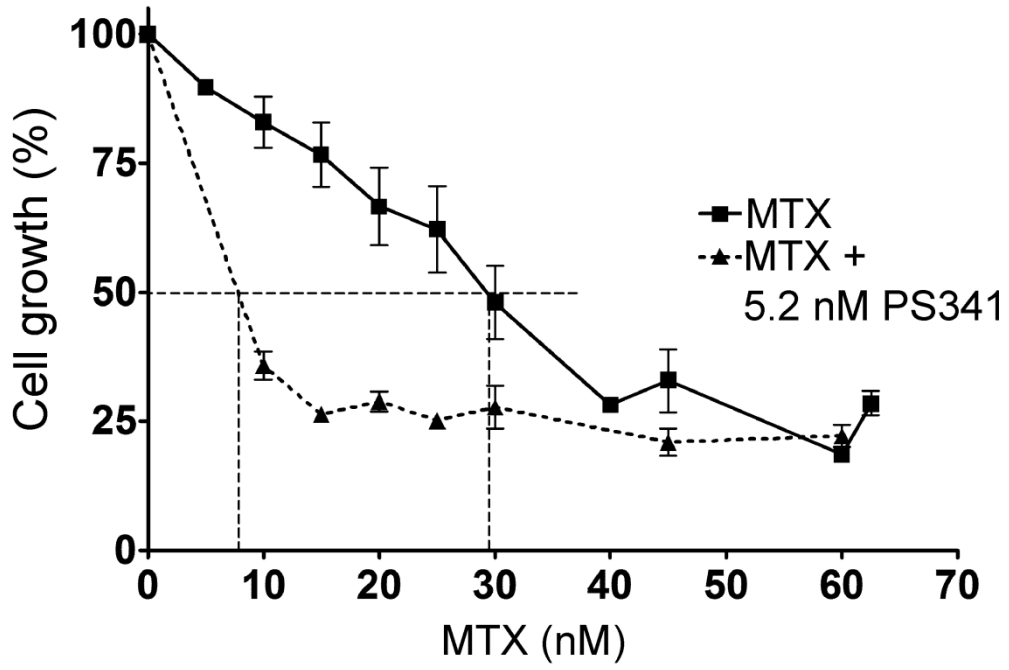

Figure 3.5 Potentiation of MTX by PS341 in K562 cells.

Cells were treated with increasing concentrations of MTX alone or in combination with 5.2 nM PS341 for 5 days followed by XTT staining. Dose–response curves were used to estimate the IC_{50} of MTX alone or in combination with PS341. Error bars represent the mean ± SEM of at least 3 separate experiments for both + and – PS341 conditions, values were normalised to the 0 nM MTX value (100%).

Investigating the effect of proteasome inhibition on the stability of MTX-induced TOP2-DNA complexes

MTX is a TOP2 poison. It stabilises TOP2-DNA complexes formed with both TOP2 isoforms in the cell. Drug-stabilised TOP2 complexes are reversible upon removal of the TOP2 poison as seen in TARDIS reversal assays (Errington *et al.*, 2004). The rate of reversal differs, depending on the drug used.

The effect of proteasome inhibition on MTX-induced TOP2 complex stability was determined using the Trapped in Agarose DNA immunostaining (TARDIS) assay, which involves embedding cells in agarose on microscopy slides followed by sodium dodecyl sulphate (SDS) and salt extraction to remove cellular components. Immunofluorescent staining with a specific primary antibody and FITC labelled secondary antibody is then used to detect covalent DNA-TOP2 adducts on the genomic DNA on the slide. FITC fluorescence of TOP2 complexes is then quantified and represents the TOP2 complex levels in individual cells (Cowell *et al.*, 2011).

K562 cells were seeded at approximately 1 x 10^5 cells per ml for 24 hours, followed by a 2 hour exposure to either 5 μM MTX alone or in combination with 50 μM MG132. Cells were then washed and placed in fresh media. For both the MG132-treated control and the combination cells, 50 μM MG132 was added back into the media. Cells were reincubated and samples were taken at 0, 1, 3, 6 (and 24, TOP2A only) hours later. Cells were processed on TARDIS microscopy slides with lysis and probed with TOP2A or TOP2B-specific antibodies. TOP2-DNA complex levels were determined by quantifying the intensity of integrated fluorescence (FITC). The mean FITC values of 5 μM MTX treated cells were set as 100% and all of the single cell values were normalised to this. The unpaired *t*-test was used to calculate the differences between cells treated with MTX alone and cells treated with MTX and MG132. Trypan blue exclusion was performed at 0 and 6 hours after drug treatment, which confirmed no major cell viability decrease within the duration of the experiment (Figure 3.6 C).

The results confirm that MTX alone induces TOP2-DNA complexes significantly above untreated control. The TOP2-DNA complex levels in MG132 treated cells were similar to untreated cells; MG132 alone did not stabilise TOP2-DNA complexes in K562 cells. This confirmed that the induction of TOP2-DNA complexes was specific to MTX. TOP2-DNA complex levels in MTX treated cells reduced with time after drug wash out. TOP2A-DNA complex levels reduced more slowly than TOP2B complexes. About 75% of TOP2A-DNA complexes remained 6 hours after drug wash-out, and reduced further to 30% after 24 hours. TOP2B-DNA complexes were significantly reduced within 6 hours. The half-life of TOP2A- and TOP2B- DNA complexes were estimated to be between 6 and 24 hours and 3 hours, respectively (Figure 3.6A and B).

The presence of MG132 slowed down the complex removal for both isoforms. For TOP2A, the complex levels remained at or above 100% 24 hours after drug wash-out, which was significantly higher than MTX alone at 24 hours (Figure 3.6A). Similarly, TOP2B complex levels showed a significant difference with and without MG132 at 3 and 6 hours. At one hour and six hours after drug wash out, 60% and 40% of TOP2B-DNA complexes remained in MTX alone treated cells, respectively. In the presence of MG132, TOP2B-DNA complex levels were 122% after a two-hour drug treatment and 118% remained at six hours after drug wash-out.

MTX induced TOP2-DNA complexes with both isoforms and the reversal times were different. This is analogous to Errington et al., 2004, who measured the stability of MTX induced TOP2-DNA complexes of both isoforms in mouse embryonic fibroblasts (MEF). After removal of MTX, TOP2-DNA complex levels were reduced and this decline was slower for TOP2A than TOP2B. Half-lives of the TOP2-DNA complexes were about 12 and 6 hours for TOP2A and TOP2B, respectively (Errington *et al.*, 2004). These results suggest that proteasomal inhibition could prolong the stability of TOP2 complexes in the cell. This might be related to the potentiation of MTX with proteasome inhibitors.

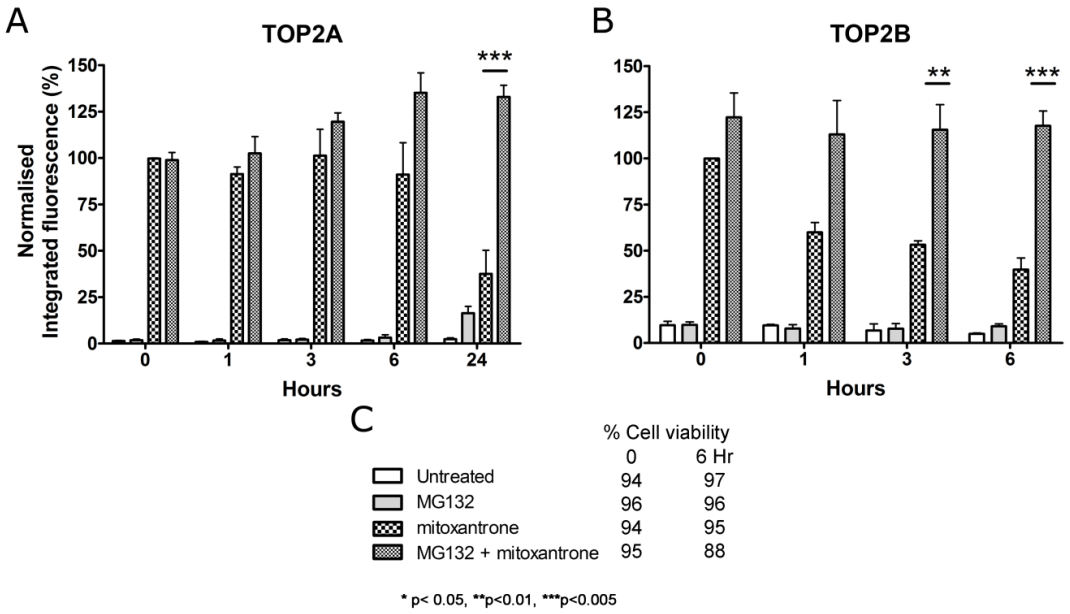

Figure 3.6 MG132 inhibits the reversal of MTX-induced TOP2A- and TOP2B-DNA complexes.

(A) and (B) K562 cells were incubated with solvent, MTX (5 μM), MG132 (50 μM) or were co-incubated with 50 μM MG132 and 5 μM MTX for 2 h. After 2 h MTX was removed, but MG132 was maintained in cell incubations that initially contained it. Levels of TOP2A and TOP2B DNA complexes at 0, 1, 3, 6 h after MTX removal (wash-out) were determined using the TARDIS assay, with an additional time point of 24 h for TOP2A. Statistical comparisons were made between the levels of TOP2-DNA complexes in the presence or absence of MG132 by unpaired *t*-test. (C) cell viability (trypan blue exclusion) under the cell treatment conditions used: ‘‘0” refers to the time at which MTX wash-out was performed and ‘‘6 h” refers to time post drug wash-out.

3.4 Proteasome inhibition and the effect of epipodophyllotoxins in the K562 cell line

Proteasomal inhibition potentiates etoposide and teniposide

VP16 and teniposide (VM26) are epipodophyllotoxins. These compounds are used in the treatment of non-Hodgkins lymphoma, leukaemia and lung cancer.

K562 cells were treated with epipodophyllotoxin alone or in combination with 95 nM MG132. Potentiation effects were detected by XTT assay after 120 hours incubation. The OD_{450nm} values for epipodophyllotoxin alone were normalised to 0 nM epipodophyllotoxin as 100%, and OD_{450nm} values of epipodophyllotoxin in combination with MG132 were normalised to 0 nM epipodophyllotoxin control in the presence of 95 nM MG132 as 100%.

The potentiation effect is presented as Pf_{50}. VP16 and VM26 significantly inhibited K562 cell growth. In combination with MG132, IC_{50} values of both drugs were reduced. Pf_{50} values for VP16 and VM26 were 1.65 and 2.62, respectively (Figure 3.7). The results suggest that the proteasome inhibitor MG132 potentiated the inhibitory effect of VP16 and VM26 on cell growth. The level of potentiation was higher with VM26.

PS341 potentiates the growth inhibitory effects of VP16 and VM26

The same potentiation assay setup and analysis which was used in the MG132 experiment was used here. The IC_{50} values of VP16 and VM26 were both reduced in the presence of PS341. The mean IC_{50} values of VM26 alone was around 60 nM, however, in the presence of PS341 it fell to around 22 nM ($p<0.0001$). The level of potentiation was greater with VM26 ($Pf_{50}=2.71$) than with VP16 ($Pf_{50}=1.24$) (Figure 3.8). The results show that proteasome inhibition by either MG132 or PS341 potentiates the effect of epipodophyllotoxins.

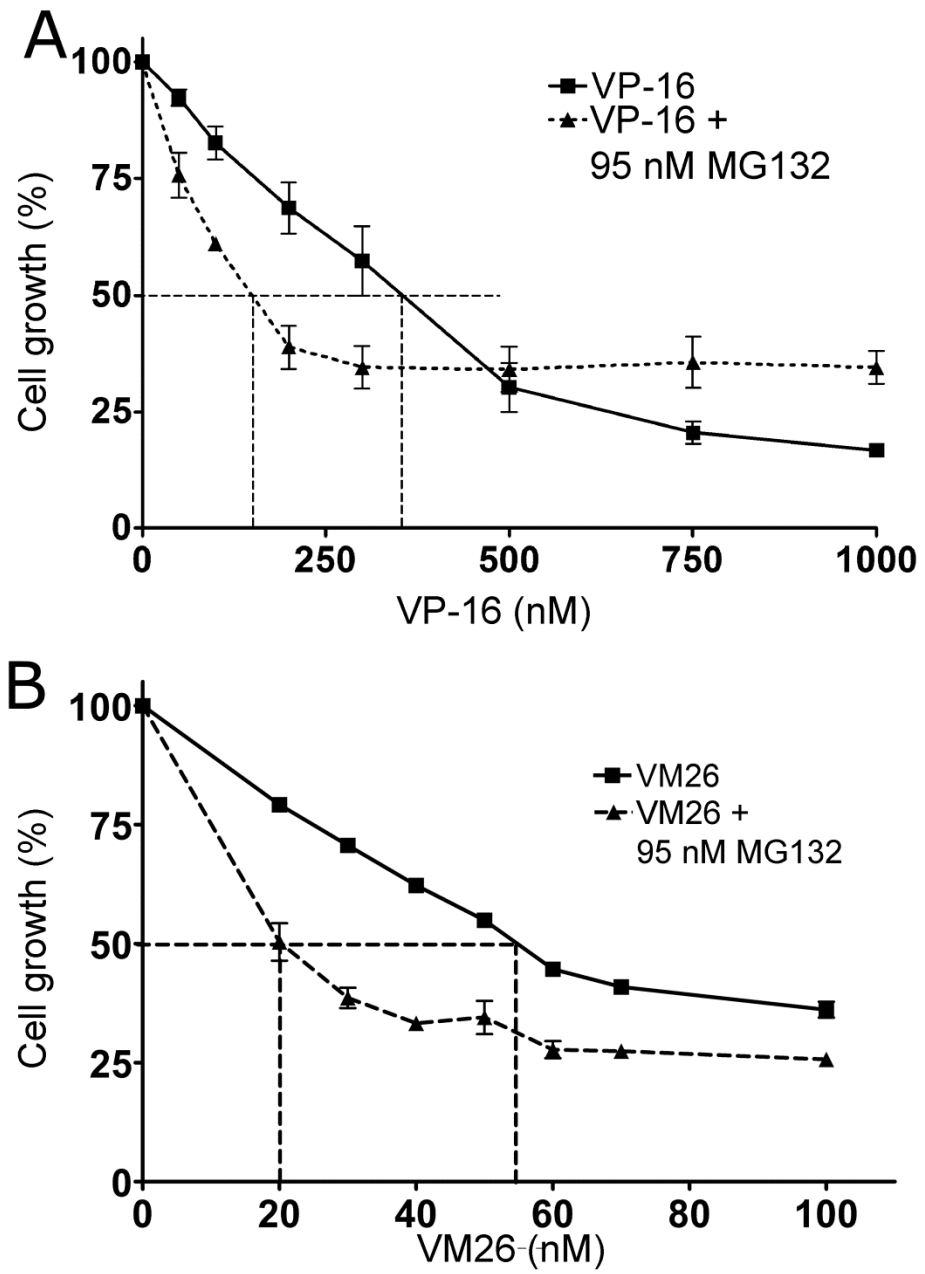

Figure 3.7 Potentiation of VP16 or VM26 by MG132 in K562 cells.

Cells were treated with increasing concentrations of VP16 (A) or teniposide (VM-26) (B) alone or in combination with 95 nM MG132 for 5 days followed by XTT staining. Dose–response curves were used to estimate the IC_{50} of epipodophyllotoxin alone or in combination with MG132. Error bars represent the mean ± SEM of at least 3 separate experiments for both + and - MG132 conditions, values were normalised to the 0 nM epipodophyllotoxin value (100%).

Etoposide +	Mean of Pf_{50}	SEM	*p*-value
MG132	1.65	0.25	0.0261
PS341	1.24	0.32	0.769

Table 3.2 Potentiation factor (Pf_{50}) summary of etoposide (VP16) in combination with proteasome inhibitors.

Statistical significance between IC_{50} values of VP16 alone and in combination with proteasome inhibitors by unpaired *t*-test (*p*-value).

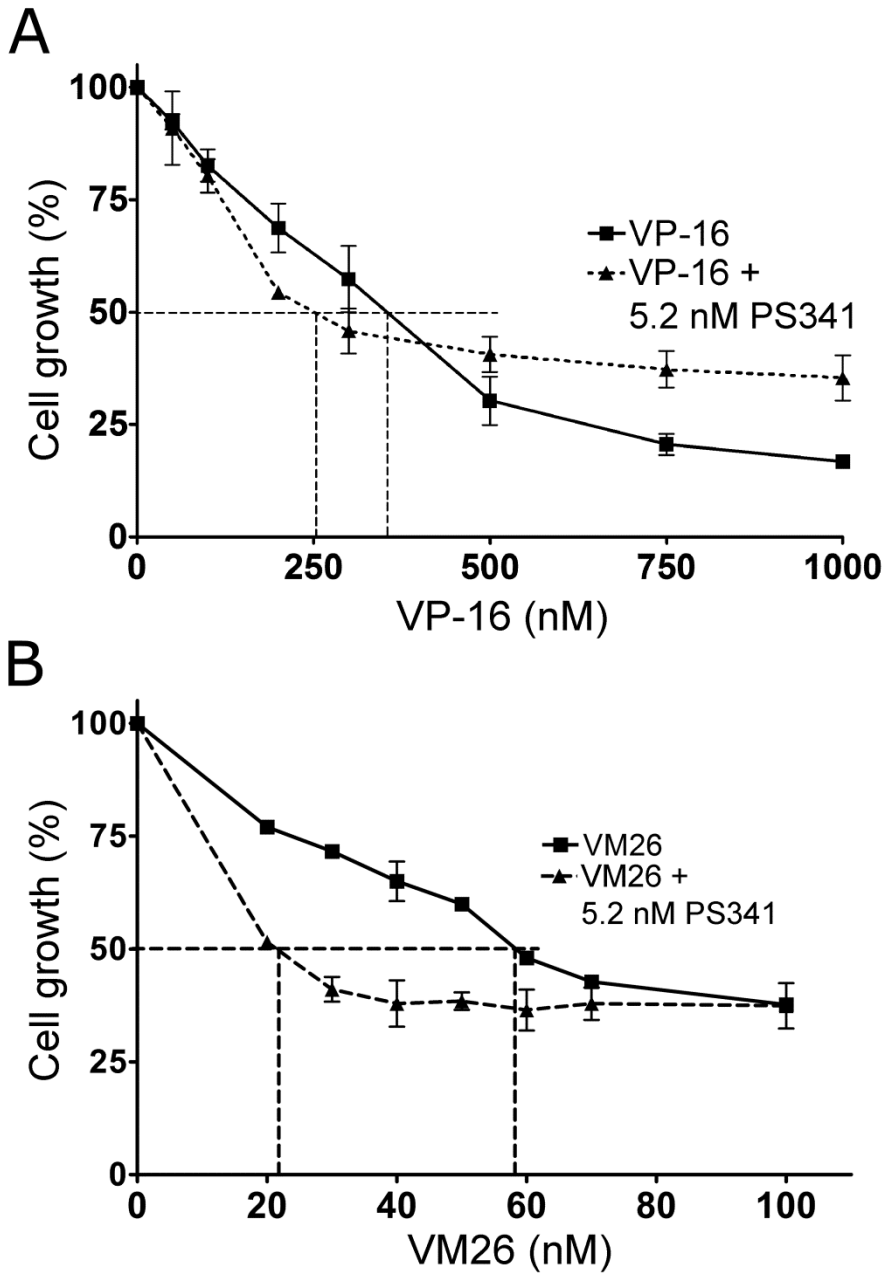

Figure 3.8 Potentiation of VP16 or VM26 by PS341 in K562 cells.

Cells were treated with increasing concentrations of VP16 (A) or VM26 (B) alone/ or in combination with 5.2 nM PS341 for 5 days followed by XTT staining. Dose–response curves were used to estimate the IC_{50} of epipodophyllotoxin alone or in combination with PS341. Error bars represent the mean ± SEM of at least 3 separate experiments for both + and – PS341 conditions. Values were normalised to the 0 nM epipodophyllotoxin value (100%).

Teniposide +	Mean of Pf_{50}	SEM	*p*-value
MG132	2.62	0.15	<0.0001
PS341	2.71	0.04	<0.0001

Table 3.3 Potentiation factor (Pf_{50}) summary of teniposide (VM26) in combination with proteasome inhibitors.

Statistical significance between IC_{50} values of VM26 alone and in combination with proteasome inhibitors by unpaired *t*-test (*p*-value).

Proteasome inhibition prolonged the half-life of VP16 induced TOP2-DNA complexes

VP16 is a TOP2 poison targeting both TOP2 isoforms to induce stabilised TOP2-DNA complexes. Errington et al,. 2004 have previously shown that VP16 stabilised TOP2-DNA complexes dissociate shortly after drug removal (Errington *et al.*, 2004). TOP2-DNA complexes are covalently bound to DNA therefore the levels of complex formation and dissociation can be observed by TARDIS.

K562 cells were seeded at approximately 1 x 10^5 cells per ml in a 6-well plate for 24 hours, and then treated with either 100 μM VP16 alone or in combination with 50 μM MG132. After a two-hour treatment, the media containing drugs was removed and replaced with fresh media. For the combination experiment, 50 μM MG132 was retained in the media. Cells were incubated for another two hours in fresh media. Samples were taken at 0, 15, 30, 60, and 120 minutes after drug removal for the TARDIS assay. TARDIS slides were probed with TOP2A (4566) or TOP2B (4555) specific antibodies for the study of TOP2-DNA complex levels. Integrated FITC readings for 100 μM VP16 treated cells were set as 100% and all the cells were normalised to this value.

The level of TOP2-DNA complexes was significantly higher in cells exposed to VP16 compared with untreated cells after exposure to VP16. In cells exposed to MG132 alone, TOP2-DNA complex levels remained at background level (no difference from untreated cells) at all time points tested, showing that MG132 does not induce a significant amount of TOP2-DNA complexes within the length of exposure time tested. Levels of both TOP2A- and TOP2B-DNA complexes were reduced after VP16 removal. After 120 minutes, TOP2-DNA complexes were reduced to the levels seen in the untreated controls.

The half-lives of TOP2A- and TOP2B-DNA complexes were about 30 and 15 minutes, respectively. In the presence of MG132, TOP2A-DNA complex levels remained elevated. 77% remained 30 minutes after drug removal,

and 54% remained 60 minutes after drug wash-out. In the presence of MG132, higher levels of TOP2B-DNA complexes (153%) were induced and the reversal of TOP2B-DNA complexes were slower than VP16 alone. After 15 minutes of drug wash-out, TOP2B-DNA complex levels in the absence and presence of MG132 were 20% and 86%, respectively. In the presence of MG132, the complex reversal rates were significantly prolonged (Figure 3.9A and B). These data are reported in Lee et al. 2016 (Lee *et al.*, 2016).

Trypan blue exclusion was used to determine cell viability throughout the VP16 exposure and drug free incubation. Cell viability was above 90% for all treatments and time points. This suggests a 2-hour exposure to 100 μM VP16 plus a 2-hour of recovery incubation did not increase membrane permeability of cells (Figure 3.9C).

The half-lives of VP16-induced TOP2A- and TOP2B- complexes are 30 and 15 minutes, respectively (Lee *et al.*, 2016). In the presence of MG132 and VP16, TOP2B complex levels were higher than seen with VP16 alone. The presence of MG132 slowed the TOP2A and B complex reversal rate in K562.

Cytotoxicity and cell cycle analysis of VP16 and MG132 in K562

Following drug wash out, VP16-stabilised TOP2-DNA complexes reversed in cells. This finding is in line with Errington et al., 2004 who reported that stabilised TOP2A- and TOP2B-DNA complexes in VP16-treated MEF cells dissociated after the VP16 was washed out. The half-life of TOP2A- and TOP2B-DNA complexes were approximately 40 and 20 minutes, respectively (Errington *et al.*, 2004). Proteasome inhibition significantly slowed down VP16-induced TOP2-DNA complex reversal rate (Figure 3.9 A and B). Trypan blue exclusion and flow cytometry data show that this observation was not due to a drop in cell viability or disturbed cell cycle distribution (Figure 3.9C and Figure 3.10).

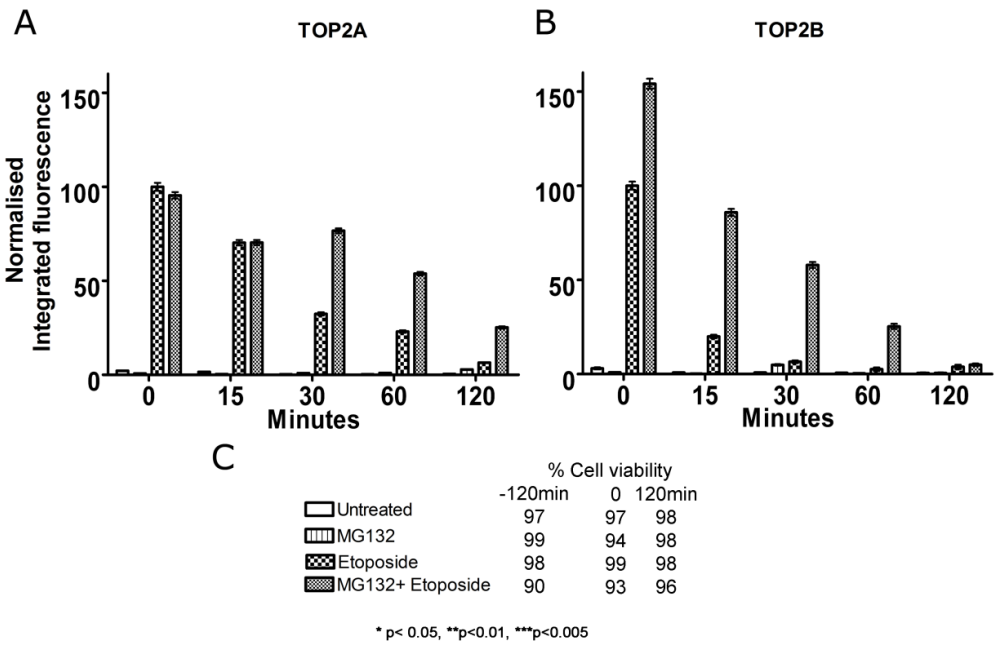

Figure 3.9 MG132 slows the reversal of VP16-induced TOP2A- and TOP2B-DNA complexes.

K562 cells were incubated with solvent, VP16 (100 μM), MG132 (50 μM) or were co-incubated with 50 μM MG132 and 100 μM VP16 for 2 h. After 2 h VP16 was removed, but MG132 was maintained in cell incubations that initially contained MG132. Levels of TOP2A (A) and TOP2B (B) DNA complexes at 0, 15, 30, 60 and 120 min after VP16 removal (wash-out) were determined using the TARDIS assay. Statistical comparisons were made between the levels of TOP2-DNA complexes in the presence or absence of MG132 by unpaired t-test. (C) cell viability (trypan blue exclusion) under the cell treatment conditions used: ''-120 min" refers to the time at which drugs were first added to cells, ''0" refers to the time at which VP16 wash-out was performed and ''120 min" refers to 2 h post drug wash-out.

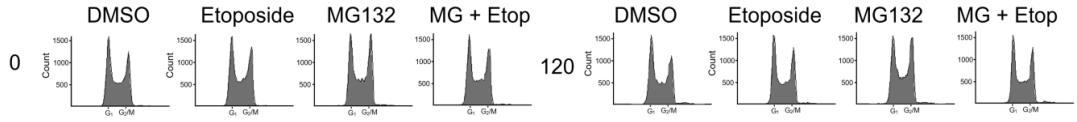

Figure 3.10 Cell cycle distribution at time of VP16 wash-out.

Cell cycle distribution at time of VP16 wash-out (''0") and 2 h after VP16 removal (''120") of cells treated with solvent (DMSO), VP16, MG132,or VP16 and MG132.

3.5 Proteasome inhibition and effect of amsacrine in the K562 cells

Proteasomal inhibition potentiates mAMSA

Amsacrine (mAMSA) is an aminoacridine, which intercalates into DNA and inhibits TOP2. Amsacrine is used to treat lymphoma and leukaemia.

K562 cells were treated with different concentrations of mAMSA alone or in combination with a fixed concentration of proteasome inhibitor (95 nM MG132) for 120 hours. Growth inhibition was measured by XTT assay. The OD_{450nm} values of mAMSA alone were normalised to 0 μM mAMSA (100%), and OD_{450nm} values of mAMSA in combination with proteasome inhibitor were normalised to 0 μM mAMSA control in the presence of 95 nM MG132 (100%) (Figure 3.11). mAMSA inhibited K562 cell growth significantly on its own. The IC_{50} value was approximately 50 nM. The IC_{50} value dropped to approximately 15 nM in the presence of MG132 (Figure 3.11). The Pf_{50} value was 2.68, therefore the growth inhibition effect of mAMSA is significantly potentiated by MG132 (Table 3.4).

PS341 potentiates the growth inhibitory effects of mAMSA

Another proteasome inhibitor (PS341) was used in combination with mAMSA to study the potentiation effect. The results show PS341 potentiated the growth inhibition effect of mAMSA. The IC_{50} value of mAMSA alone was approximately 50 nM, however, in the presence of PS341 it dropped to approximately 23 nM (Figure 3.12). The potentiation effect was statistically significant by unpaired *t*-test (Pf_{50}=1.7) (Table 3.4). mAMSA showed potentiation in combination with two different proteasome inhibitors.

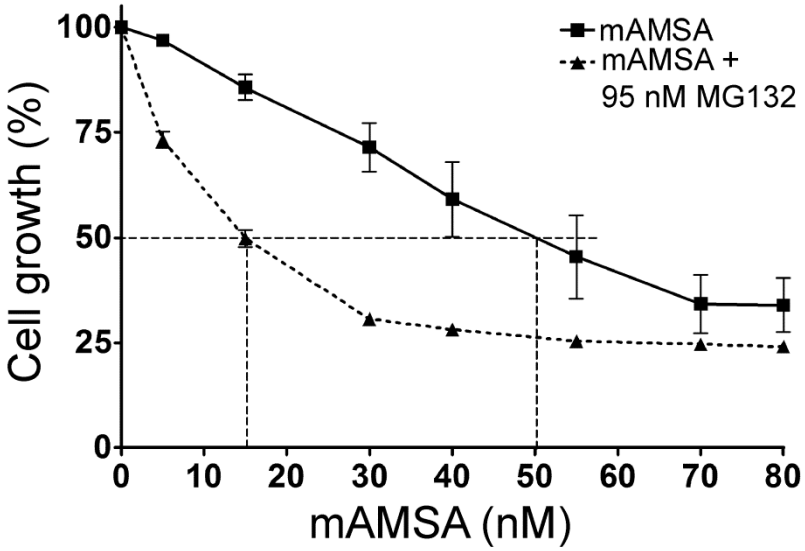

Figure 3.11 Potentiation of mAMSA by MG132 in K562 cells.

Cells were treated with increasing concentrations of mAMSA alone or in combination with 95 nM MG132 for 5 days followed by XTT staining. Dose–response curves were used to estimate the IC_{50} of mAMSA alone or in combination with MG132. Error bars represent the mean ± SEM of at least 3 separate experiments for both + and - MG132 conditions. Values were normalised to the 0 nM mAMSA value (100%).

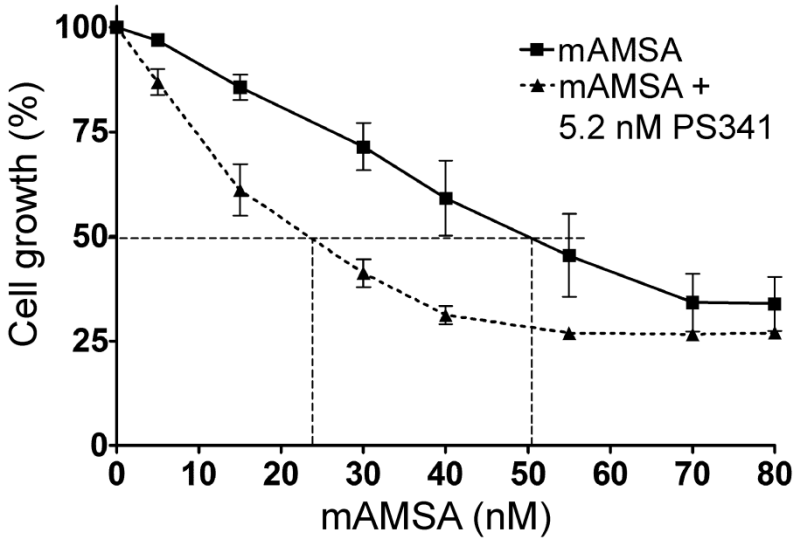

Figure 3.12 Potentiation of mAMSA by PS341 in K562 cells.

Cells were treated with increasing concentrations of mAMSA alone or in combination with 5.2 nM PS341 for 5 days followed by XTT staining. Dose–response curves were used to estimate the IC_{50} of mAMSA alone or in combination with PS341. Error bars represent the mean ± SEM of at least 3 separate experiments for both + and – PS341 conditions. Values were normalised to the 0 nM mAMSA value (100%).

mAMSA +	Mean of Pf_{50}	SEM	*p*-value
MG132	2.68	0.3	0.0005
PS341	1.7	0.35	0.0259

Table 3.4 Potentiation factor (Pf_{50}) summary of amsacrine (mAMSA) in combination with proteasome inhibitors.

Statistical significance between IC_{50} values of mAMSA alone and in combination with proteasome inhibitors by unpaired *t*-test (*p*-value).

Effect of proteasomal inhibition on mAMSA stabilised TOP2 complex stability (TARDIS reversal)

To investigate the effect of proteasomal inhibition on mAMSA stabilised TOP2 complex stability, K562 cells were seeded at approximately 1 x 10^5 cells per ml for 24 hours, and then treated with 25 μM mAMSA alone or in combination of 50 μM MG132 for 2 hours. After treatment, the drug(s) were removed by spinning down the cells, and was replaced with fresh media for further 2 hours incubation. For the cells also treated with MG132, MG132 was maintained in the fresh media. Samples were taken at 0, 15, 30, 60, and 120 minutes after drug wash out. Samples were processed onto TARDIS slides after lysis and then probed with TOP2A or TOP2B specific antibody (4566 and 4555). The mean integrated fluorescence of 25 μM mAMSA treated cells from individual experiments was set as 100% and all values of individual cells were normalised to it.

Trypan blue exclusion was used to determine cell viability before cells were treated with mAMSA (-120minute), after 2 hours mAMSA treatment (0 minute) and 2 hours (120minute) after mAMSA removal. The results showed that cell viability did not drop significantly during the period of the experiment (Figure 3.13 C).

mAMSA-stabilised TOP2-DNA complexes show a time-dependent reduction upon mAMSA removal. This was observed for both TOP2A and TOP2B. The half-lives of TOP2A- and TOP2B-DNA complexes were approximately 15 and 10 minutes, respectively. TOP2B complex levels were slightly increased in MG132 treated cells at 30, 60 and 120 minutes time points. For TOP2B, this experiment was only repeated twice, therefore unpaired *t*-test could not be used to determine statistical significance. According to the error bars the increase is unlikely to be significant (Figure 3.13 A and B).

In the presence of MG132, mAMSA stabilised higher levels of TOP2-DNA complexes than mAMSA alone at time point zero. After drug removal, the complex dissociation rate was similar to mAMSA alone treated cells. The

difference between the presence and absence of MG132 did not reach statistical significance by unpaired *t*-test at 15 mins, 30 mins, 60 mins and 120 mins. Therefore the presence of MG132 did not affect complex reversal rate (Figure 3.13 A and B).

mAMSA stabilised both isoforms of TOP2 in the cell, and the complexes decreased in a time-dependent manner upon removal of mAMSA. This finding is in line with Errington et al,. 2004, as mAMSA stabilised both TOP2A- and TOP2B-DNA complexes in MEF cells. The complex levels decreased after drug removal and half-life of both TOP2A and TOP2B complexes were approximately 15 minutes (Errington *et al.*, 2004), consistent with the results shown below (Figure 3.13).

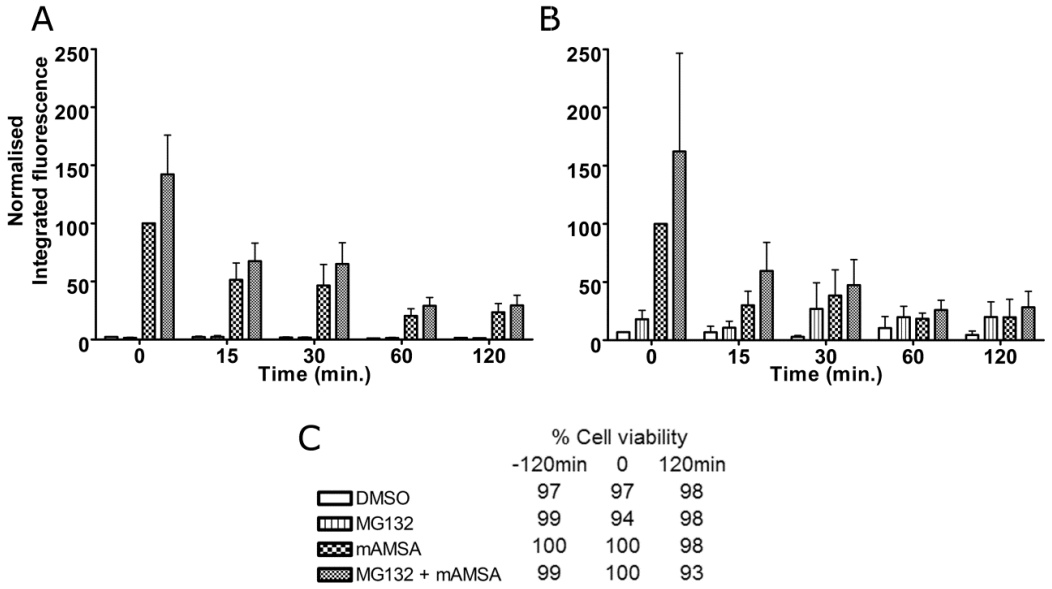

Figure 3.13 MG132 did not significantly affect the reversal of mAMSA-induced TOP2A- and TOP2B-DNA complexes.

K562 cells were incubated with solvent, mAMSA (25 μM), MG132 (50 μM) or were co-incubated with 50 μM MG132 and 25 μM mAMSA for 2 h. After 2 h mAMSA was removed, but MG132 was maintained in cell incubations that initially contained MG132. Levels of (A) TOP2A and (B) TOP2B DNA complexes at 0, 15, 30, 60, and 120 min after mAMSA removal (wash-out) were determined using the TARDIS assay. Statistical comparisons were made between the levels of TOP2-DNA complexes in the presence or absence of MG132 by unpaired t-test. (C)Cell viability (trypan blue exclusion) under the cell treatment conditions used: ''-120 min" refers to the time, at which drugs were first added to cells, ''0" refers to the time at which mAMSA wash-out was performed and ''15, 30, 60, and 120" refers to time (minutes) post drug wash-out.

3.6 Proteasomal inhibition and the effect of anthracyclines in the K562 cells

Proteasomal inhibition potentiates anthracyclines

Daunorubicin (Dau), doxorubicin (Dox), epirubicin (Epi) and idarubicin (Ida) are anthracyclines. All of these target TOP2 as a poison. These drugs are clinically used to treat leukaemia, lymphoma and breast cancer. The XTT assay was used to investigate the effect of proteasome inhibition on the growth inhibitory effects of anthracyclines.

K562 cells were seeded and treated with anthracycline alone or in combination with 95 nM MG132 for 120 hours. The OD_{450nm} values of anthracycline alone were normalised to 0 nM anthracycline, and OD_{450nm} values of anthracycline in combination with proteasome inhibitor were normalised to 0 nM anthracycline control in the presence of 95 nM MG132. The results show that all anthracyclines tested were potentiated significantly by MG132 (Figure 3.14). All Pf_{50} values were above 1.9, and Dau had the highest Pf_{50} value (Pf_{50}= 2.95) (Table 3.5 to Table 3.8).

PS341 potentiates the growth inhibitory effects of anthracyclines

To study the effect of PS341 on anthracycline-induced growth inhibition, the same experimental setup was used as for MG132. The Pf_{50} values were between 1.37 (Ida) to 1.67(Dau) (Figure 3.15 and Table 3.5 to Table 3.8).

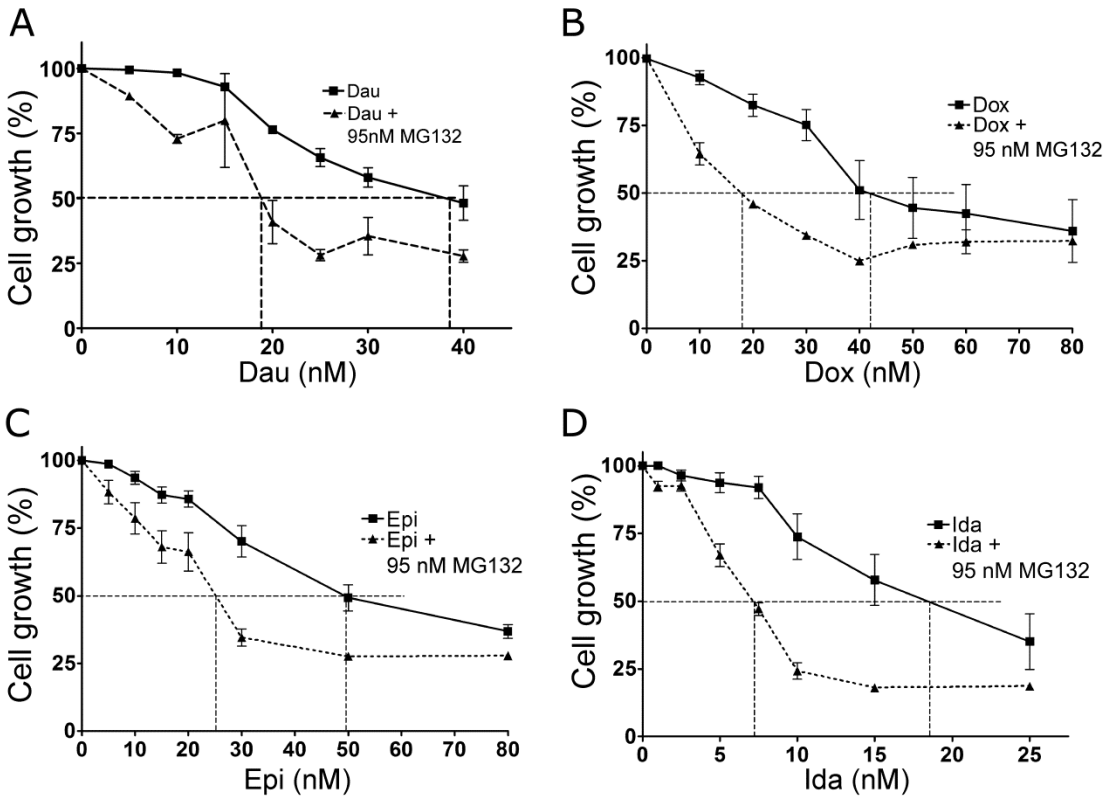

Figure 3.14 Potentiation of anthracyclines (Dau, Dox, Epi and Ida) by MG132 in K562 cells.

Cells were treated with increasing concentrations of anthracycline (A) Dau, (B) Dox, (C) Epi, and (D) Ida alone or in combination with 95 nM MG132 for 5 days followed by XTT staining. Dose–response curves were used to estimate the IC_{50} of anthracycline alone or in combination with MG132. Error bars represent the mean ± SEM of at least 3 separate experiments for both + and - MG132 conditions. Values were normalised to the 0 nM anthracycline value (100%).

Daunorubicin +	Mean of Pf_{50}	SEM	*p*-value
MG132	2.95	0.99	0.0115
PS341	1.67	0.07	0.0088

Table 3.5 Potentiation factor (Pf_{50}) summary of daunorubicin (Dau) in combination with proteasome inhibitors.

Statistical significance between IC50 values of Dau alone and in combination with proteasome inhibitors by unpaired t-test (p-value).

Doxorubicin +	Mean of Pf_{50}	SEM	*p*-value
MG132	1.93	0.31	0.0155
PS341	1.44	0.23	0.1826

Table 3.6 Potentiation factor (Pf_{50}) summary of doxorubicin (Dox) in combination with proteasome inhibitors.

Statistical significance between IC_{50} values of Dox alone and in combination with proteasome inhibitors by unpaired *t*-test (*p*-value).

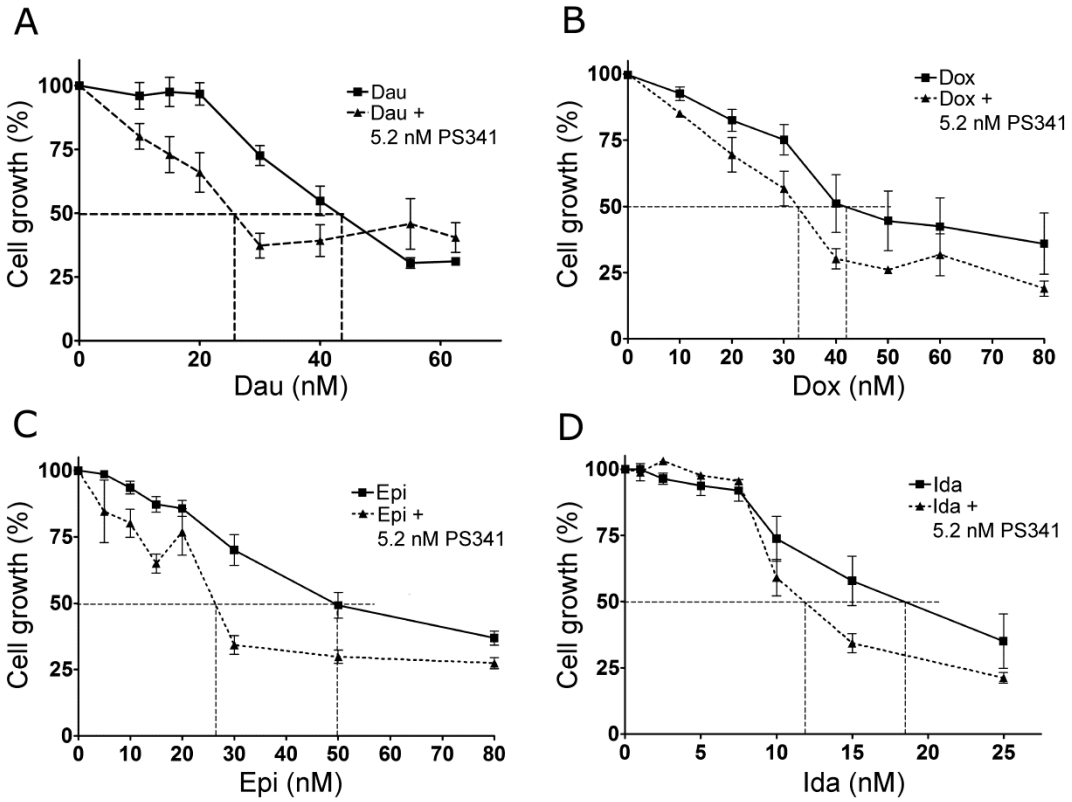

Figure 3.15 Potentiation of anthracyclines (Dau, Dox, Epi and Ida) by PS341 in K562 cells.

Cells were treated with increasing concentrations of anthracycline (A) Dau, (B) Dox, (C) Epi, and (D) Ida alone or in combination with 5.2 nM PS341 for 5 days followed by XTT staining. Dose–response curves were used to estimate the IC_{50} of anthracycline alone or in combination with PS341. Error bars represent the mean ± SEM of at least 3 separate experiments for both + and – PS341 conditions. Values were normalised to the 0 nM anthracycline value (100%).

Epirubicin +	Mean of Pf_{50}	SEM	*p*-value
MG132	1.93	0.24	0.0018
PS341	1.63	0.05	0.0056

Table 3.7 Potentiation factor (Pf_{50}) summary of epirubicin (Epi) in combination with proteasome inhibitors.

Statistical significance between IC_{50} values of Epi alone and in combination with proteasome inhibitors by unpaired *t*-test (*p*-value).

Idarubicin +	Mean of Pf_{50}	SEM	*p*-value
MG132	1.92	0.09	0.0018
PS341	1.37	0.02	0.089

Table 3.8 Potentiation factor (Pf_{50}) summary of idarubicin (Ida) in combination with proteasome inhibitors.

Statistical significance between IC_{50} values of Ida alone and in combination with proteasome inhibitors by unpaired *t*-test (*p*-value).

A

MG132 +	Mean of Pf_{50}	SEM	*p* -value
Mitoxantrone	4.58	0.54	<0.0001
Etoposide	1.65	0.25	0.0261
Teniposide	2.62	0.15	<0.0001
mAMSA	2.68	0.3	0.0005
Daunorubicin	2.95	0.99	0.0115
Doxorubicin	1.93	0.31	0.0155
Epirubicin	1.93	0.24	0.0018
Idarubicin	1.92	0.09	0.0018

B

PS341 +	Mean of Pf_{50}	SEM	*p* -value
Mitoxantrone	2.95	0.11	0.0020
Etoposide	1.24	0.32	0.7690
Teniposide	2.71	0.04	<0.0001
mAMSA	1.7	0.35	0.0259
Daunorubicin	1.67	0.07	0.0088
Doxorubicin	1.44	0.23	0.1826
Epirubicin	1.63	0.05	0.0056
Idarubicin	1.37	0.02	0.0890

Table 3.9 Summary of Pf_{50} (A) MG132 and (B) PS341.

3.7 Conclusion and discussion

Eight TOP2 poisons were tested in combination with two proteasome inhibitors. The presence of proteasome inhibitors potentiated the growth inhibition of TOP2 poison determined by XTT assay in the K562 cell line. The proteasome inhibitor MG132 potentiated all TOP2 poisons tested and PS341 potentiated five TOP2 poisons (Table 3.9). MTX demonstrated the highest level of potentiation. The results demonstrate that proteasomal inhibition can increase (potentiate) the growth inhibition of TOP2 poisons in K562 cells.

One possible explanation for the observed growth inhibition is that inhibiting the proteasome may increase the cellular protein level of TOP2. TOP2A and B protein quantitation in K562 cells treated with MG132 or PS341 was reported by Lee at al., 2016. These immuno-fluorescence data showed PS341 treatment of K562 increased the levels of TOP2A protein but not TOP2B protein. There were no changes in TOP2 protein levels

after MG132 treatment (Lee *et al.*, 2016). Thus, the potentiation by PS341 may be due to increased TOP2A protein target levels in the cells. Congdon et al., 2008 showed that treatment with PS341 increased TOP2A protein levels in a drug-resistant human multiple myeloma cell line, and the presence of PS341 potentiated the effects of TOP2 poisons (Congdon *et al.*, 2008).

The TARDIS assay was used to address the question of whether proteasome inhibition alters the kinetics of formation and removal of covalent TOP2-DNA complexes. The TARDIS assay results showed that the presence of 50 μM MG132 prolonged the half-life of VP16 or MTX stabilised covalent DNA-TOP2 complexes in cells. This was observed for complexes with both isoforms. In contrast the presence of MG132 did not alter the half-life of mAMSA stabilised DNA-TOP2 complexes in cells. These findings suggest that covalent DNA-TOP2 complex removal involves the proteasome. Increasing the half-life of the DNA-TOP2 complex provides one mechanism for MG132 to potentiate the growth inhibitory effects of MTX and VP16.

MG132 also potentiated the effects of mAMSA but the presence of MG132 did not alter the clearance rate of DNA-TOP2 complexes. This observation suggests mAMSA stabilised DNA-TOP2 complexes may be removed by other mechanism(s). Multiple pathways are involved in the removal of drug stabilised DNA-TOP2 complexes. Lee et al., 2012 previously found that the nuclease MRE11 can facilitate TOP2 complex removal (Lee *et al.*, 2012). Furthermore, the AP lyases, Ku70/80 and APE1, can remove TOP2 adducts *in vitro* (Lee, MPhil 2012). Therefore, further work is required to determine the mechanism by which MG132 potentiates growth inhibition by mAMSA.

Chapter 4. Genotoxicity of MTX alone or in combination with a proteasome inhibitor

4.1 Introduction

In the previous chapter (Chapter 3), I demonstrated that the growth inhibition by TOP2 poisons was potentiated by proteasome inhibitors (MG132 and PS341). The highest level of potentiation was seen with MTX. Drugs targeting DNA topoisomerase II are genotoxic and produce micronuclei. In this chapter, I investigated whether the combination of a proteasome inhibitor and MTX was more or less genotoxic than MTX alone. To detect *in vitro* micronuclei accurately, a two-colour assay system was used.

Micronuclei are lagging chromosome fragments or whole chromosomes that fail to attach to the spindle during the segregation process in anaphase (Figure 4.1). After cell separation, a nuclear envelope forms around these lagging chromosomes to form micronuclei (Fenech, 2000; Fenech *et al.*, 2011). Unrepaired DNA double-stranded breaks can lead to the formation of chromatid and chromosome fragments which may become micronuclei. Therefore, micronuclei can be observed in cells after exposure to radiation or DNA damaging agents as a biomarker of genotoxicity (Bryce *et al.*, 2007; Hartlerode and Scully, 2009; O'Donovan and Livingston, 2010). Applications such as Fluorescence *in situ* hybridization (FISH) or live-cell imaging can also be used to further study the micronucleus' contents and the details of formation (Norppa and Falck, 2003; Lindberg *et al.*, 2008; Huang *et al.*, 2011).

Initially, micronuclei are usually scored manually under a microscope or on microscopy images. However, manual micronuclei scoring can be time consuming. Automated methods have been developed, such as the use of software to analyse microscopy images and a specific type of flow cytometry termed fluorescence activated cell sorting (FACS) (Nusse *et al.*, 1994; Avlasevich *et al.*, 2006; Bryce *et al.*, 2007; Diaz *et al.*, 2007; Shibai-Ogata *et al.*, 2011).

In this study, manual scoring microscopy and FACS methods are used to study micronucleus formation after drug treatment.

The principle of the micronucleus assay used in this study involves staining the DNA content of nuclei and identifying micronucleated cells by the size of the micronuclei. Two different nucleic acid dyes were used. First, a cell-impermeable dye (EMA) was used to stain cells with damaged cell membranes such as apoptotic and necrotic cells staining them red. After fixation or lysis, another dye SYTOX Green or Hoechst used to stain all nuclei blue or green. The cells stained with both dyes are identified as apoptotic cells and excluded for micronucleus counting (Figure 4.2).

The criteria for identifying micronuclei manually under a microscope are based on Fenech, 2000, and are defined as small micronuclei located near to the main nucleus without overlapping each other. The size of a micronucleus is between 1/16 and 1/3 of the main nucleus. The DNA fluorescence intensity of a micronucleus and the main nucleus needs to be similar (Fenech, 2000).

The aim of this chapter was to investigate whether proteasomal inhibition potentiates cytotoxicity and reduces genotoxicity of MTX.

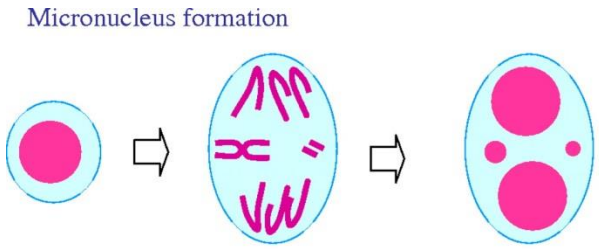

Figure 4.1 Micronucleus formation in cells undergoing nuclear division.
Adapted with permission from Fenech, 2000.

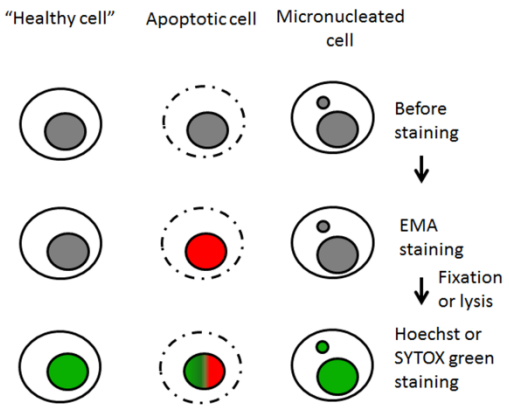

Figure 4.2 Flow chart of micronucleus assay with the use of two colour nucleic acid dyes to identify different types of cells.

4.2 Two-Colour Micronucleus (MN) assay

Early studies used acridine orange staining to detect nuclei and micronuclei. However, with this assay it is hard to distinguish between micronuclei and apoptotic blebbing. A different staining method was developed to enable exclusion of apoptotic cells from the counting process.

After drug exposure, the cells were counted prior to incubation with 2 µg/ml ethidium monoazide bromide (EMA) under a cool white light source for 30 minutes. EMA is a cell membrane impermeable nucleic acid dye which enters cells with damaged membranes, such as apoptotic or necrotic cells, and becomes covalently bound to DNA after photo-activation. Samples were then applied to microscope slides prior to fixation with methanol. Fixed cells were stained with Hoechst. Hoechst and EMA have different emission wavelengths which are detected in two different channels; 461 nm for Hoechst (blue) and 600 nm for EMA (red). Microscopy images were taken and analysed using Volocity software (Perkin-Elmer, USA). Figure 4.3 shows representative microscopy images. Figure 4.3A shows Hoechst-stained nuclei. Apoptotic cells are stained with both EMA and Hoechst, (e.g. cell marked with "X33"). Figure 4.3B and C show cells with micronuclei marked with "X1". On each slide at least 2000 cells were counted. The number of "healthy" cells, the number of micronucleated cells, and the total number of cells counted was recorded.

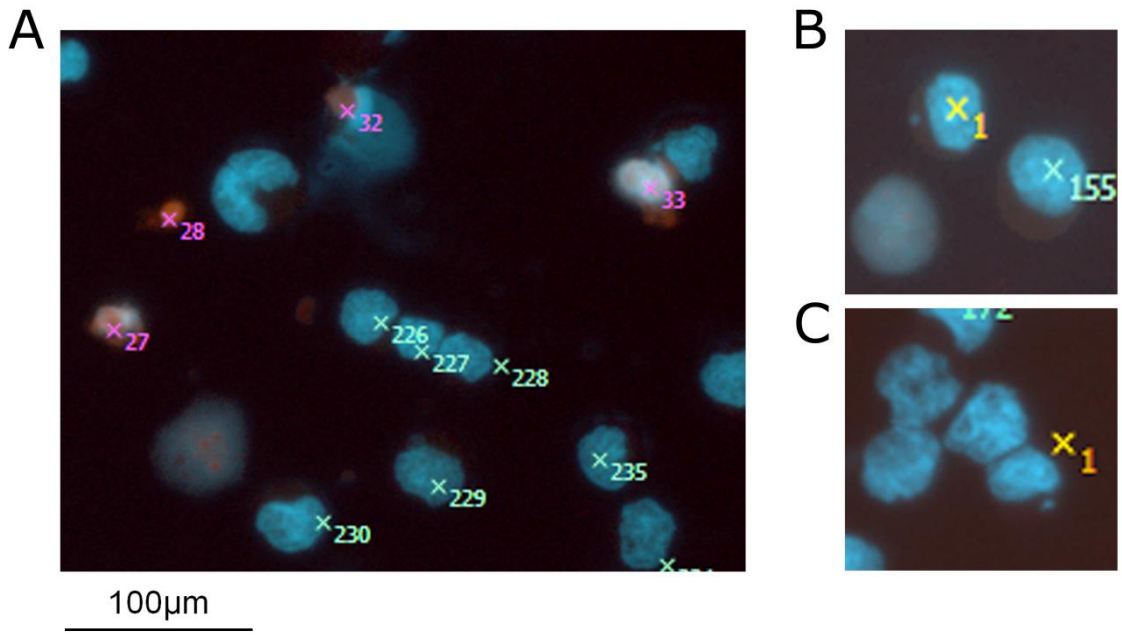

Figure 4.3 Microscopy images of cells in the micronucleus assay.

Cells were treated with 5 nM MTX for 120 hours. Apoptotic cells are stained red by EMA, and all nuclei were stained blue with Hoechst. Images are taken with magnification (x10). (A) A mixed population of cells. (B) Two zoomed in images showing cells with micronuclei.

4.3 Micronucleus assay: MTX alone or in combination with MG132 (120 hours)

Relative Increase in Cell Count (RICC)

For *in vitro* micronuclei detection, Relative Increase in Cell Count is a cytotoxicity measurement recommended in the Organisation for Economic Co-operation and Development (OECD) guidelines (Oecd). RICC is calculated using the equation shown below:

$$RICC = \frac{(Increase\ in\ number\ of\ cells\ in\ treated\ cultures(finish - starting))}{(Increase\ in\ number\ of\ cells\ in\ untreated\ control\ (finish - starting))} \times 100$$

K562 cells were treated with MTX either alone or in combination with 95 nM MG132 for 120 hours, at the concentrations determined in Chapter 3. Cell counts for each sample were taken to calculate the RICC. For micronuclei assays, an RICC lower than 40% is classed as cytotoxic. Results from cytotoxic samples need to be interpreted with caution.

Figure 4.4A shows the 120-hour RICC values. These were 82% for 95 nM MG132 alone, 52% for 5 nM MTX alone, and 25% for 5 nM MTX plus 95

nM MG132. The RICC for the combination was significantly lower than the RICC for MG132 alone (*p=0.0012*) or MTX alone (*p*=0.0046) (Figure 4.4A). The RICC for cells treated with 22.5 nM MTX alone was 14%.

Micronuclei formation assessed by microscopy (Average micronuclei)

Average percentage of micronuclei was calculated using the equation shown below:

$$\frac{Number\ cells\ with\ micronuclei}{Total\ number\ of\ cells\ counted} \times 100$$

At least 2000 cells were counted in each sample. Of the untreated control cells 0.3% had micronuclei. Cells treated with 95 nM MG132 alone were comparable to the untreated control (Figure 4.4B). MTX exposure is genotoxic; cells incubated with 5 nM MTX or 22.5 nM MTX produced significantly higher levels of micronuclei than untreated controls, 3.3% (*p*=0.0082) and 3.8% (*p*<0.0001), respectively. The combination of 5 nM MTX and 95 nM MG132 was significantly less genotoxic (0.9%) than 5 nM MTX alone (**, *p*=0.0054) (Figure 4.4B).

Micronucleus formation (Fold change) assessed by microscopy

Micronucleus formation is often reported as fold increase over the untreated control. A two-fold increase over the untreated control is classed as genotoxic. The equation used to calculate this is shown below:

$$\frac{Drug\ treated\ (Average\ micronuclei\ \%)}{Untreated\ control\ (Average\ micronuclei\ \%)}$$

MTX treatment was genotoxic. 5 nM MTX produced an eleven-fold increase in micronuclei and 22.5 nM MTX produced a twelve-fold increase in micronuclei. A combination of 5 nM MTX and 95 nM MG132 produced only a 3.5-fold increase over the untreated control. It was higher than MG132 alone (1.3-fold), but significantly lower than 5 nM MTX alone (11-fold) (*p*=0.0197) (Figure 4.4C), suggesting the combination was less genotoxic.

Summary

After a 120 hours exposure, by RICC the 22.5 nM MTX was most cytotoxic, followed by the combination of 5 nM MTX and 95 nM MG132. 5 nM MTX alone was the least cytotoxic of the three combinations tested. This is consistent with the growth inhibition assay results shown in the previous chapter. For both the % micronuclei and the fold change over the untreated control, the combination was less genotoxic than MTX alone (5 nM or 22.5 nM) when determined *in vitro* by microscopy counting at least 2000 cells per sample.

	RICC		Average micronuclei (%)		Micronuclei fold change	
	%	±SEM	%	±SEM	change	±SEM
Untreated	100.0	0.0	0.3	0.1	1.0	0.0
95 nM MG132	82.3	10.9	0.3	0.1	1.3	0.3
5 nM MTX	52.4	4.4	3.3	0.7	13.5	3.8
22.5 nM MTX	13.8	1.3	3.8	0.4	11.6	5.2
95 nM MG132+ 5 nM MTX	25.2	4.7	0.9	0.1	3.5	0.7

Table 4.1 Mean values with standard error for RICC, average (%) micronuclei and fold change show on figure 4.4.

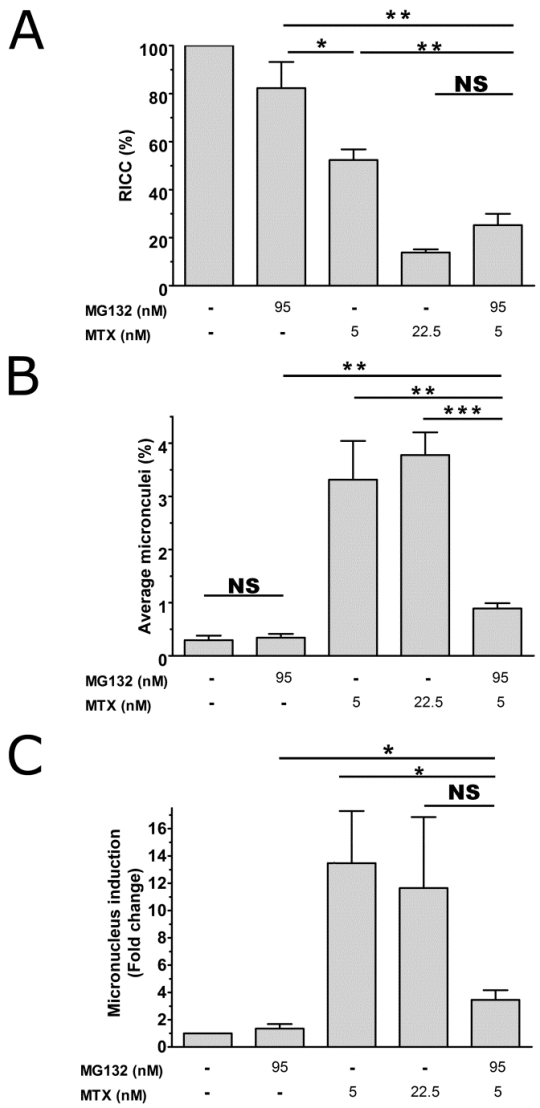

Figure 4.4 K562 cells after 120 hours treatment of MTX with or without 95 nM MG132.

(A) Relative increase in cell count (RICC), (B) Average (%) micronuclei and (C) micronucleus induction (fold change over control) determined by microscopy. (*$p \leq 0.05$, **$p \leq 0.01$, and ***$p \leq 0.005$)

4.4 *In vitro* micronucleus assay using FACS for MTX alone and in combination with MG132 (120 hours)

FACS provides an effective and robust way to determine micronuclei in a population of cells; it enables use of higher cell numbers. At least 30,000 "healthy" nuclei were counted per sample and the number of micronuclei was recorded. Genotoxicity data is presented as average micronuclei or as fold induction over untreated control. In addition, data on apoptosis (EMA positive events) and cell cycle distribution is presented.

RICC

The 120-hour RICC values were 92% for 95 nM MG132 alone, 50% for 5 nM MTX alone, and 46% in combination. The RICC for the combination was significantly lower than the RICC for MG132 alone (*p=0.012*) but not for 5 nM MTX alone (Figure 4.5A). The RICC for cells treated with 22.5 nM MTX alone was 24%.

The RICC means for this set of experiments were generally higher than the values shown in figure 4.4A, but these differences were not statistically significant.

Average % Micronucleus

The results of the flow cytometric analysis are presented as an average micronuclei percentage. In each sample at least 30,000 "healthy" nuclei were counted. Average micronuclei were calculated using the equation shown below:

$$\frac{Number\ of\ micronculei\ counted}{Number\ of\ healthy\ nuclei\ counted} \times 100$$

The average percentage of micronuclei in the untreated control was 3.9%. High levels of micronuclei were induced by 5 nM MTX (51%) or 22.5 nM MTX (174%). The average micronuclei for MTX alone or in combination with MG132 (27%) were significantly higher than the untreated control (Figure 4.5B). Cells treated with 22.5 nM MTX had an RICC lower than 40%, which is classed as a cytotoxic dose. The genotoxicity data therefore needs to be viewed with caution. This dose induced a very high level of micronuclei. Similar observations were reported in Bryce et al., 2007 and Avlasevich et al., 2006 which demonstrated that a large number of micronuclei were induced when cells were treated with cytotoxic doses of drug. After the cytotoxic treatment, FACS determined a higher level of micronuclei than determined by microscopy (Avlasevich *et al.*, 2006; Bryce *et al.*, 2007).

Micronucleus fold change over untreated control (120 hours)

Micronucleus formation results are presented as fold increase over untreated control. The ratio of micronuclei to healthy nuclei in the untreated control is set a base. Using the equation shown below:

$$\frac{Drug\ treated\ (Average\ micronuclei\ \%)}{Untreated\ control\ (Average\ micronuclei\ \%)}$$

MTX was genotoxic. 5 nM induced 13-fold higher micronuclei than the untreated control and 22.5 nM MTX induced 46-fold higher micronuclei than the control. The combination of 95 nM MG132 and 5 nM MTX only induced 7.2-fold more micronuclei than the untreated control. These results (Figure 4.5C) are consistent with the observations from the microscopy micronucleus assay shown in section 4.3 (Figure 4.4). The combination produced fewer micronuclei.

	RICC		Average micronuclei		Micronuclei (Fold change)		EMA increase (Fold change)	
	%	±SEM	%	±SEM	Fold	±SEM	Fold	±SEM
Untreated	100.0	0.0	3.9	1.0	1.0	0.0	1.0	0.0
95 nM MG132	91.7	6.1	2.9	0.7	0.8	0.0	0.9	0.1
5 nM MTX	49.5	5.9	50.8	16.5	13.0	2.9	16.3	7.9
22.5 nM MTX	23.9	7.4	173.6	42.5	46.0	5.0	18.4	8.3
95 nM MG132+ 5 nM MTX	46.0	8.3	26.6	4.4	7.2	0.7	6.2	8.3

Table 4.2 Mean values with standard error for RICC, average (%) micronuclei and micronucleus induction show on figure 4.5.

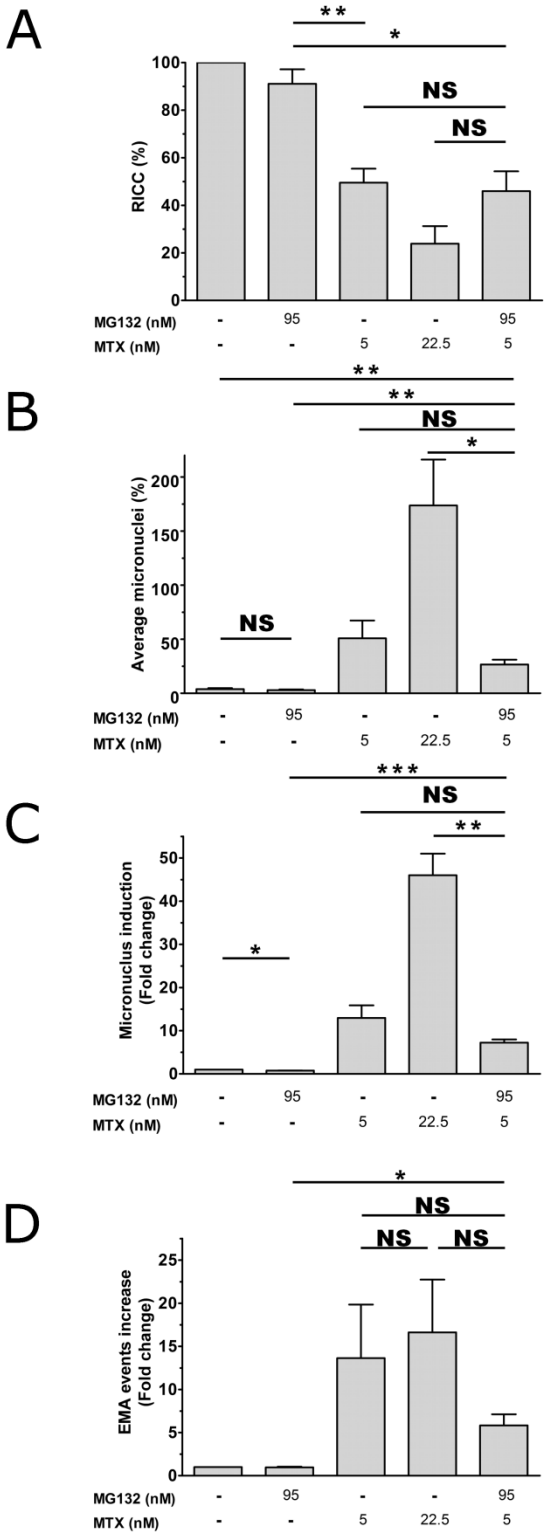

Figure 4.5 Data from K562 cells after a 120-hour treatment determined by FACS.

(A) RICC (B) Average (%) micronuclei and (C) micronucleus induction (fold change) (D) apoptosis (*$p \leq 0.05$, **$p \leq 0.01$, and ***$p \leq 0.005$)

Apoptotic measurement

The number of EMA positive events reflects the number of apoptotic cells in the sample. The ratio of healthy nuclei compared to the EMA positive events can be used to determine the level of apoptosis in each sample (Bryce *et al.*, 2007). The equation used is:

$$\frac{Drug\ treated\ (\frac{Number\ of\ EMA\ events}{Number\ of\ nuclei})}{Untreated\ control\ (\frac{Number\ of\ EMA\ events}{Number\ of\ nuclei})}$$

MG132 alone had no significant induction of apoptosis compared to untreated control. MTX induces apoptosis, which is consistent with the RICC data.

Cell cycle distribution: MTX alone or in combination with MG132 for 120 hours

FACS can detect DNA content in cells. This feature enables the cell cycle distribution within samples to be determined. K562 cells were treated with MTX alone or in combination with MG132 for 120 hours. SYTOX green was used to stain the nuclei and the fluorescence intensity of this represented DNA content. This was recorded by the FACS and was plotted as a frequency against DNA content intensity on a histogram. The frequencies of each G_1, S and G_2/M phases were calculated using specialised software FlowJo (FlowJo, USA).

In the untreated control, the distribution of G_1, S and G_2/M phases were 31%, 53% and 15%, respectively. After treatment with MG132 alone, the pattern was similar to untreated control (Figure 4.6). Cells treated with 5 nM MTX alone or the combination of 5 nM MTX and 95 nM MG132 for 120 hours showed a significant reduction of S phase cells with *p*-values of 0.0274 and 0.0088, respectively (Figure 4.6). Cells treated with 22.5 nM MTX alone accumulated in G_2/M phase and had fewer S phase cells than the untreated control (0.0012) (Figure 4.6).

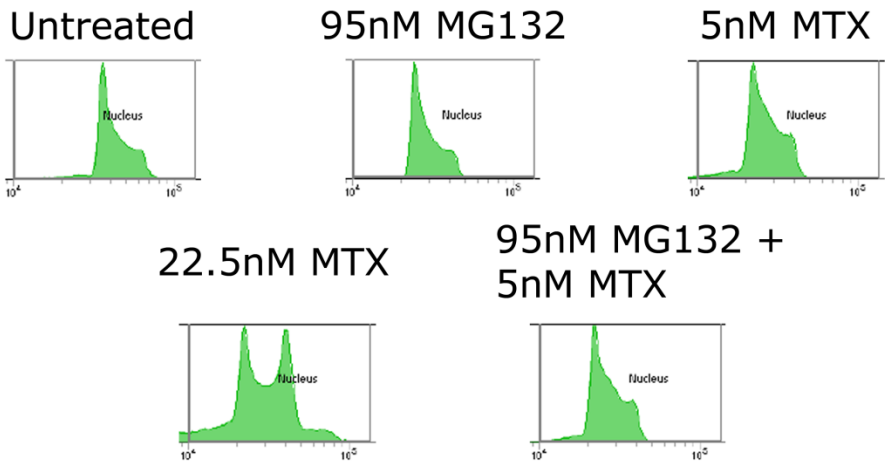

Figure 4.6 Cell cycle distribution of cells treated with MTX alone or in combination with MG132 for 120 hours.

Each plot represents at least three individual experiments.

	G_1		S		G_2/M	
	%	±SEM	%	±SEM	%	±SEM
Untreated	31.4	4.9	52.8	2.7	14.5	0.6
95 nM MG132	29.4	4.5	52.6	2.7	14.6	0.9
5 nM MTX	27.0	4.4	37.0	3.8	14.9	1.5
22.5 nM MTX	13.4	4.0	23.2	2.4	21.6	2.5
95 nM MG132 + 5 nM MTX	29.4	3.4	38.0	1.5	16.4	1.6

Table 4.3 Cell cycle distribution—Percentage of G_1, S and G_2/M phase cells in K562 cells.

Data shown on figure 4.6 is the mean of at least three experiments analysed by Flow Jo.

Summary

Cytotoxicity determined by RICC after a 120-hour exposure to the combination of 5 nM MTX plus 95 nM MG132 or 5 nM MTX or 22.5 nM MTX alone is consistent with the growth inhibition assay results shown in the previous chapter. For both the % micronuclei and the fold change over the untreated control the combination was less genotoxic than MTX alone (5 nM or 22.5 nM). This was true, when determined *in vitro* by microscopy counting of at least 2000 cells per sample or by FACS. There RICC between the combination, 5 nM and 22.5 nM MTX alone were not significantly different. The % micronuclei of the combination was lower than 22.5 nM MTX alone. However, the micronuclei levels were incredibly high by FACS. The RICC below 40% raise a concern that some of the small objects measured by FACS may not be micronuclei. Therefore, a 48-hour drug exposure was carried out using the same drug concentrations.

In vitro micronucleus assay by flow cytometric analysis: MTX alone or in combination with MG132 (48 hours)

In the previous section the 22.5 nM MTX for 120 hours was very cytotoxic and produced extremely high levels of micronuclei by FACS. The incubation time was reduced to 48 hours then FACS analysis for micronuclei was carried out. Cytotoxicity was determined in two ways: relative survival determined by FACS and RICC by cell counting. These experiments were carried out in triplicate four times (once where only RICC was determined and three times where both RICC and relative survival were determined). During the nucleic acid staining step 6-micron latex counting beads were added to each sample as an internal control (Avlasevich *et al.*, 2006; Bryce *et al.*, 2007). In the FACS analysis, at least 30,000 healthy nuclei were counted. The system also records the number of beads counted. The relative survival was calculated using the ratio of healthy nuclei to beads, taking the untreated control as 100% and normalising each sample to it. The major difference between the relative

survival and the RICC is the exclusion of the apoptotic cell population in the relative survival dataset.

Equation below:

$$\frac{Drug\ treated\ (\frac{Number\ of\ beads\ counted}{Number\ of\ healthy\ nuclei\ counted})}{Untreated\ control\ (\frac{Number\ of\ beads\ counted}{Number\ of\ healthy\ nuclei\ counted})} \times 100$$

In figure 4.7A, cytotoxicity results are presented as means with standard error of the mean for at least three experiments (relative survival as grey bars and RICC as black bars). Statistical significance was determined using the unpaired *t*-test. The cytotoxicity determined by relative survival and RICC were very similar after 48-hour drug treatments. The cytotoxic effect of MTX was dose-dependent. The relative survival of 5 nM MTX was 54%, and reduced to 23% with 22.5 nM MTX (Figure 4.7A). The relative survival values of the combination (53%) were significantly (p=0.0002) lower than MG132 alone (90%), but not significantly different from the 5 nM MTX alone.

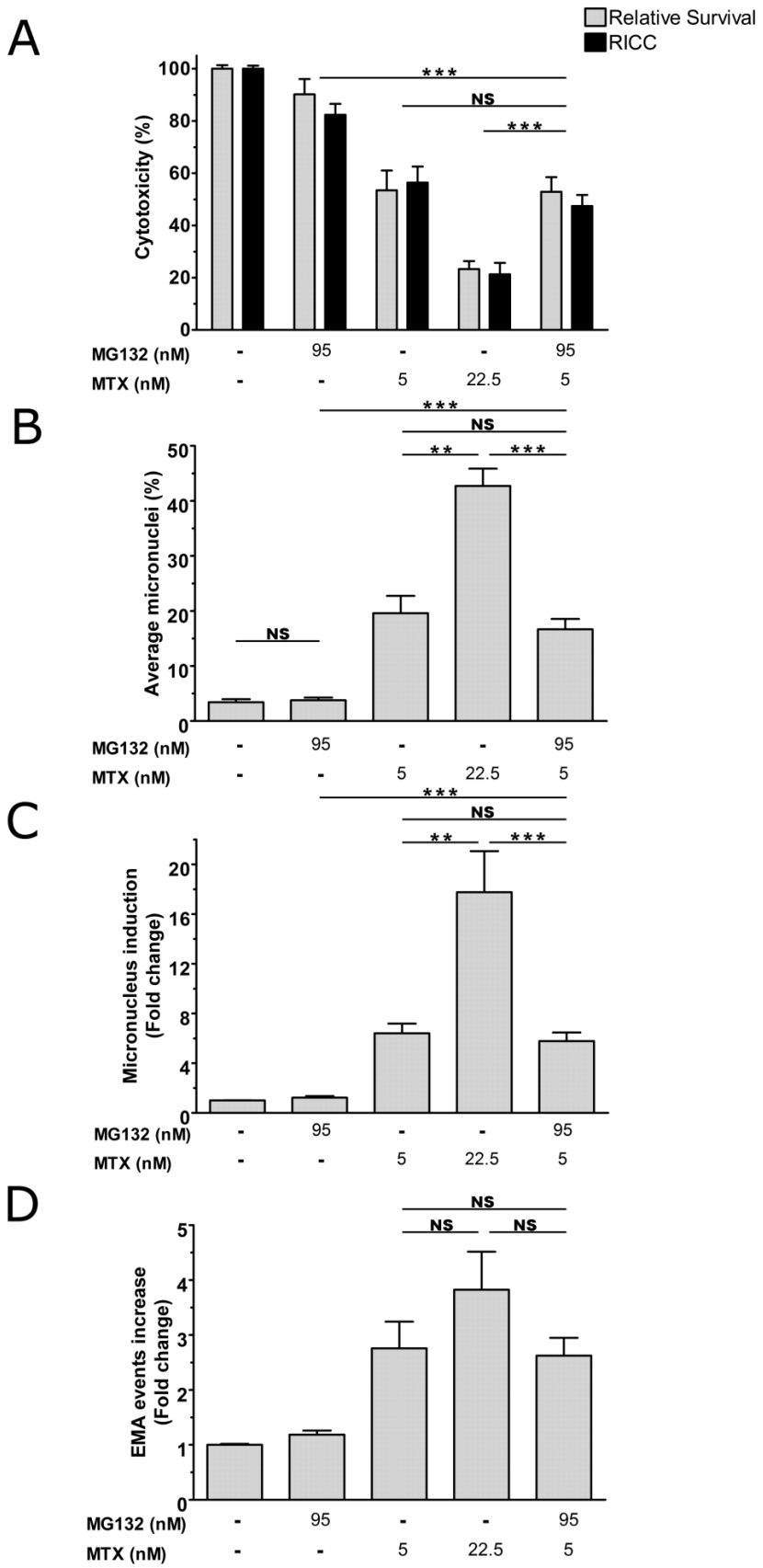

Figure 4.7 K562 cells after a 48-hour treatment of MTX with or without MG132.

(A) Relative Increase in Cell Count (RICC) black bars, relative survival – grey bars (B) Average (%) micronuclei, (C) micronucleus fold change and (D) apoptosis determined by FACS. (*p≤0.05, **p≤0.01, and ***p≤0.005)

	Relative survival		RICC		Average micronuclei		Micronuclei (Fold change)		EMA increase (Fold change)	
	%	±SEM	%	±SEM	%	±SEM	Fold	±SEM	Fold	±SEM
Untreated	100.0	1.3	100.0	1.2	3.4	0.6	1.0	0.0	1.0	0.0
95 nM MG132	90.2	5.9	82.4	4.2	3.8	0.5	1.2	0.1	1.2	0.1
5 nM MTX	53.5	7.5	56.4	6.1	19.6	3.2	6.4	0.8	2.8	0.5
22.5 nM MTX	23.3	3.1	21.3	4.4	42.7	3.2	17.8	3.3	3.8	0.7
95 nM MG132+ 5 nM MTX	52.9	5.6	47.4	4.3	16.7	1.9	5.8	0.7	2.6	0.3

Table 4.4 Mean values with standard error for RICC, relative survival, average (%) micronuclei and fold change show on figure 4.7.

Average micronucleus formation (%) induced by MTX alone or in combination with MG132 after a 48-hour incubation

At least 30,000 "healthy" nuclei were counted in each sample. The untreated control population had an average of 3.4% micronuclei. MTX induced micronuclei significantly above background. 22.5 nM MTX induced 43% micronuclei (Figure 4.7B). The combination of 5 nM MTX and 95 nM MG132 induced 17% micronuclei, significantly above background (p<0.0001), and similar to 5 nM MTX (20 % micronuclei) (Figure 4.7B and Table 4.4).

Micronucleus formation presented as fold change over untreated control (48 hours)

Fold change data had the same trend as the average micronuclei data. 95 nM MG132 alone had similar levels to the untreated control. Following treatment with 5 nM MTX there was a 6.4-fold increase in micronuclei above the control. The combination showed a 5.8-fold increase but this was not significantly lower than 5 nM MTX alone. Incubation with 22.5 nM MTX induced a 18-fold increase in micronuclei over the untreated control, significantly higher than the combination (p=0.0008) (Figure 4.7C)

Apoptotic measurement

Apoptosis induced by MTX was dose-dependent. The combination had comparable levels of apoptosis to 5 nM and 22.5 nM MTX alone (Figure 4.7D).

Cell cycle distribution: MTX alone or in combination with MG132 for 48 hours

The cell cycle distribution determined by FACS is displayed in figure 4.8. In the untreated control, the distribution of G_1, S and G_2/M phases were 37%, 50% and 15%, respectively. MTX altered the cell cycle distribution. The combination of 5 nM MTX and 95 nM MG132 produced a similar cell cycle distribution pattern as the 5 nM MTX, G_1 (26%), S (42%) and G_2/M (31%). The combination of 5 nM MTX and 95 nM MG132 had a

significantly higher population of cells at G_2/M phase than untreated control (p<0.0001) or 95 nM MG132 (p=0.0003) (Figure 4.8 and Table 4.5).

Summary

After a 48-hour exposure, the combination of 95 nM MG132 and 5 nM MTX had a lower cytotoxicity than 22.5 nM MTX. The cytotoxicity of the combination was similar as 5 nM MTX alone. The presence of 95 nM MG132 did not potentiate the cytotoxicity 5 nM MTX.

The combination of 95 nM MG132 and 5 nM MTX had lower micronuclei levels than 22.5 nM MTX alone. This might be related to the levels of cytotoxicity were differing.

There was no significant difference in cytotoxicity or genotoxicity between 5 nM MTX and 5 nM MTX plus MG132.

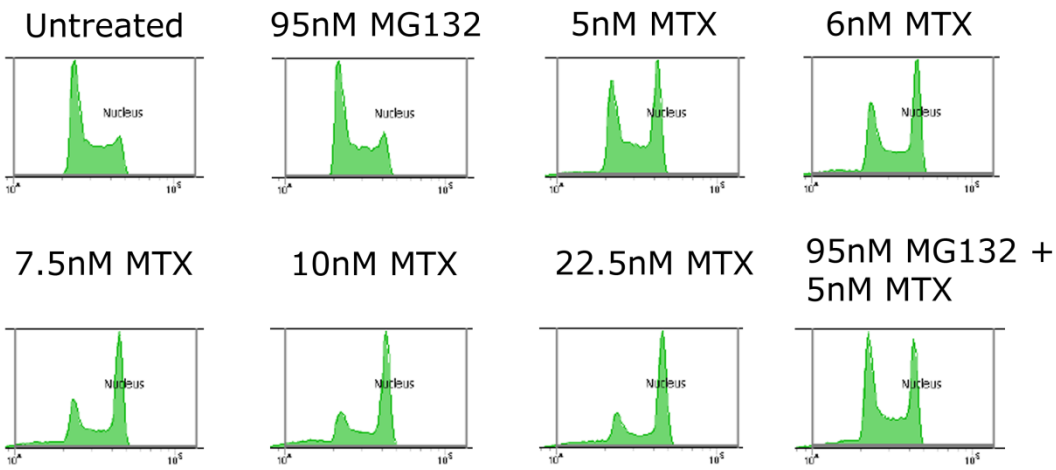

Figure 4.8 Cell cycle distribution of cells treated with MTX or MTX in combination with MG132 for 48 hours.

	G_1		S		G_2/M	
	%	±SEM	%	±SEM	%	±SEM
Untreated	37.0	2.2	49.8	1.6	14.5	0.6
95 nM MG132	31.3	3.3	54.9	2.3	16.2	0.5
5 nM MTX	27.0	1.3	44.3	0.8	29.3	1.5
6 nM MTX	23.4	1.4	43.4	2.4	29.3	3.0
7.5 nM MTX	23.4	2.0	35.9	1.6	40.1	2.2
10 nM MTX	15.3	1.5	32.8	2.2	44.1	5.3
22.5 nM MTX	11.8	1.8	21.8	1.1	67.1	3.5
95 nM MG132 + 5 nM MTX	25.8	0.5	42.4	1.5	31.0	1.5

Table 4.5 Cell cycle distribution—Percentage of G_1, S and G_2/M phase cells in K562 cells.

Data shown on figure 4.8 analysed by Flow Jo.

4.5 *In vitro* micronucleus assay with flow cytometric analysis: MTX alone and in combination with PS341 (120 hours)

Chapter 3 demonstrated that 5.2 nM PS341 potentiated the growth inhibition of MTX after a 120-hour incubation. In the XTT growth inhibition assays the IC_{50} of MTX alone was 22.5 nM, and the concentration of MTX that produced a comparable IC_{50} in combination with 5.2 nM PS341 was 7.5 nM. To determine if the PS341 combination altered genotoxicity *in vitro*, micronuclei assays by FACS were carried out. K562 cells were exposed to the drug doses used in the XTT growth inhibition assays in chapter 3.

Cytotoxicity determined by relative survival and RICC for K562 cells treated with MTX alone or in combination with PS341 for 120 hours

The RICC determinations have bigger error bars and higher survival rates than the relative survival determinations. Differences between the two measurements are statistically significant for 7.5 nM, 22.5 nM MTX and the combination of 7.5 nM MTX and 5.2 nM PS341 (Figure 4.9). All of the doses tested were classed as cytotoxic as the relative survival is lower than 40% (Figure 4.9). The relative survival of 5.2 nM PS341 alone, 7.5 nM MTX alone and 22.5 nM MTX alone were 19%, 30% and 10%, respectively. The combination of 5.2 nM PS341 and 7.5 nM MTX had relative survival of 3.3%, significantly lower than 22.5 nM MTX ($p<0.0001$). Thus the PS341 potentiated the effect of MTX after 120 hours, consistent with the data in chapter 3.

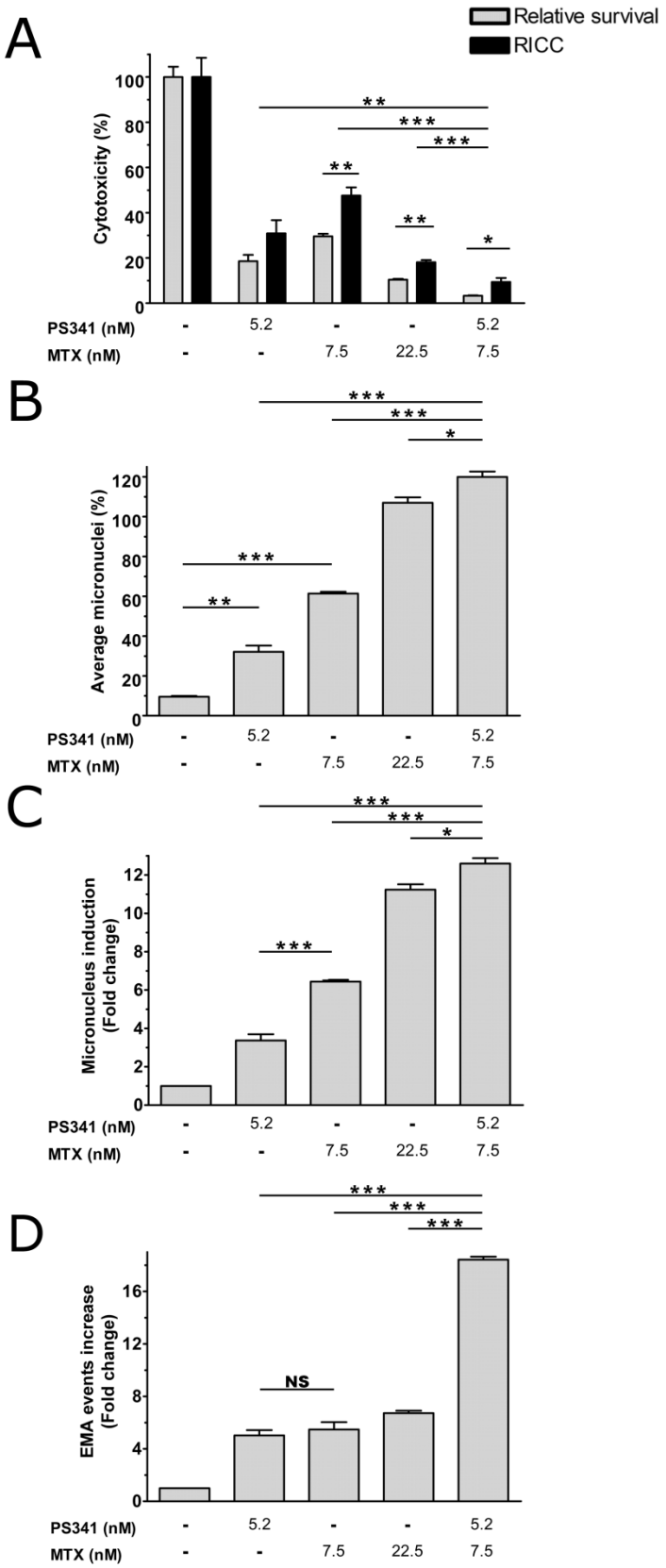

Figure 4.9 K562 cells after 120 hours treatment determined by FACS.

(A) Relative Increase in Cell Count (RICC), (B) Average (%) micronuclei and (C) micronucleus induction (fold change) and (D) apoptosis determined by FACS. (*$p \leq 0.05$, **$p \leq 0.01$, and ***$p \leq 0.005$)

	Relative survival		RICC		Average micronuclei		Micronuclei (Fold change)		EMA increase (Fold change)	
	%	±SEM	%	±SEM	%	±SEM	Fold	±SEM	Fold	±SEM
Untreated	100.0	4.5	100.0	8.5	9.5	0.4	1.0	0.0	1.0	0.0
5.2 nM PS341	18.6	2.8	30.9	5.9	32.1	3.1	3.4	0.3	5.0	0.4
7.5 nM MTX	29.6	1.1	47.6	3.6	61.4	0.9	6.4	0.1	5.5	0.6
22.5 nM MTX	10.4	0.4	18.1	1.0	107.0	2.7	11.2	0.3	6.7	0.2
5.2 nM PS341+ 7.5 nM MTX	3.3	0.2	9.4	1.7	120.0	2.7	12.6	0.3	18.4	0.2

Table 4.6 Mean values with standard error for RICC, average (%) micronuclei and fold change show on figure 4.9.

Micronucleus formation for MTX alone or in combination with PS341 presented as average micronuclei (%) (120 hours incubation)

MTX induced micronuclei significantly above the untreated control levels. In cells treated with 5.2 nM PS341 alone the percent of micronuclei recorded was 32%. This was lower than when 7.5 nM or 22.5 nM MTX was used alone, where the average micronuclei were 67% and 107%, respectively (Figure 4.9B and Table 4.6). The combination resulted in more micronuclei (120%) than 7.5 nM MTX alone and 13% more than 22.5 nM MTX alone. The levels of micronuclei increase with increasing cytotoxicity.

Micronucleus formation (PS341 + MTX) Fold change

5.2 nM PS341 alone was genotoxic, as it induced 3-fold more micronuclei than the untreated control. 7.5 nM MTX alone resulted in 6-fold increase in micronuclei and the combination caused a 12.6-fold increase, more micronuclei than either the PS341 or MTX alone. The micronuclei levels increased as the cytotoxicity level increased.

Apoptotic measurement (EMA positive events increase over untreated control)

The combination produced the highest levels of apoptosis; 18-fold over the untreated control, and significantly higher than 5.2 nM PS341, 7.5 nM MTX, or 22.5 nM MTX ($p<0.0001$) (Figure 4.9D). In these experiments both 5.2 nM PS341 and 7.5 nM MTX alone induced similar levels of apoptosis in K562, ~ 5-fold over untreated control.

Cell cycle distribution: MTX alone or in combination with PS341 for 120 hours

Figure 4.10 shows the cell cycle distribution of cells after 120 hours drug treatments.

The majority of cells in the untreated control were in S phase (60%), with fewer in G_1 (24%) and G_2/M (19%) phases respectively (Table 4.7). The 5.2 nM PS341 treated sample had more cells in G_1 phase and fewer cells in S phase (41%; p=0.0071) compared to the untreated control.

The 7.5 nM MTX treated sample had similar levels of cells in G_1 phase as the untreated control, but fewer cells in S phase (46%; p=0.0176) and more cells in G_2/M phase (26%; p=0.0203) when compared to the untreated control. Cells treated with 22.5 nM MTX or the combination of 7.5 nM MTX and 95 nM MG132 looked similar to each other with most cells in G_2/M phase.

Summary

These doses produced very high levels of cytotoxicity after 120 hours; too high for reliable micronuclei determination by FACS. To address this lower concentrations of PS341 and MTX were used for 48 hours.

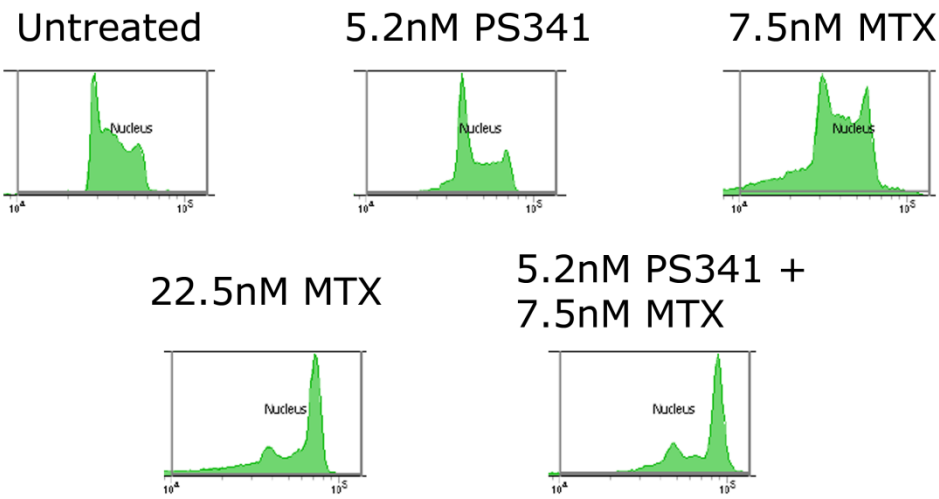

Figure 4.10 Cell cycle distribution of cells treated with MTX alone or in combination with PS341 for 120 hours.

	G_1		S		G_2/M	
	%	±SEM	%	±SEM	%	±SEM
Untreated	24.1	3.0	60.2	3.5	19.1	2.0
5.2 nM PS341	36.9	0.7	40.6	1.7	17.7	1.1
7.5 nM MTX	25.0	1.1	46.2	0.8	26.5	0.3
22.5 nM MTX	15.5	0.9	25.2	0.9	60.4	3.0
5.2 nM PS341 + 7.5 nM MTX	20.6	0.3	26.9	1.4	45.7	1.8

Table 4.7 Cell cycle distribution—Percentage of G_1, S and G_2/M phase cells in K562 cells.

Data shown on figure 4.10 analysed by Flow Jo. Each value is the mean of at least three experiments displayed in table with standard error.

4.6 *In vitro* micronucleus assay with flow cytometric analysis: MTX alone and in combination with lower doses of PS341 (48 hours)

The PS341 concentration was reduced from 5.2 nM to 2.5 nM or 3 nM and a range of MTX concentrations were tested to determine a dose-dependent response. The incubation time was also reduced to 48 hours.

Cytotoxicity was determined by both relative survival and RICC

Data for relative survival (grey) and RICC (black) are plotted on a graph shown in figure 4.11A. The values for relative survival and RICC were comparable in all samples tested. The 2.5 nM and 3 nM PS341 alone had 70% and 60% relative survival (Figure 4.11A). MTX reduced relative survival of K562 in a dose-dependent manner; 55% with 5 nM MTX and 23% with 22.5 nM MTX (Figure 4.11A). 2.5 nM PS341 in combination with 5 nM MTX reduced the relative survival to 47%. It was significantly lower than 5 nM MTX alone (p=0.0073) (Figure 4.11A). The relative survival of the combination with 3 nM PS341 was 36% and was significantly lower than combination with 2.5 nM (p=0.0053). It was also lower than 7.5 nM (41%) and 10 nM (37%) MTX alone, but the differences were not statistically significant (Figure 4.11). 22.5 nM MTX was most cytotoxic.

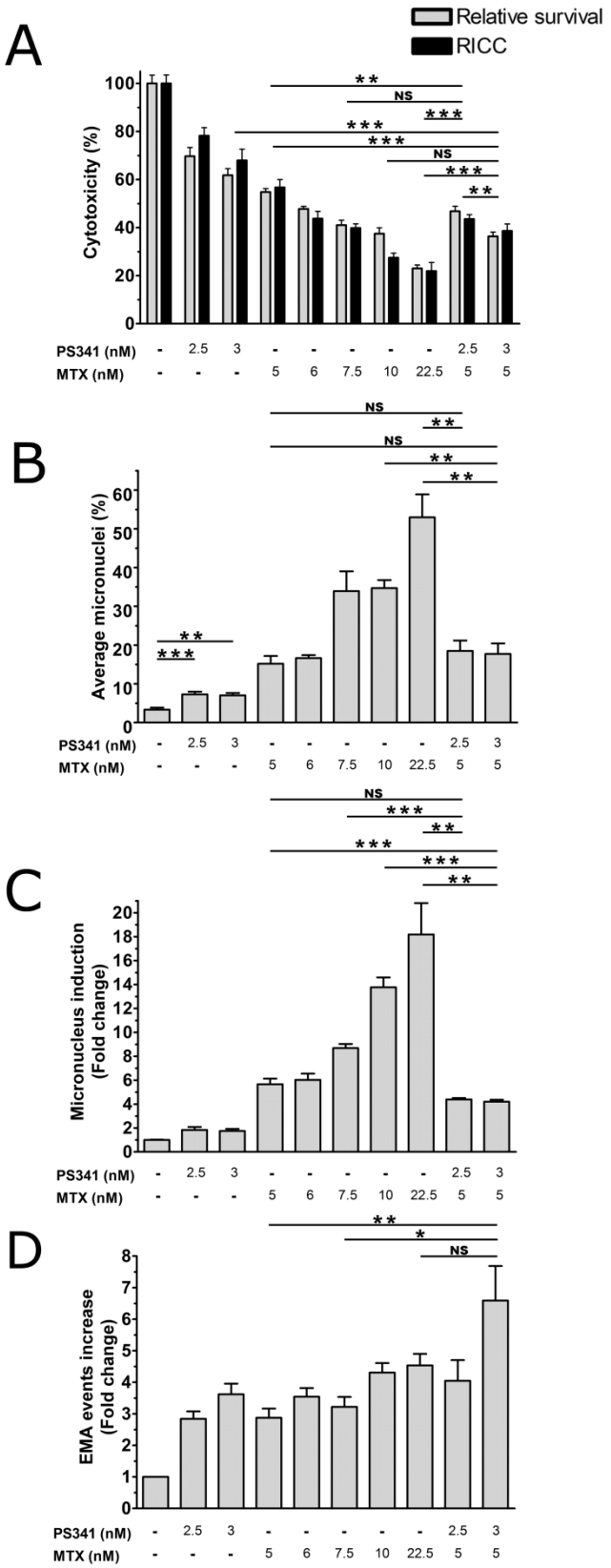

Figure 4.11 Data of K562 cells after 48 hours treatment of MTX with or without PS341.

(A) Relative Increase in Cell Count (RICC), (B) Average (%) micronuclei and (C) micronucleus induction (fold change) and (D) apoptosis determined by FACS. (*$p \leq 0.05$, **$p \leq 0.01$, and ***$p \leq 0.005$)

	Relative survival		RICC		Average micronuclei		Micronuclei (Fold change)		EMA increase (Fold change)	
	%	±SEM	%	±SEM	%	±SEM	Fold	±SEM	Fold	±SEM
Untreated	100.0	3.4	100.0	3.0	3.3	0.5	1.0	0.0	1.0	0.0
2.5 nM PS341	70.5	6.6	76.1	5.6	7.3	0.7	1.8	0.2	2.8	0.2
3 nM PS341	61.5	2.6	64.8	2.6	7.0	0.6	1.8	0.2	3.6	0.3
5 nM MTX	54.8	1.4	56.7	3.3	15.2	2.0	5.7	0.5	2.9	0.3
6 nM MTX	47.8	1.1	43.5	1.4	16.6	0.8	6.0	0.5	3.5	0.3
7.5 nM MTX	41.0	2.0	38.5	2.1	33.9	5.1	8.7	0.4	3.2	0.3
10 nM MTX	37.4	2.5	27.5	1.9	34.7	2.1	13.8	0.8	4.3	0.3
22.5 nM MTX	23.0	1.4	19.7	3.5	53.0	5.9	18.2	2.6	4.5	0.4
2.5 nM PS341 + 5 nM MTX	46.8	2.1	43.6	1.8	18.5	2.7	4.4	0.1	4.0	0.7
3 nM PS341 + 5 nM MTX	36.3	1.8	38.6	2.9	17.7	2.7	4.2	0.2	6.6	1.1

Table 4.8 Mean values with standard error for RICC, average (%) micronuclei and fold change show on figure 4.11.

Micronucleus formation with MTX alone or in combination with PS341 presented as average micronuclei (%) following a 48-hour incubation

The average level of micronuclei in the untreated control cells was 3.3%. Micronucleus levels of cells exposed to 2.5 nM or 3 nM PS341 alone were 7.3% and 7.0%, respectively, and significantly higher than untreated controls (p=0.0007 and p=0.0012, respectively) (Figure 4.11B).

MTX induced micronuclei significantly above background, and it was dose-dependent (Figure 4.11B).

The combination of 5 nM MTX with 2.5 nM PS341 generated 19% average micronuclei, higher than 2.5 nM PS341, 5 nM or 6 nM MTX alone (7.3, 15 and 16.6%, respectively) but the differences were not statistically significant (Figure 4.11B and Table 4.8). 22.5 nM MTX alone generated 53% average micronuclei. Figure 4.11A shows 5 nM and 6 nM MTX alone had comparable cytotoxicity to the combination with 2.5 nM PS341.

The combination of 5 nM MTX with 3 nM PS341 generated 17.7% average micronuclei which was similar to the combination with 2.5 nM PS341 (18.5%). Figure 4.11A shows this combination had similar cytotoxicity to 7.5 nM or 10 nM MTX alone. The average micronuclei induced by the combinations were significantly lower than that generated by 7.5 nM MTX (p=0.045) or 10 nM MTX (p=0.005) alone (Figure 4.11B).

22.5 nM MTX alone resulted in 53% average micronuclei. The combination with 2.5 nM (p=0.0043) or 3 nM PS341 (p=0.0037) had significantly lower levels of micronuclei than 22.5 nM MTX (Figure 4.11B).

Micronucleus formation in fold change over untreated control after 48 hours treatment

Figure 4.11C micronucleus formation is presented as fold increase over untreated control.

PS341 alone induced micronuclei above background but the induction was lower than two-fold over untreated control (Figure 4.11C). The micronucleus induction by MTX alone was dose-dependent which is shown by average micronuclei and fold change on figure 4.11B and C.

The combination of 5 nM MTX with 2.5 nM or 3 nM PS341 had 4.4 and 4.2 fold increase in micronuclei. The micronuclei induced by the combination of 5 nM MTX with 2.5 nM (p=0.0002) or 3 nM (p<0.0001) PS341 were significantly lower than any of the concentrations of MTX tested (Figure 4.11C). This demonstrates that the combination induced fewer micronuclei than cells treated with MTX alone.

Apoptotic measurement (EMA positive events increase over untreated control) after a 48-hour incubation

Apoptotic cells increased by 2.8-fold or 3.6-fold over the control after treatment with 2.5 nM or 3 nM PS341 alone. MTX produced a dose-dependent increase in apoptotic cells. With 5 nM MTX alone the increase was 2.9-fold, similar to 2.5 nM PS341 alone (Figure 4.11D and Table 4.8).

The combination of 3 nM PS341 and 5 nM MTX increased apoptosis to 6.6-fold above the untreated control, which was significantly higher than 3 nM PS341 alone (p=0.0323) or 5 nM MTX alone (p=0.002) (Figure 4.11D). The combination of 3 nM PS341 and 5 nM MTX had similar cytotoxicity (36.3%) to 7.5 nM or 10 nM MTX alone (41% and 37.4%) (Figure 4.11A). The apoptotic cell level of this combination was significantly higher than 7.5 nM MTX (p=0.0107), but not significantly different to 10 nM MTX alone (Figure 4.11D).

Cell cycle distribution: MTX alone or in combination with PS341 for 48 hours

DNA content of each "healthy" nucleus was recorded by FACS. The data was plotted against DNA content, displayed in figure 4.12. Cell cycle distributions were analysed by FlowJo, and statistical significances were determined using the unpaired t-test.

In the untreated control, 50% of cells were in S phase, 37% in G_1 (37%) and 15% in G_2/M. This pattern was observed in cells treated with 2.5 nM or 3 nM PS341 alone (Figure 4.12 and Table 4.9). MTX reduced the proportion of cells at G_1 and S phases. A bigger population of cells accumulated at G_2/M phase. This observation was more distinctive when MTX concentration increased (Figure 4.12). Cycle distribution of the combination with both 2.5 nM and 3 nM PS341 were similar to 5 nM or 6 nM MTX. The majority of cells were in S phase and an increased proportion of cells were in the G_2/M phase. The rise in cells in G_2/M phase was significantly higher than in the untreated control (p<0.0001) (Figure 4.12) but significantly lower than MTX alone.

Summary

A high level of micronuclei was observed in cells treated with high concentrations of MTX (7.5 nM -22.5 nM). The cytotoxicity, micronucleus formation and G_2/M accumulation of MTX alone were found to be dose-dependent.

MTX in combination with PS341 showed higher cytotoxicity, lower micronucleus formation and lower level of G_2/M phase accumulation than 5 nM MTX alone. These results suggest micronucleus formation might be related to the cell cycle distribution.

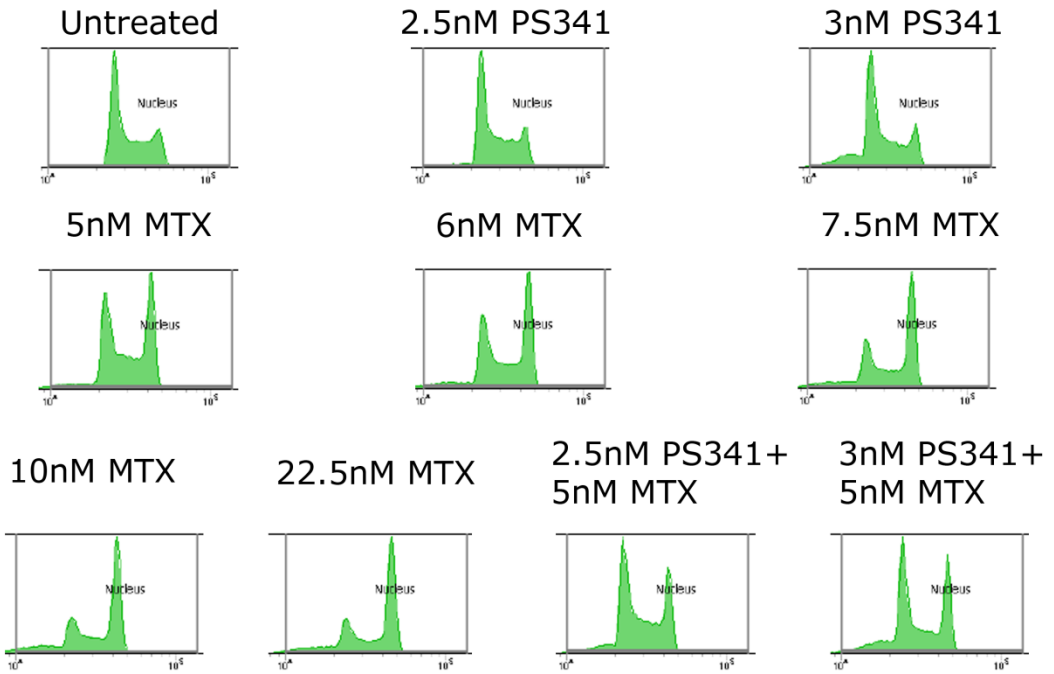

Figure 4.12 Cell cycle distribution of cells treated with MTX or in combination with PS341 for 48 hours.

	G_1		S		G_2/M	
	%	±SEM	%	±SEM	%	±SEM
Untreated	37.0	2.2	49.8	1.6	14.5	0.6
2.5 nM PS341	31.5	0.5	51.6	0.4	14.5	0.6
3 nM PS341	29.5	1.5	47.3	1.1	14.4	0.6
5 nM MTX	27.0	1.3	44.3	0.8	29.3	1.5
6 nM MTX	23.4	1.4	43.4	2.4	29.3	3.0
7.5 nM MTX	23.4	2.0	35.9	1.6	40.1	2.2
10 nM MTX	15.3	0.9	32.8	2.2	44.1	3.3
22.5 nM MTX	11.8	1.8	21.8	1.1	67.1	3.5
2.5 nM PS341 + 5 nM MTX	28.0	0.7	44.7	1.2	22.4	1.2
3 nM PS341 + 5 nM MTX	28.0	2.3	37.4	1.0	25.1	1.1

Table 4.9 Cell cycle distribution—Percentage of G_1, S and G_2/M phase cells in K562 cells.

Data shown on figure 4.12 analysed by Flow Jo. Each value is the mean of at least three experiments, displayed in table with standard error.

4.7 Conclusion and discussion

The aim of this chapter was to address the question of whether proteasomal inhibition potentiated cytotoxicity and reduced genotoxicity of MTX.

Micronucleus assays have been carried out in two ways by microscopy and by FACS to compare the combination of 95 nM MG132 and 5 nM MTX with 5 nM MTX or 22.5 nM MTX alone. Using both methods the combination induced less micronuclei than 5 nM or 22.5 nM MTX alone. The percentage of micronuclei detected by FACS was much higher than by microscopy. For example the average percentages of micronuclei detected in untreated cells by microscopy and FACS were 0.3% and 3.9%, respectively (Table 4.10).

The proteasome inhibitor PS341 potentiated the cytotoxic effect of MTX after treatment for 120 hours. However, cells exposed to these doses and combinations have a relative survival lower than 30%, too low for reliable use in FACS. Therefore the dose of PS341 was reduced from 5.2 nM to 2.5 nM or 3 nM with 5 nM MTX and cells were treated for 48 hours. PS341 potentiated 5 nM MTX. The combination of 2.5 nM or 3 nM PS341 with 5 nM MTX showed comparable cytotoxicity to 7.5 nM or 10 nM MTX. Moreover the combination produced lower genotoxicity than MTX alone. Exposure to 2.5 nM or 3 nM proteasome inhibitor alone for 48 hours was not genotoxic to K562 cells. The relative survival dropped when PS341 was combined with 5 nM MTX, and the percentage of micronuclei increased to a level similar to 5 nM or 6 nM MTX. Micronucleus induction was MTX dose-dependent. This showed that proteasomal inhibition by PS341 potentiated the cytotoxicity of MTX using two cytotoxicity assays (RICC and relative survival). The combination of 3 nM PS341 with 5 nM MTX produced fewer micronuclei than 7.5 nM, 10 nM or 22.5 nM MTX alone, and even fewer than with 5 nM and 6 nM MTX alone by fold change.

A

	RICC		Average micronuclei (%)		Micronuclei fold change	
	%	±SEM	%	±SEM	change	±SEM
Untreated	100.0	0.0	0.3	0.1	1.0	0.0
95 nM MG132	82.3	10.9	0.3	0.1	1.3	0.3
5 nM MTX	52.4	4.4	3.3	0.7	13.5	3.8
22.5 nM MTX	13.8	1.3	3.8	0.4	11.6	5.2
95 nM MG132+ 5 nM MTX	25.2	4.7	0.9	0.1	3.5	0.7

B

	RICC		Average micronuclei		Micronuclei (Fold change)		EMA increase (Fold change)	
	%	±SEM	%	±SEM	Fold	±SEM	Fold	±SEM
Untreated	100.0	0.0	3.9	1.0	1.0	0.0	1.0	0.0
95 nM MG132	91.7	6.1	2.9	0.7	0.8	0.0	0.9	0.1
5 nM MTX	49.5	5.9	50.8	16.5	13.0	2.9	16.3	7.9
22.5 nM MTX	23.9	7.4	173.6	42.5	46.0	5.0	18.4	8.3
95 nM MG132+ 5 nM MTX	46.0	8.3	26.6	4.4	7.2	0.7	6.2	8.3

Table 4.10 Summary of micronucleus data (A) Microscopy and (B) FACS.

Chapter 5. E3 ligase inhibition and the growth inhibitory effects of TOP2 poisons

5.1 Introduction

This investigation used two E3 ligase inhibitors (PRT4165 and HLI373) in combination with different groups of TOP2 poisons (MTX, epipodophyllotoxins, mAMSA and anthracyclines) to determine the effect on cell growth inhibition by XTT assay.

The ubiquitin-proteasome system (UPS) is a major protein degradation pathway in cells. Ubiquitin acts as a meditator to trigger the proteasome to degrade the target protein. The system starts with ubiquitin activation by an E1 ubiquitin activator which is then transferred to an E2 ubiquitin conjugating enzyme. Both E2 and the target protein are bound to an E3 ligase. The activated ubiquitin is transferred to the target protein. This step is repeated until a ubiquitin chain is formed on the target protein. The ubiquitin chain acts as a trigger to activate proteasome degradation (Ciechanover, 2005; Goldberg, 2007).

Cells have more than 600 different E3 ligases which largely determine substrate specificity. Therefore E3 ligase inhibition would be more specific than proteasome inhibition. Two E3 ligases, Bmi1/Ring and HDM2, have been implicated in TOP2A degradation after exposure to a TOP2 poison.

Bmi1/Ring1A is an E3 ubiquitin ligase involved in drug-induced TOP2A degradation (Alchanati *et al.*, 2009). PRT4165 was reported as a small-molecule inhibitor of Bmi1/Ring1A. It inhibits the Bmi1/Ring1A-induced ubiquitination of TOP2A and the TOP2A degradation induced by VM26 (Alchanati *et al.*, 2009).

HDM2 (called mdm2 in mouse) is an E3 ligase which interacts with and regulates the degradation of p53. HDM2 also interacts with TOP2A in the cell and is involved in VP16-induced TOP2A degradation (Nayak *et al.*, 2007). In *mdm2* knockdown MEF cells, TOP2A was not degraded after VP16 exposure (Nayak *et al.*, 2007). This suggests that inhibition of

HDM2 might prevent TOP2A degradation after exposure to VP16 (Conradt *et al.*, 2013). HLI373 is an E3 ligase inhibitor targeting HDM2 (Kitagaki *et al.*, 2008).

The aim of this chapter was to test whether inhibiting an E3 ligase reported to inhibit TOP2A degradation potentiated growth inhibition by TOP2 poisons in K562 cells.

5.2 E3 ligase inhibition and the effect of MTX on the K562 cell line

Growth inhibition by a Bmi1/Ring1A inhibitor (PRT4165) in K562 cells

For the potentiation assay, a dose of PRT4165 which inhibits K562 cell growth by 20% is needed. The XTT assay was used to determine the IC_{20} of PRT4165. K562 cells were seeded at approximately 2 x 10^3 cells per well in 96-well plates for 24 hours and then treated with increasing concentrations of PRT4165 for 120 hours. According to figure 5.1, 95 μM of PRT4165 inhibited K562 cell growth by 20%. This dose was used in potentiation assays with TOP2 poisons.

Bmi1/Ring1A inhibitor (PRT4165) potentiates growth inhibition by MTX in K562 cells

The potentiation effect was examined by XTT assay. K562 cells were treated with increasing concentrations of the TOP2 poison MTX, alone or in combination with a fixed concentration of PRT4165 (95 μM). The OD_{450nm} values of MTX alone were normalised to 0 nM MTX as 100%, and OD_{450nm} values of MTX in combination with PRT4165 were normalised to 0 nM MTX control in the presence of 95 μM PRT4165 as 100%. Figure 5.2 shows the presence of PRT4165 significantly increased growth inhibition by MTX (Pf_{50}= 3.73). This shows that MTX can be potentiated by E3 ligase inhibition in K562 cells.

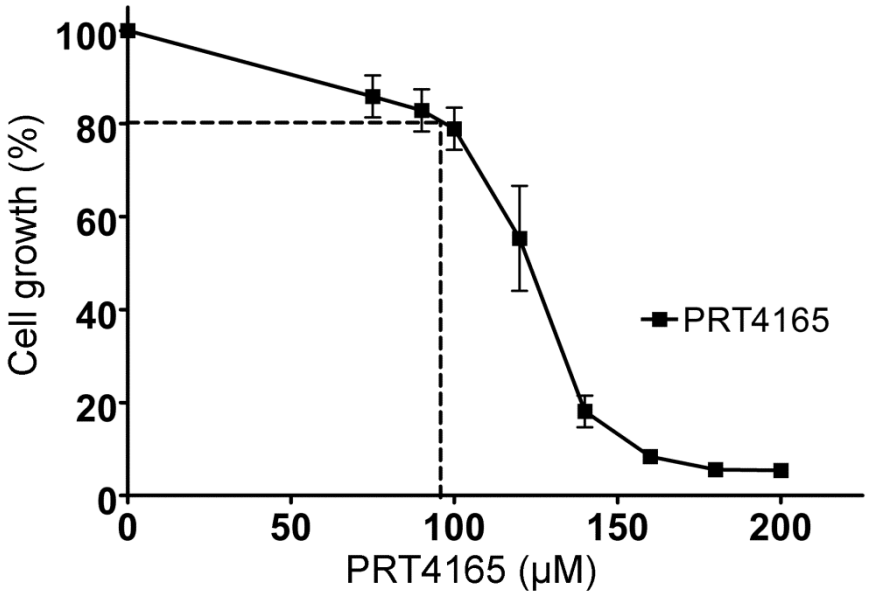

Figure 5.1 Growth inhibition curve of E3 ligase (Bmi1/Ring1A) inhibitor PRT 4165 in K562 cells.

K562 cells were seeded at approximately $2x10^3$ cells per well in a 96-well plates for 24 hours prior to PRT 4165 drug treatment. After 120 hours of drug exposure, cells were stained with XTT and OD_{450nm} was quantified. Results are means of four experiments ± standard error of the mean.

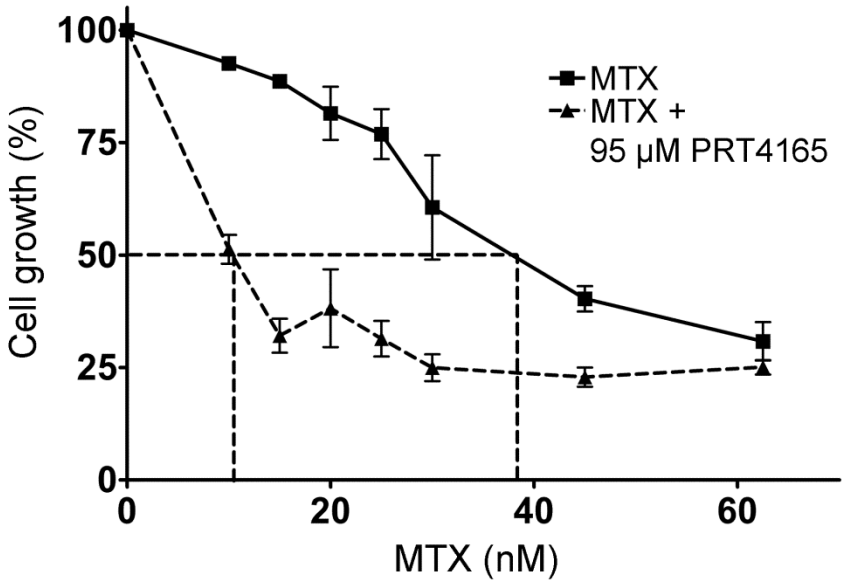

Figure 5.2 Potentiation of MTX by PRT4165 in K562 cells.

Cells were treated with increasing concentrations of MTX alone or in combination with 95 μM PRT4165 for 5 days followed by XTT staining. Dose–response curves were used to estimate the IC_{50} of MTX alone or in combination with PRT4165. Error bars represent the mean ± SEM of at least 3 separate experiments for both + and – PRT4165 conditions. Values were normalised to the 0 nM MTX value (100%).

HLI373 growth curve

For the potentiation study, the IC_{20} of HLI373 in K562 cells was required. Growth inhibition was determined by XTT assay. K562 cells were seeded and treated with HLI373 for 120 hours, followed by XTT staining. The absorbance readings of untreated cells were set at 100% and all the readings were normalised to it. The data shows approximately 3.75 μM HLI373 inhibited 20% of K562 cell growth (Figure 5.3). This concentration of HLI373 was used in combination with the TOP2 poison MTX to study whether HDM2 inhibition increases the growth inhibitory effects of MTX.

HLI373 potentiates MTX-induced growth inhibition

K562 cells were seeded and treated with a range of concentrations of MTX alone or in combination with a fixed concentration of 3.75 μM HLI373 for 120 hours. The OD_{450nm} values of MTX alone were normalised to 0 nM MTX as 100%, and OD_{450nm} values of MTX in combination with HLI373 were normalised to 0 nM MTX control in the presence of 3.75 μM HLI373 as 100%. The results show the presence of HLI373 significantly potentiated the growth inhibitory effect of MTX (Pf_{50}=4.38) (Figure 5.4). The difference between the IC_{50} values of MTX alone and in combination with HLI373 were statistically significant by unpaired *t*-test (*p*=0.0003) (Figure 5.4). This result suggests inhibition of HDM2 can potentiate the effect of MTX in cells.

Mitoxantrone +	Mean of Pf_{50}	SEM	*p*-value
PRT4165	3.73	0.035	0.002
HLI373	4.38	0.45	0.0003

Table 5.1 Potentiation factor (Pf_{50}) summary of mitoxantrone (MTX) in combination with E3 ligase inhibitors.

Statistical significance between IC_{50} values of MTX alone and in combination with E3 ligase inhibitors by unpaired *t*-test (*p*-value).

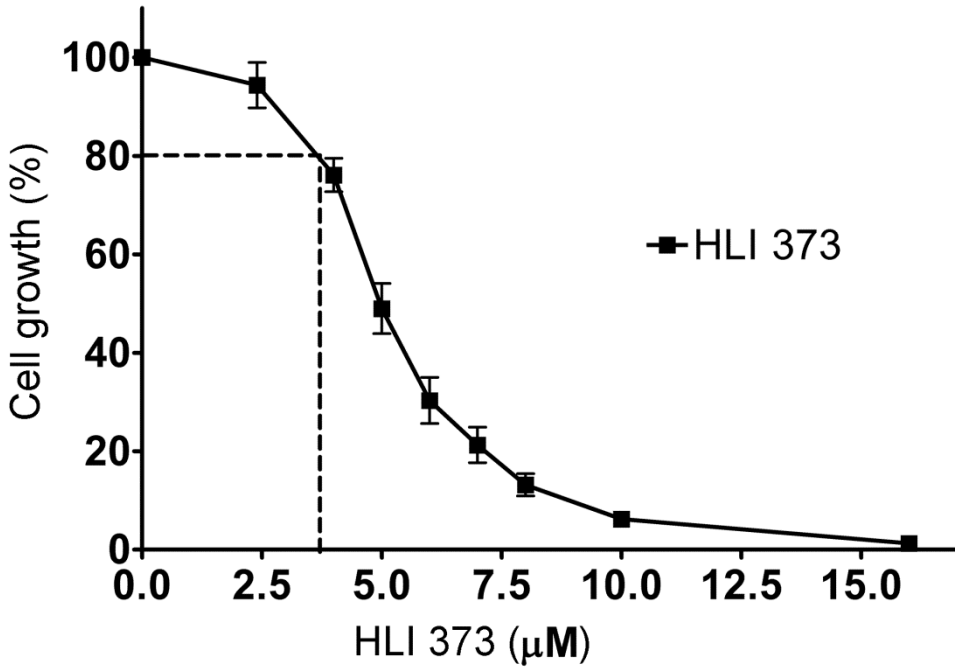

Figure 5.3 Growth inhibition curve of E3 ligase (HDM2) inhibitor HLI373 in K562 cells.

K562 cells were seeded at approximately $2x10^3$ cells/well in a 96-well plate for 24 hours prior to HLI-373 drug treatment. After 120 hours of drug exposure, cells were stained with XTT and OD_{450nm} was quantified. Results are means of four experiments ± standard error of the mean.

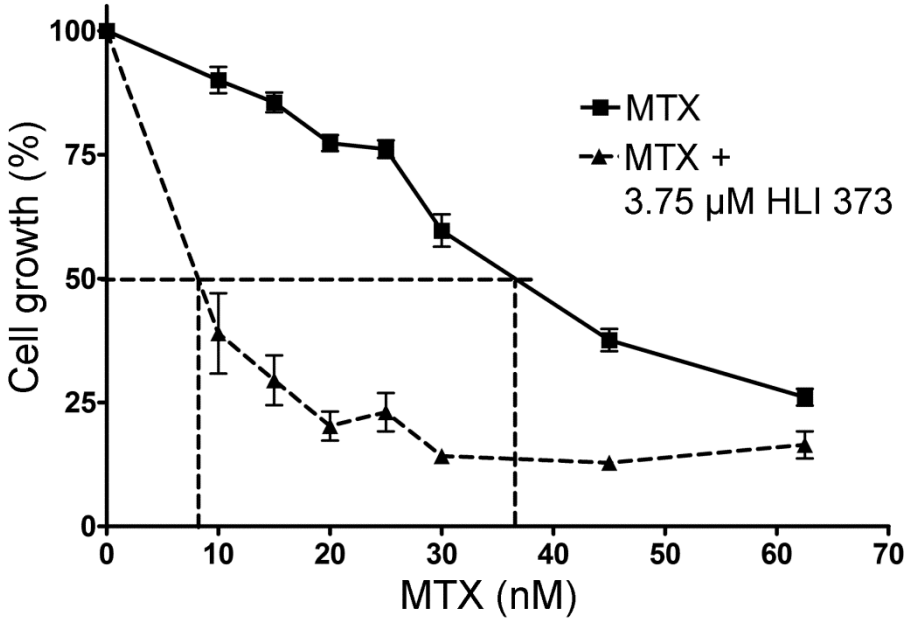

Figure 5.4 Potentiation of MTX by HLI373 in K562 cells.

Cells were treated with increasing concentrations of TOP2 poison alone or in combination with 3.75 μM HLI 373 for 5 days followed by XTT staining. Dose–response curves were used to estimate the IC_{50} of TOP2 poison alone or in combination with HLI373. Error bars represent the mean ± SEM of at least 3 separate experiments for both + and – HLI373 conditions, and values were normalised to the 0 nM of TOP2 poison value (100%).

5.3 E3 ligase inhibition and the effect of epipodophyllotoxins on the K562 cell line

Bmi1/Ring1A inhibition potentiates growth inhibition by epipodophyllotoxins

VP16 and VM26 were used to study the potentiation of epipodophyllotoxins in combination with PRT4165. Alchanati et al., 2009 demonstrated that silencing Bmi1 increased the sensitivity of HeLa cells and A549 lung cancer cells to VM26. Moreover, the cytotoxicity of VM26 was increased by PRT4165 in a synergistic manner (Alchanati *et al.*, 2009). Potentiation assays were performed to investigate the effect of PRT4165 on epipodophyllotoxin-induced growth inhibition.

K562 cells were treated with epipodophyllotoxin alone or in combination with a fixed concentration of PRT4165 (95 μM). VP16 and VM26-induced growth inhibition was potentiated by PRT4165, with both IC_{50} values reduced in the presence of PRT4165 (Figure 5.5). The effect with VM26 (Pf_{50} =2.84) was greater than with VP16 (Pf_{50} =1.76). These results show that Bmi1/Ring1A inhibition potentiates the growth inhibitory effects of epipodophyllotoxins.

HDM2 inhibition and the effect of epipodophyllotoxins in K562 cells

To investigate whether epipodophyllotoxins could also be potentiated by HDM2 inhibition, potentiation assays were performed with VP16 and VM26 in the presence of HLI373. VP16 and VM26 were used alone or in combination with the HDM2 inhibitor (HLI373) to treat K562 cells for 120 hours. Epipodophyllotoxin-induced growth inhibition was potentiated by HLI373. The potentiation factors (Pf_{50}) of VP16 and VM26 were 1.49 and 1.75, respectively. The potentiation effect toward VM26 was greater than VP16.

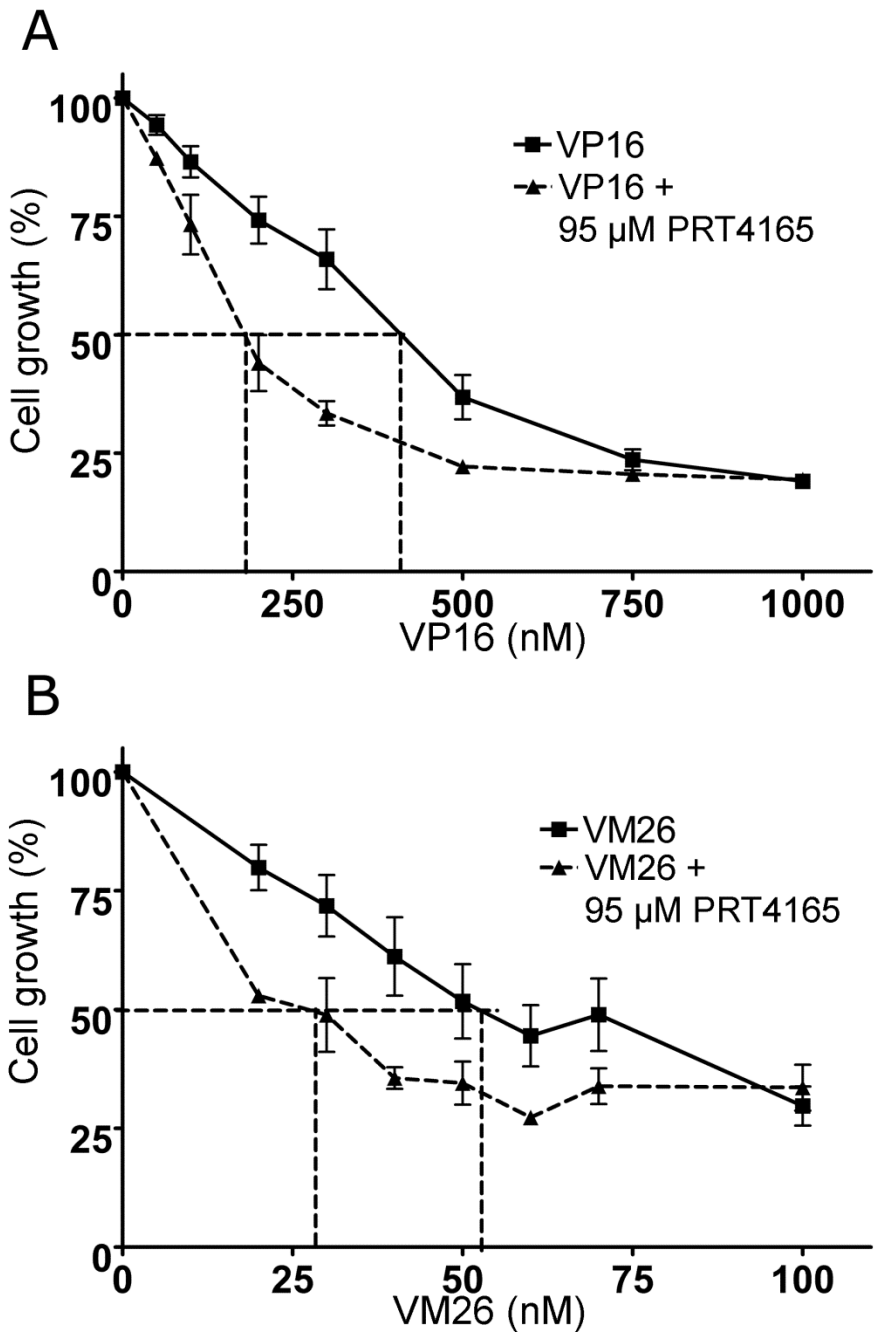

Figure 5.5 Potentiation of epipodophyllotoxins (VP16 and VM26) by PRT4165 in K562 cells.

Cells were treated with increasing concentrations of VP16 (A) or VM26 (B) alone or in combination with 95 µM PRT4165 for 5 days followed by XTT staining. Dose–response curves were used to estimate the IC_{50} of epipodophyllotoxin alone or in combination with PRT4165. Error bars represent the mean ± SEM of at least 3 separate experiments for both + and – PRT4165 conditions. Values were normalised to the 0 nM epipodophyllotoxin value (100%).

Etoposide +	Mean of Pf_{50}	SEM	*p*-value
PRT4165	1.75	0.16	0.0494
HLI373	1.49	0.13	0.022

Table 5.2 Potentiation factor (Pf_{50}) summary of VP16 in combination with E3 ligase inhibitors.

Statistical significance between IC_{50} values of etoposide (VP16) alone and in combination with E3 ligase inhibitors by unpaired *t*-test (*p*-value).

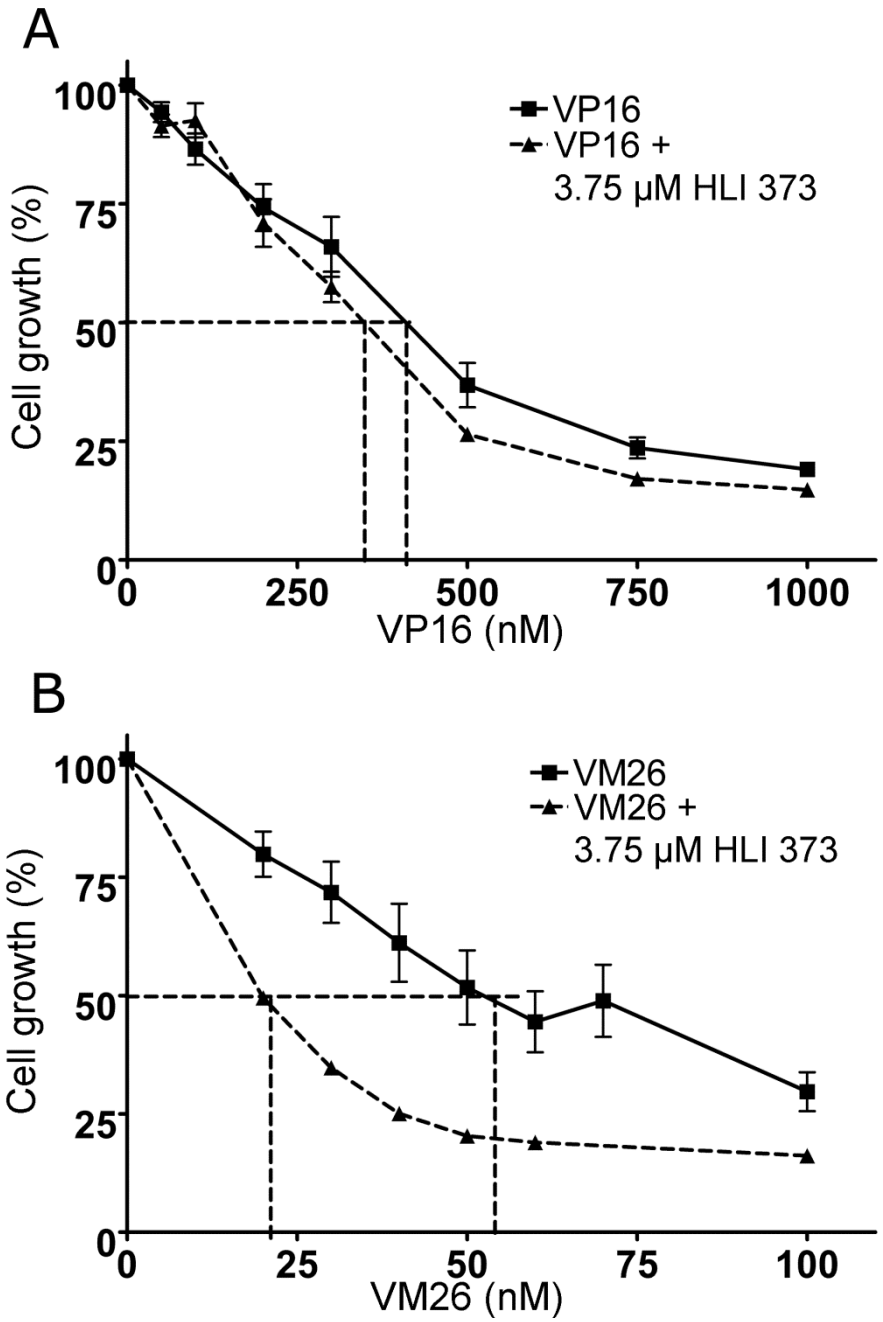

Figure 5.6 Potentiation of epipodophyllotoxins (VP16 and VM26) by HLI373 in K562 cells.

Cells were treated with increasing concentrations of VP16 (A) or VM26 (B) alone or in combination with 3.75 µM HLI373 for 5 days followed by XTT staining. Dose–response curves were used to estimate the IC_{50} of epipodophyllotoxin alone or in combination with HLI373. Error bars represent the mean ± SEM of at least 3 separate experiments for both + and – HLI373 conditions. Values were normalised to the 0 nM epipodophyllotoxin value (100%).

Teniposide +	Mean of Pf_{50}	SEM	*p*-value
PRT4165	2.84	0.59	0.015
HLI373	1.76	0.12	0.0026

Table 5.3 Potentiation factor (Pf_{50}) summary of VM26 in combination with E3 ligase inhibitors.

Statistical significance between IC_{50} values of teniposide (VM26) alone and in combination with E3 ligase inhibitors by unpaired *t*-test (*p*-value).

5.4 E3 ligase inhibition and the effect of amsacrine on the K562 cell line

Bmi1/Ring1A inhibition and the growth inhibitory effect of mAMSA in K562 cells

The effect of Bmi1/Ring1A inhibition on mAMSA-induced growth inhibition was determined by XTT assay. K562 cells were treated with mAMSA alone or in combination with a fixed concentration of PRT4165 (95 μM) for 120 hours. The OD_{450nm} values of mAMSA alone were normalised to 0 nM mAMSA (100%), and OD_{450nm} values of mAMSA in combination with PRT4165 were normalised to 0 nM mAMSA control in the presence of 95 μM PRT4165 (100%). Figure 5.7 shows that the presence of PRT4165 potentiated the growth inhibitory effect of mAMSA (Pf_{50}=1.48) (Table 5.4).

HDM2 inhibition and the growth inhibitory effect of mAMSA in K562 cells

The effect of HLI373 treatment on mAMSA-induced growth inhibition was studied by XTT assay. K562 cells were treated with mAMSA alone or in combination with 3.75 μM HLI373 for 120 hours. The OD_{450nm} values of mAMSA alone were normalised to 0 nM mAMSA (100%), and OD_{450nm} values of mAMSA in combination with HLI373 were normalised to 0 nM mAMSA control in the presence of 3.7 μM HLI373 (100%). In the presence of HLI373, the IC_{50} of mAMSA was about 65 nM (p=0.0345) (Figure 5.8). The Pf_{50} was 1.39 (Table 5.4).

mAMSA +	Mean of Pf_{50}	SEM	*p*-value
PRT4165	1.48	0.04	0.0026
HLI373	1.39	0.04	0.0345

Table 5.4 Potentiation factor (Pf_{50}) summary of mAMSA in combination with E3 ligase inhibitors.

Statistical significance between IC_{50} values of mAMSA alone and in combination with E3 ligase inhibitors by unpaired *t*-test (*p*-value).

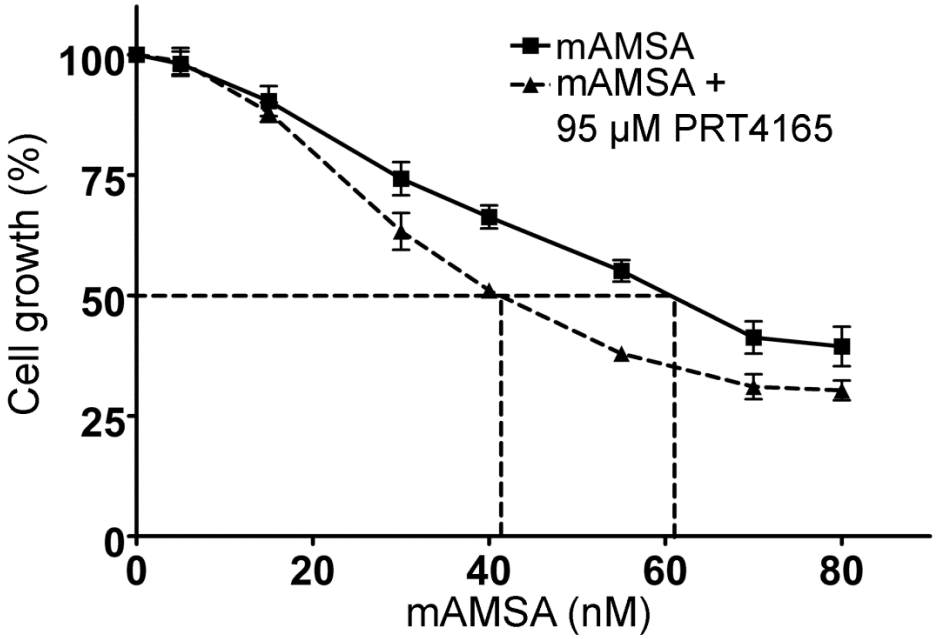

Figure 5.7 Potentiation of mAMSA by PRT4165 in K562 cells.

Cells were treated with increasing concentrations of mAMSA alone or in combination with 95 μM PRT4165 for 5 days followed by XTT staining. Dose–response curves were used to estimate the IC_{50} of mAMSA alone or in combination with PRT4165. Error bars represent the mean ± SEM of at least 3 separate experiments for both + and – PRT4165 conditions. Values were normalised to the 0 nM mAMSA value (100%).

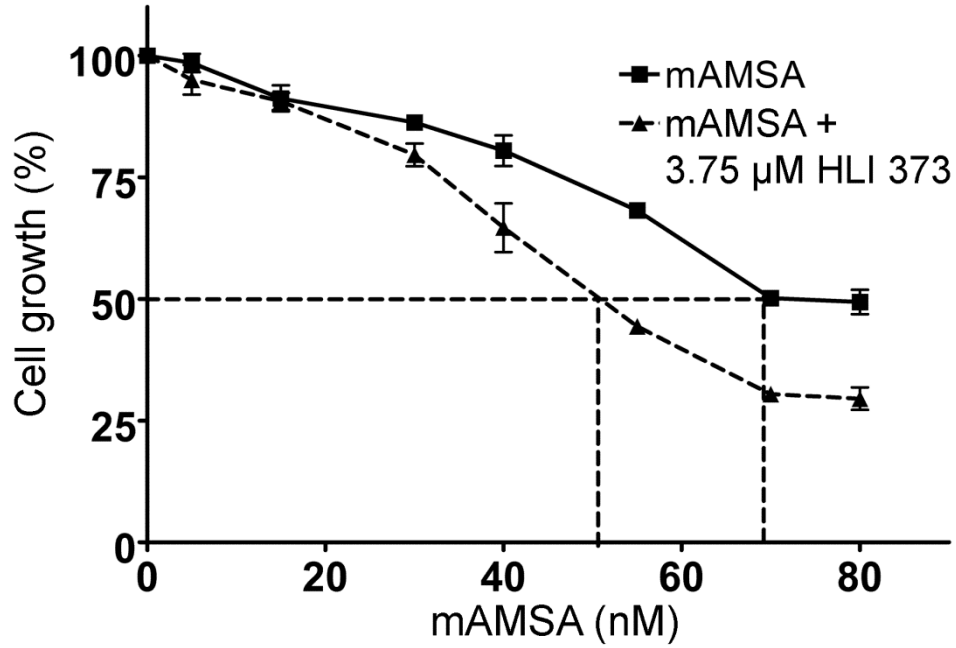

Figure 5.8 Potentiation of mAMSA by HLI373 in K562 cells.

Cells were treated with increasing concentrations of mAMSA alone or in combination with 3.75 μM HLI373 for 5 days followed by XTT staining. Dose–response curves were used to estimate the IC_{50} of mAMSA alone or in combination with HLI373. Error bars represent the mean ± SEM of at least 3 separate experiments for both + and – HLI373 conditions. Values were normalised to the 0 nM mAMSA value (100%).

5.5 E3 ligase inhibition and effect of anthracyclines in the K562 cell line

Bmi1/Ring1A inhibition and the growth inhibitory effect of anthracyclines in K562 cells

The effect of PRT4165 on anthracycline-induced growth inhibition was determined by XTT assay. Four anthracyclines (Dau, Dox, Epi, and Ida) were tested in this study. K562 cells were seeded and then treated with anthracyclines alone or in combination with a fixed concentration of PRT4165 (95 μM) for 120 hours. The OD_{450nm} values of 0 nM of anthracycline and 95 μM PRT4165 were set as 100%, and all values were normalised to it. The presence of PRT4165 reduced the IC_{50} of all anthracyclines tested (Figure 5.9). Epi had the greatest potentiation (Pf_{50} 1.91) and Dox had the lowest (Pf_{50} 1.16) (Table 5.6 and Table 5.7). The results suggest that inhibition of Bmi1/Ring1A potentiates the effect of anthracyclines in cells.

HDM2 inhibition and the growth inhibitory effect of anthracyclines in K562 cells

Four anthracyclines (Dau, Dox, Epi and Ida) were used to treat K562 cells alone or in combination with a fixed concentration (3.75 μM) of HLI373. After 120 hours treatment the XTT assay was used to determine the effect on growth inhibition. The results show that HLI373 potentiates the effect of anthracyclines (Figure 5.10). Epi had the highest potentiation effect (Pf_{50}=1.72) and Dox had the lowest (Pf_{50} =1.22) (Table 5.6 and Table 5.7). The results show that HDM2 inhibition potentiates the growth inhibition effect of anthracyclines. The level of potentiation varies depending on the drug used.

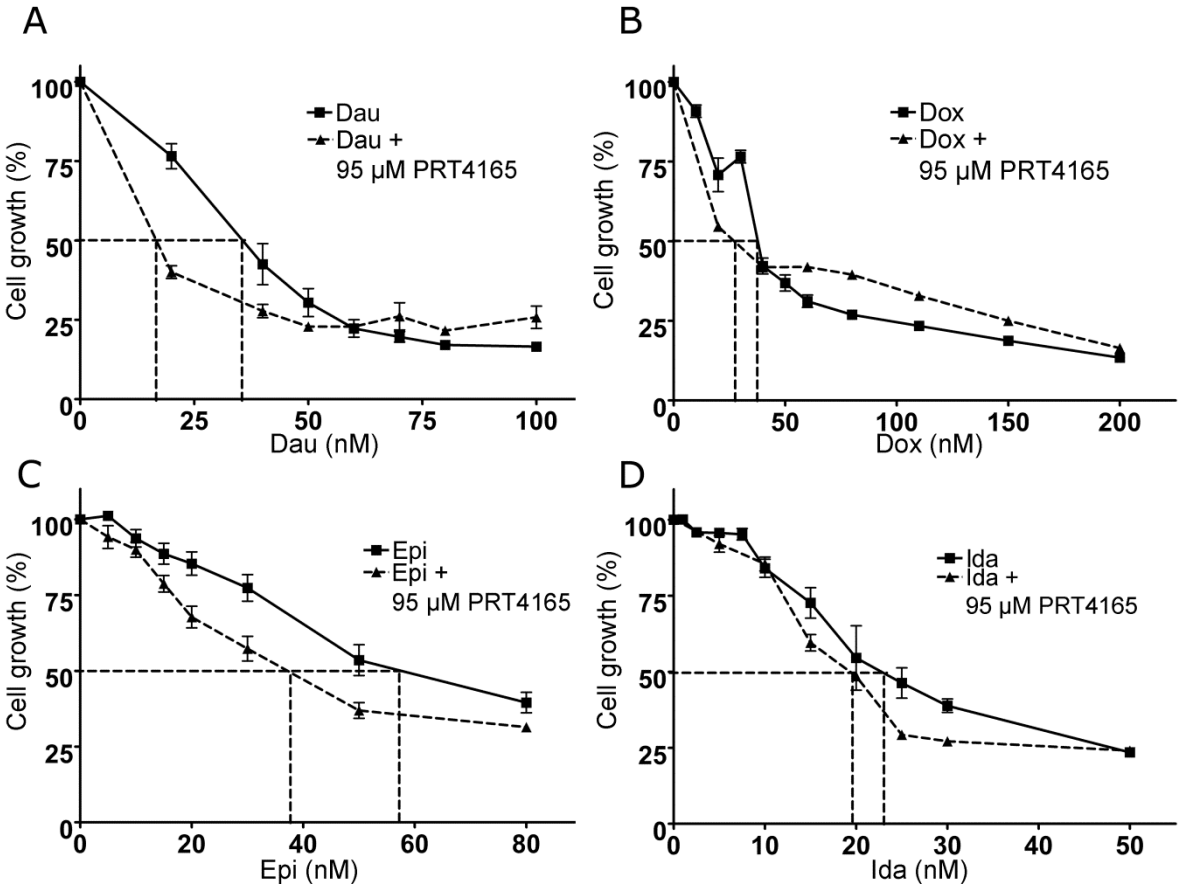

Figure 5.9 Potentiation of anthracyclines (Dau, Dox, Epi and Ida) by PRT4165 in K562 cells.

Cells were treated with increasing concentrations of anthracycline (A) Dau, (B) Dox, (C) Epi and (D) Ida alone or in combination with 95 μM PRT4165 for 5 days followed by XTT staining. Dose–response curves were used to estimate the IC_{50} of anthracycline alone or in combination with PRT4165. Error bars represent the mean ± SEM of at least 3 separate experiments for both + and – PRT4165 conditions. Values were normalised to the 0 nM anthracycline value (100%).

Daunorubicin +	Mean of Pf_{50}	SEM	*p*-value
PRT4165	1.74	0.09	0.0067
HLI373	1.41	0.04	0.0071

Table 5.5 Potentiation factor (Pf_{50}) summary of daurubicin (Dau) in combination with E3 ligase inhibitors.

Statistical significance between IC_{50} values of Dau alone and in combination with E3 ligase inhibitors by unpaired *t*-test (*p*-value).

Doxorubicin +	Mean of Pf_{50}	SEM	*p*-value
PRT4165	1.16	0.05	0.0257
HLI373	1.22	0.03	0.0024

Table 5.6 Potentiation factor (Pf_{50}) summary of Dox in combination with E3 ligase inhibitors.

Statistical significance between IC_{50} values of Dox alone and in combination with E3 ligase inhibitors by unpaired *t*-test (*p*-value).

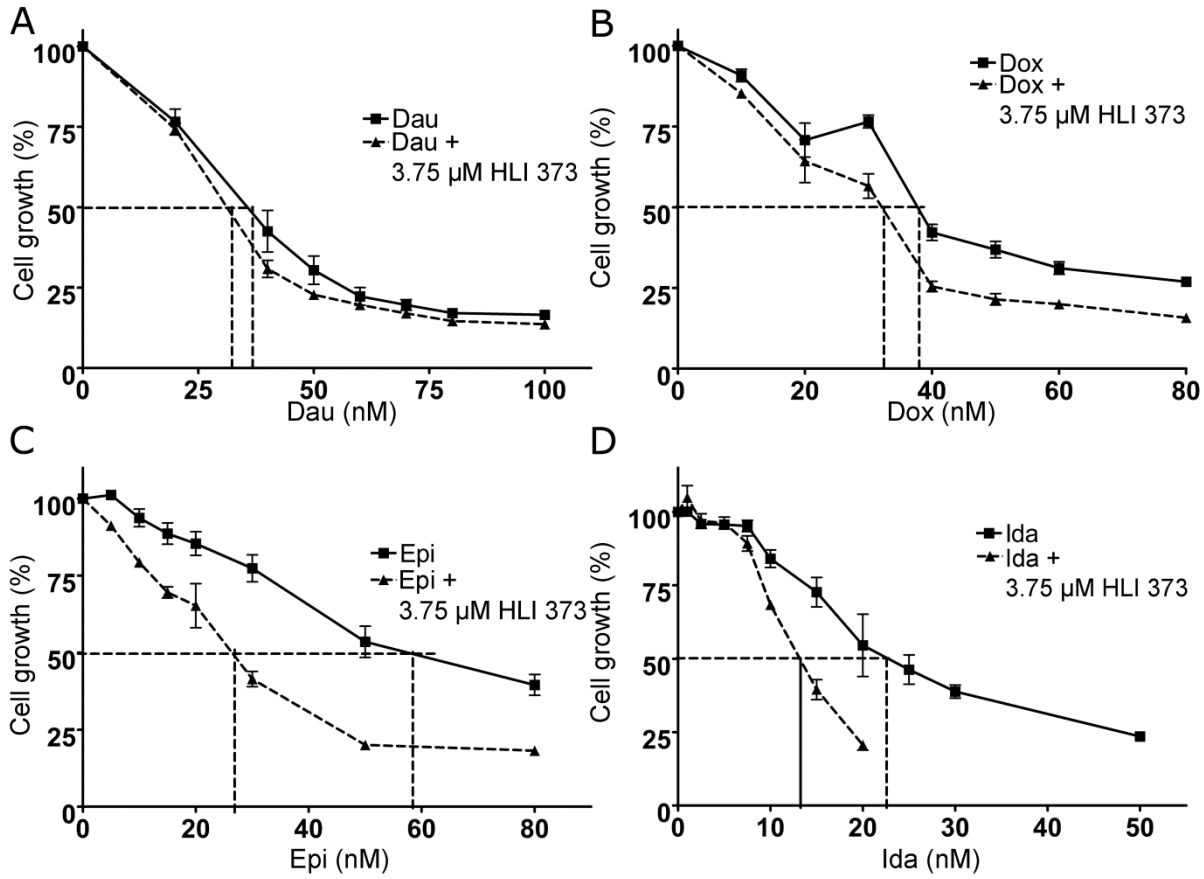

Figure 5.10 Potentiation of anthracyclines (Dau, Dox, Epi and Ida) by HLI 373 in K562 cells.

Cells were treated with increasing concentrations of anthracycline (A) Dau, (B) Dox, (C) Epi and (D) Ida alone or in combination with 3.75 μM HLI373 for 5 days followed by XTT staining. Dose–response curves were used to estimate the IC_{50} of anthracycline alone or in combination with HLI373. Error bars represent the mean ± SEM of at least 3 separate experiments for both + and – HLI373 conditions. Values were normalised to the 0 nM anthracycline value (100%).

Epirubicin +	Mean of Pf_{50}	SEM	*p*-value
PRT4165	1.91	0.07	0.0169
HLI373	1.72	0.02	0.0001

Table 5.7 Potentiation factor (Pf_{50}) summary of epirubicin (Epi) in combination with E3 ligase inhibitors.

Statistical significance between IC_{50} values of Epi alone and in combination with E3 ligase inhibitors by unpaired *t*-test (*p*-value).

Idarubicin +	Mean of Pf_{50}	SEM	*p*-value
PRT4165	1.25	0.08	0.035
HLI373	1.44	0.09	0.0328

Table 5.8 Potentiation factor (Pf_{50}) summary of idarubicin (Ida) in combination with E3 ligase inhibitors.

Statistical significance between IC_{50} values of Ida alone and in combination with E3 ligase inhibitors by unpaired *t*-test (*p*-value).

5.6 Conclusion and discussion

Two E3 ligase inhibitors were studied in combination with different TOP2 poisons. The potentiation was determined by XTT growth inhibition assay. The results show inhibition of the E3 ligase Bmi1/Ring1A potentiated all the TOP2 poisons tested. In the presence of the Bmi1/Ring1A inhibitor, PRT4165, the IC_{50} of TOP2 poisons were significantly reduced. The levels of potentiation were different for each TOP2 poison. MTX showed the greatest potentiation (Pf_{50}=3.73), followed by VM26 (Pf_{50}=2.84) (Table 5.9A). Of the four anthracyclines tested, only Epi was potentiated significantly (Pf_{50}>1.5) (Table 5.9A). The XTT assay results are consistent with a previous study which showed siRNA silencing of Bmi1 increased cell sensitivity to TOP2 poisons (Alchanati *et al.*, 2009). The siRNA silencing of Bmi1 inhibited drug-induced TOP2A degradation (Alchanati *et al.*, 2009). These results support the idea that Bmi1 facilitates TOP2A degradation after TOP2 drug exposure.

The presence of HLI373, an HDM2 inhibitor, significantly reduced the IC_{50} of all TOP2 poisons tested. The level of potentiation was different for each TOP2 poison. MTX had the greatest potentiation (Pf_{50}=4.38) followed by VM26 (Pf_{50}=1.76). Of the anthracyclines tested, Epi was potentiated the most (Pf_{50}=1.72) (Table 5.9B). The results of the potentiation assays are consistent with previous studies which showed that inhibition of HDM2 sensitised cells to VP16 in a p53 independent manner, and prevented TOP2A degradation after exposure to VP16 (Nayak *et al.*, 2007; Conradt *et al.*, 2013). HDM2 regulates p53, however K562 cells do not express p53 (Prokocimer *et al.*, 1986). The potentiation by HLI373 may be via regulation of TOP2A levels or by altering HDM2 interactions with other protein(s).

A

PRT4165+	Mean of Pf_{50}	SEM	*p* -value
Mitoxantrone	3.73	0.035	0.002
Etoposide	1.75	0.16	0.0494
Teniposide	2.84	0.59	0.015
mAMSA	1.48	0.04	0.0026
Daunorubicin	1.74	0.09	0.0067
Doxorubicin	1.16	0.05	0.0257
Epirubicin	1.91	0.07	0.0169
Idarubicin	1.25	0.08	0.035

B

HLI373+	Mean of Pf_{50}	SEM	*p* -value
Mitoxantrone	4.38	0.45	0.0003
Etoposide	1.49	0.13	0.022
Teniposide	1.76	0.12	0.0026
mAMSA	1.39	0.04	0.0345
Daunorubicin	1.41	0.04	0.0071
Doxorubicin	1.22	0.03	0.0024
Epirubicin	1.72	0.02	0.0001
Idarubicin	1.44	0.09	0.0328

Table 5.9 Summary of Pf_{50} (A) PRT4165 and (B) HLI373 in combination with TOP2 poisons.

Chapter 6. Cytotoxic and genotoxic effects of TOP2 poisons on Nalm-6 cell lines

6.1 Introduction

TOP2 poisons are used clinically for the treatment of cancer. However, TOP2 poisons are genotoxic in cells. TOP2 poisons are linked to serious adverse effects such as treatment-related secondary cancer and cardiotoxicity (Azarova *et al.*, 2007; Cowell *et al.*, 2012; Zhang *et al.*, 2012; Vejpongsa and Yeh, 2014).

Two TOP2 isoforms, TOP2A and TOP2B, exist in human cells. They have a similar reaction mechanism and are similar in structure. However, TOP2A and TOP2B differ in some of their biological functions. TOP2A is highly expressed in rapidly growing cells and is essential for cell division. Both are involved in transcription and TOP2B plays a role in ligand-mediated transcription. Evidence suggests that poisoning of TOP2B is related to secondary cancer development (Azarova *et al.*, 2007; Cowell *et al.*, 2012). Therefore, TOP2B inhibition might contribute more to TOP2 poison genotoxicity than TOP2A.

Three Nalm-6 cell lines with different expression levels for TOP2 isoforms were treated with TOP2 poisons in order to determine the contribution of each isoform to cytotoxicity and genotoxicity. This study used the human pre-B cell line Nalm-6 (wild-type) and the two derivatives of Nalm-6 to investigate the role of TOP2A and TOP2B in the growth inhibitory effect of TOP2 poisons. Nalm-$6^{TOP2A+/-}$ and Nalm-$6^{TOP2B-/-}$ cell lines have reduced expression of type II topoisomerases. TOP2A is reduced by 50% in Nalm-$6^{TOP2A+/-}$ and Nalm-$6^{TOP2B-/-}$ lack TOP2B. How this affects growth inhibition, cytotoxicity and genotoxicity has been determined.

The micronucleus assay is one of the preferred methods for studying chromosome damage. In mitosis, dividing cells contain chromosome fragments lacking centromeres and/or whole chromosomes that are unable to travel to the spindle poles. A nuclear envelope will form around

the lagging chromosome or fragment, forming a "micronucleus". The number of cells with micronuclei after drug treatment is used as a measure of chromosome damage (Fenech, 2000; Norppa and Falck, 2003). Flow cytometry is a robust and fast way to measure micronuclei in cells (Avlasevich *et al.*, 2006; Bryce *et al.*, 2007). Drugs which induce micronuclei levels two-fold higher than the untreated control are classed as genotoxic.

The aim of the work described in this chapter to study the role of TOP2 isoforms in TOP2 poison-induced growth inhibition, cytotoxicity and genotoxicity.

6.2 MTX

MTX- effect on Nalm-6 cell line growth

MTX is a TOP2 poison which stabilises TOP2-DNA complexes with both isoforms in human and mouse cell lines (Errington *et al.*, 2004; Lee *et al.*, 2016). Cells were incubated with increasing concentrations of MTX for 120 hours and growth inhibition was determined by XTT assay, as described in chapter 3. The OD_{450nm} values of 0 nM MTX treated cells were set as 100%, and all other values were normalised relative to the 0 nM MTX control values. The results are shown in figure 6.1A and table 6.1A. The growth inhibitory effect of MTX is greater in Nalm-6 WT cells than in Nalm-$6^{TOP2A+/-}$ or Nalm-$6^{TOP2B-/-}$ cells. The IC_{50} of Nalm-6 WT, Nalm-$6^{TOP2A+/-}$ and Nalm-$6^{TOP2B-/-}$ cells were approximately 4 nM, 8.5 nM and 17.4 nM, respectively. The Nalm-$6^{TOP2B-/-}$ cells were most resistant to MTX demonstrating that TOP2B plays a large role in the growth inhibitory effects of MTX (Figure 1.1A and Table 6.1A). These results are consistent with Toyoda et al 2008 and Errington et al 1999 who used clonogenic assays on human Nalm-6 or transgenic murine cell lines, respectively (Errington *et al.*, 1999; Toyoda *et al.*, 2008).

Cytotoxicity was determined by Relative Increase in Cell Count (RICC) and Relative survival; both methods were described in chapter 4. Cells were

treated with increasing concentrations of MTX for 48 hours, followed by cell counting to obtain the RICC. After that, cells were prepared for micronucleus assays. Relative survival data was obtained during the flow cytometric analysis. The data for RICC and relative survival were plotted to obtain IC_{50} values as a measure of cytotoxicity.

Figure 6.1 and Table 6.1B and C show RICC and relative survival determined during FACS, respectively. The RICC IC_{50} values were approximately 1 nM in Nalm-6 WT, 1.7 nM in Nalm-$6^{TOP2A+/-}$ and 2.8 nM in Nalm-$6^{TOP2B-/-}$ cells. The IC_{50} values from relative survival were approximately 1.2 nM in Nalm-6 WT, 2.5 nM in Nalm-$6^{TOP2A+/-}$ and 3.8 nM in Nalm-$6^{TOP2B-/-}$ cells. The relative survival rate of Nalm-6 WT cells was the lowest of the three Nalm-6 cell lines. It was significantly lower than that of Nalm-$6^{TOP2B-/-}$ cells at all doses tested (0.75 nM; p=0.0059, 1.5 nM; p=0.0056 and 3 nM; p=0.0004).

The cytotoxic effect of MTX in Nalm-6 cell lines was highest in Nalm-6 WT cells and lowest in Nalm-$6^{TOP2B-/-}$ cells (Nalm-6 WT > Nalm-$6^{TOP2A+/-}$ > Nalm-$6^{TOP2B-/-}$). This trend was the same whether determined by relative survival or RICC and similar to the growth inhibition trend. The increased resistance in the Nalm-$6^{TOP2B-/-}$ cell line reflects the importance of TOP2B in the growth inhibitory and cytotoxic effects of MTX.

A

Growth inhibition (XTT)						
	Nalm-6 WT		Nalm-6$^{TOP2B-/-}$		Nalm-6$^{TOP2A+/-}$	
MTX (nM)	Mean	SEM	Mean	SEM	Mean	SEM
0.0	100.0	0.0	100.0	0.0	101.1	1.1
1.0	111.4	10.3	92.1	14.5	82.3	5.3
1.5	118.9	12.4	122.4	25.5	101.1	5.5
2.0	118.4	8.1	124.6	29.8	89.2	2.2
2.5	101.9	6.1	114.4	24.5	102.6	7.7
5.0	17.6	5.8	96.0	10.1	83.5	0.7
7.5	-10.0	1.4	112.3	12.1	61.9	1.8
10.0	-9.5	1.7	95.0	7.5	30.9	8.9
15.0	-	-	63.3	4.1	-	-
20.0	-9.3	1.5	46.2	9.6	-6.9	0.5
25.0	-	-	11.3	2.4	-	-
30.0	-	-	2.1	2.8	-	-
40.0	-4.3	0.9	-4.7	2.0	-9.4	0.7
50.0	-	-	-2.9	2.7	-	-

B

RICC (%)						
	Nalm-6 WT		Nalm-6$^{TOP2B-/-}$		Nalm-6$^{TOP2A+/-}$	
MTX (nM)	Mean	SEM	Mean	SEM	Mean	SEM
0.00	100.0	0.0	100.0	0.0	100.0	0.0
0.75	62.4	5.7	78.7	6.4	79.6	9.4
1.50	32.4	4.3	72.7	8.7	47.9	4.8
3.00	10.8	2.5	45.9	1.1	25.5	4.0
4.50	6.3	2.2	-	-	-	-
6.00	-	-	31.9	0.9	10.8	3.5
12.00	-	-	14.7	0.0	-	-

C

Relative survival (%) (FACS)						
	Nalm-6 WT		Nalm-6$^{TOP2B-/-}$		Nalm-6$^{TOP2A+/-}$	
MTX (nM)	Mean	SEM	Mean	SEM	Mean	SEM
0.00	100.0	0.0	100.0	0.0	100.0	0.0
0.75	68.7	2.6	98.6	6.9	90.5	15.4
1.50	39.3	4.7	84.1	9.5	63.6	8.6
3.00	16.2	4.2	55.0	3.4	37.8	4.1
4.50	8.4	2.8	-	-	-	-
6.00	-	-	29.7	0.7	14.3	0.6
12.00	-	-	19.5	0.0	-	-

Table 6.1 Summary of relative survival after treatment of MTX.

Determined by (A) XTT, (B) RICC, and (C) FACS in Nalm-6 WT, Nalm-6$^{TOP2A+/-}$ and Nalm-6$^{TOP2B-/-}$ cell lines after 48 hours of MTX treatment.

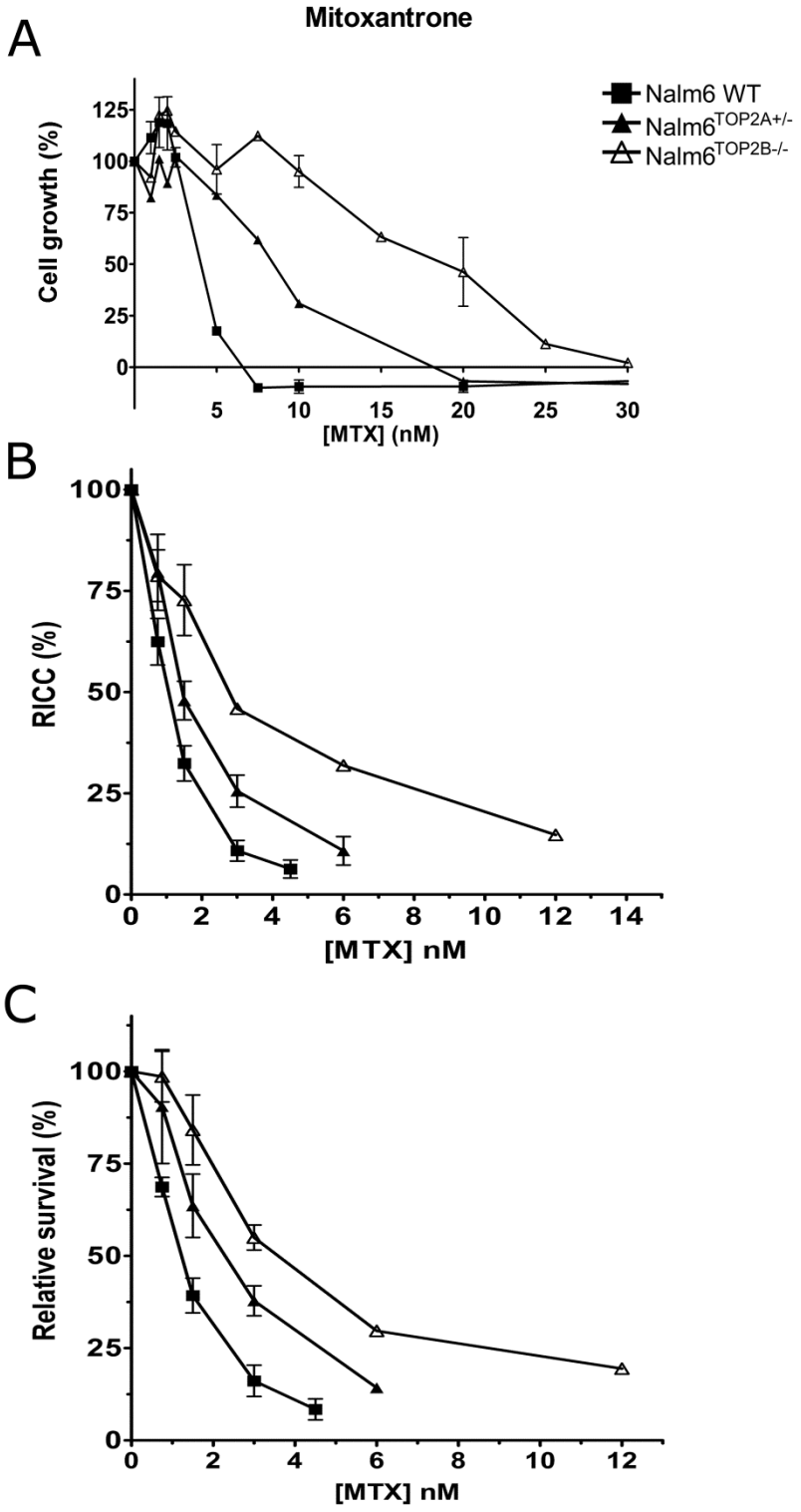

Figure 6.1 MTX-induced growth inhibition and cytotoxicity in Nalm-6 WT, Nalm-6TOP2A+/- and Nalm-6TOP2B-/- cells.

(A) Cells were treated with increasing concentrations of MTX for 120 hours and growth was determined by XTT assay (where % is inhibition of growth in relation to untreated controls). (B & C) Cells were treated with increasing concentrations of MTX for 48 hours followed by the estimation of (B) relative increase in cell count (RICC) and (C) relative survival by FACS. The value of untreated cells was set as 100% and all values normalised to it. Dose-response curves were plotted to obtain the IC_{50} of MTX in each cell line. Error bars represent the mean ± SEM of at least 3 separate experiments.

Genotoxicity of MTX in nalm6 cell lines

From this cytotoxicity data, dose ranges between 0 nM -3 nM (Nalm-6 WT), 0 nM -6 nM (Nalm-$6^{TOP2A+/-}$) and 0 nM -12 nM (Nalm-$6^{TOP2B-/-}$) were used in subsequent micronucleus assays to determine MTX genotoxicity in cell lines with differing levels of TOP2. Cells were seeded at approximately 5 x 10^4 cells per ml for 24 hours prior to incubation with MTX for 48 hours. Cells were harvested and processed for the *in vitro* micronucleus assay. Figure 6.2 shows micronucleus assay results for the three Nalm-6 cell lines in response to three different doses of MTX. This is presented as average micronuclei and micronuclei induced over untreated control. The histograms represent averages of three individual experiments. Unpaired *t*-tests were used to determine the statistical difference between cell lines at each dose.

In general, the levels of micronuclei in cells increased with dose of MTX. The average micronucleus (%) present in the Nalm-6 WT untreated control was 1.3%. The percentage went up to 3.8% or 8.3% after treatment with 0.75 nM or 1.5 nM MTX (Figure 6.2B), respectively. This increase was statistically significant as determined by *t*-test ($p<0.0001$ and $p<0.0001$, respectively). For Nalm-6 WT cells treated with 0.75 nM MTX, micronuclei were induced 3.2-fold over the untreated control (Figure 6.2C), confirming that MTX is genotoxic to Nalm-6 WT cells.

In Nalm-$6^{TOP2B-/-}$ cells, the average micronuclei without MTX treatment was 1.9%. Levels of micronuclei increased with MTX concentration. At 0.75 nM, 1.5 nM and 3 nM MTX, the percentage micronuclei increased to 2.2%, 3.8% and 5.9%, respectively (Figure 6.2B and Table 6.2B). At 1.5 nM and 3 nM MTX, the average micronuclei were significantly higher than the untreated control ($p=0.0003$ and $p=0.0002$, respectively).

According to the fold change data, there was no significant difference between 0.75 nM MTX and untreated Nalm-$6^{TOP2B-/-}$ cells (1.4-fold). Exposure to 1.5 nM and 3 nM MTX induced 2.3-fold and 3.2-fold higher

micronuclei than untreated cells. Thus at 1.5 nM and 3 nM MTX is genotoxic to Nalm-6$^{TOP2B-/-}$ cells.

In untreated Nalm-6$^{TOP2A+/-}$ cells the average micronuclei was 1.7%. This was increased to 3.3 (p=0.0042), 4.8 (p=0.0002) or 8.4% (p<0.0001) after treatment with 0.75 nM, 1.5 nM and 3nM MTX. The fold changes of micronuclei over control were 1.9-fold, 2.8-fold and 5.0-fold at 0.75 nM, 1.5 nM and 3 nM MTX, respectively. Thus, MTX is also genotoxic to Nalm-6$^{TOP2A+/-}$ cells.

Comparisons of the micronuclei levels between cell types show that the average micronuclei present in untreated Nalm-6$^{TOP2B-/-}$ cells (1.9%) was significantly higher than in untreated Nalm-6 WT cells (1.2%). However, after exposure to 0.75 nM MTX, the average micronuclei in Nalm-6 WT cells (3.8%) were significantly higher than in Nalm-6$^{TOP2B-/-}$ (2.2%; p=0.0018) and Nalm-6$^{TOP2A+/-}$ cells (3.3%; p=0.0039) (Figure 6.2B). More micronuclei were induced in Nalm-6 WT at all doses tested. The Nalm-6$^{TOP2B-/-}$ and Nalm-6$^{TOP2A+/-}$ cells produced comparable levels of micronuclei, with no significant difference between the two cell lines.

A

Relative survival						
Mitoxantrone (nM)	Nalm-6 WT		Nalm-6$^{TOP2B-/-}$		Nalm-6$^{TOP2A+/-}$	
	%	±SEM	%	±SEM	%	±SEM
0	100.0	0.0	100.0	0.0	100.0	0.0
0.75	68.7	2.6	98.6	6.9	90.5	15.4
1.5	39.3	4.7	84.1	9.5	63.6	8.6
3	16.2	4.2	55.0	3.4	37.8	4.1

B

Average micronuclei (%)						
Mitoxantrone (nM)	Nalm-6 WT		Nalm-6$^{TOP2B-/-}$		Nalm-6$^{TOP2A+/-}$	
	%	±SEM	%	±SEM	%	±SEM
0	1.3	0.1	1.9	0.2	1.7	0.3
0.75	3.8	0.2	2.2	0.1	3.3	0.1
1.5	8.3	0.9	3.8	0.2	4.8	0.1
3	16.0	2.5	5.9	0.6	8.4	0.4

C

Micronucleus induction (Fold change)						
Mitoxantrone (nM)	Nalm-6 WT		Nalm-6$^{TOP2B-/-}$		Nalm-6$^{TOP2A+/-}$	
	Fold	±SEM	Fold	±SEM	Fold	±SEM
0.75	3.2	0.4	1.4	0.1	1.9	0.3
1.5	7.0	0.8	2.3	0.2	2.8	0.4
3	10.7	1.7	3.2	0.4	5.0	0.8

D

Mitoxantrone (nM)												
Relative survival				Average micronuclei (%)				Micronucleus induction (Fold change)			
Conc.		Sig.	*p*-value	Conc.		Sig.	*p*-value	Conc.		Sig.	*p*-value
0.75	WT vs. B-/-	**	0.0059	0	WT vs. B-/-	**	0.0088	0.75	WT vs. B-/-	**	0.009
1.5	WT vs. B-/-	**	0.0056	0.75	WT vs. B-/-	**	0.0018	0.75	WT vs. A+/-	*	0.0486
1.5	WT vs. A+/-	*	0.0439	0.75	WT vs. A+/-	**	0.0039	1.5	WT vs. B-/-	**	0.0049
3	WT vs. B-/-	***	0.0004	1.5	WT vs. B-/-	**	0.0088	1.5	WT vs. A+/-	**	0.0098
3	WT vs. A+/-	*	0.0211	1.5	WT vs. A+/-	*	0.0223	3	WT vs. B-/-	**	0.0013
3	B-/- vs. A+/-	*	0.0193	1.5	B-/- vs. A+/-	*	0.0123	3	WT vs. A+/-	*	0.0363
				3	WT vs. B-/-	**	0.0022				
				3	WT vs. A+/-	*	0.0259				
				3	B-/- vs. A+/-	*	0.0390				
				0 vs. 0.75	WT	***	<0.0001				
				0 vs. 1.5	WT	***	<0.0001				
				0 vs. 3	WT	***	<0.0001				
				0 vs. 1.5	B-/-	***	0.0003				
				0 vs. 3	B-/-	***	0.0002				
				0 vs. 0.75	A+/-	**	0.0042				
				0 vs. 1.5	A+/-	***	0.0002				
				0 vs. 3	A+/-	***	<0.0001				

Table 6.2 Summary of micronucleus assay data after MTX treatment.

(A) mean of relative survival, (B) average percentage of micronuclei, (C) micronucleus induction by fold change and (D) *p*-values by unpaired *t*-test in Nalm-6 cell lines after 48 hours of MTX treatment.

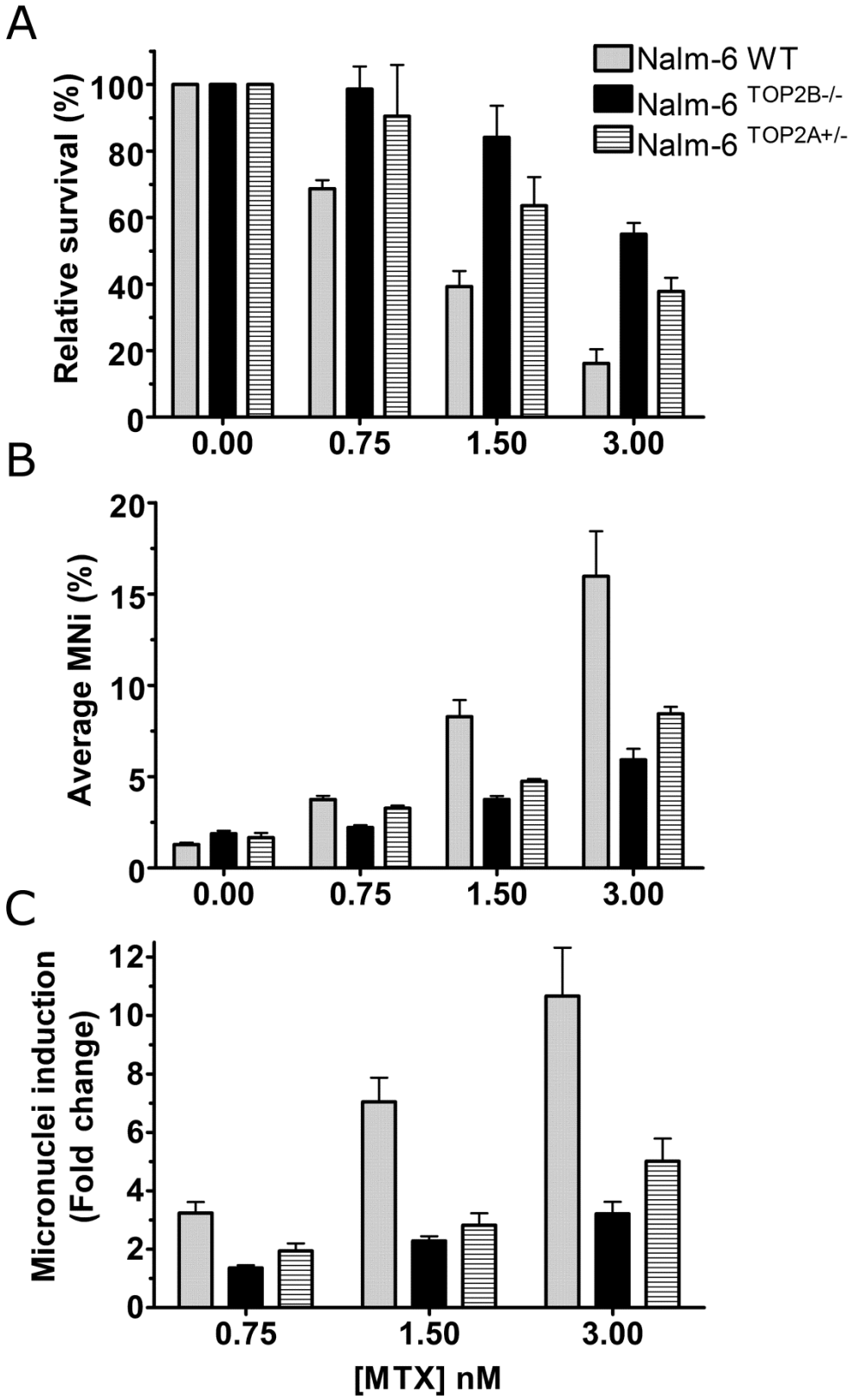

Figure 6.2 Micronucleus assay data showing cytotoxic and genotoxic effect of MTX in Nalm-6 cell lines.

Nalm-6 WT, Nalm-$6^{TOP2A+/-}$ and Nalm-$6^{TOP2B-/-}$ cells were treated with 0 nM, 0.75 nM, 1.5 nM or 3 nM MTX for 48 hours followed by micronucleus assay by FACS, (A) relative survival (%), (B) average micronuclei (%) and (C) micronuclei induced over untreated control cells (fold change).

6.3 mAMSA

Effect of mAMSA on Nalm-6 cell line growth

mAMSA is a TOP2 poison which stabilises both isoforms of TOP2 in human and mouse cell lines (Errington *et al.*, 2004). Nalm-6 cell lines were treated with increasing concentrations of mAMSA for 120 hours, and growth inhibition was detected by XTT assay. The OD_{450nm} values of the untreated control for each cell line was set as 100% and all values were normalised to the relevant control. The results are plotted on figure 6.3A.

The results show that, like MTX, Nalm-$6^{TOP2B-/-}$ cells are more tolerant to mAMSA than Nalm-6 WT or Nalm-$6^{TOP2A+/-}$ cells. The IC_{50} of Nalm-6 WT, Nalm-$6^{TOP2A+/-}$ and Nalm-$6^{TOP2B-/-}$ cells were approximately 45 nM, 33 nM and 125 nM, respectively (Figure 6.3A). This suggests that TOP2B is important in the growth inhibitory effects of mAMSA and consistent with previous studies (Errington *et al.*, 1999; Toyoda *et al.*, 2008).

Nalm-6 cells were treated with increasing concentrations of mAMSA for 48 hours followed by cytotoxicity estimation. Cytotoxicity estimation (by relative survival and RICC) was used to determine a suitable dose range for mAMSA in Nalm-6 cell lines for use in micronucleus assays. The results for both relative survival and RICC show the cell line sensitivities to mAMSA are Nalm-6 WT> Nalm-$6^{TOP2A+/-}$ > Nalm-$6^{TOP2B-/-}$. The dose range between 0 nM and 50 nM mAMSA was carried forward in micronucleus assays for all three cell lines, and was extended to 100 nM mAMSA for Nalm-$6^{TOP2B-/-}$ cells.

A

Growth inhibition (XTT)						
	Nalm-6 WT		Nalm-6$^{TOP2B-/-}$		Nalm-6$^{TOP2A+/-}$	
mAMSA (nM)	Mean	SEM	Mean	SEM	Mean	SEM
0.0	100.0	0.0	100.0	0.0	100.0	0.0
10.0	86.9	2.3	97.3	1.1	90.3	3.8
20.0	75.8	4.5	96.0	2.4	73.7	2.5
30.0	64.0	8.5	88.5	4.7	55.0	1.4
40.0	54.6	10.5	89.3	1.7	40.1	2.2
50.0	45.1	11.3	84.8	1.1	27.5	2.7
60.0	34.5	10.3	80.2	2.0	19.6	2.5
70.0	29.6	10.5	74.6	4.8	12.9	1.6
80.0	-	-	78.2	1.5	-	-
100.0	11.9	4.8	62.0	3.6	7.1	1.8
150.0	-	-	54.3	1.7	-	-
175.0	-	-	48.8	1.1	-	-
200.0	-	-	40.2	0.7	-	-

B

RICC (%)						
	Nalm-6 WT		Nalm-6$^{TOP2B-/-}$		Nalm-6$^{TOP2A+/-}$	
mAMSA (nM)	Mean	SEM	Mean	SEM	Mean	SEM
0.0	100.0	0.0	100.0	0.0	100.0	0.0
8.0	66.8	6.3	86.2	5.2	74.2	4.9
16.0	44.6	4.8	67.8	3.7	60.4	10.3
33.0	-	-	-	-	43.0	6.0
50.0	13.4	3.9	46.3	1.4	21.8	2.2
64.0	-	-	33.2	5.8	-	-
100.0	-	-	18.5	0.6	-	-

C

Relative survival (%) (FACS)						
	Nalm-6 WT		Nalm-6$^{TOP2B-/-}$		Nalm-6$^{TOP2A+/-}$	
mAMSA (nM)	Mean	SEM	Mean	SEM	Mean	SEM
0.0	100.0	0.0	100.0	0.0	100.0	0.0
8.0	67.7	4.1	84.0	2.6	86.3	8.3
16.0	42.7	2.3	67.5	2.4	66.4	2.0
33.0	-	-	-	-	37.8	0.6
50.0	10.3	1.2	36.5	2.2	21.8	1.3
64.0	-	-	28.3	1.5	-	-
100.0	-	-	15.9	0.3	-	-

Table 6.3 Summary of relative survival after mAMSA treatment.

Determined by (A) XTT, (B) RICC, and (C) FACS in Nalm-6 WT, Nalm-6$^{TOP2A+/-}$ and Nalm-6$^{TOP2B-/-}$ cell lines after 48 hours of mAMSA treatment.

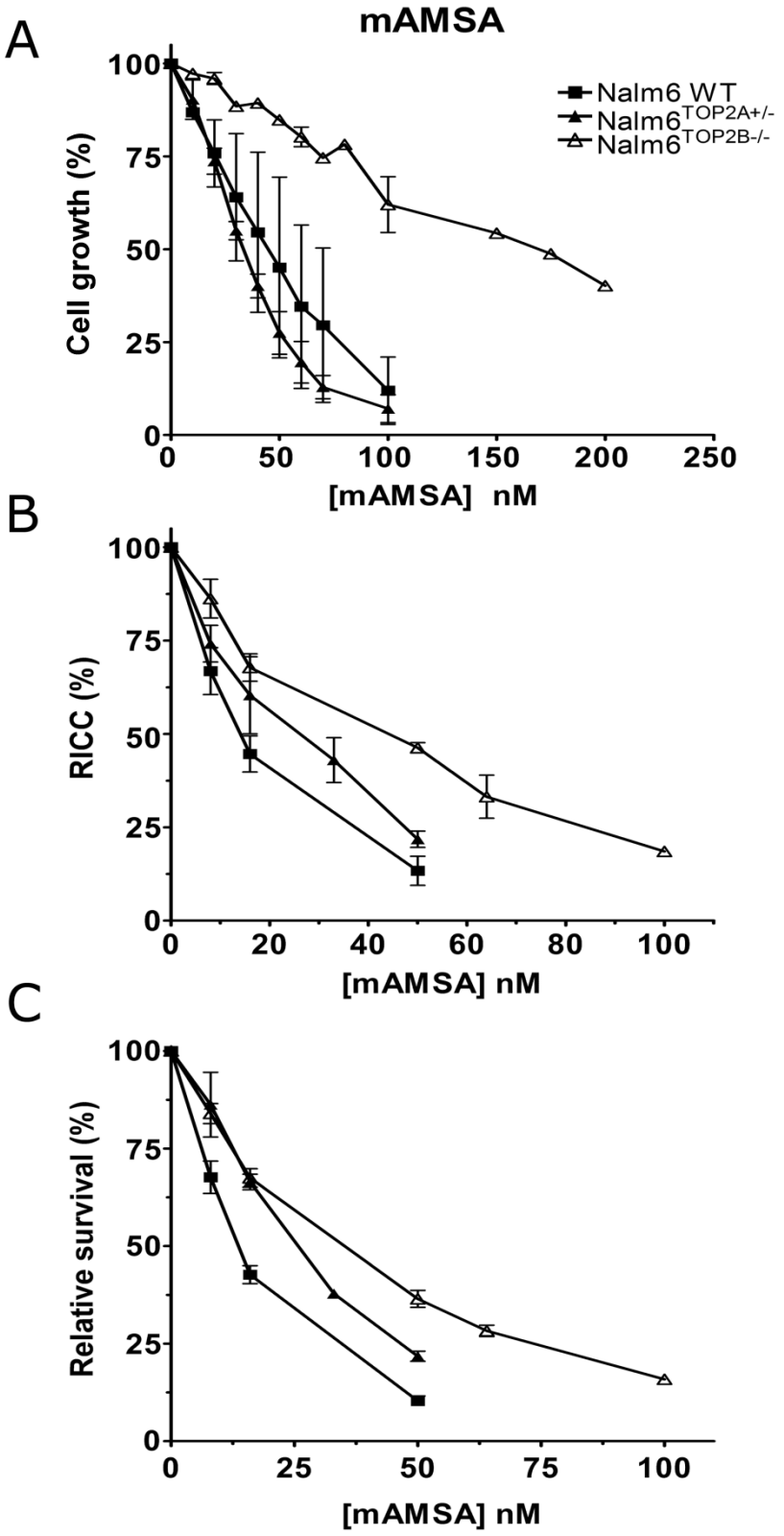

Figure 6.3 mAMSA-induced growth inhibition and cytotoxicity in Nalm-6 WT, Nalm-6$^{TOP2A+/-}$ and Nalm-6$^{TOP2B-/-}$ cells.

(A) Cells were treated with increasing concentrations of mAMSA for 120 hours and growth inhibition determined by XTT assay (where % is inhibition of growth in relation to untreated controls). Cells were treated with increasing concentrations of mAMSA for 48 hours followed by the estimation of (B) relative increase in cell count (RICC) and (C) relative survival by FACS. The value of untreated cells was set as 100% and all values normalised to it. Dose-response curves were plotted to obtain the IC_{50} of mAMSA in each cell line. Error bars represent the mean ± SEM from at least 3 separate experiments.

Genotoxicity of mAMSA

Cells were treated continuously with mAMSA for 48 hours prior to nucleic acid staining, lysis and FACS. Data are presented as relative survival, average micronucleus levels (%) and micronuclei induction over untreated control (fold change). Unpaired *t*-tests were used to determine the statistical significance in the average micronucleus levels between drug-treated and untreated controls.

Average micronucleus percentage in the Nalm-6 WT untreated control was 1.8%. Micronuclei increased significantly in a dose-related manner after treatment with mAMSA (Figure 6.4). At 8 nM the average micronuclei and fold change were 5.0% (p=0.0005 versus untreated cells) and 3.3-fold, respectively. This shows that mAMSA is genotoxic to Nalm-6 WT cells at the lowest dose tested.

The background micronuclei level for untreated Nalm-6$^{TOP2B-/-}$ cells was 2.6%. Micronuclei were significantly induced after treatment with 8 nM (4.6%; p=0.0342) or 16 nM (5.8%; p=0.0273) mAMSA (Figure 6.4B). The fold change was above 2 at 16 nM, confirming that at this dose mAMSA was genotoxic in the Nalm-6$^{TOP2B-/-}$ cells (Figure 6.4C). The levels of micronuclei increased with dose at 50 nM, 66 nM and 100 nM. However, relative survival was reduced below 40% above 50 nM, and FACS micronuclei determinations need to be viewed with caution when the survival drops below 40% (please see appendix figure 2).

Micronuclei levels in untreated Nalm-6$^{TOP2A+/-}$ cells were 2.4%. Micronuclei were induced significantly after treatment with mAMSA. At 8 nM and 16 nM, micronuclei levels increased to 4.3% (p=0.0226) and 7.5% (p=0.0005), respectively (Figure 6.4B). Fold change over the untreated control was 1.8-fold and 3.2-fold at 8 nM and 16 nM (Figure 6.4C). Therefore 16 nM mAMSA is genotoxic to Nalm-6$^{TOP2A+/-}$ cells at 16 nM and above. The level of micronuclei increased further to 16.5-fold at 50 nM mAMSA. By 50 nM the relative survival had dropped below 40%.

When comparing micronuclei levels between cell lines, untreated Nalm-6$^{TOP2B-/-}$ cells had higher levels of micronuclei than untreated Nalm-6 WT cells (p=0.0410) .

However, after treatment with 16 nM or 50 nM mAMSA, micronucleus levels in Nalm-6$^{TOP2B-/-}$ cells were lower than the other two cell lines (Figure 6.4B). This observation was more apparent when measured in fold change; micronuclei levels in Nalm-6$^{TOP2B-/-}$ cells were significantly lower than in Nalm-6 WT at 8n M (1.7 vs. 3.3; p=0.0013 and 16 nM (2.1 vs. 4.9; p=0.0004). The difference between Nalm-6 WT and Nalm-6$^{TOP2A+/-}$ cells was also significant (p<0.05).

In conclusion, mAMSA significantly induced micronuclei in all three cell lines, but higher doses were needed to reach two-fold above the untreated control significance for both Nalm-6$^{TOP2B-/-}$ and Nalm-6$^{TOP2A+/-}$ cells. This confirmed that the level of TOP2 is important for micronuclei formation, and that both isoforms are involved in the formation of micronuclei.

A

Relative survival						
mAMSA (nM)	Nalm-6 WT		Nalm-6$^{TOP2B-/-}$		Nalm-6$^{TOP2A+/-}$	
	%	±SEM	%	±SEM	%	±SEM
0	100.0	0.0	100.0	0.0	100.0	0.0
8	67.7	4.1	84.0	2.6	86.3	8.3
16	42.7	2.3	67.5	2.4	66.4	2.0
50	10.3	1.2	36.5	2.2	21.8	1.3

B

Average micronuclei (%)						
mAMSA (nM)	Nalm-6 WT		Nalm-6$^{TOP2B-/-}$		Nalm-6$^{TOP2A+/-}$	
	%	±SEM	%	±SEM	%	±SEM
0	1.9	0.2	2.6	0.2	2.4	0.2
8	5.0	0.6	4.6	1.0	4.3	0.6
16	9.1	0.8	5.8	1.5	7.5	0.7
50	17.4	1.6	10.8	2.3	16.5	0.7

C

Micronucleus induction (Fold change)						
mAMSA (nM)	Nalm-6 WT		Nalm-6$^{TOP2B-/-}$		Nalm-6$^{TOP2A+/-}$	
	Fold	±SEM	Fold	±SEM	Fold	±SEM
8	3.3	0.3	1.7	0.3	1.8	0.3
16	4.9	0.3	2.1	0.3	3.2	0.5
50	8.3	2.1	4.0	0.6	7.0	0.6

D

mAMSA (nM)											
Relative survival				Average micronuclei (%)				Micronucleus induction			
Conc.		Sig.	*p* -value	Conc.		Sig.	*p* -value	Conc.		Sig.	*p* -value
8	WT vs. B-/-	*	0.0283	0	WT vs. B-/-	*	0.0410	8	WT vs. B-/-	*	0.001
16	WT vs. B-/-	***	0.0003	0 vs. 8	WT	***	0.0005	8	WT vs. A+/-	*	0.0196
16	WT vs. A+/-	***	0.0003	0 vs. 16	WT	***	<0.0001	16	WT vs. B-/-	***	0.0004
50	WT vs. B-/-	***	0.0002	0 vs. 8	B-/-	*	0.0342	16	WT vs. A+/-	**	0.0088
50	WT vs. A+/-	**	0.0032	0 vs. 16	B-/-	*	0.0273	50	B-/- vs. A+/-	*	0.0145
50	B-/- vs. A+/-	**	0.0033	0 vs. 8	A+/-	*	0.0226	8 vs 16	WT vs. B-/-	*	0.0495
				0 vs. 16	A+/-	***	0.0005				

Table 6.4 Summary of micronucleus assay data after mAMSA treatment.

(A) mean of relative survival, (B) average percentage of micronuclei, (C) micronucleus induction by fold change and (D) *p*-values by unpaired *t*-test in Nalm-6 cell lines after 48 hours of mAMSA treatment.

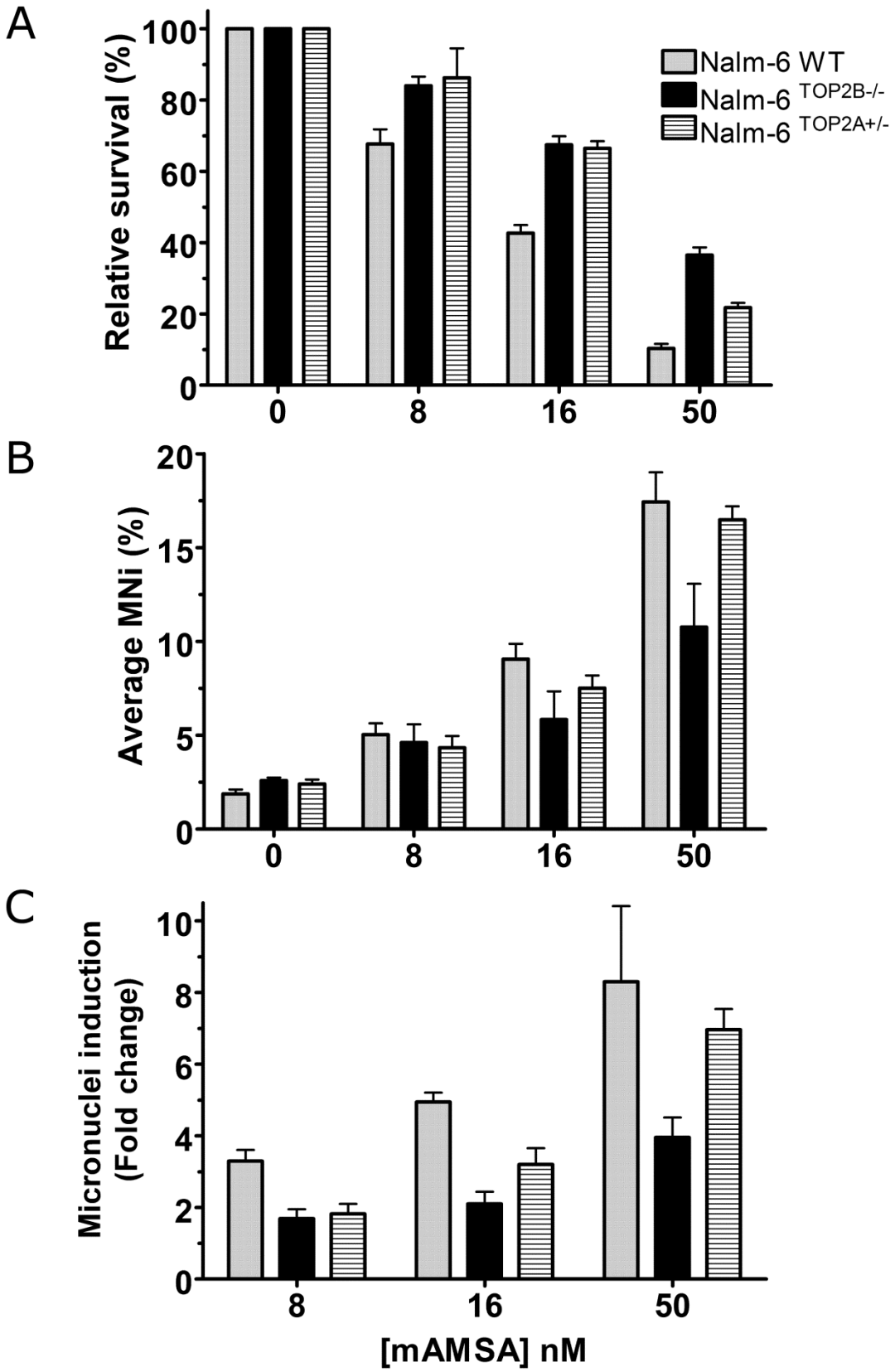

Figure 6.4 Micronucleus assay data showing the cytotoxic and genotoxic effect of mAMSA on Nalm-6 cell lines.

Nalm-6 WT, Nalm-$6^{TOP2A+/-}$ and Nalm-$6^{TOP2B-/-}$ cells were treated with 0 nM, 8 nM, 16 nM and 50 nM mAMSA for 48 hours followed by micronucleus assay. (A) relative survival (%), (B) average micronuclei (%) and (C) micronuclei induced over untreated control cells (fold change).

6.4 Anthracyclines

Effect of anthracyclines (Dox) on Nalm-6 cell line growth

Dox is an anthracycline derivative of Dau (Arcamone *et al.*, 1969a; Arcamone *et al.*, 1969b). It has cardiotoxic side effects. Knocking out TOP2B in cardiomyocytes' prevents cardiotoxicity (Capranico *et al.*, 1992; Zhang *et al.*, 2012; Vejpongsa and Yeh, 2014).

Nalm-6 cell lines with reduced amounts of TOP2A (Nalm-$6^{TOP2A+/-}$) or lacking TOP2B (Nalm-$6^{TOP2B-/-}$) were treated with a range of Dox concentrations for 120 hours. The growth inhibitory effect of Dox was determined by XTT assay. The results show that both Nalm-$6^{TOP2A+/-}$ cells and Nalm-$6^{TOP2B-/-}$ cells tolerate higher doses of Dox than wild type cells, suggesting both TOP2A and TOP2B are targeted by Dox. The IC_{50} of Dox was 23.3 nM in Nalm-$6^{TOP2A+/-}$ cells and 13.5 nM in Nalm-$6^{TOP2B-/-}$ cells, compared to 9.4 nM in Nalm-6 WT cells (

Figure 6.5). Nalm-$6^{TOP2A+/-}$ cells were significantly more resistant to Dox than Nalm-$6^{TOP2B-/-}$ cells (p=0.0220), suggesting the growth inhibitory effects of Dox may be largely due to targeting of TOP2A.

Nalm-6 cell lines were treated with Dox for 48 hours followed by cytotoxicity estimation by RICC and relative survival. A summary of this data is shown in table 6.5B and C. The relative survival of Nalm-$6^{TOP2A+/-}$ cells in response to 6 nM Dox was slightly higher than Nalm-$6^{TOP2B-/-}$ (p=0.42) and Nalm-6 WT cells (p=0.0214). However, by RICC, the cytotoxicity of Dox was similar in all three cell lines (

Figure 6.5C).

A

Growth inhibition (XTT)						
	Nalm-6 WT		Nalm-6$^{TOP2B-/-}$		Nalm-6$^{TOP2A+/-}$	
Dox (nM)	Mean	SEM	Mean	SEM	Mean	SEM
0.0	100.0	0.0	100.0	0.0	100.0	0.0
5.0	92.0	2.9	96.8	4.8	94.6	4.5
10.0	42.5	6.4	71.8	4.8	92.2	4.0
15.0	14.7	2.7	41.2	1.7	86.9	1.4
17.5	8.3	0.8	26.4	3.0	81.6	7.8
20.0	4.0	0.7	16.8	1.2	60.7	7.5
25.0	1.5	0.4	5.3	0.6	36.2	9.2
27.5	0.9	0.4	2.6	0.5	30.9	10.8
30.0	1.4	0.4	2.3	0.9	26.7	9.7

B

RICC (%)						
	Nalm-6 WT		Nalm-6$^{TOP2B-/-}$		Nalm-6$^{TOP2A+/-}$	
Dox (nM)	Mean	SEM	Mean	SEM	Mean	SEM
0.0	100.0	0.0	100.0	0.0	100.0	0.0
3.0	86.3	7.6	89.2	7.1	89.5	11.5
6.0	56.5	6.4	65.8	3.0	67.2	9.8
9.5	37.5	4.3	47.5	4.8	43.9	1.0
12.0	-	-	48.9	0.0	51.7	5.3
20.0	-	-	16.1	6.3	-	-

C

Relative survival (%) (FACS)						
	Nalm-6 WT		Nalm-6$^{TOP2B-/-}$		Nalm-6$^{TOP2A+/-}$	
Dox (nM)	Mean	SEM	Mean	SEM	Mean	SEM
0.0	100.0	0.0	100.0	0.0	100.0	0.0
3.0	92.3	3.9	98.0	6.4	100.0	10.9
6.0	61.6	2.8	76.2	4.7	87.8	12.0
9.5	35.0	6.1	53.1	1.6	58.8	7.2
12.0	-	-	47.1	0.0	49.2	0.5
20.0	-	-	21.1	0.6	-	-

Table 6.5 Summary of relative survival after Dox treatment.

Determined by (A) XTT, (B) RICC, and (C) FACS in Nalm-6 WT, Nalm-6$^{TOP2A+/-}$ and Nalm-6$^{TOP2B-/-}$ cell lines after 48 hours of Dox treatment

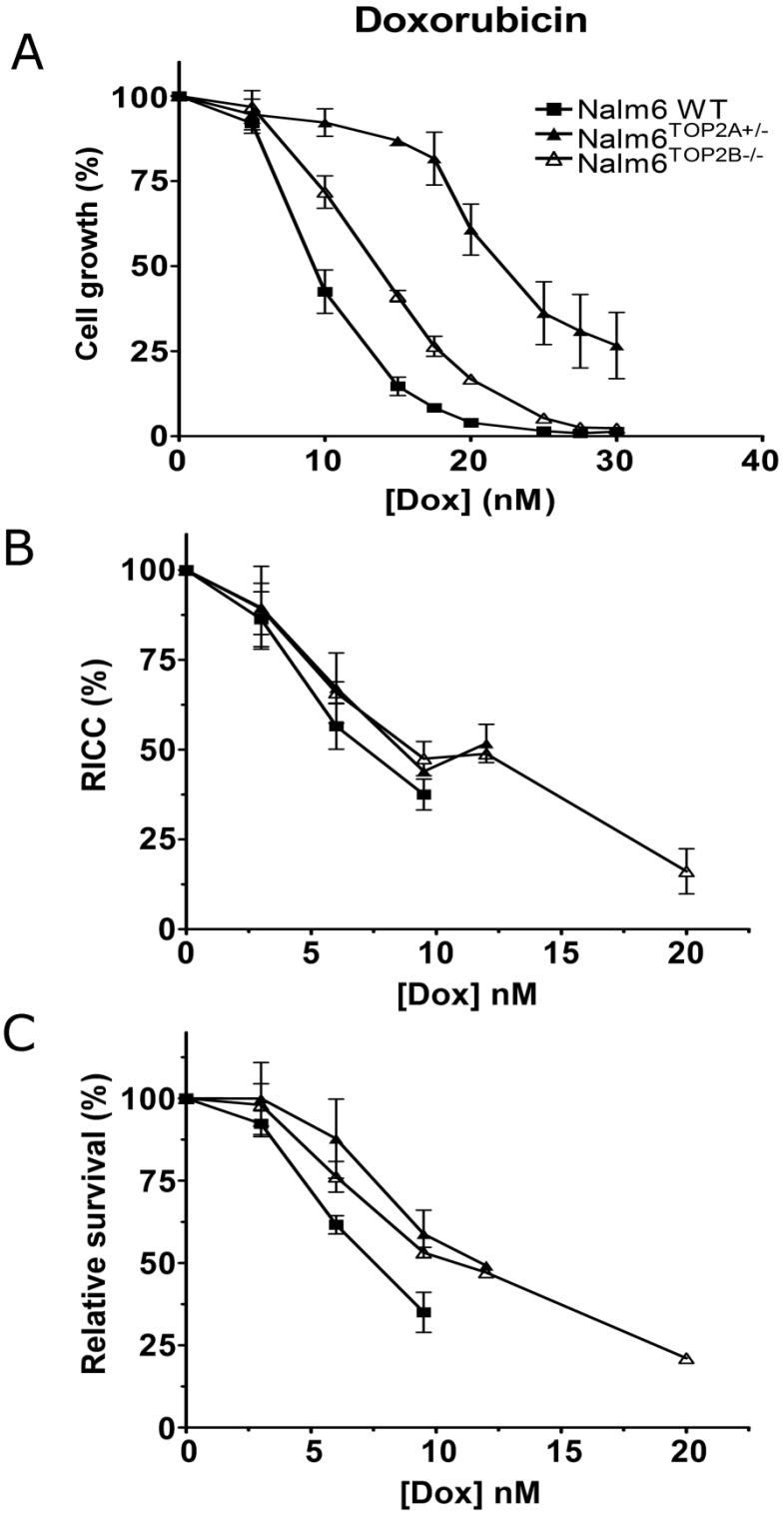

Figure 6.5 Dox-induced growth inhibition and cytotoxicity in Nalm-6 WT, Nalm-6$^{TOP2A+/-}$ and Nalm-6$^{TOP2B-/-}$ cells.

(A) Cells were treated with increasing concentrations of Dox for 120 hours and growth inhibition determined by XTT assay (where % is inhibition of growth in relation to untreated controls). (B & C) Cells were treated with increasing concentrations of Dox for 48 hours followed by the estimation of (B) relative increase in cell count (RICC) and (C) relative survival by FACS. The value of untreated cells was set as 100% and all values normalised to it. Dose-response curves were plotted to obtain the IC_{50} of Dox in each cell line. Error bars represent the mean ± SEM of at least 3 separate experiments.

Genotoxicity of anthracyclines (Dox) on Nalm6 cell lines

Cells were treated with 0 nM, 3 nM, 6 nM and 9.5 nM Dox for 48 hours. Genotoxicity data from flow cytometry analysis is shown as average micronucleus (%) and micronuclei induced over untreated control (fold change). In untreated Nalm-6 WT cells the average micronucleus level was 1.3%. This increased significantly after treatment with Dox. At 3 nM, 6 nM and 9.5 nM, micronucleus levels were 2.4% (p=0.01), 6.6% (p=0.0002) and 16% (p<0.0001), respectively (Figure 6.6B). Dox induced micronuclei to two-fold over untreated control at 3 nM, (Figure 6.6C). Therefore, Dox is genotoxic to Nalm-6 WT cells.

Average micronucleus levels in untreated Nalm-6$^{TOP2B-/-}$ cells was 1.9%. Micronucleus induction by Dox was dose-related. The average percentages of micronuclei were significantly higher than untreated control at 6 nM (4.5%; p=0.0018) and 9.5 nM (8.2%; p<0.0001). Micronuclei induction over control at 3 nM was 1.7. This increased to 2.8 fold at 6 nM, confirming that Dox is genotoxic to Nalm-6$^{TOP2B-/-}$ cells. As TOP2B is absent in Nalm-6$^{TOP2B-/-}$ cells, this indicates that Dox can induce micronuclei in cells only expressing TOP2A.

The micronuclei level in untreated Nalm-6$^{TOP2A+/-}$ cells was 1.7%. Dox induced micronuclei in Nalm-6$^{TOP2A+/-}$ cells in a dose-dependent manner. This was significantly higher than untreated control (1.7%) from 6 nM (3.9%; p=0.0245) and 9.5 nM (5.9%; p=0.0105) (Figure 6.6B). According to the fold change data, Dox induced more than two-fold induction at 6 nM.

When comparing micronuclei levels between each cell line, Nalm-6$^{TOP2B-/-}$ cells contained a higher level of micronuclei than Nalm-6 WT cells at 0 nM. However, after treatment with 6 nM or 9.5 nM Dox, Nalm-6 WT cells had higher levels of micronuclei than Nalm-6$^{TOP2A+/-}$ or Nalm-6$^{TOP2B-/-}$ cells (Figure 6.6C). This observation is more apparent when presented as fold change. At 6 nM and 9.5 nM the fold change of Nalm-6 WT was 5.1 and 10.7, respectively. This was significantly higher Nalm-6$^{TOP2B-/-}$ cells at 2.8-

fold (p=0.031) and 4.5-fold (p=0.001), respectively. Therefore, Dox is genotoxic to all three Nalm-6 cell lines tested, but is most genotoxic to Nalm-6 WT cells. Although the levels of micronuclei in Nalm-6$^{TOP2A+/-}$ cells were slightly lower than in Nalm-6$^{TOP2B-/-}$ cells, this difference was not statistically significant.

A

Relative survival						
Doxorubicin (nM)	Nalm-6 WT		Nalm-6$^{TOP2B-/-}$		Nalm-6$^{TOP2A+/-}$	
	%	±SEM	%	±SEM	%	±SEM
0	100.0	0.0	100.0	0.0	100.0	0.0
3	92.3	3.9	98.0	6.4	100.0	10.9
6	61.6	2.8	76.2	4.7	87.8	12.0
9.5	35.0	6.1	53.1	1.6	58.8	7.2

B

Average micronuclei (%)						
Doxorubicin (nM)	Nalm-6 WT		Nalm-6$^{TOP2B-/-}$		Nalm-6$^{TOP2A+/-}$	
	%	±SEM	%	±SEM	%	±SEM
0	1.3	0.1	1.9	0.2	1.7	0.3
3	2.4	0.4	2.8	0.5	2.1	0.2
6	6.6	0.9	4.5	0.6	3.9	0.8
9.5	16.0	1.6	8.2	0.7	5.9	1.2

C

Micronucleus induction (Fold change)						
Doxorubicin (nM)	Nalm-6 WT		Nalm-6$^{TOP2B-/-}$		Nalm-6$^{TOP2A+/-}$	
	Fold	±SEM	Fold	±SEM	Fold	±SEM
3	2.0	0.4	1.7	0.3	1.2	0.1
6	5.1	0.6	2.8	0.4	2.2	0.0
9.5	10.7	1.2	4.5	0.5	3.3	0.1

D

Doxorubicin (nM)											
Relative survival				Average micronuclei (%)				Micronucleus induction			
Conc.		Sig.	*p* -value	Conc.		Sig.	*p* -value	Conc.		Sig.	*p* -value
6	WT vs. B-/-	*	0.0241	9.5	WT vs. B-/-	**	0.0022	6	WT vs. B-/-	*	0.031
6	WT vs. A+/-	*	0.0214	9.5	B-/- vs. A+/-	**	0.0074	6	WT vs. A+/-	**	0.0098
9.5	WT vs. B-/-	*	0.0104	0 vs. 3	WT	**	0.0100	9.5	WT vs. B-/-	**	0.001
				0 vs. 6	WT	***	0.0002	9.5	WT vs. A+/-	**	0.0031
				0 vs. 9.5	WT	***	<0.0001				
				0 vs. 6	B-/-	**	0.0018				
				0 vs. 9.5	B-/-	***	<0.0001				
				0 vs. 6	A+/-	*	0.0245				
				0 vs. 9.5	A+/-	*	0.0105				

Table 6.6 Summary of micronucleus assay data after Dox treatment.

(A) Mean of relative survival, (B) average percentage of micronuclei, (C) micronucleus induction by fold change and (D) *p*-values by unpaired *t*-test in Nalm-6 cell lines after 48 hours of Dox treatment.

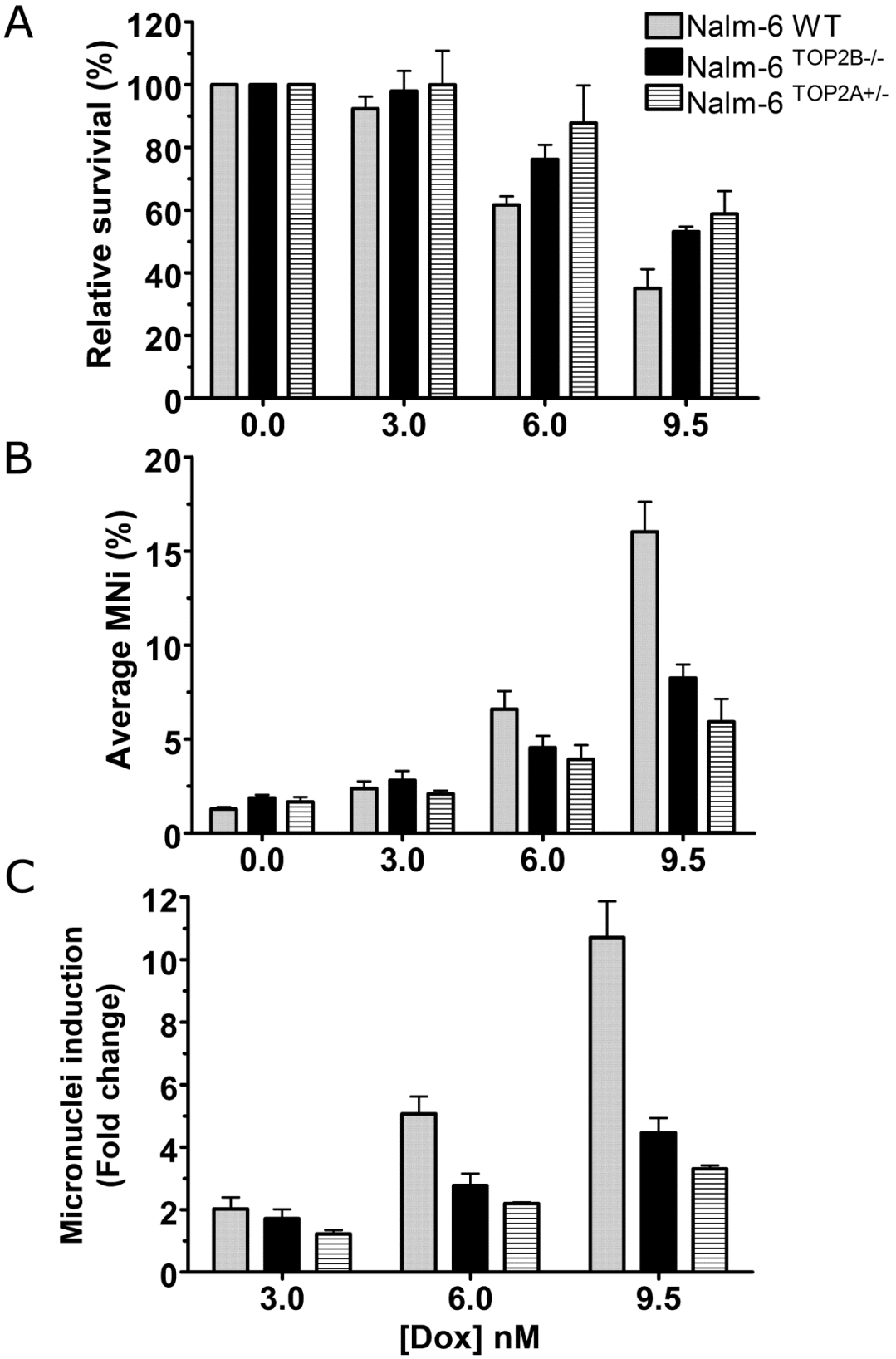

Figure 6.6 Micronucleus assay data showing cytotoxicity and genotoxicity of Dox in Nalm-6 cell lines.

Nalm-6 WT, Nalm-$6^{TOP2A+/-}$ and Nalm-$6^{TOP2B-/-}$ cells were treated with 0 nM, 3 nM, 6 nM and 9.5 nM Dox for 48 hours followed by micronucleus assay by FACS (A) relative survival (%), (B) average micronuclei (%) and (C) micronuclei induced over untreated control cells (fold change).

Effect of anthracyclines (Epi) on Nalm-6 cell line growth

Epi is a 4'-epi-isomer of Dox. Nalm-6 cell lines were treated with increasing concentrations of Epi for 120 hours. The growth inhibitory effect was determined by XTT assay. Epi inhibited growth both in the absence of TOP2B (in Nalm-$6^{TOP2B-/-}$ cells) and in cells with reduced levels of TOP2A (Nalm-$6^{TOP2A+/-}$ cells). The growth inhibitory effect of Epi in all three cell lines was similar, with an IC_{50} of 12 nM and 12.8 nM in Nalm-6 WT and Nalm-$6^{TOP2B-/-}$, and 16 nM in Nalm-$6^{TOP2A+/-}$ cells. According to the IC_{50}, Nalm-$6^{TOP2A+/-}$ cells are slightly more tolerant to Epi than Nalm-6 WT (p=0.0156) (Figure 6.7A).

Nalm-6 cell lines were treated with Epi for 48 hours followed by cytotoxicity estimation by RICC and relative survival. The relative survival of Nalm-$6^{TOP2A+/-}$ cells in response to Epi was slightly higher than Nalm-$6^{TOP2B-/-}$ and Nalm-6 WT cells. The difference in relative survival between Nalm-$6^{TOP2A+/-}$ and Nalm-$6^{TOP2B-/-}$ cells was not significant. The trends of relative survival and RICC are very similar.

A

Growth inhibition (XTT)						
	Nalm-6 WT		Nalm-6$^{TOP2B-/-}$		Nalm-6$^{TOP2A+/-}$	
Epi (nM)	Mean	SEM	Mean	SEM	Mean	SEM
0.0	100.0	0.0	100.0	0.0	100.0	0.0
5.0	95.9	4.6	87.5	4.1	102.1	4.6
10.0	77.8	3.0	63.5	4.8	94.2	5.5
15.0	26.7	2.3	31.3	2.9	55.1	4.9
17.5	13.8	1.0	17.3	2.0	39.8	6.3
20.0	9.5	0.4	12.5	1.9	24.4	2.8
25.0	5.3	0.7	4.5	0.6	14.2	1.8
30.0	3.0	0.2	2.0	0.4	7.4	1.1
50.0	2.7	0.4	0.5	0.3	1.6	0.4

B

RICC (%)						
	Nalm-6 WT		Nalm-6$^{TOP2B-/-}$		Nalm-6$^{TOP2A+/-}$	
Epi (nM)	Mean	SEM	Mean	SEM	Mean	SEM
0.0	100.0	0.0	100.0	0.0	100.0	0.0
3.0	74.3	6.8	80.7	4.7	91.7	4.9
6.0	52.8	6.5	68.2	2.0	73.8	3.4
9.5	34.0	3.7	51.6	1.0	55.8	2.7
12.0	-	-	29.7	3.9	54.7	2.7
13.0	20.3	0.9	-	-	-	-
20.0	-	-	5.9	0.0	-	-

C

Relative survival (%) (FACS)						
	Nalm-6 WT		Nalm-6$^{TOP2B-/-}$		Nalm-6$^{TOP2A+/-}$	
Epi (nM)	Mean	SEM	Mean	SEM	Mean	SEM
0.0	100.0	0.0	100.0	0.0	100.0	0.0
3.0	82.2	4.4	96.3	5.6	102.5	8.7
6.0	58.5	3.6	76.7	13.5	84.2	11.7
9.5	31.8	5.9	57.4	3.6	65.5	14.1
12.0	-	-	38.3	2.9	47.3	2.0
13.0	17.8	0.2	-	-	-	-
20.0	-	-	11.2	0.0	-	-

Table 6.7 Summary of relative survival after Epi treatment.

Determined by (A) XTT, (B) RICC, and (C) FACS in Nalm-6 WT, Nalm-6$^{TOP2A+/-}$ and Nalm-6$^{TOP2B-/-}$ cell lines after 48 hours of Epi treatment.

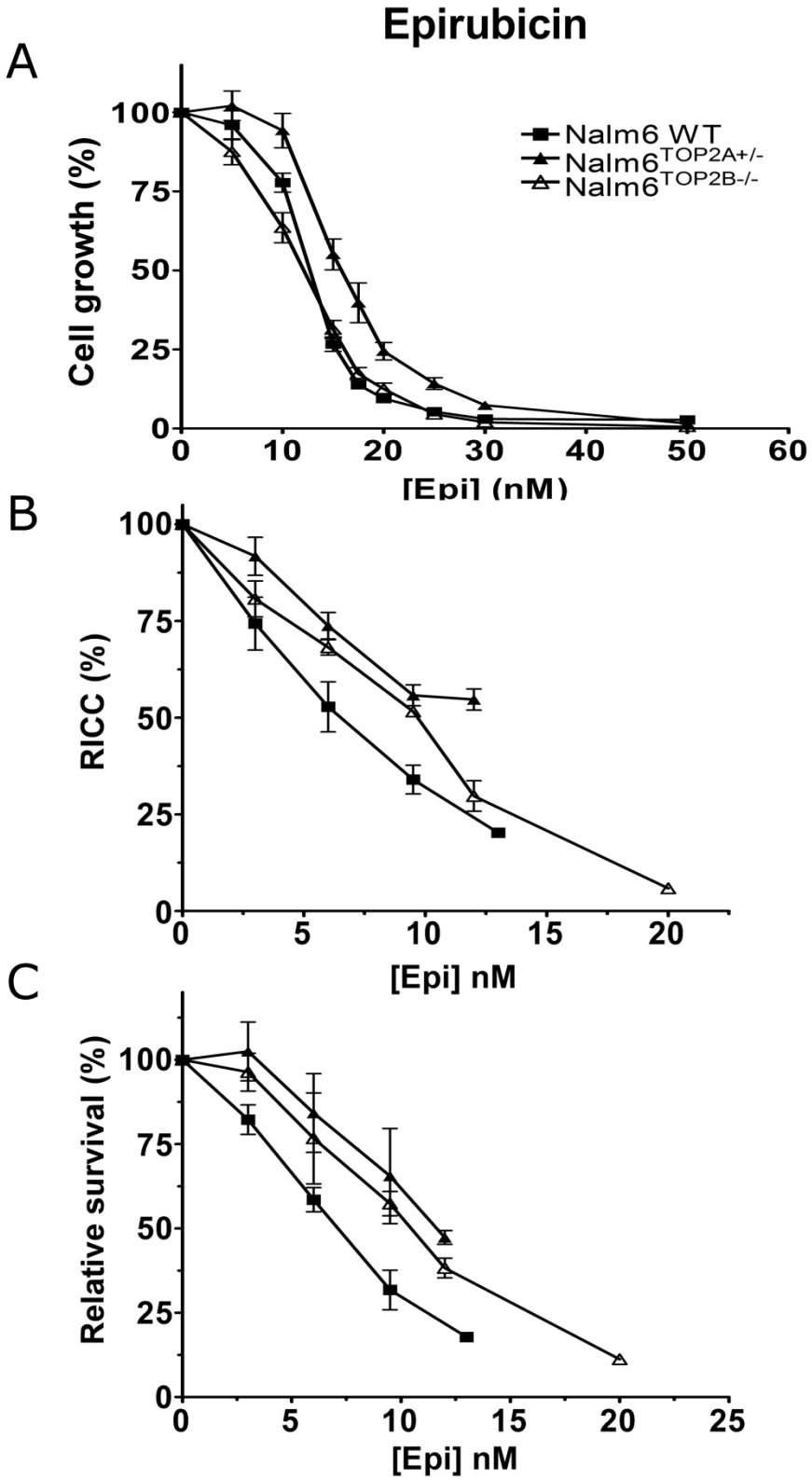

Figure 6.7 Epi-induced growth inhibition and cytotoxicity in Nalm-6 WT, Nalm-6$^{TOP2A+/-}$ and Nalm-6$^{TOP2B-/-}$ cells.

(A) Cells were treated with increasing concentrations of Epi for 120 hours and growth inhibition determined by XTT assay (where % is inhibition of growth in relation to untreated controls). (B & C) Cells were treated with increasing concentrations of Epi for 48 hours followed by the estimation of (B) relative increase in cell count (RICC) and (C) relative survival by FACS. The value of untreated cells was set as 100% and all values normalised to it.

Genotoxicity of anthracyclines (Epi) on Nalm6 cell lines

Cells were treated with 0 nM, 3 nM, 6 nM or 9.5 nM Epi for 48 hours. Data from flow cytometry analysis is shown as relative survival, average micronucleus (%) and micronuclei induced over untreated (fold change). Before treatment with Epi, the average micronucleus level in Nalm-6 WT cells was 1.3%. This increased to 2.2% and 4.7% at 3 nM and 6 nM Epi, respectively. These increases were significant compared to untreated control, with *p*-values of 0.0107 and 0.0002, respectively (Figure 6.8B). Epi induced micronuclei 1.8-fold or 4.0-fold over untreated cells at 3 nM or 6 nM, with relative survival levels of 82% and 59% (Figure 6.8A) respectively. Epi is genotoxic to Nalm-6 WT cells. The fold change at 6 nM is 3.9.

Epi induced micronuclei in Nalm-$6^{TOP2B-/-}$ cells in a dose-dependent manner. At 6 nM the percentage micronuclei of Nalm-$6^{TOP2B-/-}$ was 4.1%, significantly higher than the untreated control (p=0.0027). The relative survival was 77%. Micronuclei were induced more than two-fold at 6 nM (Figure 6.8C). Therefore, Epi is genotoxic to Nalm-$6^{TOP2B-/-}$ cells at 6 nM and above. Epi induced micronuclei in Nalm-$6^{TOP2A+/-}$ cells in a dose-dependent manner. The micronucleus levels were significantly higher than background at 6 nM and 9.5 nM Epi, with *p*-values of 0.0151 and 0.0041, respectively. The relative survival at 6 nM and 9.5 nM was around 85% and 65%. Micronuclei fold changes were 1.4 and 1.8 at 3 nM and 6 nM, respectively. The dose required to induce greater than two-fold over control is higher than 6 nM. At 9.5 nM the fold change was 4.

Figure 6.8B shows that micronuclei levels in each Nalm-6 cell line were very similar at 3 nM Epi. At 6 nM, the average micronucleus level was higher in Nalm-6 WT cells, but this was not statistically significant. This is more apparent when comparing fold changes. At 6 nM Epi, the fold change was significantly higher in Nalm-6 WT cells compared to Nalm-$6^{TOP2B-/-}$ (p=0.0445) or Nalm-$6^{TOP2A+/-}$ (p=0.0108). Overall, Nalm-$6^{TOP2B-/-}$ cells and Nalm-$6^{TOP2A+/-}$ cells had lower levels of micronuclei than Nalm-6 WT after exposure to the same concentration of Epi, confirming that

micronuclei formation is reduced when there is less TOP2. There are no significant differences between Nalm-6$^{TOP2B-/-}$ and Nalm-6$^{TOP2A+/-}$ cells. This suggests that Epi-induced micronucleus formation is mediated via both TOP2 isoforms.

A

Relative survival						
Epirubicin (nM)	Nalm-6 WT		Nalm-6$^{TOP2B-/-}$		Nalm-6$^{TOP2A+/-}$	
	%	±SEM	%	±SEM	%	±SEM
0	100.0	0.0	100.0	0.0	100.0	0.0
3	82.2	4.4	96.3	5.6	102.5	8.7
6	58.5	3.6	76.7	13.5	84.2	11.7
9.5	31.8	5.9	57.4	3.6	65.5	14.1

B

Average micronuclei (%)						
Epirubicin (nM)	Nalm-6 WT		Nalm-6$^{TOP2B-/-}$		Nalm-6$^{TOP2A+/-}$	
	%	±SEM	%	±SEM	%	±SEM
0	1.3	0.1	1.9	0.2	1.7	0.3
3	2.2	0.3	2.3	0.2	2.4	0.3
6	4.7	0.6	4.1	0.5	3.2	0.3
9.5	15.4	4.6	7.0	0.4	7.1	1.3

C

Micronucleus induction (Fold change)						
Epirubicin (nM)	Nalm-6 WT		Nalm-6$^{TOP2B-/-}$		Nalm-6$^{TOP2A+/-}$	
	Fold	±SEM	Fold	±SEM	Fold	±SEM
3	1.8	0.2	1.4	0.2	1.4	0.2
6	3.9	0.4	2.5	0.4	1.8	0.2
9.5	10.2	3.0	3.9	0.4	4.0	0.3

D

Epirubicin (nM)												
Relative survival				Average micronuclei (%)				Micronucleus induction			
Conc.		Sig.	*p* -value	Conc.		Sig.	*p* -value	Conc.		Sig.	*p* -value
9.5	WT vs. B-/-	**	0.0073	0	WT vs. B-/-	**	0.0088	6	WT vs. B-/-	*	0.045
				9.5	WT vs. B-/-	*	0.0495	6	WT vs. A+/-	*	0.0108
				0 vs. 3	WT	*	0.0107	9.5	WT vs. B-/-	*	0.015
				0 vs. 6	WT	***	0.0002				
				0 vs. 9.5	WT	**	0.0022				
				0 vs. 6	B-/-	**	0.0027				
				0 vs. 9.5	B-/-	***	<0.0001				
				0 vs. 6	A+/-	*	0.0151				
				0 vs. 9.5	A+/-	**	0.0041				

Table 6.8 Summary of micronucleus assay results after Epi treatment.

(A) Mean of relative survival, (B) average percentage of micronuclei, (C) micronucleus induction by fold change and (D) *p*-values by unpaired *t*-test in Nalm-6 cell lines after 48 hours of Epi treatment.

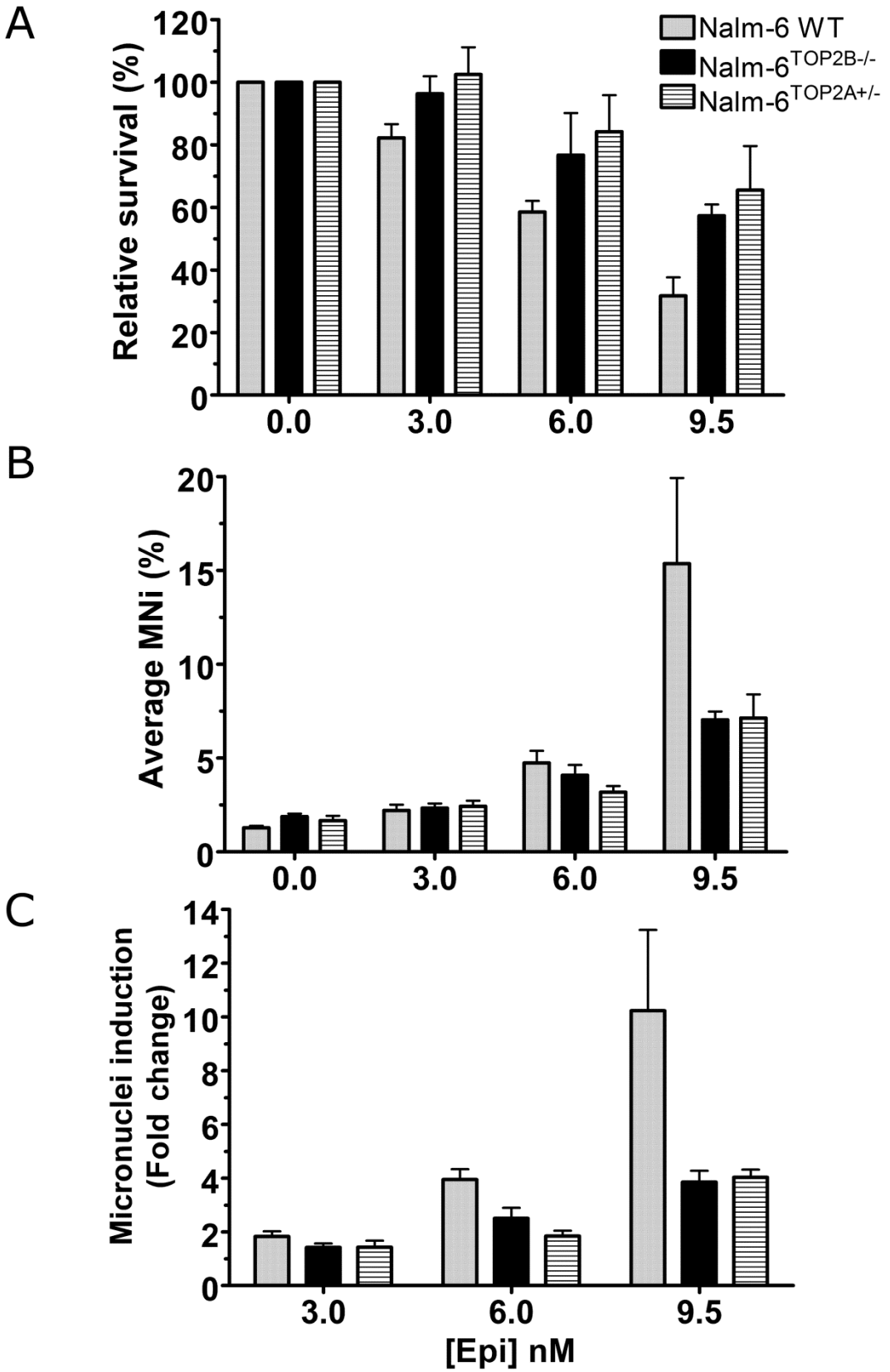

Figure 6.8 Micronucleus assay data showing the cytotoxic and genotoxic effect of Epi in Nalm-6 cell lines.

Nalm-6 WT, Nalm-$6^{TOP2A+/-}$ and Nalm-$6^{TOP2B-/-}$ cells were treated with 0 nM, 3 nM, 6 nM or 9.5 nM Epi for 48 hours followed by micronucleus assay by FACS. (A) Relative survival (%), (B) average micronuclei (%) and (C) micronuclei induced over untreated control cells (fold change).

6.5 VM26

Effect of VM26 on Nalm6 cell line growth

VM26 is a TOP2 poison which targets both isoforms of TOP2. To study the role of each TOP2 isoform on the growth inhibitory effect of VM26, Nalm-6 cells were treated with increasing concentrations of VM26 for 120 hours. Growth inhibition was detected by XTT assay. The results are plotted on figure 6.9A. A summary of the data is shown on table 6.9. The IC_{50} of VM26 is higher in Nalm-$6^{TOP2A+/-}$ (20 nM) and Nalm-$6^{TOP2B-/-}$ (18 nM) cells compared to Nalm-6 WT (10 nM) cells. The IC_{50} difference between Nalm-$6^{TOP2A+/-}$ and Nalm-$6^{TOP2B-/-}$ cells is not significant.

Cytotoxicity estimation (relative survival and RICC) was used to determine an appropriate dose range of VM26 in Nalm-6 cell lines for use in micronuclei assays. Nalm-6 cells were treated with VM26 for 48 hours followed by cytotoxicity estimation. A summary of relative survival data determined by FACS and RICC are shown on table 6.9B and C. Relative survival data shows that Nalm-$6^{TOP2A+/-}$ cells were more tolerant to VM26 than Nalm-6 WT and Nalm-$6^{TOP2B-/-}$ cells. At 4 nM the relative survival of Nalm-$6^{TOP2A+/-}$ (95.5%) was significantly higher Nalm-6 WT (55.1%; p=0.0002) and Nalm-$6^{TOP2B-/-}$ (61.7%; p=0.0072), respectively. The RICC differences between Nalm-$6^{TOP2A+/-}$ and Nalm-$6^{TOP2B-/-}$ cells at 2 nM, 4 nM and 10 nM were not significant.

A

Growth inhibition (XTT)						
	Nalm-6 WT		Nalm-6$^{TOP2B-/-}$		Nalm-6$^{TOP2A+/-}$	
VM26 (nM)	Mean	SEM	Mean	SEM	Mean	SEM
0.0	100.0	0.0	100.0	0.0	100.0	0.0
10.0	49.2	3.8	72.1	2.9	76.8	6.3
15.0	33.9	2.5	57.1	2.9	64.4	4.3
20.0	20.1	0.6	44.1	2.4	54.0	12.3
25.0	12.0	0.3	29.6	0.6	38.9	4.8
30.0	7.8	0.1	22.3	1.1	25.8	3.8
50.0	2.2	0.2	7.3	0.5	9.0	2.1
70.0	1.0	0.2	4.0	0.2	3.7	0.4
100.0	0.8	0.2	3.2	0.5	2.4	0.3

B

RICC (%)						
	Nalm-6 WT		Nalm-6$^{TOP2B-/-}$		Nalm-6$^{TOP2A+/-}$	
VM26 (nM)	Mean	SEM	Mean	SEM	Mean	SEM
0.0	100.0	0.0	100.0	0.0	100.0	0.0
2.0	74.1	7.1	101.8	15.7	84.1	8.6
4.0	46.0	3.3	67.5	2.7	75.5	12.8
10.0	20.0	1.1	43.8	4.3	36.8	0.8
12.0	-	-	31.4	3.2	-	-
16.0	-	-	-	-	37.7	3.7

C

Relative survival (%) (FACS)						
	Nalm-6 WT		Nalm-6$^{TOP2B-/-}$		Nalm-6$^{TOP2A+/-}$	
VM26 (nM)	Mean	SEM	Mean	SEM	Mean	SEM
0.0	100.0	0.0	100.0	0.0	100.0	0.0
2.0	80.8	4.5	93.4	1.9	111.8	3.1
4.0	55.1	3.0	61.7	4.5	95.5	4.9
10.0	26.3	5.5	31.1	1.1	67.4	6.3
12.0	-	-	25.0	0.9	-	-
16.0	-	-	-	-	38.2	3.1

Table 6.9 Summary of relative survival after VM26 treatment.

Determined by (A) XTT, (B) RICC, and (C) FACS in Nalm-6 WT, Nalm-6$^{TOP2A+/-}$ and Nalm-6$^{TOP2B-/-}$ cell lines after 48 hours of VM26 treatment.

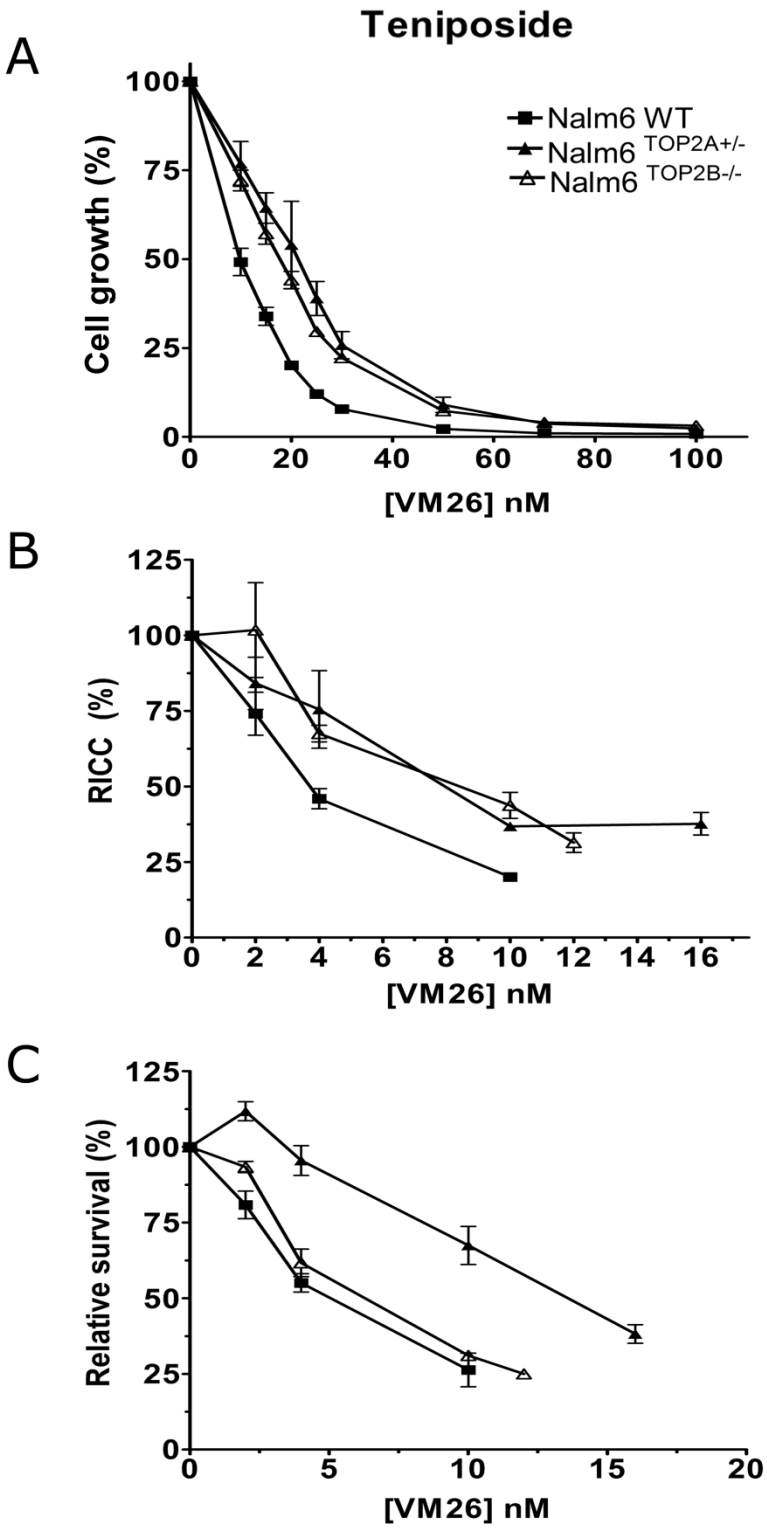

Figure 6.9 VM26-induced growth inhibition and cytotoxicity in Nalm-6 WT, Nalm-6$^{TOP2A+/-}$ and Nalm-6$^{TOP2B-/-}$ cells.

(A) Cells were treated with increasing concentrations of VM26 for 120 hours and growth inhibition determined by XTT assay (where % is inhibition of growth in relation to untreated controls). (B & C) Cells were treated with increasing concentrations of VM26 for 48 hours followed by the estimation of (B) relative increase in cell count (RICC) and (C) relative survival by FACS. The value of untreated cells was set as 100% and all values normalised to it. Dose-response curves were plotted to obtain the IC_{50} of VM26 in each cell line. Error bars represent the mean ± SEM of at least 3 separate experiments.

Genotoxicity of VM26 in Nalm-6 cell lines

Cells were treated with 0 nM, 2 nM, 4 nM and 10 nM VM26 for 48 hours. Data from flow cytometry analysis are presented as relative survival, average micronucleus (%) and micronuclei induced over untreated control (fold change). VM26 induced micronuclei in Nalm-6 WT cells in a dose-related manner. It significantly induced micronuclei above untreated control (1.9%) at 2 nM (3.8%; p=0.0139) and 4 nM (6.7%; p=0.0007) with a relative survival of approximately 80% and 55%, respectively (Figure 6.10). At 2 nM, VM26 induced micronuclei 2.5-fold over background. Thus VM26 is genotoxic to Nalm-6 WT cells.

In Nalm-$6^{TOP2B-/-}$ cells 2 nM VM26 induced a low level of micronuclei (3.3%). The induction rose significantly above background (2.6%) at 4 nM (4.9%; p=0.0488) with relative survival around 60%. The induction was more significant at 10 nM (10.3%; p=0.0010), when the relative survival dropped to 30%. In fold changes, cells treated with 2 nM or 4 nM, had 1.2-fold and 1.8-fold increase in micronuclei (Figure 6.10C), respectively. Therefore, VM26 is genotoxic to Nalm-$6^{TOP2B-/-}$ cells, inducing micronuclei significantly above background at 4 nM or higher.

VM26 induced micronuclei in Nalm-$6^{TOP2A+/-}$ cells in a dose-dependent manner. At 2 nM, the average micronuclei level was 1.3%. The induction became statistically significant from 4 nM (4.4%; p=0.0061), while relative survival remained high at 96%. Micronuclei were induced 2.9-fold over control at 10 nM VM26. Therefore, VM26 is genotoxic to Nalm-$6^{TOP2A+/-}$ cells.

Levels of micronuclei induced by VM26 in each cell line were similar at 2 nM and 4 nM. However, at 10 nM VM26 Nalm-$6^{TOP2A+/-}$ cells had significantly lower levels of micronuclei than Nalm-6 WT (average percentage of micronuclei; p=0.0044). VM26 formed similar levels of micronuclei in Nalm-$6^{TOP2B-/-}$ and Nalm-$6^{TOP2A+/-}$ cells. Fold change levels of micronuclei were higher in Nalm-6 WT cells than in Nalm-$6^{TOP2B-/-}$ or Nalm-$6^{TOP2A+/-}$ cells at 4 nM (p=0.0026) or 10 nM (p=0.0464) (Figure

6.10C and Table 6.10D), respectively. Reduced TOP2 levels in cells can increase tolerance to VM26 and reduce micronuclei formation compared to wild type cells.

A

Relative survival						
Teniposide (nM)	Nalm-6 WT		Nalm-6$^{TOP2B-/-}$		Nalm-6$^{TOP2A+/-}$	
	%	±SEM	%	±SEM	%	±SEM
0	100.0	0.0	100.0	0.0	100.0	0.0
2	80.8	4.5	93.4	1.9	111.8	3.1
4	55.1	3.0	61.7	4.5	95.5	4.9
10	26.3	5.5	31.1	1.1	67.4	6.3

B

Average micronuclei (%)						
Teniposide (nM)	Nalm-6 WT		Nalm-6$^{TOP2B-/-}$		Nalm-6$^{TOP2A+/-}$	
	%	±SEM	%	±SEM	%	±SEM
0	1.9	0.2	2.6	0.2	2.4	0.2
2	3.8	0.6	3.3	0.2	3.8	0.7
4	6.7	1.1	4.9	1.3	4.4	0.4
10	12.6	0.5	10.3	1.5	6.8	0.6

C

Micronucleus induction (Fold change)						
Teniposide (nM)	Nalm-6 WT		Nalm-6$^{TOP2B-/-}$		Nalm-6$^{TOP2A+/-}$	
	Fold	±SEM	Fold	±SEM	Fold	±SEM
2	2.5	0.3	1.2	0.1	1.5	0.2
4	3.5	0.3	1.8	0.3	1.8	0.1
10	5.8	0.9	4.0	0.5	2.9	0.5

D

Teniposide (nM)											
Relative survival				Average micronuclei (%)				Micronucleus induction			
Conc.		Sig.	*p*-value	Conc.		Sig.	*p*-value	Conc.		Sig.	*p*-value
2	WT vs. A+/-	**	0.0036	10	WT vs. A+/-	**	0.0440	2	WT vs. B-/-	*	0.016
2	B-/- vs. A+/-	**	0.0072	0 vs 2	WT	*	0.0139	4	WT vs. B-/-	**	0.0026
4	WT vs. A+/-	***	0.0002	0 vs 4	WT	***	0.0007	4	WT vs. A+/-	**	0.0021
4	B-/- vs. A+/-	**	0.0072	0 vs 4	B-/-	*	0.0488	10	WT vs. B-/-	*	0.0486
10	WT vs. A+/-	**	0.0080	0 vs 10	B-/-	**	0.0010	10	WT vs. A+/-	*	0.0464
10	B-/- vs. A+/-	***	0.0003	0 vs 4	A+/-	**	0.0061				
				0 vs 10	A+/-	***	0.0007				

Table 6.10 Summary of micronucleus assay results after VM26 treatment.

(A) Mean of relative survival, (B) average percentage of micronuclei, (C) micronucleus induction by fold change and (D) *p*-values by unpaired *t*-test in Nalm-6 cell lines after 48 hours of VM26 treatment.

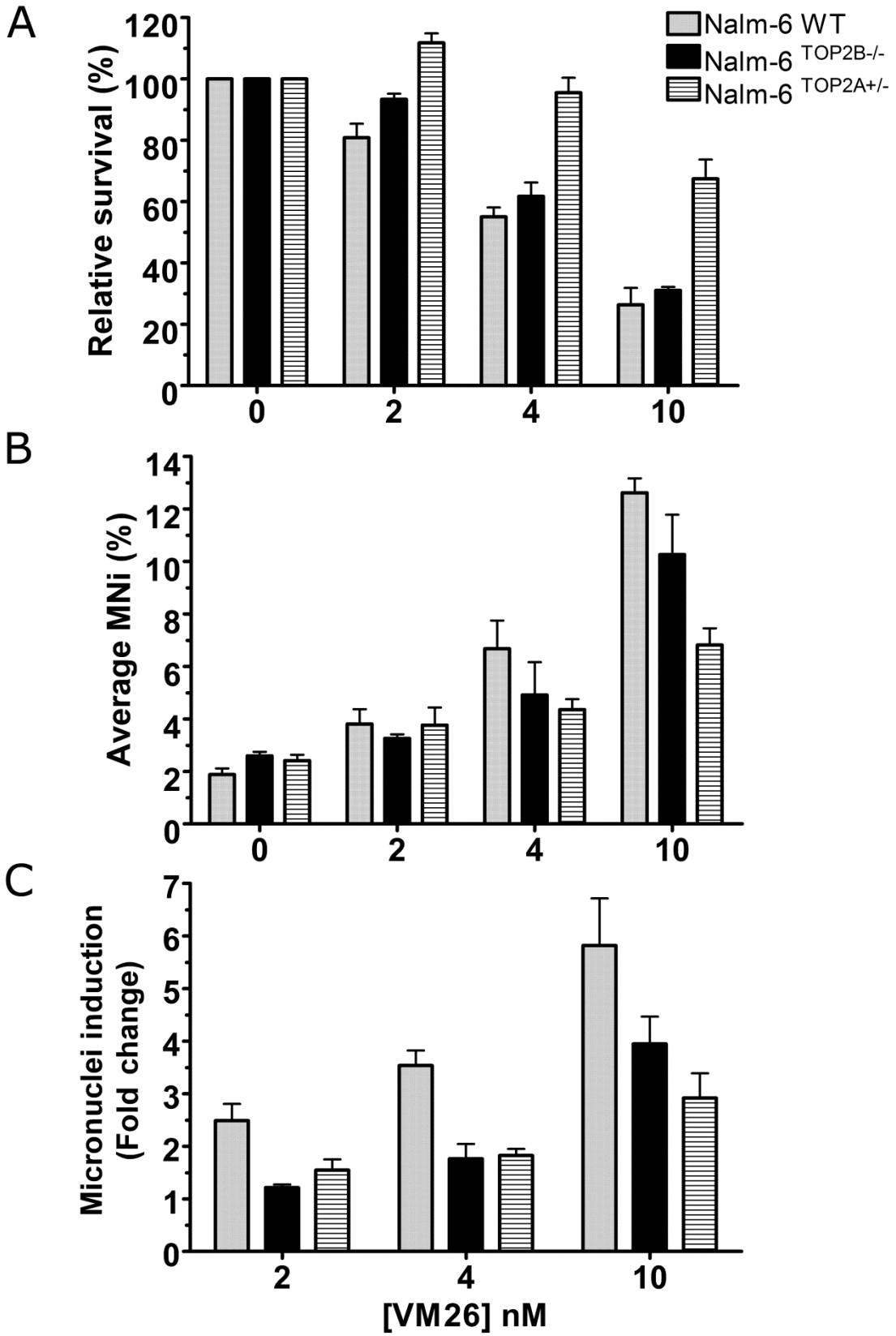

Figure 6.10 Micronucleus assay data showing the cytotoxicity and genotoxicity of VM26 in Nalm-6 cell lines.

Nalm-6 WT, Nalm-$6^{TOP2A+/-}$ and Nalm-$6^{TOP2B-/-}$ cells were treated with 0 nM, 2 nM, 4 nM and 10 nM VM26 for 48 hours followed by micronucleus assay. The results of (A) relative survival (%), (B) average micronuclei (%) and (C) micronuclei induced over untreated control cells (fold change) were plotted on graphs.

6.6 VP16

Effect of VP16 on Nalm6 cell line growth

VP16 is a TOP2 poison (epipodophyllotoxin) which targets both isoforms of TOP2 stabilising both TOP2A- and TOP2B- DNA complexes in cells. This is reported in human and murine cells (Willmore *et al.*, 1998; Errington *et al.*, 2004; Lee *et al.*, 2016). Studies suggest that TOP2A rather than TOP2B is important in VP16 cytotoxicity (Errington *et al.*, 1999; Toyoda *et al.*, 2008). Nalm-6 cell lines were treated with a range of VP16 concentrations for 120 hours, and growth inhibition was determined by XTT assay. The data is shown in table 6.11A. The results show sensitivity to VP16 was reduced with lower levels of TOP2A or TOP2B, suggesting that VP16 targets both isoforms of TOP2 (in support of previous studies). Tolerance to VP16 in Nalm-6 cell lines is ranked Nalm-$6^{TOP2A+/-}$ > Nalm-$6^{TOP2B-/-}$ > Nalm-6 WT. IC_{50} values were approximately 86 nM, 157 nM and 264 nM for Nalm-6 WT, Nalm-$6^{TOP2B-/-}$ and Nalm-$6^{TOP2A+/-}$, respectively. This suggests TOP2A is particularly important in VP16-induced growth inhibition.

Nalm-6 cells were treated with VP16 for 48 hours. Cytotoxicity estimation by relative survival and RICC are displayed on Figure 6.11 B and C. The mean and standard error of results are summarised and displayed in Table 6.11B (RICC) and C (relative survival). The relative survival results show that Nalm-$6^{TOP2A+/-}$ cells are more tolerant to VP16 than Nalm-6 WT and Nalm-$6^{TOP2B-/-}$ cells. At 85 nM relative survival of Nalm-$6^{TOP2A+/-}$, Nalm-$6^{TOP2B-/-}$ and Nalm-6 WT were 71%, 44% (p=0.0025), and 37% (p=0.0056), respectively; the differences were significant. The RICC results show that VP16 cytotoxicity in Nalm-$6^{TOP2A+/-}$ and Nalm-$6^{TOP2B-/-}$ cells is similar at dose range 0 nM – 40 nM, but Nalm-$6^{TOP2A+/-}$ cells became more tolerant at dose range 80 nM – 120 nM (Figure 6.11B). At 85 nM RICC of Nalm-$6^{TOP2B-/-}$ (41%) was significantly lower than Nalm-$6^{TOP2A+/-}$ (58%; p=0.0413).

The data suggest TOP2A is important in VP16 cytotoxicity which is consistent with previous studies and XTT results (Errington *et al.*, 1999; Onda *et al.*, 2008).

A

Growth inhibition (XTT)						
	Nalm-6 WT		Nalm-6$^{TOP2B-/-}$		Nalm-6$^{TOP2A+/-}$	
VP16 (nM)	Mean	SEM	Mean	SEM	Mean	SEM
0.0	100.0	0.0	100.0	0.0	100.0	0.0
75.0	65.6	7.2	85.4	10.2	87.8	2.5
100.0	36.7	2.7	80.3	12.9	96.8	5.2
125.0	18.8	1.2	69.0	13.3	86.9	2.8
150.0	10.5	1.3	57.4	12.0	82.4	8.4
200.0	3.1	0.6	37.0	9.4	73.8	4.8
300.0	0.8	0.3	12.3	1.2	36.9	2.5
400.0	0.1	0.2	5.2	1.1	14.5	1.2
500.0	1.1	0.3	2.9	0.9	6.0	1.3

B

RICC (%)						
	Nalm-6 WT		Nalm-6$^{TOP2B-/-}$		Nalm-6$^{TOP2A+/-}$	
VP16 (nM)	Mean	SEM	Mean	SEM	Mean	SEM
0.0	100.0	0.0	100.0	0.0	100.0	0.0
22.5	69.2	1.8	88.5	2.4	82.5	8.3
45.0	47.2	4.3	70.1	7.8	72.5	3.5
85.0	22.5	1.7	41.0	3.1	57.8	6.9
90.0	-	-	40.0	2.8	-	-
110.0	-	-	39.1	0.0	67.6	2.5

C

Relative survival (%) (FACS)						
	Nalm-6 WT		Nalm-6$^{TOP2B-/-}$		Nalm-6$^{TOP2A+/-}$	
VP16 (nM)	Mean	SEM	Mean	SEM	Mean	SEM
0.0	100.0	0.0	100.0	0.0	100.0	0.0
22.5	82.9	4.9	83.8	7.0	103.7	3.5
45.0	57.4	2.6	66.2	3.5	83.3	3.2
85.0	36.5	4.7	43.9	3.3	70.5	4.2
90.0	-	-	40.7	0.6	-	-
110.0	-	-	35.5	0.0	54.3	3.0

Table 6.11 Summary of relative survival after VP16 treatment.

Determined by (A) XTT, (B) RICC, and (C) FACS in Nalm-6 WT, Nalm-6$^{TOP2A+/-}$ and Nalm-6$^{TOP2B-/-}$ cell lines after 48 hours of VP16 treatment.

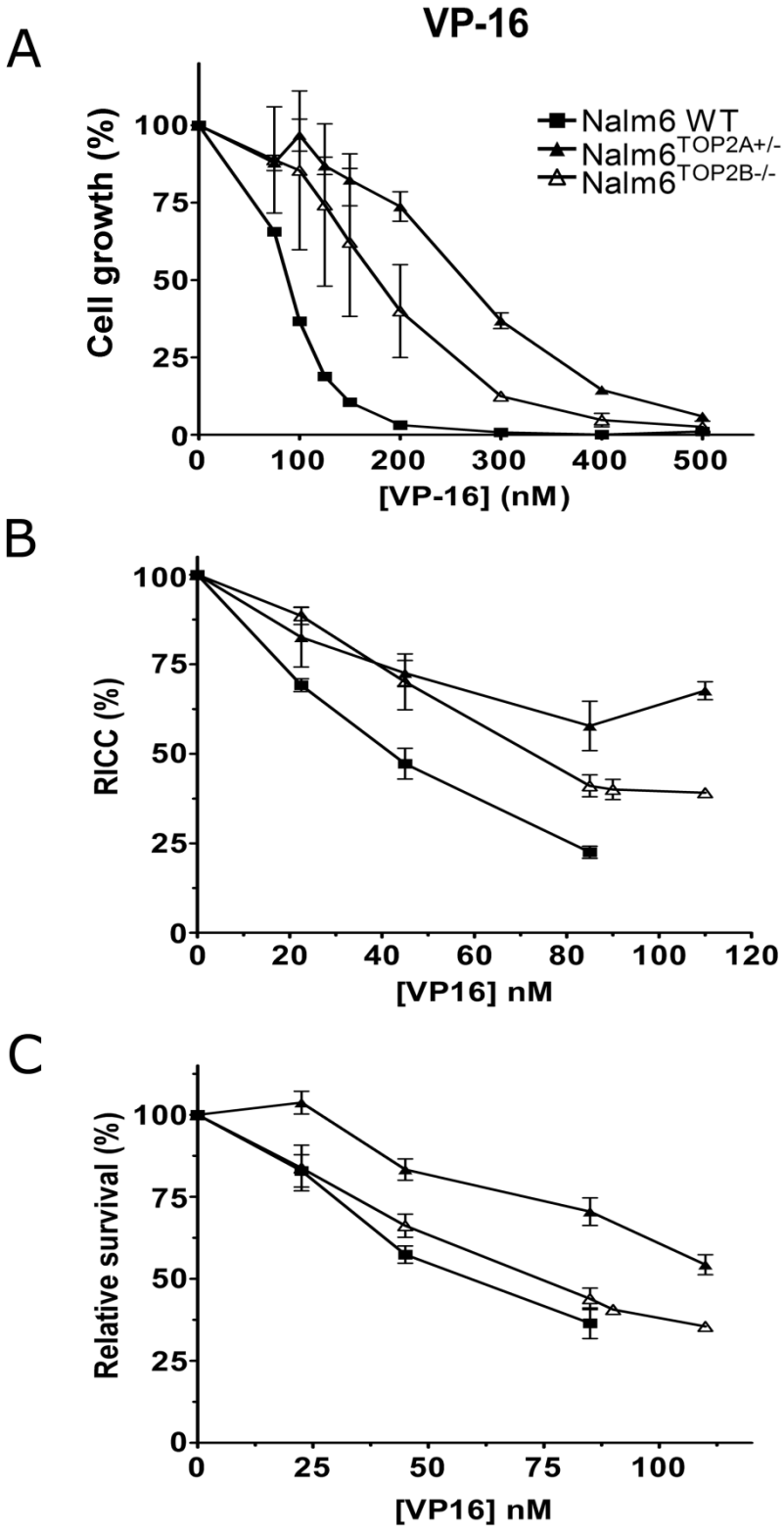

Figure 6.11 VP16-induced growth inhibition and cytotoxicity in Nalm-6 WT, Nalm-6$^{TOP2A+/-}$ and Nalm-6$^{TOP2B-/-}$ cells.

(A) Cells were treated with increasing concentrations of VP16 for 120 hours and growth inhibition determined by XTT assay (where % is inhibition of growth in relation to untreated controls). Cells were treated with increasing concentrations of VP16 for 48 hours followed by the estimation of (B) relative increase in cell count (RICC) and (C) relative survival by FACS. The value of untreated cells was set as 100% and all values normalised to it. Dose-response curves were plotted to obtain the IC_{50} of VP16 in each cell line. Error bars represent the mean ± SEM of at least 3 separate experiments.

Genotoxicity of VP16 in Nalm6 cell lines

Cells were treated with VP16 for 48 hours followed by the micronucleus assay. The flow cytometric analysis results are presented as relative survival, average micronuclei (%) and micronuclei induction over untreated control (fold change).

VP16 induced micronuclei in Nalm-6 WT cells significantly above background (1.9%) at 22.5 nM (3.4%; p=0.0285) and 45 nM (6.8%; p=0.0001). The relative survival at these two doses remained above 50%. This observation was similar with in fold change. The induction was dose-dependent. 22.5 nM induced micronuclei higher than two-fold above untreated cells (Figure 6.12C).

VP16 induced micronuclei in Nalm-6$^{TOP2B-/-}$ cells. The induction was VP16 dose-dependent. For average micronuclei, induction by VP16 was statistically significant compared to untreated control (2.6%) at 22.5 nM (5.1%; p=0.0159) and 45 nM (6.5%; p=0.0057). At these doses, relative survival were 84% and 66%, respectively (Table 6.12). At 22.5 nM, VP16 increased micronuclei nearly two-fold (1.9) over control (Figure 6.12C). This was 2.4-fold and 3.3-fold at 45 nM and 85 nM, respectively. VP16 is genotoxic to Nalm-6$^{TOP2B-/-}$ cells.

VP16 increased micronucleus formation in Nalm-6$^{TOP2A+/-}$ cells. The micronuclei levels in Nalm-6$^{TOP2A+/-}$ cells was induced significantly above background level (2.4%) at 45 nM (4.1%; p=0.0051) and 85 nM VP16 (p=0.0012). Relative survival was 83% and 70%, respectively (Figure 6.12A and B). 45 nM VP16 induced micronuclei more than two-fold over control (Figure 6.12C), thus VP16 is genotoxic to Nalm-6$^{TOP2A+/-}$ cells.

The average micronuclei induced by 85 nM VP16 in Nalm-6 WT cells were significantly higher than in Nalm-6$^{TOP2A+/-}$ cells (p=0.0115) (Figure 6.12B and Table 6.12D). The difference in micronuclei levels between Nalm-6 WT and Nalm-6$^{TOP2A+/-}$ cells was clearer when presented as fold change over untreated control. The difference was significant at both 45 nM (p=0.0462) and 85 nM (p=0.0383) (Figure 6.12C and Table 6.12D). VP16

induced slightly higher levels of micronuclei in Nalm-6$^{TOP2B-/-}$ than Nalm-6$^{TOP2A+/-}$ cells. However, according to unpaired *t*-test, the difference was not significant (Figure 6.12B and C). Overall, reduced TOP2 levels can reduce micronucleus formation in response to VP16.

A

Relative survival						
Etoposide (nM)	Nalm-6 WT		Nalm-6$^{TOP2B-/-}$		Nalm-6$^{TOP2A+/-}$	
	%	±SEM	%	±SEM	%	±SEM
0	100.0	0.0	100.0	0.0	100.0	0.0
22.5	82.9	4.9	83.8	7.0	103.7	3.5
45	57.4	2.6	66.2	3.5	83.3	3.2
85	36.5	4.7	43.9	3.3	70.5	4.2

B

Average micronuclei (%)						
Etoposide (nM)	Nalm-6 WT		Nalm-6$^{TOP2B-/-}$		Nalm-6$^{TOP2A+/-}$	
	%	±SEM	%	±SEM	%	±SEM
0	1.9	0.2	2.6	0.2	2.4	0.2
22.5	3.4	0.6	5.1	1.0	4.1	0.9
45	6.8	0.8	6.5	1.2	5.0	0.6
85	11.5	1.1	8.5	0.8	6.2	0.6

C

Micronucleus induction (Fold change)						
Etoposide (nM)	Nalm-6 WT		Nalm-6$^{TOP2B-/-}$		Nalm-6$^{TOP2A+/-}$	
	Fold	±SEM	Fold	±SEM	Fold	±SEM
22.5	2.3	0.4	1.9	0.2	1.7	0.4
45	3.7	0.4	2.4	0.2	2.1	0.3
85	5.3	0.9	3.3	0.4	2.6	0.1

D

Etoposide (nM)											
Relative survival				Average micronuclei (%)				Micronucleus induction			
Conc.		Sig.	*p* -value	Conc.		Sig.	*p* -value	Conc.		Sig.	*p* -value
22.5	WT vs. A+/-	*	0.0244	0	WT vs. B-/-	*	0.0410	45	WT vs. A+/-	*	0.0462
45	WT vs. A+/-	***	0.0006	85	WT vs. A+/-	*	0.0115	85	WT vs. B-/-	*	0.049
45	B-/- vs. A+/-	*	0.0234	0 vs. 22.5	WT	*	0.0285	85	WT vs. A+/-	*	0.0383
85	WT vs. A+/-	**	0.0056	0 vs. 45	WT	***	0.0001				
85	B-/- vs. A+/-	**	0.0025	0 vs. 85	WT	***	<0.0001				
85	B-/- vs. A+/- (RICC)	*	0.0413	0 vs. 22.5	B-/-	*	0.0159				
				0 vs. 45	B-/-	**	0.0057				
				0 vs. 85	B-/-	***	0.0001				
				0 vs. 45	A+/-	**	0.0051				
				0 vs. 85	A+/-	**	0.0012				

Table 6.12 Summary of micronucleus assay results after VP16 treatment.

(A) Mean of relative survival, (B) average percentage of micronuclei, (C) micronucleus induction by fold change and (D) *p*-values by unpaired *t*-test in Nalm-6 cell lines after 48 hours of VP16 treatment.

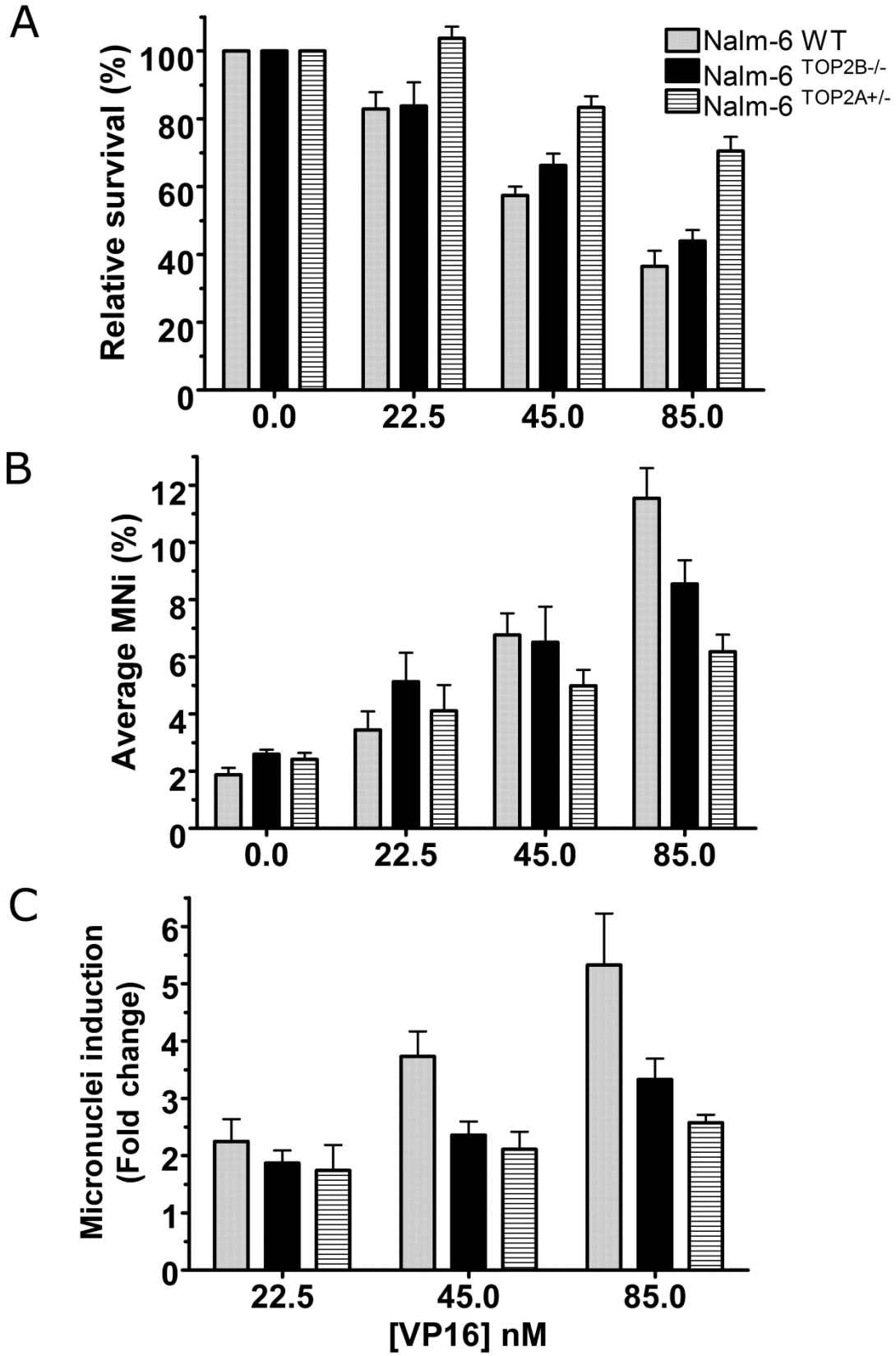

Figure 6.12 Micronucleus assay data showing the cytotoxicity and genotoxicity of VP16 in Nalm-6 cell lines.

Nalm-6 WT, Nalm-$6^{TOP2A+/-}$ and Nalm-$6^{TOP2B-/-}$ cells were treated with 0 nM, 22.5 nM, 45 nM or 85 nM VP16 for 48 hours followed by micronucleus assay. The results of (A) relative survival (%), (B) average micronuclei (%) and (C) micronuclei induced over untreated control cells (fold change) were plotted on graphs.

6.7 Conclusion and discussion

The aim of this chapter was to determine the role of both TOP2 isoforms in growth inhibition, cytotoxicity and genotoxicity.

The results of growth inhibition (XTT) and cytotoxicity studies (RICC and relative survival by FACS) show that all of the TOP2 poisons tested target both isoforms of TOP2. With 48 hours of continuous exposure, drug cytotoxicity was lower in Nalm-6$^{TOP2B-/-}$ and Nalm-6$^{TOP2A+/-}$ cells than in Nalm-6 WT cells. The pattern of growth inhibition and cytotoxicity varied according to the TOP2 poison tested. Two main patterns emerged. The first pattern, where the Nalm-6$^{TOP2B-/-}$ was most resistant (MTX and mAMSA) and the second pattern, where the Nalm-6$^{TOP2A+/-}$ was most resistant (Epi, Dox, VP16 and VM26). The pattern of Nalm-6 cell line resistance towards MTX and mAMSA were similar (Nalm-6$^{TOP2B-/-}$ > Nalm-6$^{TOP2A+/-}$> Nalm-6 WT). The results were consistent between XTT, RICC and relative survival. The patterns of Dox and Epi were similar to each other. Growth inhibition assay results show Nalm-6$^{TOP2A+/-}$ cells were most resistant to Dox and Epi. The cytotoxicity assay (RICC and relative survival) showed that both Nalm-6$^{TOP2A+/-}$ and Nalm-6$^{TOP2B-/-}$ cells were more resistant than wild type cells, but there was no significant difference between Nalm-6$^{TOP2A+/-}$and Nalm-6$^{TOP2B-/-}$. The XTT and relative survival results showed that the Nalm-6$^{TOP2A+/-}$ cells were most resistant to VP16 and VM26. This confirms that growth inhibition and cytotoxicity of TOP2 poisons are dependent on TOP2. This is consistent with previous studies (Errington *et al.*, 1999; Toyoda *et al.*, 2008).

Six TOP2 poisons were tested with the XTT, RICC, relative survival and *in vitro* micronucleus assay in three Nalm-6 cell lines. For 48 hours of continuous exposure, all the agents tested had generated micronuclei above background levels. The induction of micronuclei was TOP2 poison dose-dependent. This finding confirms that TOP2 poisons are genotoxic.

Three different Nalm-6 cell lines were treated with the same dose of TOP2 poison to determine the levels of micronuclei. The Nalm-6$^{TOP2B-/-}$ and

Nalm-6$^{TOP2A+/-}$ cells had lower levels of micronuclei than Nalm-6 WT cells, presumably because they have less target protein.

The patterns of micronucleus induction varied between different TOP2 poisons. Micronucleus induction data is presented in two ways. The percentage of cells with micronuclei (average micronuclei %) and fold increase over control levels.

For the six drugs analysed in the three cell lines the wild type cells in all cases displayed significantly more micronuclei than either Nalm-6$^{TOP2A+/-}$ or Nalm-6$^{TOP2B-/-}$, when measured by fold change. There were no significant differences between Nalm-6$^{TOP2B-/-}$ and Nalm-6$^{TOP2A+/-}$, except with MTX when measured by percentage of micronuclei.

A

MTX	Nalm-6 WT						Nalm-6 $^{TOP2B-/-}$						Nalm-6 $^{TOP2A+/-}$					
	Relative survival		Average micronuclei		Micronucleus induction		Relative survival		Average micronuclei		Micronucleus induction		Relative survival		Average micronuclei		Micronucleus induction	
nM	%	SEM	%	SEM	Fold	SEM	%	SEM	%	SEM	Fold	SEM	%	SEM	%	SEM	Fold	SEM
0.0	100.0	0.0	1.3	0.1	1.0	0.0	100.0	0.0	1.9	0.2	1.0	0.0	100.0	0.0	1.7	0.3	1.0	0.0
0.8	68.7	2.6	3.8	0.2	3.2	0.4	98.6	6.9	2.2	0.1	1.4	0.1	90.5	15.4	3.3	0.1	1.9	0.3
1.5	39.3	4.7	8.3	0.9	7.0	0.8	84.1	9.5	3.8	0.2	2.3	0.2	63.6	8.6	4.8	0.1	2.8	0.4
3.0	16.2	4.2	16.0	2.5	10.7	1.7	55.0	3.4	5.9	0.6	3.2	0.4	37.8	4.1	8.4	0.4	5.0	0.8
4.5	8.4	2.8	11.1	1.7	7.5	1.0	-	-	-	-	-	-	-	-	-	-	-	-
6.0	-	-	-	-	-	-	29.7	0.7	9.8	0.9	4.5	0.6	14.3	0.6	17.2	1.1	13.0	0.8
12.0	-	-	-	-	-	-	19.5	0.0	12.0	0.0	5.0	0.0	-	-	-	-	-	-

B

mAMSA	Nalm-6 WT						Nalm-6 $^{TOP2B-/-}$						Nalm-6 $^{TOP2A+/-}$					
	Relative survival		Average micronuclei		Micronucleus induction		Relative survival		Average micronuclei		Micronucleus induction		Relative survival		Average micronuclei		Micronucleus induction	
nM	%	SEM	%	SEM	Fold	SEM	%	SEM	%	SEM	Fold	SEM	%	SEM	%	SEM	Fold	SEM
0.0	100.0	0.0	1.9	0.2	1.0	0.0	100.0	0.0	2.6	0.2	1.0	0.0	100.0	0.0	2.4	0.2	1.0	0.0
8.0	67.7	4.1	5.0	0.6	3.3	0.3	84.0	2.6	4.6	1.0	1.7	0.3	86.3	8.3	4.3	0.6	1.8	0.3
16.0	42.7	2.3	9.1	0.8	4.9	0.3	67.5	2.4	5.8	1.5	2.1	0.3	66.4	2.0	7.5	0.7	3.2	0.5
33.0	-	-	-	-	-	-	-	-	-	-	-	-	37.8	0.6	12.1	0.2	5.1	0.1
50.0	10.3	1.2	17.4	1.6	8.3	2.1	36.5	2.2	10.8	2.3	4.0	0.6	21.8	1.3	16.5	0.7	7.0	0.6
64.0	-	-	-	-	-	-	28.3	1.5	13.3	1.2	5.6	0.6	-	-	-	-	-	-
100.0	-	-	-	-	-	-	15.9	0.3	19.6	0.3	8.1	0.4	-	-	-	-	-	-

Table 6.13 Summary tables of micronucleus assay data (A) MTX and (B) mAMSA.

A

Dox	Nalm-6 WT						Nalm-6 $^{TOP2B-/-}$						Nalm-6 $^{TOP2A+/-}$					
	Relative survival		Average micronuclei		Micronucleus induction		Relative survival		Average micronuclei		Micronucleus induction		Relative survival		Average micronuclei		Micronucleus induction	
nM	%	SEM	%	SEM	Fold	SEM	%	SEM	%	SEM	Fold	SEM	%	SEM	%	SEM	Fold	SEM
0.0	100.0	0.0	1.3	0.1	1.0	0.0	100.0	0.0	1.9	0.2	1.0	0.0	100.0	0.0	1.7	0.3	1.0	0.0
3.0	92.3	3.9	2.4	0.4	2.0	0.4	98.0	6.4	2.8	0.5	1.7	0.3	100.0	10.9	2.1	0.2	1.2	0.1
6.0	61.6	2.8	6.6	0.9	5.1	0.6	76.2	4.7	4.5	0.6	2.8	0.4	87.8	12.0	3.9	0.8	2.2	0.0
9.5	35.0	6.1	16.0	1.6	10.7	1.2	53.1	1.6	8.2	0.7	4.5	0.5	58.8	7.2	5.9	1.2	3.3	0.1
12.0	-	-	-	-	-	-	47.1	0.0	10.6	0.0	4.4	0.0	49.2	0.5	9.1	0.3	6.8	0.2
20.0	-	-	-	-	-	-	21.1	0.6	19.8	0.2	9.1	0.4	-	-	-	-	-	-

B

Epi	Nalm-6 WT						Nalm-6 $^{TOP2B-/-}$						Nalm-6 $^{TOP2A+/-}$					
	Relative survival		Average micronuclei		Micronucleus induction		Relative survival		Average micronuclei		Micronucleus induction		Relative survival		Average micronuclei		Micronucleus induction	
nM	%	SEM	%	SEM	Fold	SEM	%	SEM	%	SEM	Fold	SEM	%	SEM	%	SEM	Fold	SEM
0.0	100.0	0.0	1.3	0.1	1.0	0.0	100.0	0.0	1.9	0.2	1.0	0.0	100.0	0.0	1.7	0.3	1.0	0.0
3.0	82.2	4.4	2.2	0.3	1.8	0.2	96.3	5.6	2.3	0.2	1.4	0.2	102.5	8.7	2.4	0.3	1.4	0.2
6.0	58.5	3.6	4.7	0.6	3.9	0.4	76.7	13.5	4.1	0.5	2.5	0.4	84.2	11.7	3.2	0.3	1.8	0.2
9.5	31.8	5.9	15.4	4.6	10.2	3.0	57.4	3.6	7.0	0.4	3.9	0.4	65.5	14.1	7.1	1.3	4.0	0.3
12.0	-	-	-	-	-	-	38.3	2.9	12.5	0.1	5.7	0.2	47.3	2.0	8.4	0.6	6.3	0.5
13.0	17.8	0.2	24.8	4.8	16.7	2.9	-	-	-	-	-	-	-	-	-	-	-	-
20.0	-	-	-	-	-	-	11.2	0.0	27.5	0.0	11.5	0.0	-	-	-	-	-	-

Table 6.14 Summary tables of micronucleus assay data (A) Dox and (B) Epi.

A

VM26	Nalm-6 WT						Nalm-6$^{TOP2B-/-}$						Nalm-6$^{TOP2A+/-}$					
	Relative survival		Average micronuclei		Micronucleus induction		Relative survival		Average micronuclei		Micronucleus induction		Relative survival		Average micronuclei		Micronucleus induction	
nM	%	SEM	%	SEM	Fold	SEM	%	SEM	%	SEM	Fold	SEM	%	SEM	%	SEM	Fold	SEM
0.0	100.0	0.0	1.9	0.2	1.0	0.0	100.0	0.0	2.6	0.2	1.0	0.0	100.0	0.0	2.4	0.2	1.0	0.0
2.0	80.8	4.5	3.8	0.6	2.5	0.3	93.4	1.9	3.3	0.2	1.2	0.1	111.8	3.1	3.8	0.7	1.5	0.2
4.0	55.1	3.0	6.7	1.1	3.5	0.3	61.7	4.5	4.9	1.3	1.8	0.3	95.5	4.9	4.4	0.4	1.8	0.1
10.0	26.3	5.5	12.6	0.5	5.8	0.9	31.1	1.1	10.3	1.5	4.0	0.5	67.4	6.3	6.8	0.6	2.9	0.5
12.0	-	-	-	-	-	-	25.0	0.9	11.9	0.8	4.9	0.4	-	-	-	-	-	-
16.0	-	-	-	-	-	-	-	-	-	-	-	-	38.2	3.1	10.5	0.7	4.4	0.3

B

VP16	Nalm-6 WT						Nalm-6$^{TOP2B-/-}$						Nalm-6$^{TOP2A+/-}$					
	Relative survival		Average micronuclei		Micronucleus induction		Relative survival		Average micronuclei		Micronucleus induction		Relative survival		Average micronuclei		Micronucleus induction	
nM	%	SEM	%	SEM	Fold	SEM	%	SEM	%	SEM	Fold	SEM	%	SEM	%	SEM	Fold	SEM
0.0	100.0	0.0	1.9	0.2	1.0	0.0	100.0	0.0	2.6	0.2	1.0	0.0	100.0	0.0	2.4	0.2	1.0	0.0
22.5	82.9	4.9	3.4	0.6	2.3	0.4	83.8	7.0	5.1	1.0	1.9	0.2	103.7	3.5	4.1	0.9	1.7	0.4
45.0	57.4	2.6	6.8	0.8	3.7	0.4	66.2	3.5	6.5	1.2	2.4	0.2	83.3	3.2	5.0	0.6	2.1	0.3
85.0	36.5	4.7	11.5	1.1	5.3	0.9	43.9	3.3	8.5	0.8	3.3	0.4	70.5	4.2	6.2	0.6	2.6	0.1
90.0	-	-	-	-	-	-	40.7	0.6	9.2	0.8	3.8	0.4	-	-	-	-	-	-
110.0	-	-	-	-	-	-	35.5	0.0	12.1	0.0	5.2	0.0	54.3	3.0	7.9	0.1	3.3	0.0

Table 6.15 Summary tables of micronucleus assay data (A) VM26 and (B) VP16.

Chapter 7. Conclusions and Overview

Chapter 3 presents data demonstrating that proteasome inhibitors can potentiate the growth-inhibitory effects of TOP2 poisons in a K562 cell line. Two proteasome inhibitors were used: MG132, an investigational drug, and PS341-a clinically-important proteasome inhibitor (Trade names Velcade or Bortezomib)- which has Food and Drug Administration (FDA) approval for use in multiple myeloma and mantle cell lymphoma and which is being studied in other chemotherapy regimens (Sterz *et al.*, 2008). These agents were used at a fixed concentration (that alone produced 20% cell growth inhibition) in combination with increasing concentrations of various TOP2 poisons. The greatest potentiation for both agents was seen with mitoxantrone, with a Pf_{50} of 4.58 for MG132 and PF_{50} 2.95 for PS341. PS341 significantly potentiated the growth inhibition of three TOP2 poisons in K562 cells: mitoxantrone, mAMSA and epirubicin, while MG132 potentiated all six TOP2 poisons. Both MG132 and PS341 target the same protease component within the proteasome, namely the β5 subunit (Lightcap *et al.*, 2000; Kisselev and Goldberg, 2001), so it is not entirely clear why the potentiation effects differ. We found that a 120-hour exposure to PS341 increased the intracellular protein level of TOP2A, however, MG132 did not. This drug-specific increase in TOP2A target level may contribute to the observed differences in potentiation. Previous reports have suggested that PS341 increases the sensitivity of cells to anti-topoisomerase II drugs by increasing levels of TOP2 drug target in the cell (Ogiso *et al.*, 2000; Congdon *et al.*, 2008).

It is possible the MG132 potentiation of anti-topoisomerase II drugs is mediated by multiple mechanisms. Proteasome inhibition will cause the accumulation of ubiquitin conjugates and reduce free ubiquitin (Xu *et al.*, 2004). Ubiquitination plays a key role in the cellular response to DNA damage. MG132 has been shown to inhibit focus formation involving DNA damage signalling proteins and DNA repair proteins, such as BRCA1,

53BP1 and Rad51, after exposure to IR and cisplatin (Jacquemont and Taniguchi, 2007). Therefore, as well as reducing the processivity of the proteasome, MG132 and PS341 may potentiate the growth inhibitory effects of anti-topoisomerase II drugs by reducing the repair of double-strand breaks once TOP2-DNA complexes have been processed.

The levels of TOP2-DNA complexes in the presence and absence of MG132 were measured using the TARDIS assay. This experimental approach required higher levels of both the TOP2 drug and MG132. Inhibition of the proteasome increased the levels of TOP2 complexes seen with etoposide but not with mAMSA, consistent with the idea that there are multiple possible mechanisms by which proteasomal inhibition affects TOP2 drug effects.

Drug stabilised DNA-TOP2 complexes can be removed by a number of mechanisms (Figure 7.1). For example, proteasomal proteases may degrade TOP2 protein bound to DNA, leaving a 5' phosphotyrosyl-adduct on a DSB or a SSB, to be removed by TDP2 or FEN1, respectively (Salmena *et al.*, 2001; Cortes Ledesma *et al.*, 2009; Schellenberg *et al.*, 2012; Gao *et al.*, 2014a; Kametani *et al.*, 2016). Moreover, a number of nucleases such as MRE11 and DNA2, or AP lyases such as KU70/80 and APE1 can remove stabilised TOP2 complexes to facilitate DSB repair (Ayene *et al.*, 2005; Roberts *et al.*, 2010; Lee, 2012; Lee *et al.*, 2012; Tammaro *et al.*, 2016). Different mechanism(s) or a combination of mechanisms may be involved in the removal of TOP2 complexes stabilised by different TOP2 poisons. This may explain the differences observed with mAMSA and etoposide stabilised complexes in response to proteasomal inhibition with MG132.

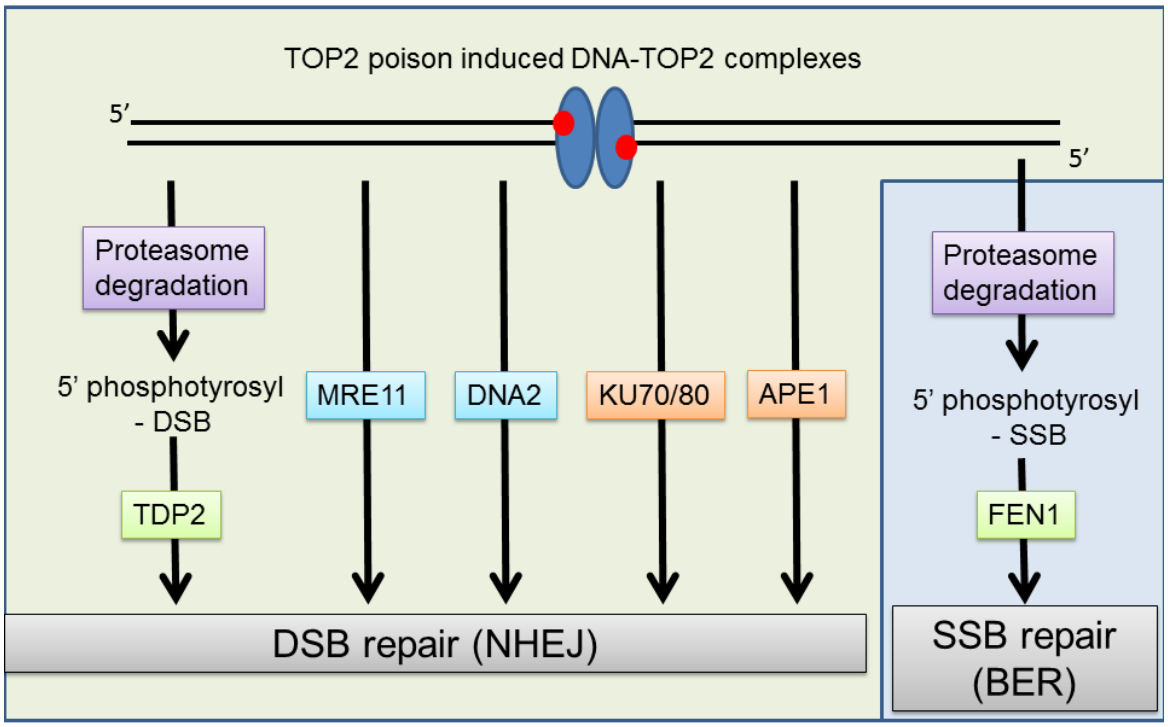

Figure 7.1 Schematic summary of the different processes involved in the removal of TOP2 complexes. The various stabilising compounds may affect different pathways.

Clinically, targeting the ubiquitin proteasome system in combination with existing therapies may allow treatment intensification. For example, a low dose of PS341 in combination with a TOP2 drug such as mitoxantrone may significantly increase the effectiveness without increasing toxicity.

One type of toxicity investigated in this study is genotoxicity, for which a standard measure is to determine the percentage of micronuclei formed following exposure to drugs. In Chapter 4, the effects of combinations of proteasome inhibitors and the TOP2 poison mitoxantrone on the generation of micronuclei were examined *in vitro*. Two methods of assessment were used: a slide-based manual counting method and an automated method using FACS. For the slide-based method, at least 2000 cells were counted per drug condition, whereas for the FACS-based method around 30,000 cells were analysed. However, the experimental protocol for the FACS-based method involves cell lysis of the cells which can lead to background problems if high levels of cell debris are present following exposure to high drug doses. The increased background signal can result in misleadingly high levels of micronuclei-sized particles. These

experiments showed that low levels of a proteasome inhibitor can actually reduce the level of micronuclei without reducing cytotoxicity. Further studies will be required to determine if these combinations also reduce other types of cellular toxicity.

Type II DNA topoisomerases can be ubiquitinated via a series of enzymatic steps. Ubiquitin is activated by an E1 activation enzyme, then transferred to an E2 ubiquitin-conjugating enzyme, and both the E2 and the target protein are then bound to an E3 ligase. Cells possess more than 600 E3 ligases exhibiting different substrate specificities. Two E3 ligases-Bmi1/Ring1A and HDM2-have been reported to interact with TOP2A (Nayak *et al.*, 2007; Kitagaki *et al.*, 2008; Alchanati *et al.*, 2009; Conradt *et al.*, 2013). Small molecule inhibitors for these two E3 ligases such as PRT4165 and HLI373 have been described in the literature and are commercially available. Experiments in Chapter 5 showed that both of these compounds can potentiate the growth inhibition by some TOP2 poisons. Further work will be required to work out the mechanism(s) underlying the potentiation.

Anthracycline therapy is in wide use in the clinic; however the dose that can be used is limited by toxicity such as cardiotoxicity. A murine model system showed that TOP2B removal from cardiomyocytes reduced the cardiac damage induced by doxorubicin (Zhang *et al.*, 2012). This observation led to the suggestion that drugs targeting only TOP2A would be of clinical value in reducing cardiotoxicity. To investigate the effect of the two isoforms on genotoxicity, studies in Chapter 6 measured micronuclei in three Nalm-6 cells lines with differing levels of TOP2A and TOP2B (Nalm-6 WT, Nalm-6$^{TOP2A+/-}$, and Nalm-6$^{TOP2B-/-}$). All six TOP2 poisons examined were found to generate micronuclei in a dose-dependent manner. Further work will be required to investigate the contribution of TOP2 isoforms to genotoxicity and cardiotoxicity.

In conclusion, studies described in this thesis have investigated the role of the proteasome in the processing of stabilised TOP2-DNA complexes.

Proteasomal inhibition potentiated the growth inhibition of TOP2 poisons. Potentiation is possibly mediated by prolonging the stabilisation of TOP2-DNA complexes. The association of proteasome and other DNA signalling protein and DNA repair proteins, such as BRCA1, 53BP1 and Rad51, may also contribute to the potentiation. Co-inhibition of proteasome and TOP2 has the potential to reduce the genotoxicity of TOP2 poisons during treatment. Further work will be required to understand the mechanism of by which stabilised TOP2-DNA complexes are removed. Thus, the work described here offers a potentially important approach to improving current cancer treatment.

Chapter 8. References

Akimitsu, N., Adachi, N., Hirai, H., Hossain, M.S., Hamamoto, H., Kobayashi, M., Aratani, Y., Koyama, H. and Sekimizu, K. (2003) 'Enforced cytokinesis without complete nuclear division in embryonic cells depleting the activity of DNA topoisomerase IIalpha', *Genes Cells*, 8(4), pp. 393-402.

Alchanati, I., Teicher, C., Cohen, G., Shemesh, V., Barr, H.M., Nakache, P., Ben-Avraham, D., Idelevich, A., Angel, I., Livnah, N., Tuvia, S., Reiss, Y., Taglicht, D. and Erez, O. (2009) 'The E3 ubiquitin-ligase Bmi1/Ring1A controls the proteasomal degradation of Top2alpha cleavage complex - a potentially new drug target', *PLoS One*, 4(12), p. e8104.

Arcamone, F., Cassinelli, G., Fantini, G., Grein, A., Orezzi, P., Pol, C. and Spalla, C. (1969a) 'Adriamycin, 14-hydroxydaunomycin, a new antitumor antibiotic from S. peucetius var. caesius', *Biotechnol Bioeng*, 11(6), pp. 1101-10.

Arcamone, F., Franceschi, G., Penco, S. and Selva, A. (1969b) 'Adriamycin (14-hydroxydaunomycin), a novel antitumor antibiotic', *Tetrahedron Lett*, (13), pp. 1007-10.

Avlasevich, S.L., Bryce, S.M., Cairns, S.E. and Dertinger, S.D. (2006) 'In vitro micronucleus scoring by flow cytometry: differential staining of micronuclei versus apoptotic and necrotic chromatin enhances assay reliability', *Environ Mol Mutagen*, 47(1), pp. 56-66.

Ayene, I.S., Ford, L.P. and Koch, C.J. (2005) 'Ku protein targeting by Ku70 small interfering RNA enhances human cancer cell response to topoisomerase II inhibitor and gamma radiation', *Mol Cancer Ther*, 4(4), pp. 529-36.

Azarova, A.M., Lyu, Y.L., Lin, C.P., Tsai, Y.C., Lau, J.Y., Wang, J.C. and Liu, L.F. (2007) 'Roles of DNA topoisomerase II isozymes in chemotherapy and secondary malignancies', *Proc Natl Acad Sci U S A*, 104(26), pp. 11014-9.

Berger, J.M., Gamblin, S.J., Harrison, S.C. and Wang, J.C. (1996) 'Structure and mechanism of DNA topoisomerase II', *Nature*, 379(6562), pp. 225-32.

Bryce, S.M., Bemis, J.C., Avlasevich, S.L. and Dertinger, S.D. (2007) 'In vitro micronucleus assay scored by flow cytometry provides a comprehensive evaluation of cytogenetic damage and cytotoxicity', *Mutat Res*, 630(1-2), pp. 78-91.

Capranico, G., Tinelli, S., Austin, C.A., Fisher, M.L. and Zunino, F. (1992) 'Different patterns of gene expression of topoisomerase II isoforms in differentiated tissues during murine development', *Biochim Biophys Acta*, 1132(1), pp. 43-8.

Chen, M.C., Chen, C.H., Chuang, H.C., Kulp, S.K., Teng, C.M. and Chen, C.S. (2011) 'Novel mechanism by which histone deacetylase inhibitors facilitate topoisomerase IIalpha degradation in hepatocellular carcinoma cells', *Hepatology*, 53(1), pp. 148-59.

Ciechanover, A. (2005) 'Proteolysis: from the lysosome to ubiquitin and the proteasome', *Nat Rev Mol Cell Biol*, 6(1), pp. 79-87.

Congdon, L.M., Pourpak, A., Escalante, A.M., Dorr, R.T. and Landowski, T.H. (2008) 'Proteasomal inhibition stabilizes topoisomerase IIalpha protein and reverses resistance to the topoisomerase II poison ethonafide (AMP-53, 6-ethoxyazonafide)', *Biochem Pharmacol*, 75(4), pp. 883-90.

Conradt, L., Henrich, A., Wirth, M., Reichert, M., Lesina, M., Algul, H., Schmid, R.M., Kramer, O.H., Saur, D. and Schneider, G. (2013) 'Mdm2 inhibitors synergize with topoisomerase II inhibitors to induce p53-independent pancreatic cancer cell death', *Int J Cancer*, 132(10), pp. 2248-57.

Cortes Ledesma, F., El Khamisy, S.F., Zuma, M.C., Osborn, K. and Caldecott, K.W. (2009) 'A human 5'-tyrosyl DNA phosphodiesterase that repairs topoisomerase-mediated DNA damage', *Nature*, 461(7264), pp. 674-8.

Cowell, I.G., Sondka, Z., Smith, K., Lee, K.C., Manville, C.M., Sidorczuk-Lesthuruge, M., Rance, H.A., Padget, K., Jackson, G.H., Adachi, N. and Austin, C.A. (2012) 'Model for MLL translocations in therapy-related leukemia involving topoisomerase IIbeta-mediated DNA strand breaks and gene proximity', *Proc Natl Acad Sci U S A*, 109(23), pp. 8989-94.

Cowell, I.G., Tilby, M.J. and Austin, C.A. (2011) 'An overview of the visualisation and quantitation of low and high MW DNA adducts using the trapped in agarose DNA immunostaining (TARDIS) assay', *Mutagenesis*, 26(2), pp. 253-60.

Dereuddre, S., Delaporte, C. and Jacquemin-Sablon, A. (1997) 'Role of topoisomerase II beta in the resistance of 9-OH-ellipticine-resistant Chinese hamster fibroblasts to topoisomerase II inhibitors', *Cancer Res*, 57(19), pp. 4301-8.

Diaz, D., Scott, A., Carmichael, P., Shi, W. and Costales, C. (2007) 'Evaluation of an automated in vitro micronucleus assay in CHO-K1 cells', *Mutat Res*, 630(1-2), pp. 1-13.

Errington, F., Willmore, E., Leontiou, C., Tilby, M.J. and Austin, C.A. (2004) 'Differences in the longevity of topo IIalpha and topo IIbeta drug-stabilized cleavable complexes and the relationship to drug sensitivity', *Cancer Chemother Pharmacol*, 53(2), pp. 155-62.

Errington, F., Willmore, E., Tilby, M.J., Li, L., Li, G., Li, W., Baguley, B.C. and Austin, C.A. (1999) 'Murine transgenic cells lacking DNA topoisomerase IIbeta are resistant to acridines and mitoxantrone: analysis of cytotoxicity and cleavable complex formation', *Mol Pharmacol*, 56(6), pp. 1309-16.

Felix, C.A. (1998) 'Secondary leukemias induced by topoisomerase-targeted drugs', *Biochim Biophys Acta*, 1400(1-3), pp. 233-55.

Felix, C.A. (2001) 'Leukemias related to treatment with DNA topoisomerase II inhibitors', *Med Pediatr Oncol*, 36(5), pp. 525-35.

Felix, C.A., Kolaris, C.P. and Osheroff, N. (2006) 'Topoisomerase II and the etiology of chromosomal translocations', *DNA Repair (Amst)*, 5(9-10), pp. 1093-108.

Fenech, M. (2000) 'The in vitro micronucleus technique', *Mutat Res*, 455(1-2), pp. 81-95.

Fenech, M., Kirsch-Volders, M., Natarajan, A.T., Surralles, J., Crott, J.W., Parry, J., Norppa, H., Eastmond, D.A., Tucker, J.D. and Thomas, P. (2011) 'Molecular mechanisms of micronucleus,

nucleoplasmic bridge and nuclear bud formation in mammalian and human cells', *Mutagenesis*, 26(1), pp. 125-32.

Gao, R., Huang, S.Y., Marchand, C. and Pommier, Y. (2012) 'Biochemical characterization of human tyrosyl DNA phosphodiesterase 2 (TDP2/TTRAP): a Mg2+/Mn2+-dependent phosphodiesterase specific for the repair of topoisomerase cleavage complexes', *J Biol Chem*.

Gao, R., Schellenberg, M.J., Huang, S.-y.N., Abdelmalak, M., Marchand, C., Nitiss, K.C., Nitiss, J.L., Williams, R.S. and Pommier, Y. (2014a) 'Proteolytic degradation of topoisomerase II (TOP2) enables the processing of Top2·DNA and Top2·RNA covalent complexes by tyrosyl-DNA-phosphodiesterase 2 (TDP2)', *Journal of Biological Chemistry*, 289(26), pp. 17960-17969.

Gao, R., Schellenberg, M.J., Huang, S.Y., Abdelmalak, M., Marchand, C., Nitiss, K.C., Nitiss, J.L., Williams, R.S. and Pommier, Y. (2014b) 'Proteolytic degradation of topoisomerase II (TOP2) enables the processing of Top2-DNA and -RNA covalent complexes by tyrosyl-DNA-phosphodiesterase 2 (TDP2)', *J Biol Chem*.

Goldberg, A.L. (2007) 'Functions of the proteasome: from protein degradation and immune surveillance to cancer therapy', *Biochem Soc Trans*, 35(Pt 1), pp. 12-7.

Hartlerode, A.J. and Scully, R. (2009) 'Mechanisms of double-strand break repair in somatic mammalian cells', *Biochem J*, 423(2), pp. 157-68.

Huang, Y., Fenech, M. and Shi, Q. (2011) 'Micronucleus formation detected by live-cell imaging', *Mutagenesis*, 26(1), pp. 133-8.

Jacquemont, C. and Taniguchi, T. (2007) 'Proteasome function is required for DNA damage response and fanconi anemia pathway activation', *Cancer Res*, 67(15), pp. 7395-405.

Kametani, Y., Takahata, C., Narita, T., Tanaka, K., Iwai, S. and Kuraoka, I. (2016) 'FEN1 participates in repair of the 5'-phosphotyrosyl terminus of DNA single-strand breaks', *Carcinogenesis*, 37(1), pp. 56-62.

Kisselev, A.F. and Goldberg, A.L. (2001) 'Proteasome inhibitors: from research tools to drug candidates', *Chem Biol*, 8(8), pp. 739-58.

Kitagaki, J., Agama, K.K., Pommier, Y., Yang, Y. and Weissman, A.M. (2008) 'Targeting tumor cells expressing p53 with a water-soluble inhibitor of Hdm2', *Mol Cancer Ther*, 7(8), pp. 2445-54.

Koeffler, H.P. and Golde, D.W. (1980) 'Human myeloid leukemia cell lines: a review', *Blood*, 56(3), pp. 344-50.

Larsen, A.K., Escargueil, A.E. and Skladanowski, A. (2003) 'Catalytic topoisomerase II inhibitors in cancer therapy', *Pharmacol Ther*, 99(2), pp. 167-81.

Lee, D.H. and Goldberg, A.L. (1998) 'Proteasome inhibitors: valuable new tools for cell biologists', *Trends Cell Biol*, 8(10), pp. 397-403.

Lee, K.C. (2012) 'Molecular pharmacology of DNA topoisomerase II: a study to investigate DNA-topoisomerase II complex removal mechanisms', *MPhil*.

Lee, K.C., Bramley, R.L., Cowell, I.G., Jackson, G.H. and Austin, C.A. (2016) 'Proteasomal inhibition potentiates drugs targeting DNA topoisomerase II', *Biochem Pharmacol*, 103, pp. 29-39.

Lee, K.C., Padget, K., Curtis, H., Cowell, I.G., Moiani, D., Sondka, Z., Morris, N.J., Jackson, G.H., Cockell, S.J., Tainer, J.A. and Austin, C.A. (2012) 'MRE11 facilitates the removal of human topoisomerase II complexes from genomic DNA', *Biology Open*, 1(9), pp. 863-873.

Lightcap, E.S., McCormack, T.A., Pien, C.S., Chau, V., Adams, J. and Elliott, P.J. (2000) 'Proteasome inhibition measurements: clinical application', *Clin Chem*, 46(5), pp. 673-83.

Lindberg, H.K., Falck, G.C., Jarventaus, H. and Norppa, H. (2008) 'Characterization of chromosomes and chromosomal fragments in human lymphocyte micronuclei by telomeric and centromeric FISH', *Mutagenesis*, 23(5), pp. 371-6.

Madabhushi, R., Gao, F., Pfenning, A.R., Pan, L., Yamakawa, S., Seo, J., Rueda, R., Phan, T.X., Yamakawa, H., Pao, P.C., Stott,

R.T., Gjoneska, E., Nott, A., Cho, S., Kellis, M. and Tsai, L.H. (2015) 'Activity-induced DNA breaks govern the expression of neuronal early-response genes', *Cell*, 161(7), pp. 1592-605.

Mao, Y., Desai, S.D., Ting, C.Y., Hwang, J. and Liu, L.F. (2001) '26 S proteasome-mediated degradation of topoisomerase II cleavable complexes', *J Biol Chem*, 276(44), pp. 40652-8.

Martensson, S., Nygren, J., Osheroff, N. and Hammarsten, O. (2003) 'Activation of the DNA-dependent protein kinase by drug-induced and radiation-induced DNA strand breaks', *Radiat Res*, 160(3), pp. 291-301.

Nalepa, G., Rolfe, M. and Harper, J.W. (2006) 'Drug discovery in the ubiquitin-proteasome system', *Nat Rev Drug Discov*, 5(7), pp. 596-613.

Nayak, M.S., Yang, J.M. and Hait, W.N. (2007) 'Effect of a single nucleotide polymorphism in the murine double minute 2 promoter (SNP309) on the sensitivity to topoisomerase II-targeting drugs', *Cancer Res*, 67(12), pp. 5831-9.

Nitiss, J.L. (2009) 'Targeting DNA topoisomerase II in cancer chemotherapy', *Nat Rev Cancer*, 9(5), pp. 338-50.

Norppa, H. and Falck, G.C. (2003) 'What do human micronuclei contain?', *Mutagenesis*, 18(3), pp. 221-33.

Nusse, M., Beisker, W., Kramer, J., Miller, B.M., Schreiber, G.A., Viaggi, S., Weller, E.M. and Wessels, J.M. (1994) 'Measurement of micronuclei by flow cytometry', *Methods Cell Biol*, 42 Pt B, pp. 149-58.

O'Donovan, P.J. and Livingston, D.M. (2010) 'BRCA1 and BRCA2: breast/ovarian cancer susceptibility gene products and participants in DNA double-strand break repair', *Carcinogenesis*, 31(6), pp. 961-7.

Oecd *Test No. 487: In Vitro Mammalian Cell Micronucleus Test*. OECD Publishing.

Ogiso, Y., Tomida, A., Lei, S., Omura, S. and Tsuruo, T. (2000) 'Proteasome inhibition circumvents solid tumor resistance to topoisomerase II-directed drugs', *Cancer Res*, 60(9), pp. 2429-34.

Onda, T., Toyoda, E., Miyazaki, O., Seno, C., Kagaya, S., Okamoto, K. and Nishikawa, K. (2008) 'NK314, a novel topoisomerase II inhibitor, induces rapid DNA double-strand breaks and exhibits superior antitumor effects against tumors resistant to other topoisomerase II inhibitors', *Cancer Lett*, 259(1), pp. 99-110.

Pommier, Y., Huang, S.Y., Gao, R., Das, B.B., Murai, J. and Marchand, C. (2014) 'Tyrosyl-DNA-phosphodiesterases (TDP1 and TDP2)', *DNA Repair (Amst)*, 19, pp. 114-29.

Pommier, Y., Leo, E., Zhang, H. and Marchand, C. (2010) 'DNA topoisomerases and their poisoning by anticancer and antibacterial drugs', *Chem Biol*, 17(5), pp. 421-33.

Prokocimer, M., Shaklai, M., Bassat, H.B., Wolf, D., Goldfinger, N. and Rotter, V. (1986) 'Expression of p53 in human leukemia and lymphoma', *Blood*, 68(1), pp. 113-8.

Roberts, S.A., Strande, N., Burkhalter, M.D., Strom, C., Havener, J.M., Hasty, P. and Ramsden, D.A. (2010) 'Ku is a 5'-dRP/AP lyase that excises nucleotide damage near broken ends', *Nature*, 464(7292), pp. 1214-7.

Rowley, J.D. (1998) 'The critical role of chromosome translocations in human leukemias', *Annu Rev Genet*, 32, pp. 495-519.

Rowley, J.D. and Olney, H.J. (2002) 'International workshop on the relationship of prior therapy to balanced chromosome aberrations in therapy-related myelodysplastic syndromes and acute leukemia: overview report', *Genes Chromosomes Cancer*, 33(4), pp. 331-45.

Salmena, L., Lam, V., McPherson, J.P. and Goldenberg, G.J. (2001) 'Role of proteasomal degradation in the cell cycle-dependent regulation of DNA topoisomerase IIalpha expression', *Biochem Pharmacol*, 61(7), pp. 795-802.

Schellenberg, M.J., Appel, C.D., Adhikari, S., Robertson, P.D., Ramsden, D.A. and Williams, R.S. (2012) 'Mechanism of repair of 5'-topoisomerase II-DNA adducts by mammalian tyrosyl-DNA phosphodiesterase 2', *Nat Struct Mol Biol*, 19(12), pp. 1363-71.

Shi, K., Kurahashi, K., Gao, R., Tsutakawa, S.E., Tainer, J.A., Pommier, Y. and Aihara, H. (2012) 'Structural basis for recognition of 5'-phosphotyrosine adducts by Tdp2', *Nat Struct Mol Biol*, 19(12), pp. 1372-7.

Shibai-Ogata, A., Kakinuma, C., Hioki, T. and Kasahara, T. (2011) 'Evaluation of high-throughput screening for in vitro micronucleus test using fluorescence-based cell imaging', *Mutagenesis*, 26(6), pp. 709-19.

Shinagawa, H., Miki, Y. and Yoshida, K. (2008) 'BRCA1-mediated ubiquitination inhibits topoisomerase II alpha activity in response to oxidative stress', *Antioxid Redox Signal*, 10(5), pp. 939-49.

Smith, M.A., Rubinstein, L., Anderson, J.R., Arthur, D., Catalano, P.J., Freidlin, B., Heyn, R., Khayat, A., Krailo, M., Land, V.J., Miser, J., Shuster, J. and Vena, D. (1999) 'Secondary leukemia or myelodysplastic syndrome after treatment with epipodophyllotoxins', *J Clin Oncol*, 17(2), pp. 569-77.

Sterz, J., von Metzler, I., Hahne, J.C., Lamottke, B., Rademacher, J., Heider, U., Terpos, E. and Sezer, O. (2008) 'The potential of proteasome inhibitors in cancer therapy', *Expert Opin Investig Drugs*, 17(6), pp. 879-95.

Sunter, N.J., Cowell, I.G., Willmore, E., Watters, G.P. and Austin, C.A. (2010) 'Role of topoisomerase IIbeta in DNA damage response following IR and etoposide', *J Nucleic Acids*, 2010.

Tammaro, M., Liao, S., Beeharry, N. and Yan, H. (2016) 'DNA double-strand breaks with 5' adducts are efficiently channeled to the DNA2-mediated resection pathway', *Nucleic Acids Res*, 44(1), pp. 221-31.

Thakurela, S., Garding, A., Jung, J., Schubeler, D., Burger, L. and Tiwari, V.K. (2013) 'Gene regulation and priming by topoisomerase IIalpha in embryonic stem cells', *Nat Commun*, 4, p. 2478.

Tiwari, V.K., Burger, L., Nikoletopoulou, V., Deogracias, R., Thakurela, S., Wirbelauer, C., Kaut, J., Terranova, R., Hoerner,

L., Mielke, C., Boege, F., Murr, R., Peters, A.H., Barde, Y.A. and Schubeler, D. (2012) 'Target genes of topoisomerase IIbeta regulate neuronal survival and are defined by their chromatin state', *Proc Natl Acad Sci U S A*, 109(16), pp. E934-43.

Toyoda, E., Kagaya, S., Cowell, I.G., Kurosawa, A., Kamoshita, K., Nishikawa, K., Iiizumi, S., Koyama, H., Austin, C.A. and Adachi, N. (2008) 'NK314, a topoisomerase II inhibitor that specifically targets the alpha isoform', *J Biol Chem*, 283(35), pp. 23711-20.

Vejpongsa, P. and Yeh, E.T. (2014) 'Topoisomerase 2beta: a promising molecular target for primary prevention of anthracycline-induced cardiotoxicity', *Clin Pharmacol Ther*, 95(1), pp. 45-52.

Wang, J.C. (2002) 'Cellular roles of DNA topoisomerases: a molecular perspective', *Nat Rev Mol Cell Biol*, 3(6), pp. 430-40.

Wendorff, T.J., Schmidt, B.H., Heslop, P., Austin, C.A. and Berger, J.M. (2012) 'The structure of DNA-bound human topoisomerase II alpha: conformational mechanisms for coordinating inter-subunit interactions with DNA cleavage', *J Mol Biol*, 424(3-4), pp. 109-24.

Willmore, E., de Caux, S., Sunter, N.J., Tilby, M.J., Jackson, G.H., Austin, C.A. and Durkacz, B.W. (2004) 'A novel DNA-dependent protein kinase inhibitor, NU7026, potentiates the cytotoxicity of topoisomerase II poisons used in the treatment of leukemia', *Blood*, 103(12), pp. 4659-65.

Willmore, E., Frank, A.J., Padget, K., Tilby, M.J. and Austin, C.A. (1998) 'Etoposide targets topoisomerase IIalpha and IIbeta in leukemic cells: isoform-specific cleavable complexes visualized and quantified in situ by a novel immunofluorescence technique', *Mol Pharmacol*, 54(1), pp. 78-85.

Wu, C.C., Li, T.K., Farh, L., Lin, L.Y., Lin, T.S., Yu, Y.J., Yen, T.J., Chiang, C.W. and Chan, N.L. (2011) 'Structural basis of type II topoisomerase inhibition by the anticancer drug etoposide', *Science*, 333(6041), pp. 459-62.

Xiao, H. and Goodrich, D.W. (2005) 'The retinoblastoma tumor suppressor protein is required for efficient processing and repair

of trapped topoisomerase II-DNA-cleavable complexes', *Oncogene*, 24(55), pp. 8105-13.

Xu, Q., Farah, M., Webster, J.M. and Wojcikiewicz, R.J. (2004) 'Bortezomib rapidly suppresses ubiquitin thiolesterification to ubiquitin-conjugating enzymes and inhibits ubiquitination of histones and type I inositol 1,4,5-trisphosphate receptor', *Mol Cancer Ther*, 3(10), pp. 1263-9.

Yang, X., Li, W., Prescott, E.D., Burden, S.J. and Wang, J.C. (2000) 'DNA topoisomerase IIbeta and neural development', *Science*, 287(5450), pp. 131-4.

Yun, J., Kim, Y.I., Tomida, A. and Choi, C.H. (2009) 'Regulation of DNA topoisomerase IIalpha stability by the ECV ubiquitin ligase complex', *Biochem Biophys Res Commun*, 389(1), pp. 5-9.

Zeng, Z., Cortes-Ledesma, F., El Khamisy, S.F. and Caldecott, K.W. (2011) 'TDP2/TTRAP is the major 5'-tyrosyl DNA phosphodiesterase activity in vertebrate cells and is critical for cellular resistance to topoisomerase II-induced DNA damage', *J Biol Chem*, 286(1), pp. 403-9.

Zhang, A., Lyu, Y.L., Lin, C.P., Zhou, N., Azarova, A.M., Wood, L.M. and Liu, L.F. (2006) 'A protease pathway for the repair of topoisomerase II-DNA covalent complexes', *J Biol Chem*, 281(47), pp. 35997-6003.

Zhang, S., Liu, X., Bawa-Khalfe, T., Lu, L.S., Lyu, Y.L., Liu, L.F. and Yeh, E.T. (2012) 'Identification of the molecular basis of doxorubicin-induced cardiotoxicity', *Nat Med*, 18(11), pp. 1639-42.

Chapter 9. Appendices

List of appendix figures

List of appendix tables

A

Relative survival						
Mitoxantrone (nM)	Nalm-6 WT		Nalm-6$^{TOP2B-/-}$		Nalm-6$^{TOP2A+/-}$	
	%	±SEM	%	±SEM	%	±SEM
0	100.0	0.0	100.0	0.0	100.0	0.0
0.75	68.7	2.6	98.6	6.9	90.5	15.4
1.5	39.3	4.7	84.1	9.5	63.6	8.6
3	16.2	4.2	55.0	3.4	37.8	4.1
4.5	8.4	2.8	-	-	-	-
6	-	-	29.7	0.7	14.3	0.6
12	-	-	19.5	0.0	-	-

B

Average micronuclei (%)						
Mitoxantrone (nM)	Nalm-6 WT		Nalm-6$^{TOP2B-/-}$		Nalm-6$^{TOP2A+/-}$	
	%	±SEM	%	±SEM	%	±SEM
0	1.3	0.1	1.9	0.2	1.7	0.3
0.75	3.8	0.2	2.2	0.1	3.3	0.1
1.5	8.3	0.9	3.8	0.2	4.8	0.1
3	16.0	2.5	5.9	0.6	8.4	0.4
4.5	11.1	1.7	-	-	-	-
6	-	-	9.8	0.9	17.2	1.1
12	-	-	12.0	0.0	-	-

C

Micronucleus induction (Fold change)						
Mitoxantrone (nM)	Nalm-6 WT		Nalm-6$^{TOP2B-/-}$		Nalm-6$^{TOP2A+/-}$	
	Fold	±SEM	Fold	±SEM	Fold	±SEM
0	1.0	0.0	1.0	0.0	1.0	0.0
0.75	3.2	0.4	1.4	0.1	1.9	0.3
1.5	7.0	0.8	2.3	0.2	2.8	0.4
3	10.7	1.7	3.2	0.4	5.0	0.8
4.5	7.5	1.0	-	-	-	-
6	-	-	4.5	0.6	13.0	0.8
12	-	-	5.0	0.0	-	-

Appendix table 1 Summary tables of appendix figure 1.

(A) Relative survival, (B) average percentage of micronuclei and (C) Micronucleus induction (fold change)

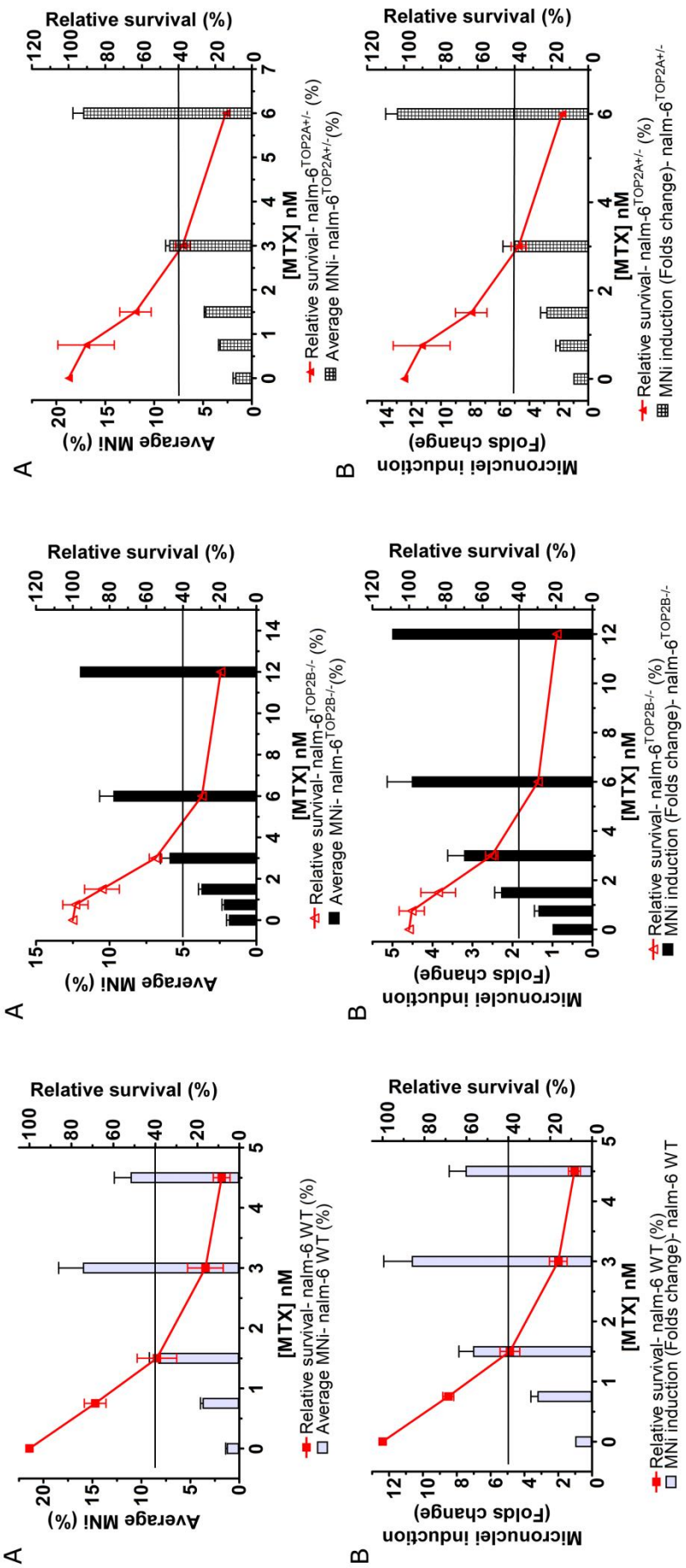

Appendix figure 1 Micronucleus formation in Nalm-6 cell lines after 48 hours exposure to MTX.

Data presented in average percentage of micronuclei (Row A) and fold change (Row B).

A

Relative survival						
mAMSA (nM)	Nalm-6 WT		Nalm-6$^{TOP2B-/-}$		Nalm-6$^{TOP2A+/-}$	
	%	±SEM	%	±SEM	%	±SEM
0	100.0	0.0	100.0	0.0	100.0	0.0
8	67.7	4.1	84.0	2.6	86.3	8.3
16	42.7	2.3	67.5	2.4	66.4	2.0
33	-	-	-	-	37.8	0.6
50	10.3	1.2	36.5	2.2	21.8	1.3
64	-	-	28.3	1.5	-	-
100	-	-	15.9	0.3	-	-

B

Average micronuclei (%)						
mAMSA (nM)	Nalm-6 WT		Nalm-6$^{TOP2B-/-}$		Nalm-6$^{TOP2A+/-}$	
	%	±SEM	%	±SEM	%	±SEM
0	1.9	0.2	2.6	0.2	2.4	0.2
8	5.0	0.6	4.6	1.0	4.3	0.6
16	9.1	0.8	5.8	1.5	7.5	0.7
33	-	-	-	-	12.1	0.2
50	17.4	1.6	10.8	2.3	16.5	0.7
64	-	-	13.3	1.2	-	-
100	-	-	19.6	0.3	-	-

C

Micronucleus induction (Fold change)						
mAMSA (nM)	Nalm-6 WT		Nalm-6$^{TOP2B-/-}$		Nalm-6$^{TOP2A+/-}$	
	Fold	±SEM	Fold	±SEM	Fold	±SEM
0	1.0	0.0	1.0	0.0	1.0	0.0
8	3.3	0.3	1.7	0.3	1.8	0.3
16	4.9	0.3	2.1	0.3	3.2	0.5
33	-	-	-	-	5.1	0.1
50	8.3	2.1	4.0	0.6	7.0	0.6
64	-	-	5.6	0.6	-	-
100	-	-	8.1	0.4	-	-

Appendix table 2 Summary tables of appendix figure 2.

(A) Relative survival, (B) average percentage of micronuclei and (C) Micronucleus induction (fold change)

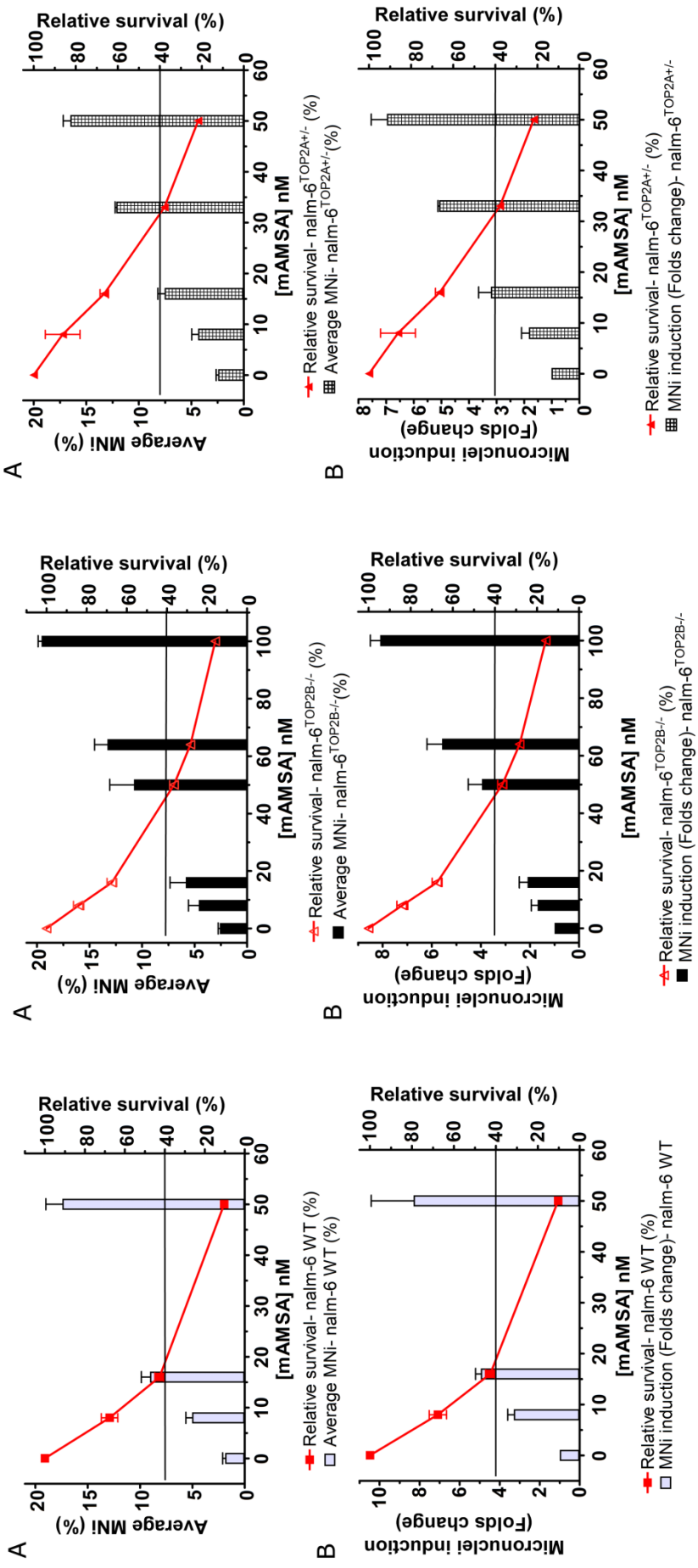

Appendix figure 2 Micronucleus formation in Nalm-6 cell lines after 48 hours exposure to mAMSA.

Data presented in average percentage of micronuclei (Row A) and fold change (Row B).

A

Relative survival						
Doxorubicin (nM)	Nalm-6 WT		Nalm-6$^{TOP2B-/-}$		Nalm-6$^{TOP2A+/-}$	
	%	±SEM	%	±SEM	%	±SEM
0	100.0	0.0	100.0	0.0	100.0	0.0
3	92.3	3.9	98.0	6.4	100.0	10.9
6	61.6	2.8	76.2	4.7	87.8	12.0
9.5	35.0	6.1	53.1	1.6	58.8	7.2
12	-	-	47.1	0.0	49.2	0.5
20	-	-	21.1	0.6	-	-

B

Average micronuclei (%)						
Doxorubicin (nM)	Nalm-6 WT		Nalm-6$^{TOP2B-/-}$		Nalm-6$^{TOP2A+/-}$	
	%	±SEM	%	±SEM	%	±SEM
0	1.3	0.1	1.9	0.2	1.7	0.3
3	2.4	0.4	2.8	0.5	2.1	0.2
6	6.6	0.9	4.5	0.6	3.9	0.8
9.5	16.0	1.6	8.2	0.7	5.9	1.2
12	-	-	10.6	0.0	9.1	0.3
20	-	-	19.8	0.2	-	-

C

Micronucleus induction (Fold change)						
Doxorubicin (nM)	Nalm-6 WT		Nalm-6$^{TOP2B-/-}$		Nalm-6$^{TOP2A+/-}$	
	Fold	±SEM	Fold	±SEM	Fold	±SEM
0	1.0	0.0	1.0	0.0	1.0	0.0
3	2.0	0.4	1.7	0.3	1.2	0.1
6	5.1	0.6	2.8	0.4	2.2	0.0
9.5	10.7	1.2	4.5	0.5	3.3	0.1
12	-	-	4.4	0.0	6.8	0.2
20	-	-	9.1	0.4	-	-

Appendix table 3 Summary tables of appendix figure 3.

(A) Relative survival, (B) average percentage of micronuclei and (C) Micronucleus induction (fold change)

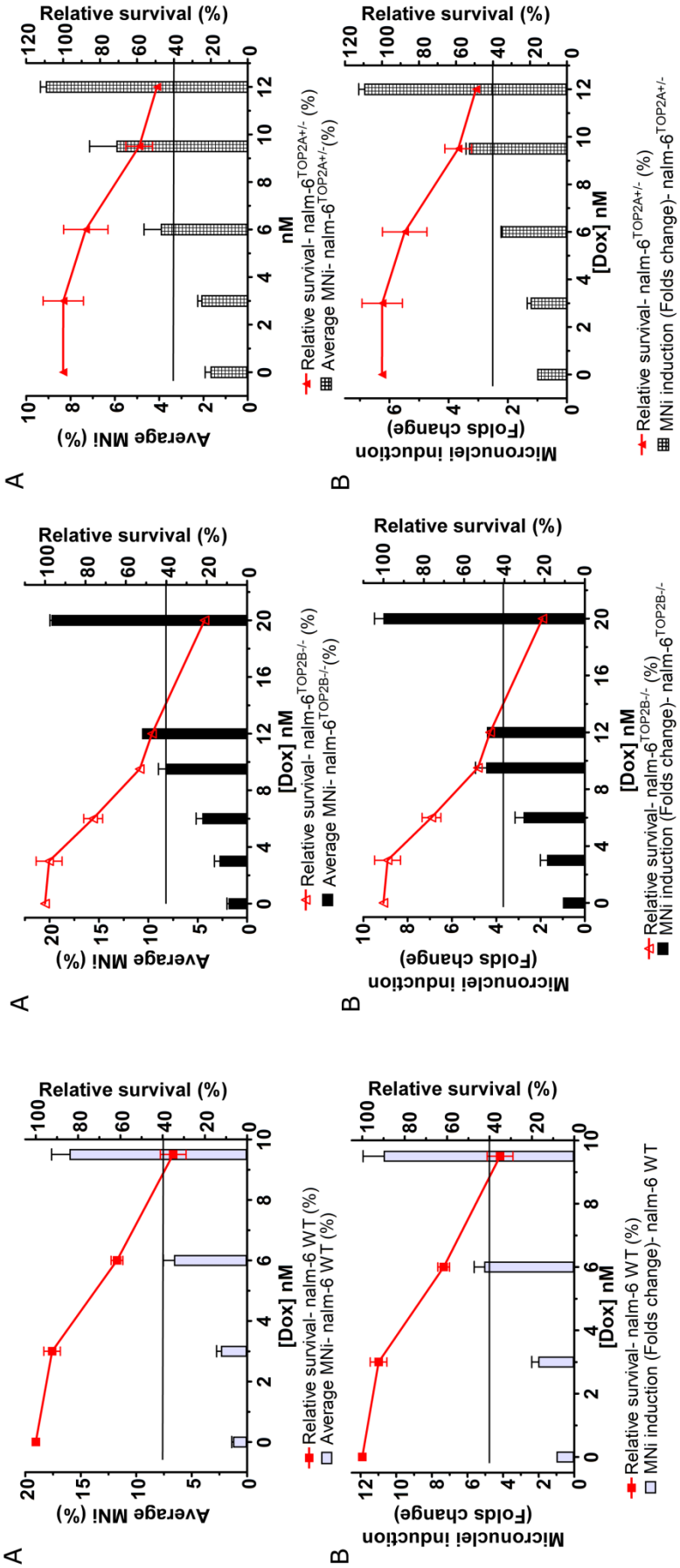

Appendix figure 3 Micronucleus formation in Nalm-6 cell lines after 48 hours exposure to Dox.

Data presented in average percentage of micronuclei (Row A) and fold change (Row B).

A

Relative survival						
Epirubicin (nM)	Nalm-6 WT		Nalm-6$^{TOP2B-/-}$		Nalm-6$^{TOP2A+/-}$	
	%	±SEM	%	±SEM	%	±SEM
0	100.0	0.0	100.0	0.0	100.0	0.0
3	82.2	4.4	96.3	5.6	102.5	8.7
6	58.5	3.6	76.7	13.5	84.2	11.7
9.5	31.8	5.9	57.4	3.6	65.5	14.1
12	-	-	38.3	2.9	47.3	2.0
13	17.8	0.2	-	-	-	-
20	-	-	11.2	0.0	-	-

B

Average micronuclei (%)						
Epirubicin (nM)	Nalm-6 WT		Nalm-6$^{TOP2B-/-}$		Nalm-6$^{TOP2A+/-}$	
	%	±SEM	%	±SEM	%	±SEM
0	1.3	0.1	1.9	0.2	1.7	0.3
3	2.2	0.3	2.3	0.2	2.4	0.3
6	4.7	0.6	4.1	0.5	3.2	0.3
9.5	15.4	4.6	7.0	0.4	7.1	1.3
12	-	-	12.5	0.1	8.4	0.6
13	24.8	4.8	-	-	-	-
20	-	-	27.5	0.0	-	-

C

Micronucleus induction (Fold change)						
Epirubicin (nM)	Nalm-6 WT		Nalm-6$^{TOP2B-/-}$		Nalm-6$^{TOP2A+/-}$	
	Fold	±SEM	Fold	±SEM	Fold	±SEM
0	1.0	0.0	1.0	0.0	1.0	0.0
3	1.8	0.2	1.4	0.2	1.4	0.2
6	3.9	0.4	2.5	0.4	1.8	0.2
9.5	10.2	3.0	3.9	0.4	4.0	0.3
12	-	-	5.7	0.2	6.3	0.5
13	16.7	2.9	-	-	-	-
20	-	-	11.5	0.0	-	-

Appendix table 4 Summary tables of appendix figure 4.

(A) Relative survival, (B) average percentage of micronuclei and (C) Micronucleus induction (fold change)

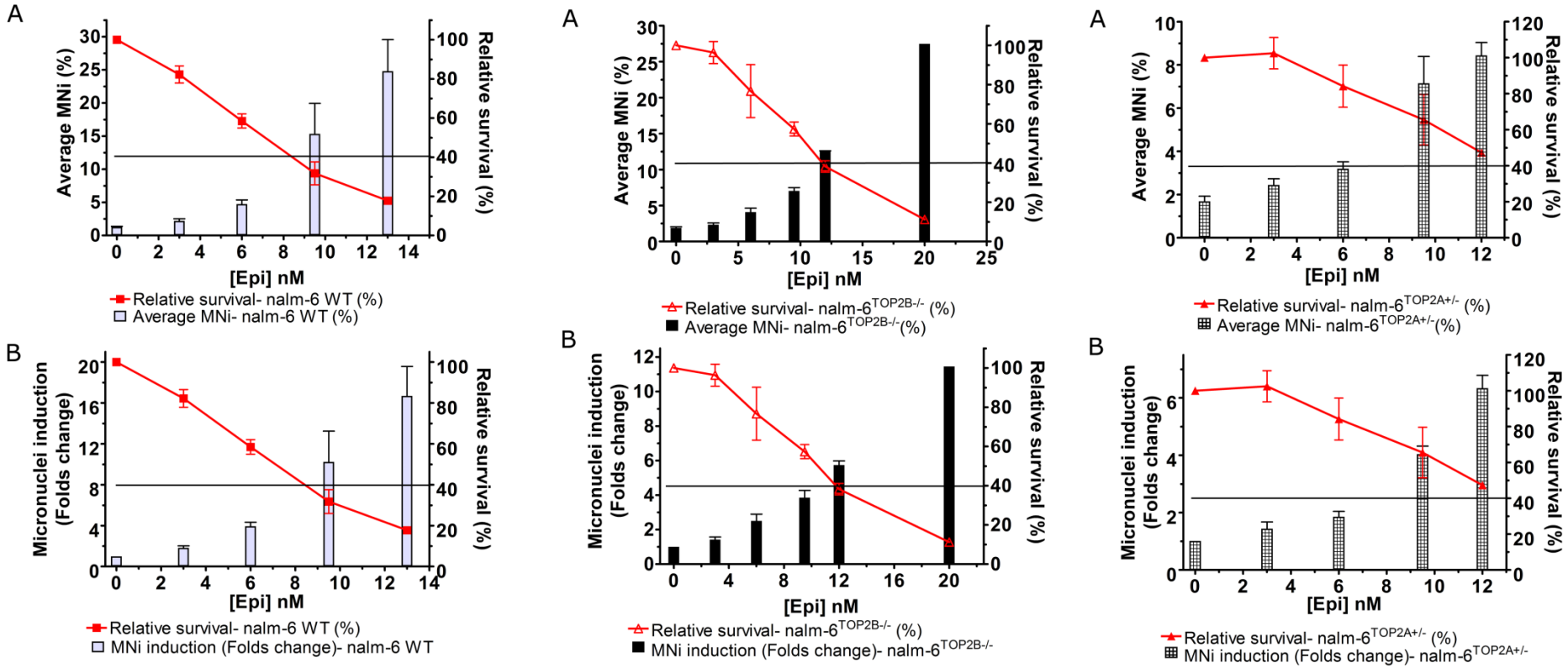

Appendix figure 4 Micronucleus formation in Nalm-6 cell lines after 48 hours exposure to Epi.

Data presented in average percentage of micronuclei (Row A) and fold change (Row B).

A

Relative survival						
Teniposide (nM)	Nalm-6 WT		Nalm-6$^{TOP2B-/-}$		Nalm-6$^{TOP2A+/-}$	
	%	±SEM	%	±SEM	%	±SEM
0.0	100.0	0.0	100.0	0.0	100.0	0.0
2.0	80.8	4.5	93.4	1.9	111.8	3.1
4.0	55.1	3.0	61.7	4.5	95.5	4.9
10.0	26.3	5.5	31.1	1.1	67.4	6.3
12.0	-	-	25.0	0.9	-	-
16.0	-	-	-	-	38.2	3.1

B

Average micronuclei (%)						
Teniposide (nM)	Nalm-6 WT		Nalm-6$^{TOP2B-/-}$		Nalm-6$^{TOP2A+/-}$	
	%	±SEM	%	±SEM	%	±SEM
0	1.9	0.2	2.6	0.2	2.4	0.2
2	3.8	0.6	3.3	0.2	3.8	0.7
4	6.7	1.1	4.9	1.3	4.4	0.4
10	12.6	0.5	10.3	1.5	6.8	0.6
12	-	-	11.9	0.8	-	-
16	-	-	-	-	10.5	0.7

C

Micronucleus induction (Fold change)						
Teniposide (nM)	Nalm-6 WT		Nalm-6$^{TOP2B-/-}$		Nalm-6$^{TOP2A+/-}$	
	Fold	±SEM	Fold	±SEM	Fold	±SEM
0	1.0	0.0	1.0	0.0	1.0	0.0
2	2.5	0.3	1.2	0.1	1.5	0.2
4	3.5	0.3	1.8	0.3	1.8	0.1
10	5.8	0.9	4.0	0.5	2.9	0.5
12	-	-	4.9	0.4	-	-
16	-	-	-	-	4.4	0.3

Appendix table 5 Summary tables of appendix figure 5.

(A) Relative survival, (B) average percentage of micronuclei and (C) Micronucleus induction (fold change)

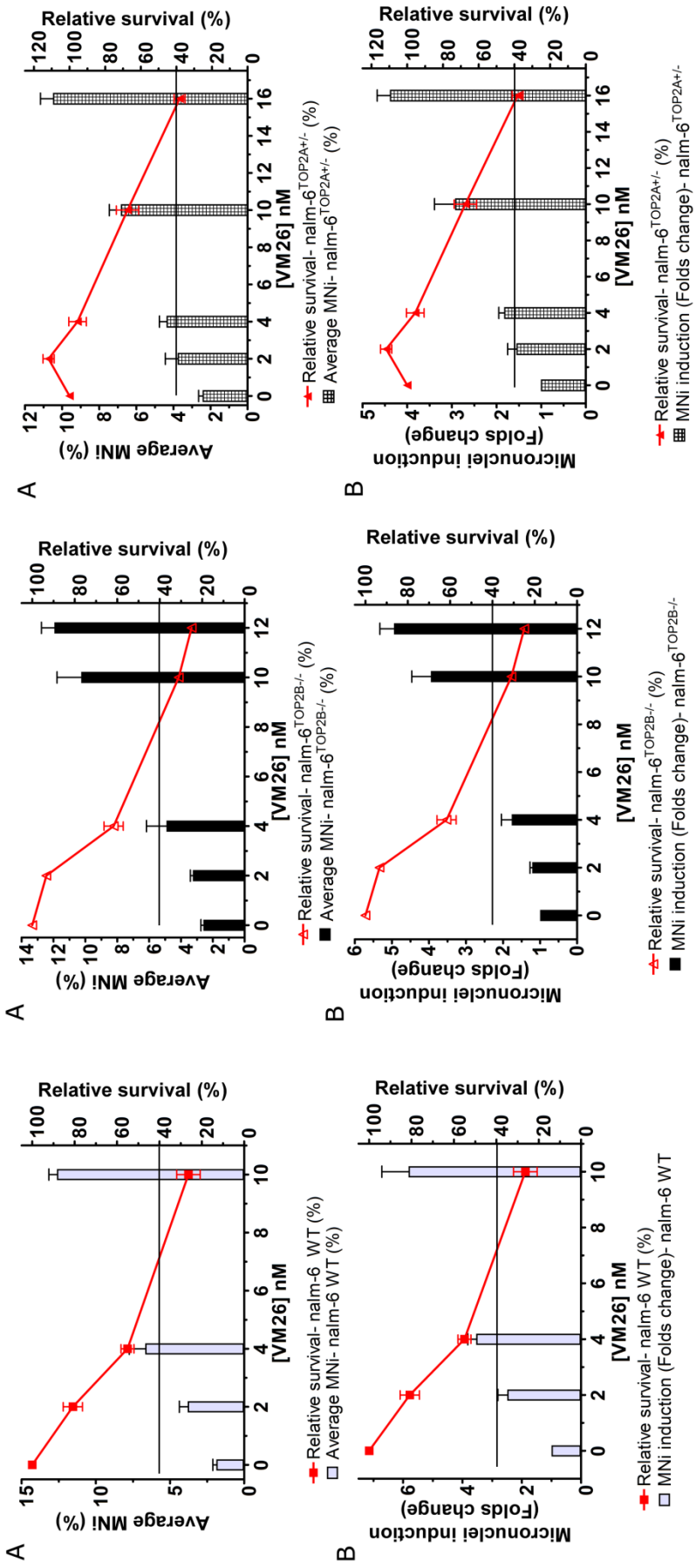

Appendix figure 5 Micronucleus formation in Nalm-6 cell lines after 48 hours exposure to VM26.

Data presented in average percentage of micronuclei (Row A) and fold change (Row B).

A

Relative survival						
Etoposide (nM)	Nalm-6 WT		Nalm-6$^{TOP2B-/-}$		Nalm-6$^{TOP2A+/-}$	
	%	±SEM	%	±SEM	%	±SEM
0	100.0	0.0	100.0	0.0	100.0	0.0
22.5	82.9	4.9	83.8	7.0	103.7	3.5
45	57.4	2.6	66.2	3.5	83.3	3.2
85	36.5	4.7	43.9	3.3	70.5	4.2
90	-	-	40.7	0.6	-	-
110	-	-	35.5	0.0	54.3	3.0

B

Average micronuclei (%)						
Etoposide (nM)	Nalm-6 WT		Nalm-6$^{TOP2B-/-}$		Nalm-6$^{TOP2A+/-}$	
	%	±SEM	%	±SEM	%	±SEM
0	1.9	0.2	2.6	0.2	2.4	0.2
22.5	3.4	0.6	5.1	1.0	4.1	0.9
45	6.8	0.8	6.5	1.2	5.0	0.6
85	11.5	1.1	8.5	0.8	6.2	0.6
90	-	-	9.2	0.8	-	-
110	-	-	12.1	0.0	7.9	0.1

C

Micronucleus induction (Fold change)						
Etoposide (nM)	Nalm-6 WT		Nalm-6$^{TOP2B-/-}$		Nalm-6$^{TOP2A+/-}$	
	Fold	±SEM	Fold	±SEM	Fold	±SEM
0	1.0	0.0	1.0	0.0	1.0	0.0
22.5	2.3	0.4	1.9	0.2	1.7	0.4
45	3.7	0.4	2.4	0.2	2.1	0.3
85	5.3	0.9	3.3	0.4	2.6	0.1
90	-	-	3.8	0.4	-	-
110	-	-	5.2	0.0	3.3	0.0

Appendix table 6 Summary tables of appendix figure 6.

(A) Relative survival, (B) average percentage of micronuclei and (C) Micronucleus induction (fold change)

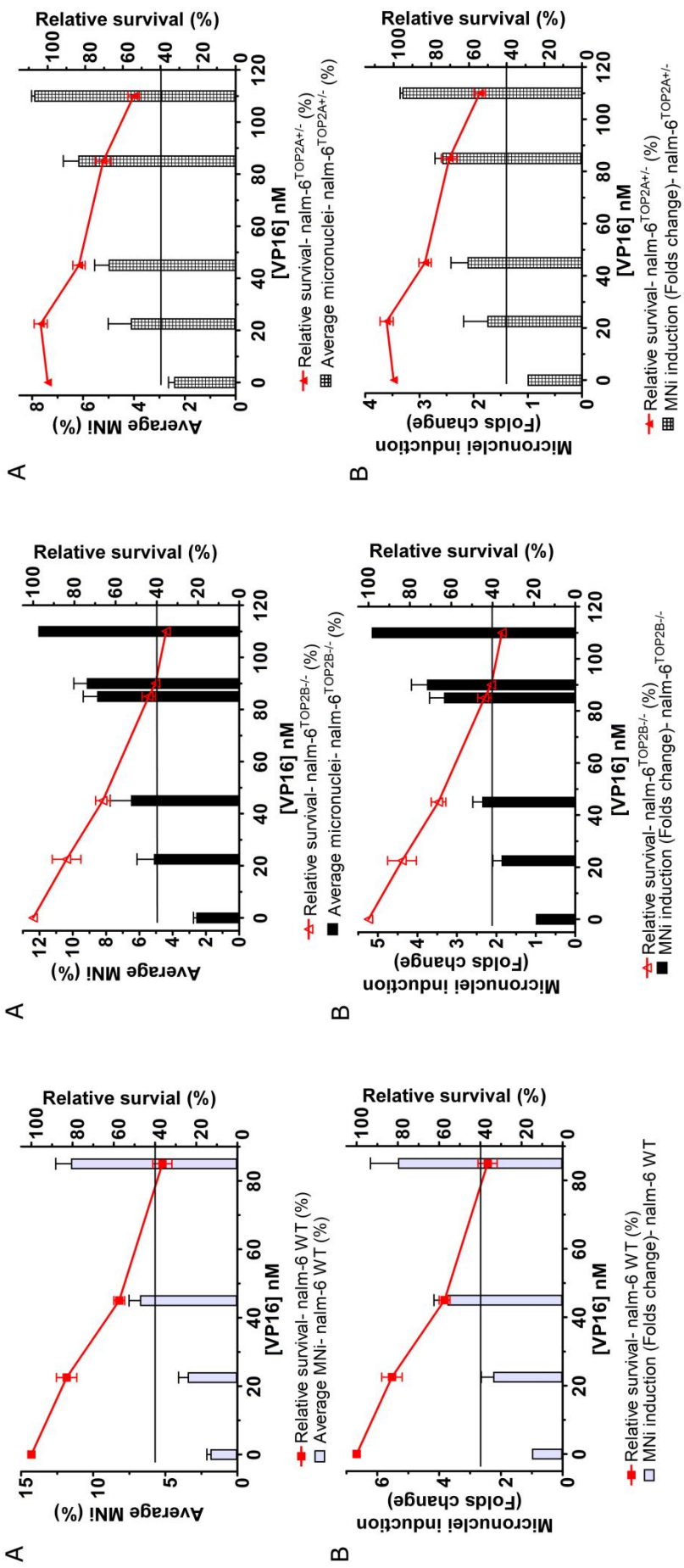

Appendix figure 6 Micronucleus formation in Nalm-6 cell lines after 48 hours exposure to VP16.

Data presented in average percentage of micronuclei (Row A) and fold change (Row B).

OXFORD UNIVERSITY PRESS LICENSE
TERMS AND CONDITIONS
Jul 01, 2016

This Agreement between Ka Cheong Lee ("You") and Oxford University Press ("Oxford University Press") consists of your license details and the terms and conditions provided by Oxford University Press and Copyright Clearance Center.

License Number	3900220547824
License date	Jul 01, 2016
Licensed content publisher	Oxford University Press
Licensed content publication	Mutagenesis
Licensed content title	An overview of the visualisation and quantitation of low and high MW DNA adducts using the trapped in agarose DNA immunostaining (TARDIS) assay:
Licensed content author	Ian G. Cowell, Michael J. Tilby, Caroline A. Austin
Licensed content date	03/01/2011
Type of Use	Thesis/Dissertation
Institution name	
Title of your work	Molecular Pharmacology of DNA topoisomerase II drugs
Publisher of your work	n/a
Expected publication date	Jul 2016
Permissions cost	0.00 USD
Value added tax	0.00 USD
Total	0.00 USD
Requestor Location	Ka Cheong Lee Newcastle University Medical School Newcastle upon Tyne, NE2 4HH United Kingdom Attn: Ka Cheong Lee
Publisher Tax ID	GB125506730
Billing Type	Invoice
Billing Address	Ka Cheong Lee Newcastle University Medical School Newcastle upon Tyne, United Kingdom NE2 4HH Attn: Ka Cheong Lee
Total	0.00 USD

ELSEVIER LICENSE
TERMS AND CONDITIONS
Jul 01, 2016

This Agreement between Ka Cheong Lee ("You") and Elsevier ("Elsevier") consists of your license details and the terms and conditions provided by Elsevier and Copyright Clearance Center.

License Number	3900220178887
License date	Jul 01, 2016
Licensed Content Publisher	Elsevier
Licensed Content Publication	Chemistry & Biology
Licensed Content Title	DNA Topoisomerases and Their Poisoning by Anticancer and Antibacterial Drugs
Licensed Content Author	Yves Pommier,Elisabetta Leo,HongLiang Zhang,Christophe Marchand
Licensed Content Date	28 May 2010
Licensed Content Volume Number	17
Licensed Content Issue Number	5
Licensed Content Pages	13
Start Page	421
End Page	433
Type of Use	reuse in a thesis/dissertation
Portion	figures/tables/illustrations
Number of figures/tables/illustrations	1
Format	both print and electronic
Are you the author of this Elsevier article?	No
Will you be translating?	No
Order reference number	
Original figure numbers	Figure 5 A and B
Title of your thesis/dissertation	Molecular Pharmacology of DNA topoisomerase II drugs
Expected completion date	Jul 2016
Estimated size (number of pages)	180
Elsevier VAT number	GB 494 6272 12
Requestor Location	Ka Cheong Lee Newcastle University Medical School Newcastle upon Tyne, NE2 4HH United Kingdom Attn: Ka Cheong Lee
Total	0.00 USD

ELSEVIER LICENSE
TERMS AND CONDITIONS
Jul 01, 2016

This Agreement between Ka Cheong Lee ("You") and Elsevier ("Elsevier") consists of your license details and the terms and conditions provided by Elsevier and Copyright Clearance Center.

License Number	3900220747071
License date	Jul 01, 2016
Licensed Content Publisher	Elsevier
Licensed Content Publication	Mutation Research/Genetic Toxicology and Environmental Mutagenesis
Licensed Content Title	In vitro micronucleus assay scored by flow cytometry provides a comprehensive evaluation of cytogenetic damage and cytotoxicity
Licensed Content Author	Steven M. Bryce,Jeffrey C. Bemis,Svetlana L. Avlasevich,Stephen D. Dertinger
Licensed Content Date	15 June 2007
Licensed Content Volume Number	630
Licensed Content Issue Number	1-2
Licensed Content Pages	14
Start Page	78
End Page	91
Type of Use	reuse in a thesis/dissertation
Intended publisher of new work	other
Portion	figures/tables/illustrations
Number of figures/tables/illustrations	2
Format	both print and electronic
Are you the author of this Elsevier article?	No
Will you be translating?	No
Order reference number	
Original figure numbers	Figure 1 and figure 2
Title of your thesis/dissertation	Molecular Pharmacology of DNA topoisomerase II drugs
Expected completion date	Jul 2016
Estimated size (number of pages)	180
Elsevier VAT number	GB 494 6272 12
Requestor Location	Ka Cheong Lee Newcastle University Medical School Newcastle upon Tyne, NE2 4HH United Kingdom Attn: Ka Cheong Lee
Total	0.00 USD

ELSEVIER LICENSE
TERMS AND CONDITIONS
Jul 01, 2016

This Agreement between Ka Cheong Lee ("You") and Elsevier ("Elsevier") consists of your license details and the terms and conditions provided by Elsevier and Copyright Clearance Center.

License Number	3900220933607
License date	Jul 01, 2016
Licensed Content Publisher	Elsevier
Licensed Content Publication	Mutation Research/Fundamental and Molecular Mechanisms of Mutagenesis
Licensed Content Title	The in vitro micronucleus technique
Licensed Content Author	Michael Fenech
Licensed Content Date	20 November 2000
Licensed Content Volume Number	455
Licensed Content Issue Number	1-2
Licensed Content Pages	15
Start Page	81
End Page	95
Type of Use	reuse in a thesis/dissertation
Intended publisher of new work	other
Portion	figures/tables/illustrations
Number of figures/tables/illustrations	1
Format	both print and electronic
Are you the author of this Elsevier article?	No
Will you be translating?	No
Order reference number	
Original figure numbers	Figure 1
Title of your thesis/dissertation	Molecular Pharmacology of DNA topoisomerase II drugs
Expected completion date	Jul 2016
Estimated size (number of pages)	180
Elsevier VAT number	GB 494 6272 12
Requestor Location	Ka Cheong Lee Newcastle University Medical School Newcastle upon Tyne, NE2 4HH United Kingdom Attn: Ka Cheong Lee
Total	0.00 USD

NATURE PUBLISHING GROUP LICENSE
TERMS AND CONDITIONS
Jul 01, 2016

This Agreement between Ka Cheong Lee ("You") and Nature Publishing Group ("Nature Publishing Group") consists of your license details and the terms and conditions provided by Nature Publishing Group and Copyright Clearance Center.

License Number	3900221174160
License date	Jul 01, 2016
Licensed Content Publisher	Nature Publishing Group
Licensed Content Publication	Nature Reviews Molecular Cell Biology
Licensed Content Title	Proteolysis: from the lysosome to ubiquitin and the proteasome
Licensed Content Author	Aaron Ciechanover
Licensed Content Date	Jan 1, 2005
Licensed Content Volume Number	6
Licensed Content Issue Number	1
Type of Use	reuse in a dissertation / thesis
Requestor type	academic/educational
Format	print and electronic
Portion	figures/tables/illustrations
Number of figures/tables/illustrations	1
High-res required	no
Figures	Figure 2A
Author of this NPG article	no
Your reference number	
Title of your thesis / dissertation	Molecular Pharmacology of DNA topoisomerase II drugs
Expected completion date	Jul 2016
Estimated size (number of pages)	180
Requestor Location	Ka Cheong Lee Newcastle University Medical School Newcastle upon Tyne, NE2 4HH United Kingdom Attn: Ka Cheong Lee
Billing Type	Invoice
Billing Address	Ka Cheong Lee Newcastle University Medical School Newcastle upon Tyne, United Kingdom NE2 4HH Attn: Ka Cheong Lee
Total	0.00 USD